U. S. Department of
Transportation
**Federal Railroad
Administration**

Commuter Rail Seat Testing and Analysis

Office of Research
and Development
Washington, D.C. 20590

Railroad Systems Safety

DOT/FRA/ORD-01/06

**Final Report
July 2002**

**This document is available to the public through the National Technical Information Service, Springfield, VA 22161
This document is also available on the FRA web site at www.fra.dot.gov**

REPORT DOCUMENTATION PAGE	*Form Approved OMB No. 0704-0188*

1. AGENCY USE ONLY (Leave blank)	2. REPORT DATE July 2002	3. REPORT TYPE AND DATES COVERED Final Report June 1998 – April 1999

4. TITLE AND SUBTITLE Commuter Rail Seat Testing and Analysis	5. FUNDING NUMBERS RR028/R0001
6. AUTHOR(S) C. VanIngen-Dunn, J. Manning	

7. PERFORMING ORGANIZATION NAME(S) AND ADDRESS(ES) Simula Technologies, Inc.* 10016 S. 51st Street Phoenix, AZ 85044	8. PERFORMING ORGANIZATION REPORT NUMBER DOT-VNTSC-FRA-02-10
9. SPONSORING/MONITORING AGENCY NAME(S) AND ADDRESS(ES) U.S. Department of Transportation Federal Railroad Administration Office of Research and Development 1120 Vermont Avenue, NW – Mail Stop 20 Washington, DC 20590	10. SPONSORING/MONITORING AGENCY REPORT NUMBER DOT/FRA/ORD-01/06

11. SUPPLEMENTARY NOTES
*under contract to: U.S. Department of Transportation
John A. Volpe National Transportation Systems Center
Research and Special Programs Administration
55 Broadway
Cambridge, MA 02142-1093

12a. DISTRIBUTION/AVAILABILITY STATEMENT This document is available to the U.S. public through the National Technical Information Service, Springfield VA 22161. This document is also available on the FRA web site at www.fra.dot.gov.	12b. DISTRIBUTION CODE

13. ABSTRACT (Maximum 200 words)

The need to determine the structural integrity and passenger safety provided by existing commuter rail seats was identified by the Construction/Structural Subgroup of the American Public Transportation Association's (APTA) Passenger Rail Equipment Safety Standards (PRESS) Task Force. Recognizing the importance of this information, the Federal Railroad Administration (FRA) authorized funding for commuter rail seat testing and analysis to establish a baseline of information about these seats in a dynamic rail collision environment. Results describing the current level of seat strength and occupant compatibility with these seats were used to help develop the new APTA Passenger Rail Equipment Safety Standards that were published in May 1999.

This report presents the results of the testing and analysis of the two-passenger C-3 seat, the three-passenger M-Style seat, and the three-passenger Walkover seat used in this study.

14. SUBJECT TERMS commuter rail, M-style seat, Walkover seat, static testing, dynamic testing, structural integrity, occupant safety	15. NUMBER OF PAGES 204
	16. PRICE CODE

17. SECURITY CLASSIFICATION OF REPORT Unclassified	18. SECURITY CLASSIFICATION OF THIS PAGE Unclassified	19. SECURITY CLASSIFICATION OF ABSTRACT Unclassified	20. LIMITATION OF ABSTRACT

PREFACE

This work was performed as part of the Equipment Safety Research Program sponsored by the Office of Research and Development of the Federal Railroad Administration (FRA). The author would like to thank Dr. Tom Tsai, Program Manager, and Claire Orth, Division Chief, Equipment and Operating Practices Division, Office of Research and Development, FRA, for their support.

The work described in this report was performed at the request of the American Public Transportation Association (APTA), and was coordinated through APTA Passenger Rail Equipment Safety Standards Construction/Structural Subcommittee. The author would like to thank Tom Peacock, APTA, for his assistance in coordinating this effort.

The work was initiated by David Tyrell, Senior Engineer, Volpe Center, and monitored by Mr. Tyrell and John Zolock, Senior Engineer, Volpe Center.

METRIC/ENGLISH CONVERSION FACTORS

ENGLISH TO METRIC

LENGTH (APPROXIMATE)

1 inch (in)	=	2.5 centimeters (cm)
1 foot (ft)	=	30 centimeters (cm)
1 yard (yd)	=	0.9 meter (m)
1 mile (mi)	=	1.6 kilometers (km)

AREA (APPROXIMATE)

1 square inch (sq in, in^2)	=	6.5 square centimeters (cm^2)
1 square foot (sq ft, ft^2)	=	0.09 square meter (m^2)
1 square yard (sq yd, yd^2)	=	0.8 square meter (m^2)
1 square mile (sq mi, mi^2)	=	2.6 square kilometers (km^2)
1 acre = 0.4 hectare (he)	=	4,000 square meters (m^2)

MASS - WEIGHT (APPROXIMATE)

1 ounce (oz)	=	28 grams (gm)
1 pound (lb)	=	0.45 kilogram (kg)
1 short ton = 2,000 pounds (lb)	=	0.9 tonne (t)

VOLUME (APPROXIMATE)

1 teaspoon (tsp)	=	5 milliliters (ml)
1 tablespoon (tbsp)	=	15 milliliters (ml)
1 fluid ounce (fl oz)	=	30 milliliters (ml)
1 cup (c)	=	0.24 liter (l)
1 pint (pt)	=	0.47 liter (l)
1 quart (qt)	=	0.96 liter (l)
1 gallon (gal)	=	3.8 liters (l)
1 cubic foot (cu ft, ft^3)	=	0.03 cubic meter (m^3)
1 cubic yard (cu yd, yd^3)	=	0.76 cubic meter (m^3)

TEMPERATURE (EXACT)

[(x-32)(5/9)] F = y C

METRIC TO ENGLISH

LENGTH (APPROXIMATE)

1 millimeter (mm)	=	0.04 inch (in)
1 centimeter (cm)	=	0.4 inch (in)
1 meter (m)	=	3.3 feet (ft)
1 meter (m)	=	1.1 yards (yd)
1 kilometer (km)	=	0.6 mile (mi)

AREA (APPROXIMATE)

1 square centimeter (cm^2)	=	0.16 square inch (sq in, in^2)
1 square meter (m^2)	=	1.2 square yards (sq yd, yd^2)
1 square kilometer (km^2)	=	0.4 square mile (sq mi, mi^2)
10,000 square meters (m^2)	=	1 hectare (ha) = 2.5 acres

MASS - WEIGHT (APPROXIMATE)

1 gram (gm)	=	0.036 ounce (oz)
1 kilogram (kg)	=	2.2 pounds (lb)
1 tonne (t)	=	1,000 kilograms (kg)
	=	1.1 short tons

VOLUME (APPROXIMATE)

1 milliliter (ml)	=	0.03 fluid ounce (fl oz)
1 liter (l)	=	2.1 pints (pt)
1 liter (l)	=	1.06 quarts (qt)
1 liter (l)	=	0.26 gallon (gal)
1 cubic meter (m^3)	=	36 cubic feet (cu ft, ft^3)
1 cubic meter (m^3)	=	1.3 cubic yards (cu yd, yd^3)

TEMPERATURE (EXACT)

[(9/5) y + 32] C = x F

QUICK INCH - CENTIMETER LENGTH CONVERSION

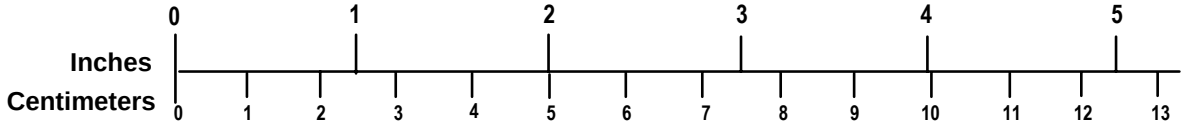

QUICK FAHRENHEIT - CELSIUS TEMPERATURE CONVERSION

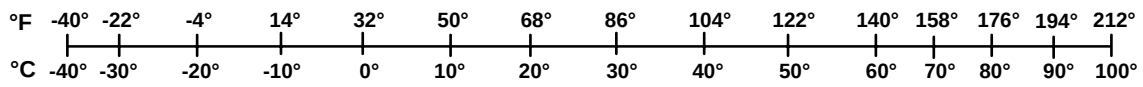

For more exact and or other conversion factors, see NIST Miscellaneous Publication 286, Units of Weights and Measures. Price $2.50 SD Catalog No. C13 10286

Updated 6/17/98

TABLE OF CONTENTS

Section **Page**

TABLE OF CONTENTS (cont.)

LIST OF FIGURES

LIST OF TABLES

EXECUTIVE SUMMARY

The Construction/Structural Subgroup of the American Public Transportation Association's (APTAs) Passenger Rail Equipment Safety Standards (PRESS) Task Force identified the need to determine the structural integrity and passenger safety provided by existing commuter rail seats. Results describing the current level of seat strength and occupant compatibility with these seats were used to help develop the new APTA Passenger Rail Equipment Safety Standards which were published in May of 1999. Recognizing the importance of this information, the Federal Railroad Administration (FRA) authorized funding for commuter rail seat testing and analysis to establish a baseline of information about these seats in a dynamic rail collision environment.

Three test outcomes were defined as the desirable indicators for demonstrating an acceptable level of structural integrity and passenger safety of the commuter rail seats. These test outcomes were:

- All seat components should remain attached (or should not become free-flying objects).
- Passengers should remain compartmentalized between the two seat rows.
- Occupant injury should be within acceptable injury criteria.

The John A. Volpe National Transportation Systems Center (Volpe Center) contracted with Simula Technologies, Inc., located in Phoenix, Arizona, through the U.S. Army Proving Ground, located in Yuma, Arizona. The program's Contract Number was DAAD01-98-C-0010. The program's start date was June 16, 1998. A 6-1/2-month program was approved and consisted of static testing, dynamic testing, and computer modeling and analysis of the following three commuter rail seat types:

- The two-passenger C-3 seat.
- The three-passenger M-Style seat.
- The three-passenger Walkover seat.

Quasi-static testing was first conducted on each seat to determine the relative stiffness of the seats. The stiffness characteristics (load-deflection curves) from these tests were used to build lumped-mass computer models of each seat with the MADYMO computer modeling software program. Seat/occupant models were then run using different seat and occupant parameters to assess the relative effect of these parameters on occupant safety. The test parameters that were varied included the seat pitch, crash pulse, occupant size, and occupant location. The results of the parametric analysis were used to help define the Dynamic Test Plan. Dynamic testing was then conducted to determine the collision performance of each seat design.

The dynamic tests were conducted with two seats in a tandem configuration, separated one behind the other by 32 inches (seat pitch). Anthropomorphic test devices (ATD) of varying sizes were placed, unrestrained, in the rear seat row. A triangular dynamic crash pulse of 250-msec duration and 8-G peak acceleration (for an occupant secondary impact velocity of 22 mph) was used to represent a typical in-line collision at 35 mph or above for occupants in the first coach car (behind the locomotive). The data recorded from the seat attachment load cells and the ATDs' instrumentation were reviewed, analyzed, and compared with the predicted results from the computer modeling.

All tests were successfully completed and clearly indicated how commuter rail seats and their occupants are most likely to respond in a dynamic loading environment.

Cushion detachment was the primary source of flying objects and occurred in the C-3 (partial detachment) and M-Style seats (complete detachment).

Compartmentalization appears to be at least a partially effective occupant restraint for the tested seats. The C-3 seats were the most effective at compartmentalization. The M-Style and Walkover seat tests also demonstrated some compartmentalization; however, in both of these cases, an occupant landed on the aisle-side floor. It is unknown whether the occupants in the Walkover seat would have projected completely over the front-row seats if they had not been as closely tethered to the rear seat row (all ATDs were tethered in all tests to prevent severe damage to them). Therefore, the conservative conclusion is to consider that these two seats did not effectively compartmentalize the occupants.

The 5th-percentile female and 50th-percentile male occupants in the stiff C-3 seat measured neck and femur injury loads that exceeded the injury criteria. The 5th-percentile female in the M-Style seat measured a neck flexion load that exceeded the injury criteria in Table 2.

The outcome of these dynamic tests suggests that stiffer seats like the C-3 seat improve passenger compartmentalization, but increase the likelihood of neck injuries caused by impacting the seat in front of them. More compliant seats, like the M-Style and the Walkover seats, increase the risk of passengers projecting beyond the seat in front of them. However, they do reduce the risk of injuries caused by occupants impacting the seat back. The results also demonstrated that these tests were repeatable and provided consistent information. Since the seats were rigidly mounted to the test fixture, it was not possible to account for the effect of the rail car structure on the outcome of the tests. To account for this situation, the seat attachment loads were all measured to provide some information regarding seat attachment strength.

It could be expected that the occupant injury and seat loading outcomes identified would be worse as the seat pitch increases. The seat/occupant models created in this program correlate well to the testing (see section 7) and may be used in future analyses to assess the effect of changes in seat configuration and collision dynamics.

1. INTRODUCTION

With the current emphasis on train occupant safety and passenger rail car crashworthiness, there has been preliminary activity toward the development of new standards that better define rail seat design requirements for dynamic conditions. Consequently, there is a heightened interest in knowing the level of crashworthiness of existing seats. The objective of this program effort is to establish the level of existing commuter rail passenger seat crashworthiness. More importantly, this program provides the information needed to establish new seat safety standards. In particular, this program will help define the acceptable criteria for commuter rail passenger seat crashworthiness and establish a corresponding method by which commuter seats should be tested to demonstrate structural integrity and passenger safety.

Passenger seating in rail cars can either enhance the safety environment within the car interior or can be a hazard, depending on the details of seating design, the seating arrangement in the car, and the strength of the seat's attachment to the car structure. There are several issues in rail passenger seat design that need to be addressed, only some of which could be addressed through the testing conducted in this program. The seat design issues that should be considered are:

- *Seat Strength* - Is the seat back strong enough to prevent the occupants from bending the seat back and impacting other interior features (tertiary impact)? Does the seat need to be strong enough to allow for the mounting of passenger restraints, such as lap belts, in the future? If so, does the seat need to be strong enough to (1) absorb the energy of a passenger impacting the seat back, and (2) resist the force of restrained passengers? How does the current trend towards cantilever-mounted seats affect the strength of the seat attachment and the compliance of the seat back structure?

- *Seat Attachment Strength* - Is the seat and its means of attachment to the car strong enough to prevent the seat from becoming detached from the car and thus becoming a projectile during a collision? Are the stanchion posts attached to the seat strong enough to stay attached if a passenger happens to be holding onto one during a crash?

- *Secondary Impact Features of the Seat* - Is the seat back padded? Have all sharp corners and edges been removed? Is the back structure compliant enough to absorb the energy of impacting passengers, and yet not fold over completely, thus allowing a tertiary impact? Are grab handles or seat-mounted stanchion posts padded or compliantly mounted? Should the seat be designed to mitigate injuries? If so, what measurements and criteria should be used? Should measurements include human tolerance data such as head injury criterion (HIC), femur load, chest acceleration, etc.? What crash pulse should be used for any sled testing?

- *Seating Arrangement in the Car* - Are seats arranged transversely in the car? Do seats face one another? Do they face bulkheads or partitions? Are there tables between facing seats? Are seats arranged longitudinally? Do longitudinal seats have armrests to prevent passengers from sliding during an accident? What trade-off should be made regarding operational and quality of service issues compared to maximizing safety? How do the requirements of the Americans with Disabilities Act of 1990 affect this?

- *Seat Design* - Does the seat back recline? Does the fact that the seat reclines increase or decrease its crashworthiness? Is the seat back recline mechanism strong enough and suitably compliant to contribute to compartmentalization? Is the seat back sufficiently padded to reduce injury? Does the seat rotate? Is there a rotation lock, and is the lock of sufficient strength to prevent rotation during a crash? Is there a tray table mounted to the seat back or in the armrest? Can it deploy accidentally

during a collision? Does it pose a safety hazard when it is deployed? Will objects mounted to the seat such as cushions, grab handles, pedestals, etc., stay attached to the seat or will they fly around in the car, with the potential to cause injuries? Are all corners and edges of the seat rounded to prevent injury?

This testing and analysis program addressed some of these issues. A preliminary assessment of seat and occupant safety was determined through the development of dynamic occupant computer models of three commuter seats and the quasi-static testing associated with developing these models. A parametric analysis of 40 test configurations was used to help predict dynamic test results and define the dynamic test protocol. The parameters chosen for evaluation were: 1) the crash pulse, 2) the seat pitch, and 3) ATD size and seating position. The results of dynamic testing helped establish a baseline from which future rail seats can be designed.

These results are provided in this report along with a description of the seats (Section 2), the test set-up and implementation of both the static and dynamic testing (Section 3), the quasi-static test results (Section 4), the dynamic test results (Section 5), the seat/occupant modeling results (Section 6), and a comparison between the dynamic test results and the seat/occupant modeling output (Section 7). The program conclusions and recommendations are provided in Sections 8 and 9, respectively. Appendix A provides a detailed seat description, Appendix B provides the static test results, Appendix C provides the crash pulses and seat attachment loads from the dynamic testing, Appendix D provides the seat/occupant modeling results, and Appendix E compares the dynamic test results and the seat/occupant modeling output to injury thresholds. The dynamic test results and the seat/occupant modeling output data are presented on one chart for each data channel in Appendix F. Finally, a background discussion of terms of existing standards and current practice is provided in Appendix G.

2. SEAT DESCRIPTION

A description and corresponding schematic of each of the three seat types is provided. A detailed description of each seat is presented in Appendix A.

Three rail seat types manufactured by Coach and Car Equipment Corporation (CCEC), located in Elk Grove Village, Illinois, were selected for testing. These three seats and some of the property owners who install them are:

- **Two-passenger C-3 seat**
  Long Island Rail Road (LIRR) (cantilever seat)
  Peninsula Corridor Joint Powers Board (Caltrain) (non-cantilever mounted seat)
  Northern Virginia - Virginia Rail Express (VRE) (non-cantilever mounted seat)

- **Three-passenger M-Style seat**
  Metro North
  LIRR
  South Eastern Pennsylvania Transit Authority (SEPTA)
  Northern Indiana (NICTD)
  New Jersey Transit (NJT)
  Maryland (MARC)

- **Three-passenger Walkover seat**
  Chicago Metra
  NJT
  Caltrain

2.1 C-3 SEAT

The C-3 seat that was tested is a fixed-position, two-passenger, cantilever-mounted seat design (See Figure 1). This seat is designed without a floor pedestal which is typically required to provide vertical support on the aisle side. Instead, the seat is attached to the wall of the train car at three mounting points, two located along the lower edge of the seat pan, and one located on the edge of the seat back. In order to accomplish this mounting configuration, the frame of the seat is constructed of 2-inch diameter round and 2-inch square steel tubing. A plastic shroud covers the rear portion of the seat while the seat back and seat cushion are clipped in place. Armrests are incorporated in the design on both ends of the seat.

2.2 M-STYLE SEAT

The M-Style seat is a fixed-position, three-passenger, traditional seat design (see Figure 1). Traditional mounting is used to attach the seat to the car: one mount attaches the seat to the wall of the car and a pedestal connects the seat to the floor. The pedestal is located under the aisle-side passenger seat. The seat frame, like the C-3, is constructed of both round and square steel tubing, but of smaller dimensions (1.25-inch diameter round and 1.25-inch square, respectively). The inboard armrest is part of the seat, while the outboard armrest is part of the train car. Three cushions are used for this seat: one for the seat pan and two for the seat back. All cushions are held in place with clips.

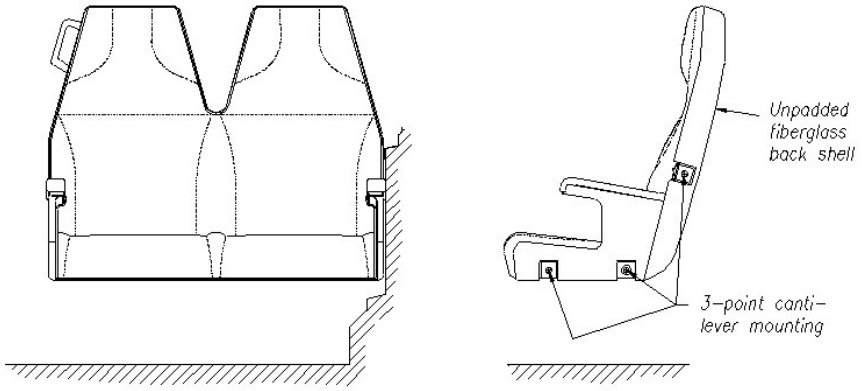

2 Passenger LIRR C-3 Seat

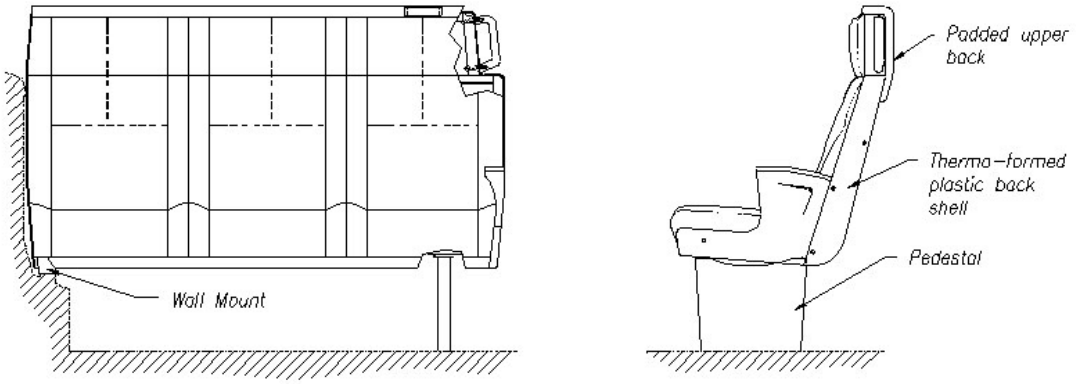

3 Passenger M-Style Seat

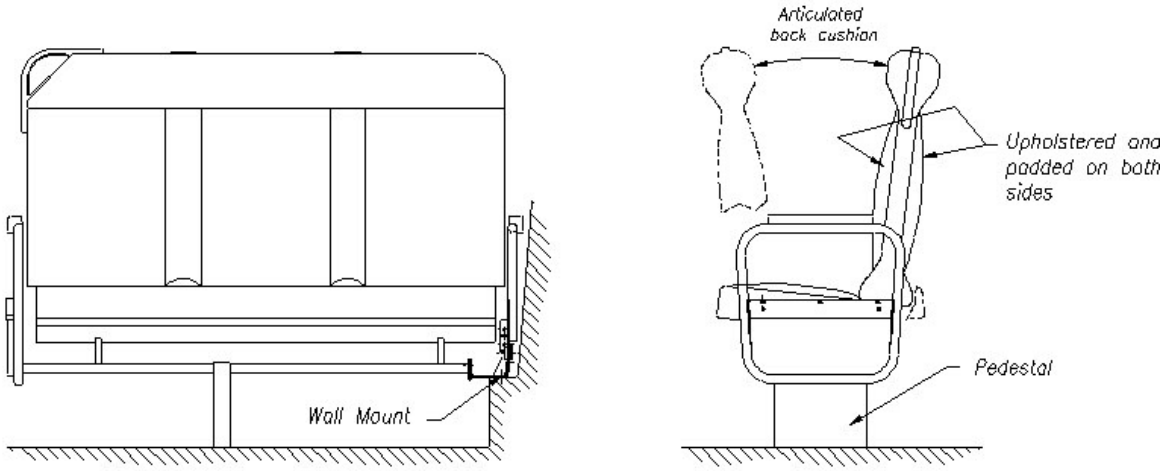

3 Passenger Walkover Seat

Figure 1. Commuter Rail Seats Tested and Analyzed

2.3 WALKOVER SEAT

The Walkover seat is a three-passenger seat with a back cushion that rotates about a pivot point to provide seated passengers with the option of changing the direction that they face in the train. (See Figure 1). The seat is attached to the car with two mounting positions. One mount connects the seat to the wall of the train while the other mount is a pedestal that connects the seat to the floor. The base of the seat is constructed of steel tubing, which supports the linkage mechanism used to pivot the seat back cushion forward and aftward, and houses the inertial locking device associated with it. The locking device is designed so that, in the event of a sudden stop, it engages (due to inertial force effects on the mechanism) to prevent the seat back from rotating about its pivot point. A full description of the inertial locking device can be found in Appendix A. The seat cushion is held in place with clips while the seat back slides over two tubes attached to the pivot mechanism.

3. TEST SETUP AND IMPLEMENTATION

All testing was conducted at Simula Technologies, Inc., in Phoenix, Arizona. One single test fixture was designed and manufactured to accommodate all three seat types in both the static and dynamic testing configurations. A single seat was attached to the test fixture for static testing. Two seats of one type, set 32 inches apart, were attached to the same fixture for dynamic testing. A description of the test setup for each test and seat type is provided in this section.

3.1 QUASI-STATIC TEST SETUP

3.1.1 C-3 and M-Style Seats

For quasi-static testing, one seat was loaded onto the test fixture and loaded until failure. The mounting structure was made of channeled steel designed to minimize structural flexing (see Figure 2). The seats were mounted to steel adapters which were, in turn, mounted to three-axis load cells. The load cells were then mounted to the test structure at the wall mount (and floor mount for the M-Style seat).

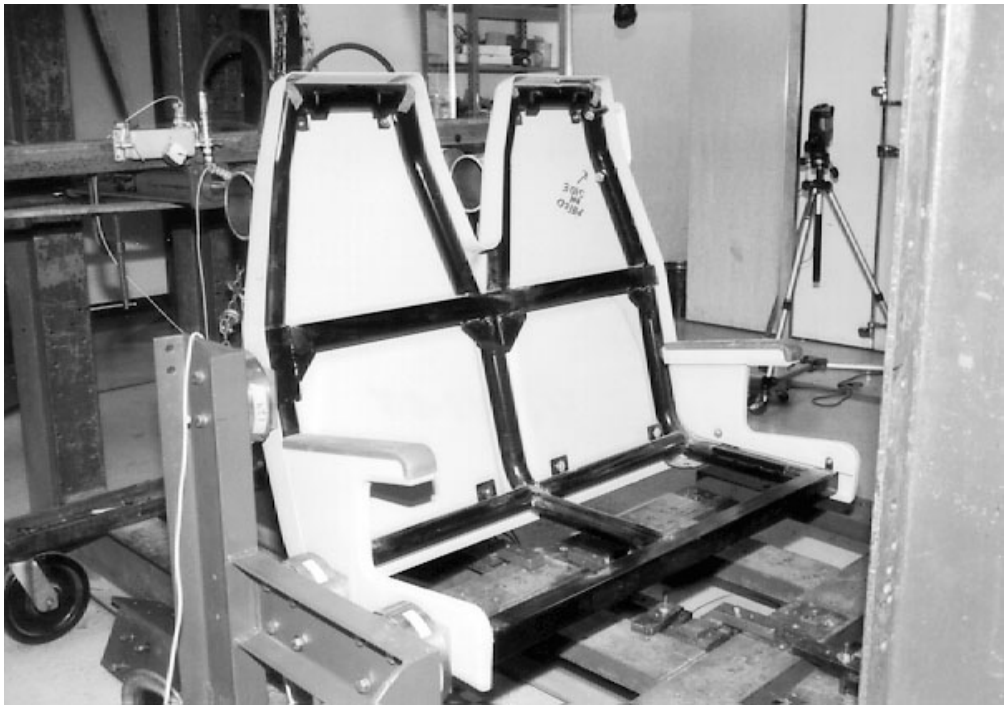

Figure 2. C-3 Commuter Seat Setup for Static Testing in the Test Frame

A single hydraulic ram and load form was used to apply a load to each position of each seat back simultaneously at a constant rate of 2 inches/minute until failure. Horizontal seat displacements were assumed to be equivalent to the displacement of the ram, which was measured using a string potentiometer. No vertical displacements were measured. The applied loads were measured using a single-axis load cell mounted between the ram and the load form. The typical static seat test setup is shown in Figure 3.

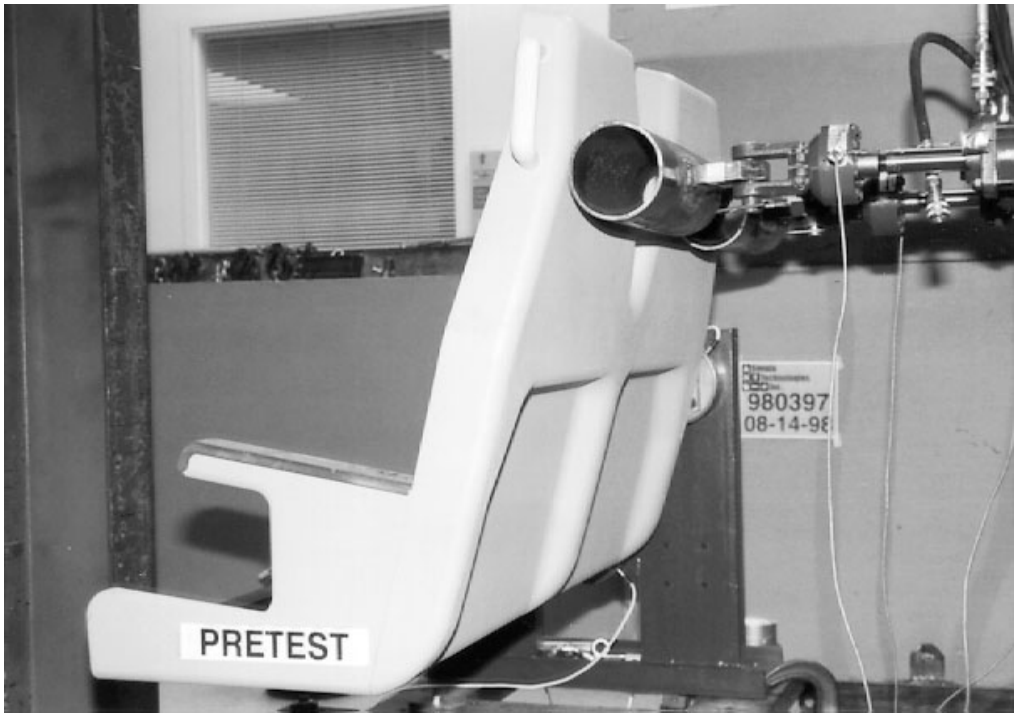

Figure 3. Typical Static Test with C-3 Commuter Seat and Hydraulic Ram

Two tests were conducted on each seat type. The first test condition represented the occupant's knees loading into the seat back. The point chosen for the C-3 was 21.0 inches from the floor, while the point for the M-Style was 21.75 inches from the floor. The second test condition was an approximation of head/chest contact with the seat back. The point chosen for both the C-3 and M-Style seats was 8 inches below the top of the seat back.

3.1.2 Walkover Seat

Static loads on the Walkover seat were applied at different locations from the other two seats. The construction of the Walkover seat suggested that the changes in seat stiffness would be greatest from one end of the seat to the other rather than from the top to the bottom of the seat back. Reflecting its name, the Walkover seat is designed with a seat back rotation mechanism that allows occupants to change the direction they face (see Figure 4).

When the Walkover seat is decelerated, the seat back travels forward from its initial position, rotating about the pivot at the base of the seat back. Free travel continues until the bi-directional ratchet (BDR) on the side of the seat swings forward and engages the upper and lower rack. From the point of engagement until the seat back has traveled to the opposite side, resistance to motion is provided by the upper rack loading the forward torsion bar. After the upper seat frame contacts the forward stop, any additional energy in the system is removed by rotating the seat base and/or deforming the seat back.

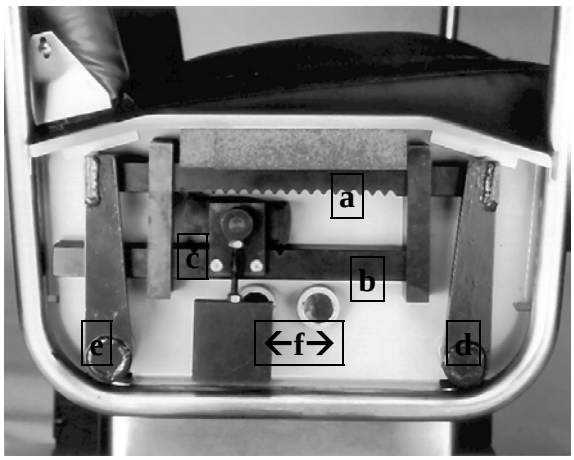

a. Upper Rack
b. Lower Rack
c. BDR
d. Forward Torsion Bar
e. Rear Torsion Bar
f. Pivot Points

Figure 4. Walkover Seat Back Rotation Mechanism

Based on factors such as the seat deceleration rate and the motion of the BDR, the seat back could be in any of several positions when the lock initially engages (see Figure 5). The location of the seat back when the lock engages has a large effect on its ability to restrain the occupant. The most effective condition is created when the seat locks immediately (see Figure 5a). The longer it takes to engage the lock, the further forward the seat back will be, and the greater the space will be for the occupant to travel forward (see Figures 5b and 5c). The outcome is a decreased effectiveness of the seat in restraining or compartmentalizing the occupant.

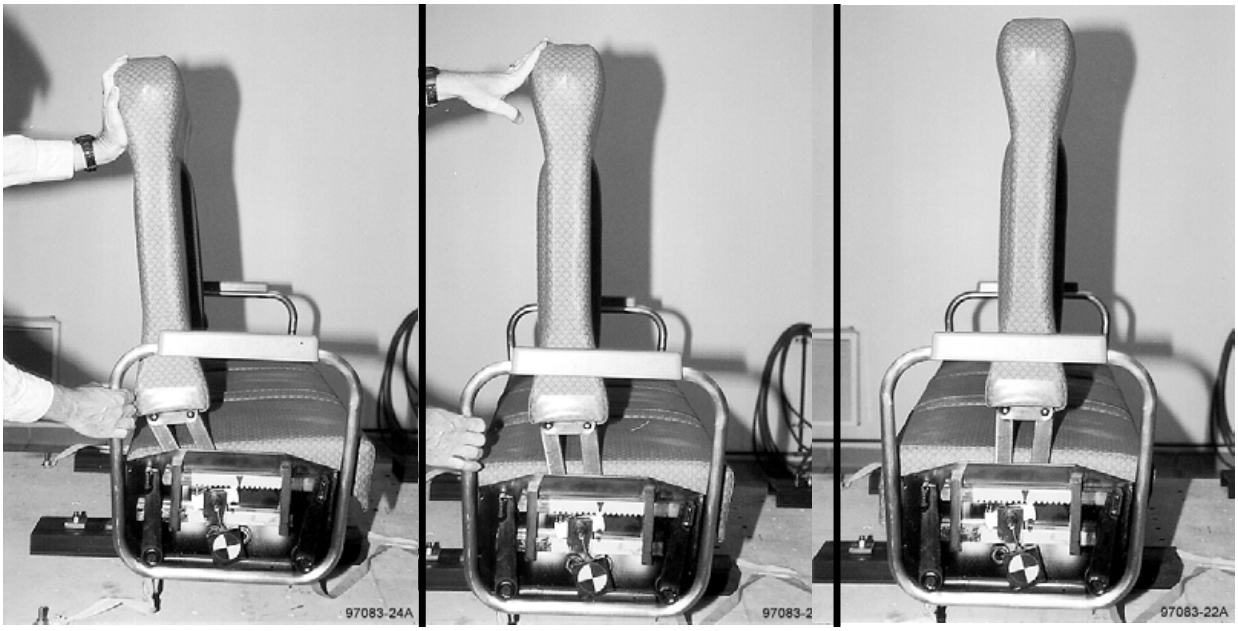

a) immediate (early) locking **b) mid-locking** **c) delayed (late) locking**

Figure 5. Three Walkover Seat Back Positions

Six tests were conducted on the Walkover seat: three to measure the torque/rotation characteristics of the locking mechanism, and three to measure seat back stiffness. For the first three tests, the seat back was removed and a clamp was installed on the guide tube. The hydraulic ram was mounted to the clamp and the inertial lock was engaged. In this first test, the lock was engaged at the point that would keep the seat back as upright and as far aft as possible, representing the condition of early locking (see Figure 6). In the second test, the seat tube was moved to the mid-point of rotation before engaging the lock (see Figure 7). In the third test, the guide tubes were moved to three-quarters of the total rotation distance before the inertial locking device was engaged, representing the late locking condition (see Figure 8). In all testing, the ram was extended at a rate of 2 inches/minute until the seat tube reached the seat stop.

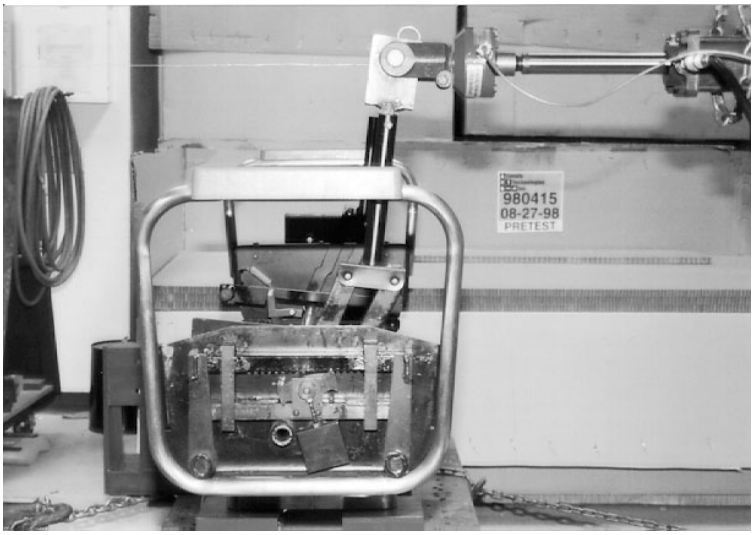

Figure 6. Walkover Seat Torque/Rotation Test: Early-Locking Position

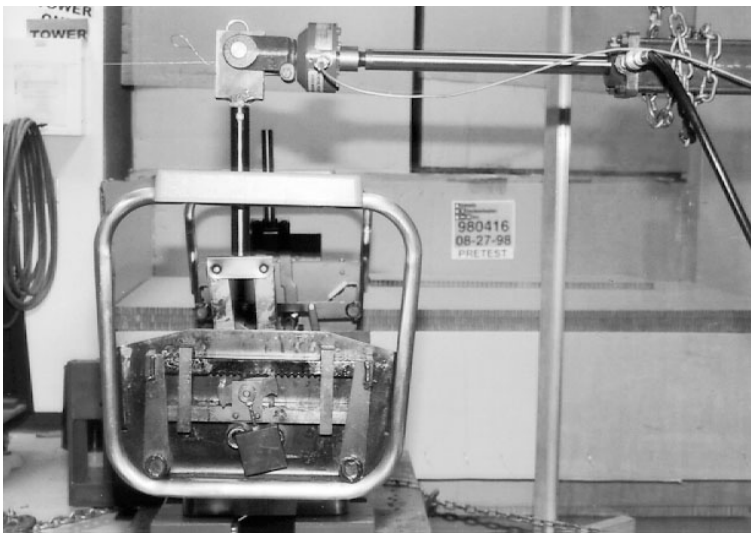

Figure 7. Walkover Seat Torque/Rotation Test: Mid-Locking Position

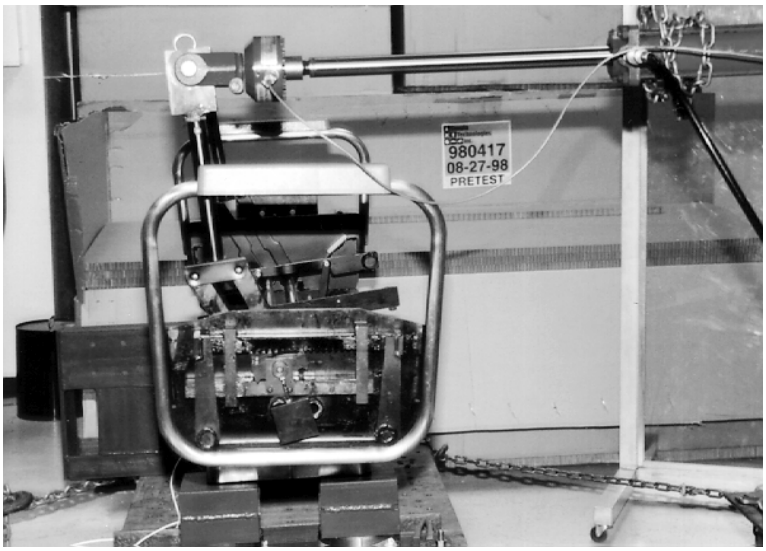

Figure 8. Walkover Seat Torque/Rotation Test: Late-Locking Position

Having established the point of force application and the ram displacement, it was then possible to develop torque/rotation tables for all three locking conditions. A computer model of the seat was developed to represent the torque/rotation characteristics for the locking condition that was typified in dynamic testing.

The stiffness characteristics of the seat back and structure were measured in the last three tests. In each test, the lock was disengaged and the seat back was placed against the forward-most (late-locking) stop. The hydraulic ram and load form were placed at a point 6.5 inches below the top of the seat back, behind one passenger seat position. A load was applied at a rate of 2 inches/minute until seat failure occurred. Horizontal displacement of each seat was assumed to be equivalent to the displacement of the ram which was measured with a string potentiometer. In the first test, the hydraulic ram applied the load to the seat back on the aisle-side of the seat. The ram was moved for each of the next two tests to apply the load behind the center and window seat positions, respectively.

3.2 DYNAMIC TEST SETUP

A total of six dynamic tests were conducted. In each of the six tests (two tests were conducted on each seat type), two seats were mounted one behind the other to represent a conventional seat configuration. While a typical seat pitch is between 32 and 34 inches, the seat pitch used in the dynamic tests was 32 inches.

The front row seat in every test was empty and the back row seat was occupied with the specified size, number, and location of unrestrained ATDs. Two ATD configurations were tested and are identified as Test Type 1 and Test Type 2. Test Type 1 consisted of all 50th-percentile male ATDs, and Test Type 2 consisted of a range of ATD sizes from 5th percentile female to 95th percentile male. The size and position of the ATDs for Test Types 1 and 2 are listed in Table 1 for each seat. A comparison of weight, seating height, and stature for each dummy is given in Table 2.

Hybrid II and III ATDs were utilized during the testing. The mass properties and dimensions are nearly the same for both models. The Hybrid III model features and articulated neck, with neck load cell, and a more biofidelic thorax that measures chest deflection.

Table 1. Occupant Positions for Dynamic Testing

Seat Type	Test Type	Test Number	Aisle Seat	Center Seat	Window Seat
C-3	1	98-0480	Hybrid II 50th	N/A	Hybrid III 50th
C-3	2	98-0481	Hybrid III 95th	N/A	Hybrid III 5th
M-Style	1	98-0507	Hybrid II 50th	Hybrid II 50th	Hybrid III 50th
M-Style	2	98-0506	Hybrid III 95th	Hybrid II 50th	Hybrid III 5th
Walkover	1	98-0508	Hybrid II 50th	Hybrid II 50th	Hybrid III 50th
Walkover	2	98-0509	Hybrid III 95th	Hybrid II 50th	Hybrid III 5th

Table 2. Comparison of Weight, Sitting Height, and Stature for Hybrid III ATDs

	5th percentile female	50th percentile male	95th percentile male
Weight (lbs.)	108.7	171.3	223
Sitting Height (inches)	31.1	34.8	36.8
Stature (inches)	59.0	68.7	73.4

The seats were rigidly mounted to the test fixture in a manner mimicking the mounting arrangement in a rail car. Tri-axial load cells were mounted at each floor and/or wall attachment point to measure the longitudinal, vertical, and lateral loads transferred from the seat to the floor or wall at that site during the dynamic loading of the seat. The location of and peak loads measured by the load cells are provided in Appendices B and C. The time history measured at each load cell is provided in Appendix F.

Prior to each test, a digitizer arm was used to locate the initial position of the aisle and window-side ATDs. The coordinates with respect to a designated origin were determined for targets located on the ATD's head, arm, hip and knee. The motion of the ATD was measured with an Image Express program which tracks the location of the targets during the dynamic sequence.

All dynamic sled tests were conducted with a triangular crash pulse of 250 msec duration and an 8 G peak acceleration occurring at approximately 125 msec. Figure 9 shows the ideal triangular crash pulse and a corresponding crash pulse that was produced during an actual sled test.

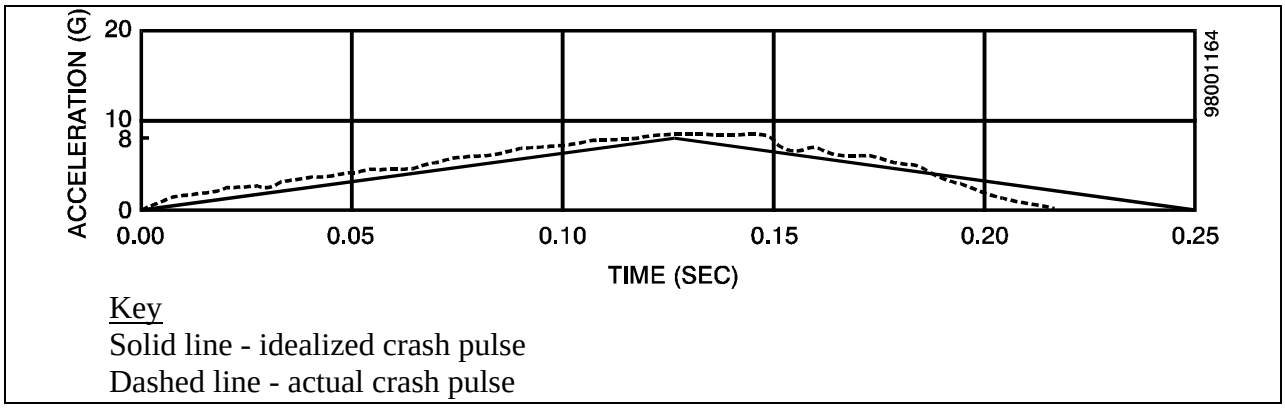

Figure 9. Rail Crash Pulse (Idealized and Actual)

A calibration test was conducted to ensure that the desired crash pulse could be achieved. This calibration test was conducted for the heaviest seat/ATD configuration. All subsequent test configurations were ballasted to attain the heaviest seat/ATD test configuration to ensure that the desired crash pulse was achieved.

The test sled was instrumented with accelerometers to measure sled deceleration with respect to time. The ATDs were instrumented to measure head, neck, chest, and femur loads.

A diagram of the deceleration sled is shown in Figure 10. The pullback sled is attached to the primary sled which is attached to the drop weight and drawn back using the winch. The pullback distance is determined by a computer program which also is used to calculate the shape and amount of the energy-absorbing honeycomb cardboard stack required to generate the specified impact velocity, peak deceleration, and onset rate. After the pullback sled is secured to the track, a pin is pulled which connects the pullback to the primary sled, and the primary sled is released. The weight drops, pulling the sled toward the honeycomb cardboard mounted on the barrier face. When the weight hits the ground, the sled will have reached the desired velocity, the tow cable drops away, and the sled coasts at a constant velocity into the impact with the honeycomb stack.

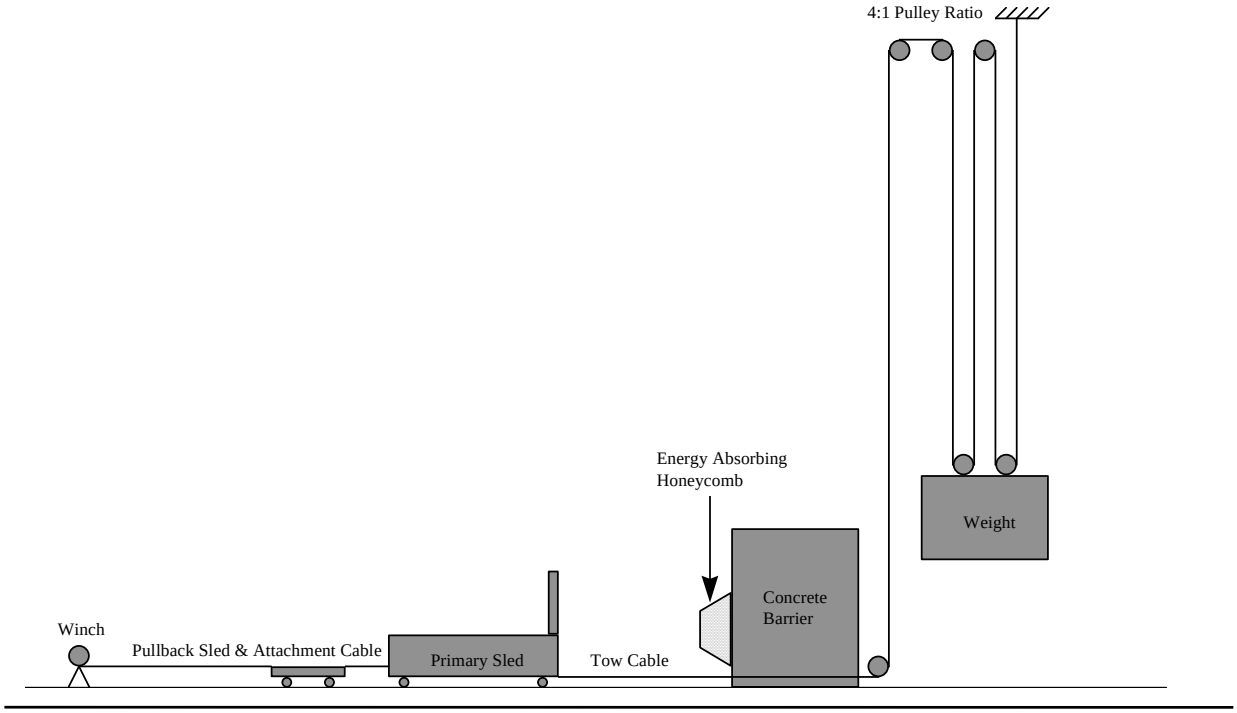

Figure 10. Deceleration Sled Schematic

Three high-speed 16-mm cameras (1000 frames/sec) and one high-speed video camera (500 frames/sec) recorded the motions of the seats and ATDs during each of the test runs. The high-speed 16-mm cameras taped the tests from the right side, left side and front. The high-speed video camera taped the tests from the right side (window side) of the seat, except in the case of the C-3 seat, which was taped from the aisle side. Still photographs were taken before and after each test to document deformations in the seat structure and changes in ATD positions.

4. QUASI-STATIC TEST RESULTS

The conducting static tests were conducted to determine the stiffness characteristics of the seats and the loads that developed at the attachment points. This information was incorporated into the seat/occupant computer models and used to predict the dynamic responses of the seats during testing. The seat stiffness characteristics were measured when the load was independently applied to the upper seat back and the lower seat back. In the case of the Walkover seat, the stiffness was measured when the load was applied along the length of the seat back (aisle-side to window-side). Loads were also measured with load cells at the seat attachments. Seat stiffness curves and attachment loads are provided in Appendix B.

4.1 SEAT STIFFNESS CHARACTERISTICS

4.1.1 C-3 Seat

The results of the two tests conducted on the C-3 seat suggested that the window side of the seat was stiffer than the aisle side of the seat.

Upper Seat Back Loading - Loading the C-3 upper seat back caused the entire seat to rotate forward and the frame at the wall attachment to buckle. Figures 11 and 12 show these two outcomes of the test.

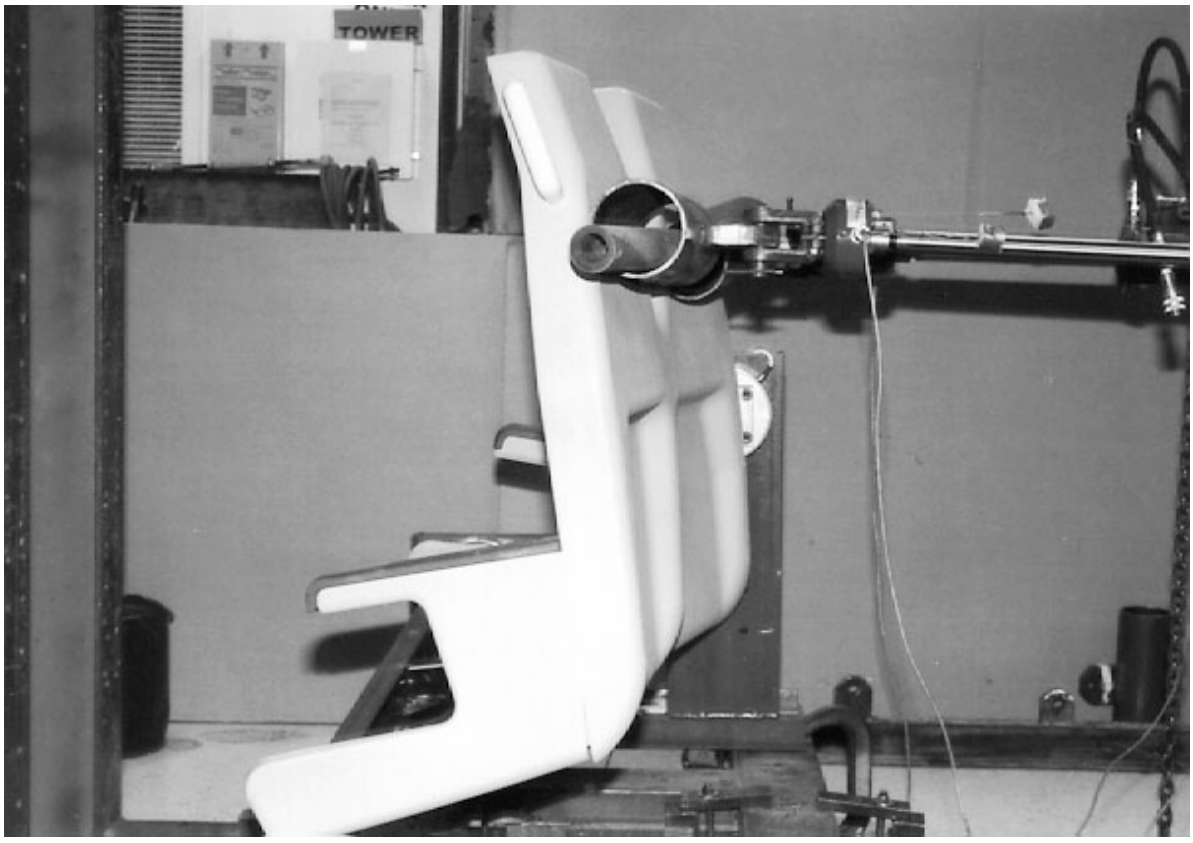

Figure 11. C-3 Upper (Post-test) - Seat Rotated Forward

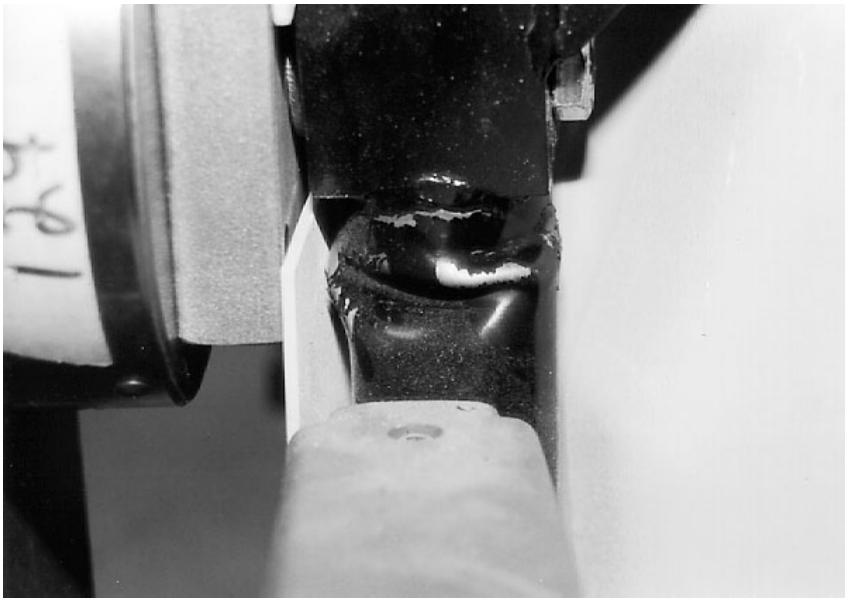

Figure 12. C-3 Upper (Post-test) - Buckled Frame at Wall Attachment Point

Lower Seat Back Loading - Loading the C-3 lower seat back caused the plastic shroud to crack as the load form penetrated through the seat back. Both cushions popped off at the top attachment points. Figure 13 shows this outcome of the test.

Figure 13. C-3 Lower (Post-test) - Plastic Shroud Cracked and Back Cushions Detached

4.1.2 M-Style Seat

The results of the two tests conducted on the M-Style seat suggested that, unlike the other two seat types, the aisle side, rather than the window side, of the seat was stiffer due to the strong pedestal attachment.

Upper Seat Back Loading - Loading the M-Style upper seat back caused the following to happen: (1) the entire seat rotated forward, (2) the plastic shroud buckled at the armrest, and (3) the square beam attachments buckled forward. Figures 14 and 15 show these outcomes.

Lower Seat Back Loading - Loading the M-Style lower seat back caused the pedestal and square beam attachments to buckle, the plastic shroud to crack, and the seat cushions to pop out. Figures 16 and 17 show these outcomes.

Figure 14. M-Style Upper (Post-test) - Seat Rotated Forward and Plastic Shroud Buckled at Armrest

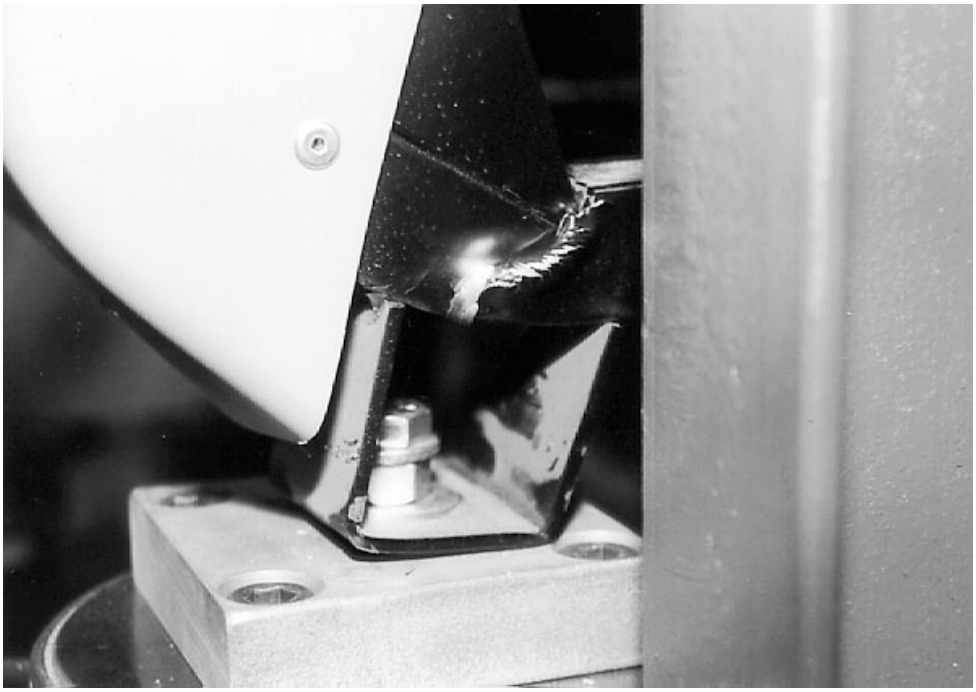

Figure 15. M-Style Upper (Post-test) - Square Beam Attachment Buckled

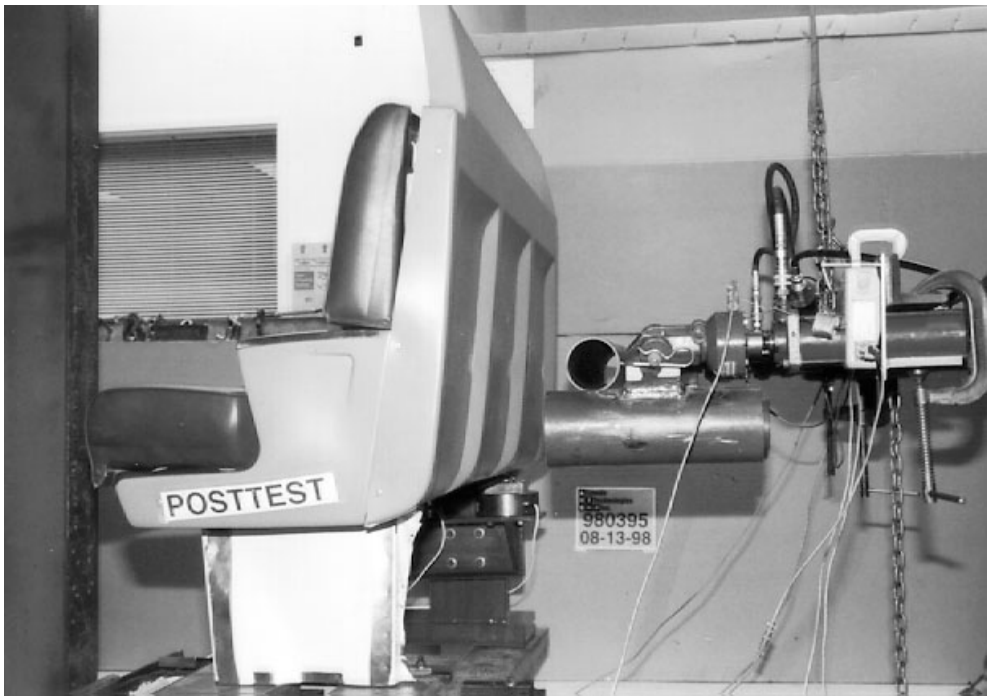

Figure 16. M-Style Lower (Post-test) - Pedestal Attachment Buckled and Seat Cushions Detached

Figure 17. M-Style Lower (Post-test) - Plastic Shroud Cracked

4.1.3 Walkover Seat

All static tests on the Walkover seat were conducted with the seat back rotated forward to the late-locking position. The results of the tests suggested that the aisle and window sides of the seat were stiffer than the middle seat because there is nothing to support the center portion of the seat back.

Aisle Side Seat Back Loading - Loading the Walkover aisle-side seat back caused the seat back to bend slightly forward from its stopped position against the torsion bar. Figure 18 shows this outcome.

Middle Seat Back Loading - Loading the Walkover middle seat back caused the seat back to buckle quite severely. Figure 19 shows this outcome.

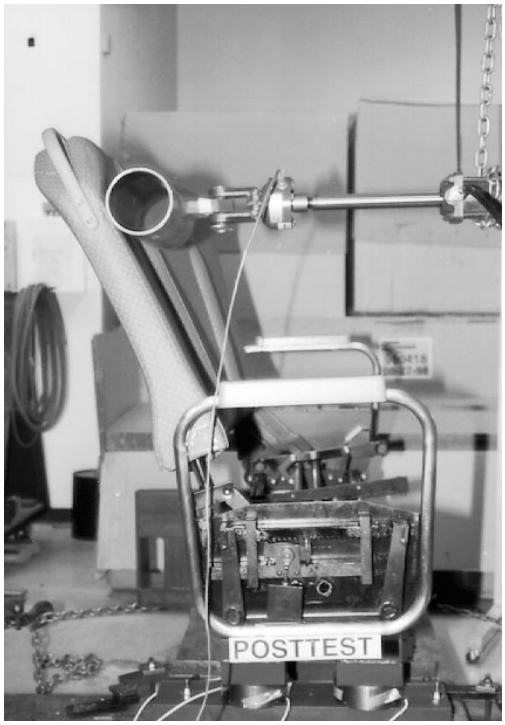

Figure 18. Walkover Seat - Aisle (Post-test) - Seat Back Bends Slightly Forward

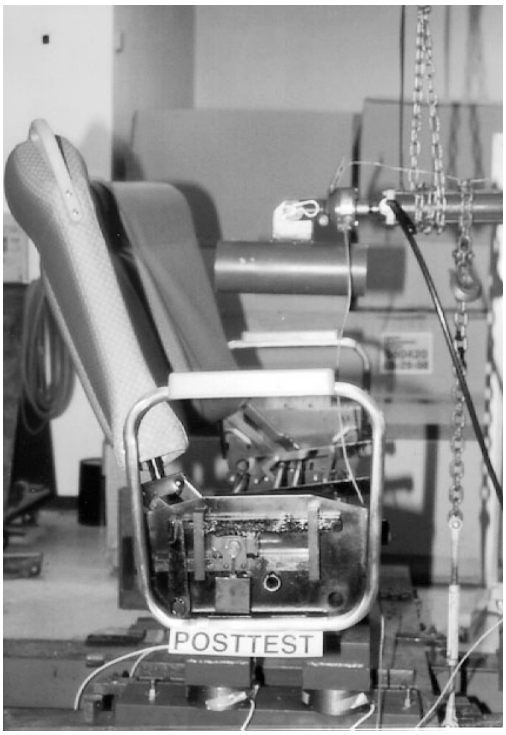

Figure 19. Walkover Seat - Middle (Post-test) - Seat Back Bows Forward in the Middle

Window-Side Seat Back Loading - Loading the Walkover window-side seat back caused the seat back to bend slightly forward from its stopped position against the torsion bar. Figures 20 shows this outcome.

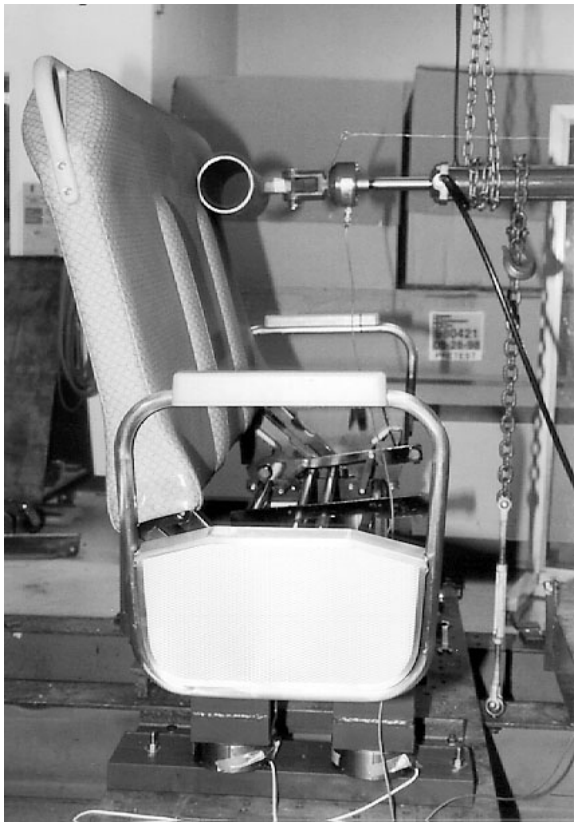

Figure 20. Walkover Seat - Window (Post-test) - Seat Back Bends Slightly Forward

4.2 SEAT LOAD CELL PEAK VALUES

Peak loads were measured from the load cells that interfaced the seats and the test fixture in each static test. These loads, provided in Appendix B, were used to build the computer models of each seat. Similar loads were measured at the attachments during the dynamic tests.

5. DYNAMIC TEST RESULTS

The purpose for conducting dynamic testing was to observe the seat/occupant response to dynamic loading conditions. An in-line train collision environment was described by a triangular pulse of 250 msec in duration with an 8-G peak. The recorded pulse from each test is printed in Appendix C. All seats were separated by a 32-inch pitch and the rear seat was occupied with unrestrained ATDs. Two tests were conducted for each seat type and differed by ATD type, size, and location. The following two seat/occupant scenarios were tested:

- Type 1 Test - Hybrid III 50th-percentile male in the window seat, and Hybrid II 50th percentile male in the middle and aisle seats (see Figure 21).

- Type 2 Test - Hybrid III 5th-percentile female in the window seat, Hybrid III 50th-percentile male in the middle seat, and Hybrid III 95th-percentile male in the aisle seat (see Figure 22).

5.1 DYNAMIC TEST EVALUATION CRITERIA

In anticipation of dynamic testing, the following three test outcomes were defined as the desirable indicators for seats demonstrating an acceptable level of structural integrity and passenger safety:

- All seat components should remain attached (or should not become free-flying objects).

- Passengers should remain compartmentalized between the two seat rows.

- Occupant injury loads should be within acceptable injury criteria (see Table 2).

Seat component attachment was determined by observing which, if any, seat components detached from the seat's main frame. Seat-to-car attachment, however, could not be determined, because the seats were rigidly mounted to the test fixture. Load cells placed between the seat and test fixture measured the forces that developed at the attachment points. Information about the rail car structure(s), to which the seats would be installed, can then be used to help determine whether the seat/floor or seat/wall attachments are strong enough to support the loads in a collision environment. The peak seat attachment loads measured during dynamic testing are provided in Appendix C, and the load curves are compared to the corresponding modeling output curves in Appendix F.

5.2 OCCUPANT INJURY CRITERIA

Table 3 lists the injury criteria that were used to assess the measured loads in the ATDs. The criteria for the 95th-percentile male are identified in Reference 1. The criteria for the 5th-percentile female were identified from the rule modifying the Federal Motor Vehicle Safety Standard (FMVSS) 208, recently presented by the National Highway Traffic Safety Administration (NHTSA). This NHTSA rule introduces the use of neck injury criteria for both the 5th-percentile female and 50th-percentile male. The remaining criteria for the 50th-percentile male (HIC, chest, and femur) were identified from the current FMVSS 208 Standards (Reference 2). The same criteria for HIC and femur are required by the Federal Aviation Administration (FAA) (Reference 3). Appendix E provides a comparison of normalized injury data to the corresponding injury criteria, and Appendix F compares the test data to the corresponding modeling output curves.

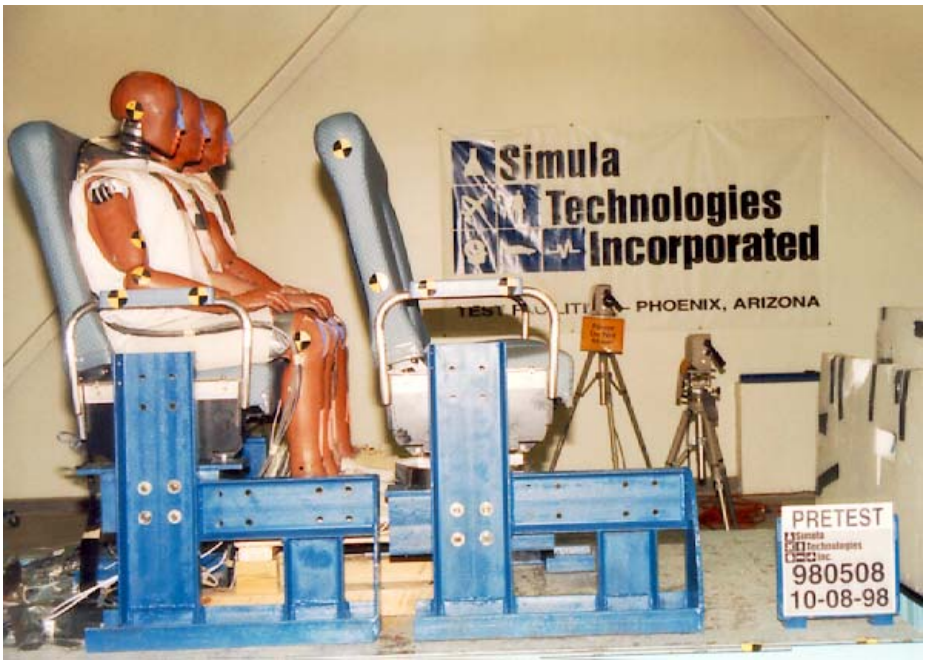

Figure 21. Type 1 Test - All 50th-Percentile ATDs - Hybrid III 50th-Percentile Male in Window Seat, Hybrid II 50th-Percentile Male in Middle Seat, and Hybrid II 50th-Percentile Male in Aisle Seat

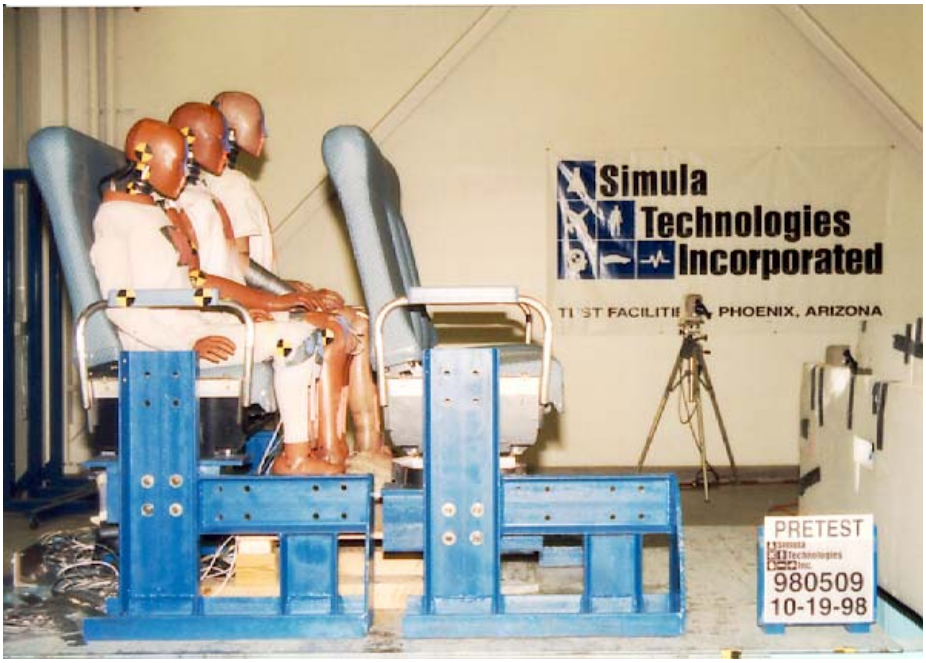

Figure 22. Type 2 Test - 95th-Percentile Male, 50th-Percentile Male, and 5th-Percentile Female ATDs -Hybrid III 5th-Percentile Female in Window Seat, Hybrid III 50th-Percentile Male in Middle Seat, and Hybrid III Male 95th-Percentile in Aisle Seat

Outcomes of the dynamic testing revealed inconsistencies in the neck results. Specifically, while the neck in most cases appeared to go into extreme extension (head tips backward toward the back), the data

indicated that the peak moments were occurring in flexion. A study independent from this program was conducted to investigate the reason for this apparent discrepancy.

Table 3. Injury Criteria

	5th (Female)	50th (Male)	95th (Male)
HIC	1,000[4]	1,000[2][3]	1,000([1])
Neck Fx (lb)	+/- 438[4]	+/- 697[4]	+/-856([1])
Neck Fz (lb)	+468 / -567[4]	+742 / -900[4]	+910/-1,104([1])
Neck My (ft-lb)	+70 / -21[4]	+140/-42[4]	+190/-58([1])
Chest (G)	60[4]	60[2]	60([1])
Femur (lb)	-1,530[4]	-2,250[2][3]	-2,594([1])

Notes:
(1) – Reference 1
(2) – Reference 2
(3) – Reference 3
(4) – FMVSS Rule

Preliminary indications suggest that the neck in the ATD assumes an S-shape upon impact and is actually in flexion at the top of the neck where the load cell is located. Meanwhile, the lower part of the neck, which can be easily observed on film, is in extension. While the automotive industry recently has been mandating the use of neck injury criteria to certify their vehicles, it is possible that they may have not observed the phenomenon experienced here because of the lack of visibility during their testing. Most of their tests involve airbags, which typically obscure a clear view of the neck response and its correlation to the loads that are measured.

5.3 DYNAMIC SLED TEST RESULTS

The seat structures deformed similarly in dynamic testing as they did in static testing, but with more severe outcomes. All the test results are compared to the projected corresponding computer modeling output and are provided in Appendix F.

5.3.1 C-3 Seat

In both tests of the C-3 seat, the seat stayed intact and the front seat's back cushions detached from the upper portion of the seat back (Figures 23 and 24). The lower portion of the front seat's back cushions remained attached. The results suggest that the seat is very stiff and deforms very little under dynamic loading conditions. This stiff seat design was instrumental in compartmentalizing the occupant. However, due to its rigidity, the 50th-percentile male seated in the window seat in the Type 1 Test produced neck shear loads that exceeded the injury criteria (Table 4). The 5th-percentile female also experienced neck loads (shear and flexion) and femur loads that exceeded the injury criteria (Table 5). Hybrid II ATDs are not equipped to measure neck forces andmoments, thus they are listed in the following tables as "not recorded."

Table 4. C-3 Seat/Occupant Loads - Type 1 Test (98-0480)

	Criteria	H2II 50th Male (Aisle)	HIII 50th Male (Window)
HIC	1,000	562	846
Neck Fx (lb)	+/-697	not recorded	**-807**
Neck Fz (lb)	+742/-900	not recorded	576
Neck My (ft-lb)	+140/-42	not recorded	116
Chest (G)	60	32	28
Femur (lb)	-2,250	-1,237 R	-1,024 L

Figure 23. C-3 Seat Post-test - Type 1 Test (98-0480)

Table 5. C-3 seat/Occupant Loads - Type 2 Test (98-0481)

	HIII 95th Male (Aisle)		HIII 5th Female (Window)	
	Criteria	**Recorded Loads**	**Criteria**	**Recorded Loads**
HIC	1,000	481	1,000	570
Neck Fx (lb)	+/-856	not recorded	+/-438	**-438**
Neck Fz (lb)	+910/-1,104	not recorded	+468/-567	-149
Neck My (ft-lb)	+190/-58	not recorded	+70/-21	**+92**
Chest (G)	60	34	60	26
Femur (lb)	-2,594	-789	-1,530	**-2,084**

Figure 24. C-3 Seat Post-test - Type 2 Test (98-0481)

5.3.2 M-Style Seat

In both tests of the M-Style seat, the seats stayed intact; however, *all* the cushions from both seats completely detached and became hazardous flying objects during the collision (see Figures 25 and 26). The M-Style seat is a more compliant seat than the C-3 seat, which was evidenced by the reduction in the injury loads measured in the ATDs (Table 6). Only one injury load in the 5th-percentile female ATD exceeded the injury criteria, and this criteria limit was exceeded by only 2 foot-pounds (Table 7). While the reduced seat stiffness correspondingly reduced the injury loads, the risk against occupant compartmentalization increased. The 50th-percentile ATD in the aisle seat (Type 1 Test) landed on the

test lab floor (Figure 25). However, the ATD did not catapult over the front row seat; therefore, the seat could possibly be considered to have compartmentalized the occupants.

Table 6. M-Style Seat/Occupant Loads - Type 1 Test (98-0507)

	HII 50th Male (Aisle)		HII 50th Male (Middle)		HIII 50th Male (Window)	
	Criteria	**Recorded Loads**	**Criteria**	**Recorded Loads**	**Criteria**	**Recorded Loads**
HIC	1,000	231	1,000	219	1,000	356
Neck Fx (lb)	+/-697	NR	+/-697	NR	+/-697	-207
Neck Fz (lb)	+742/-900	NR	+742/-900	NR	+742/-900	+268
Neck My (ft-lb)	+140/-42	NR	+140/-42	NR	+140/-42	+32
Chest (G)	60	15	60	18	60	20
Femur (lb)	-2,250	-694	-2,250	-884	-2,250	-819

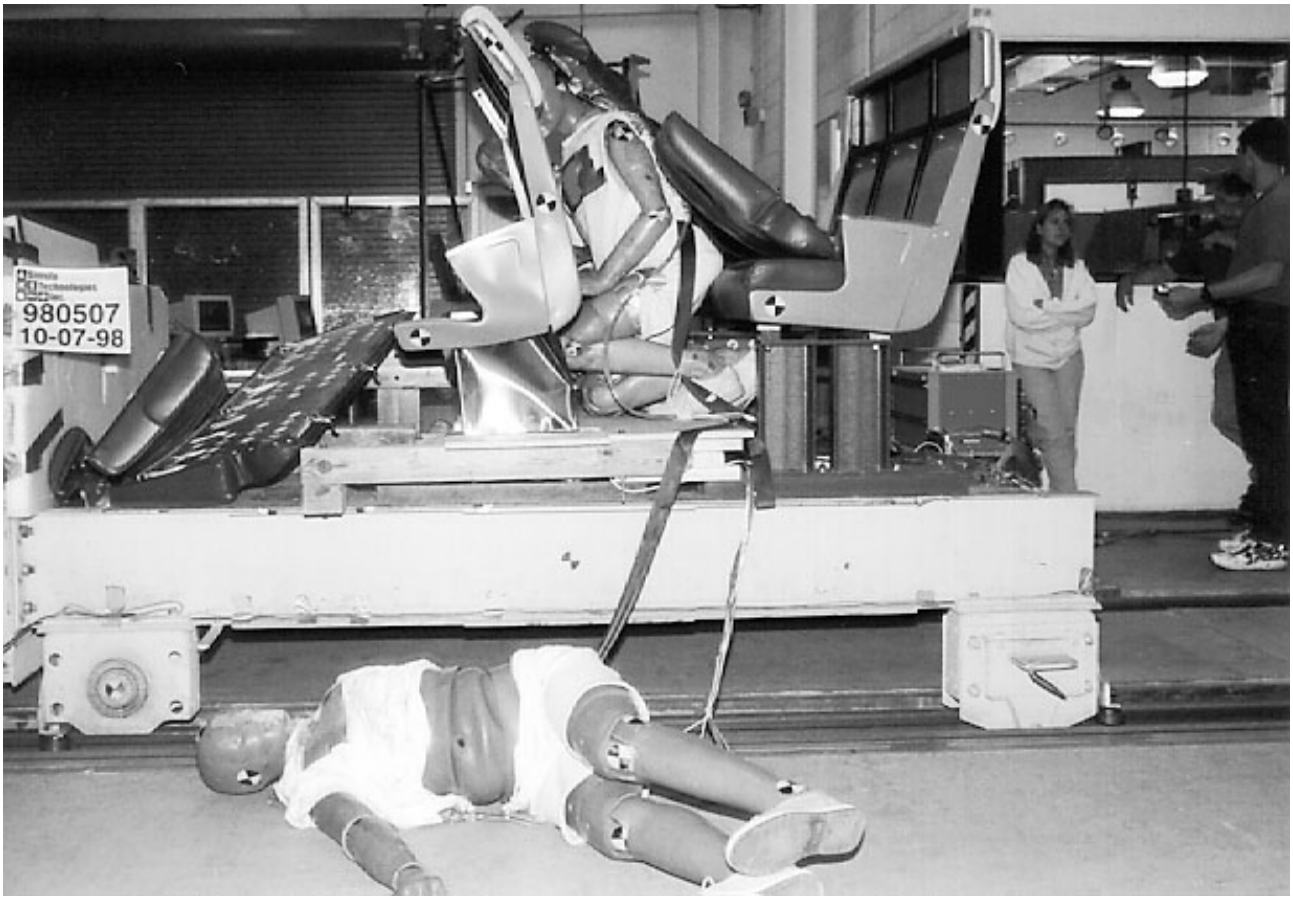

Figure 25. M-Style Seat Post-test - Type 1 Test (98-0507)

Table 7. M-Style Seat/Occupant Loads - Type 2 Test (98-0506)

	HIII 95th Male (Aisle)		HIII3 50th Male (Middle)		HIII 5th Female (Window)	
	Criteria	Recorded Loads	Criteria	Recorded Loads	Criteria	Recorded Loads
HIC	1,000	164	1,000	217	1,000	738
Neck Fx (lb)	+/-856	-459	+/-697	NR	+/-438	-333
Neck Fz (lb)	+910/-1,104	+462	+742/-900	NR	+468/-567	+272
Neck My (ft-lb)	+190/-58	+95	+140/-42	NR	+70/-21	**+72**
Chest (G)	60	26	60	11	60	33
Femur (lb)	-2,594	-554	-2,250	-622	-1,530	-650

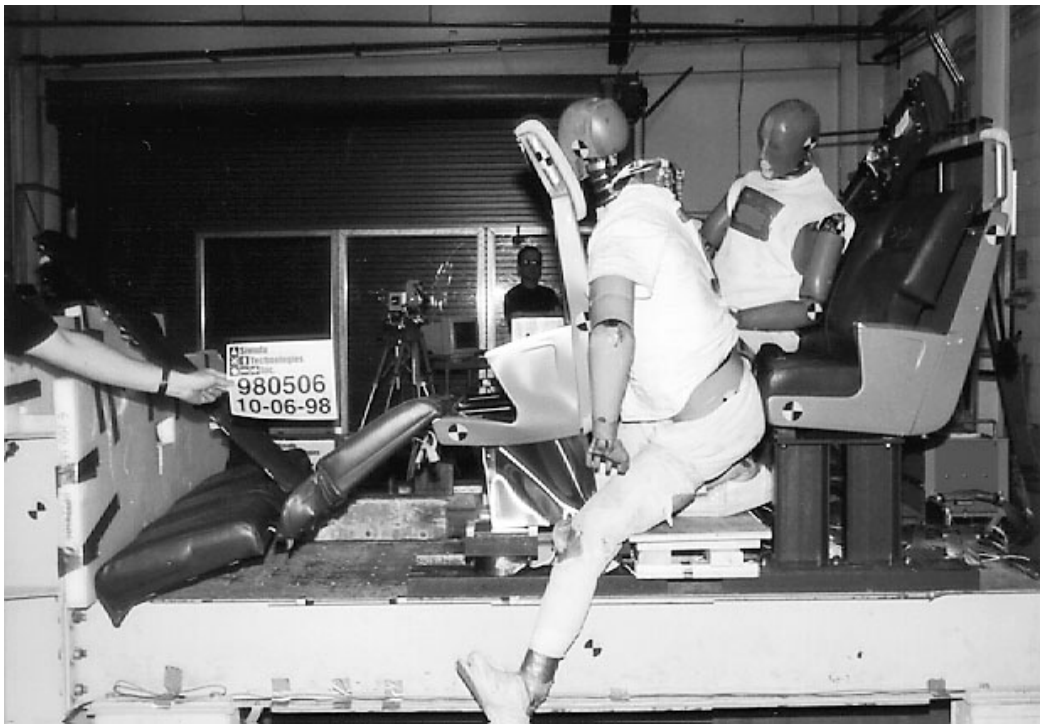

Figure 26. M-Style Seat Post-test - Type 2 Test (98-0506)

5.3.3 Walkover Seat

In both tests of the Walkover seats, the seats stayed intact and the cushions remained attached (Figures 27 and 28). The Walkover seat back rotated forward before locking in place, thereby increasing the distance through which the occupants could travel. As in all the tests, each ATD was tethered with a strap from a point at its lower lumbar spine to the seat. The purpose for tethering the ATDs was to protect them from

extensive damage (such as broken clavicle bones, knees, sensor damage, etc.) that could occur if the ATDs flew free of the seats and impacted stationary objects. It appears that the ATD trajectory may have been limited by the length of the tether and that untethered ATDs could possibly have catapulted over the seat back and been thrown forward beyond the forward seat.

The ATD's knees impacted the bottom cushion, bending the attachment clips, and causing the ATD and the cushion to continue forward. As the ATD's knees loaded the bottom cushion, the upper body rotated forward and impacted the upper seat back which continued to move forward. This motion caused the ATD to extend its knees as the upper torso led the trajectory. The upper seat back bent somewhat as the ATDs flailed on top of it. The large deformation of the seat back, and its movement, helped keep the measured injury loads to a minimum (Tables 8 and 9).

Table 8. Walkover Seat/Occupant Loads - Type 1 Test (98-0508)

	HII 50th Male (Aisle)		HII 50th Male (Middle)		HIII 50th Male (Window)	
	Criteria	Recorded Loads	Criteria	Recorded Loads	Criteria	Recorded Loads
HIC	1,000	125	1,000	51	1,000	44
Neck Fx (lb)	+/-697	NR	+/-697	NR	+/-697	-430
Neck Fz (lb)	+742/-900	NR	+742/-900	NR	+742/-900	-342
Neck My (ft-lb)	+140/-42	NR	+140/-42	NR	+140/-42	+97
Chest (G)	60	15	60	16	60	12
Femur (lb)	-2,250	-722	-2,250	-814	-2,250	-762

Figure 27. Walkover Seat Post-test - Type 1 Test (98-0508)

Table 9. Walkover Seat/Occupant Loads - Type 2 Test (98-0509)

	HIII 95th Male (Aisle)		HIII 50th Male (Middle)		HIII 5th Female (Window)	
	Criteria	**Recorded Loads**	**Criteria**	**Recorded Loads**	**Criteria**	**Recorded Loads**
HIC	1,000	142	1,000	24	1,000	46
Neck Fx (lb)	+/-856	-524	+/-697	NR	+/-438	-267
Neck Fz (lb)	+910/-1,10	-384	+742/-900	NR	+468/-567	-253
Neck My (ft-lb)	+190/-58	128	+140/-42	NR	+70/-21	37
Chest (G)	60	11	60	10.4	60	13
Femur (lb)	-2,594	-598	-2,250	-751	-1,391	-508

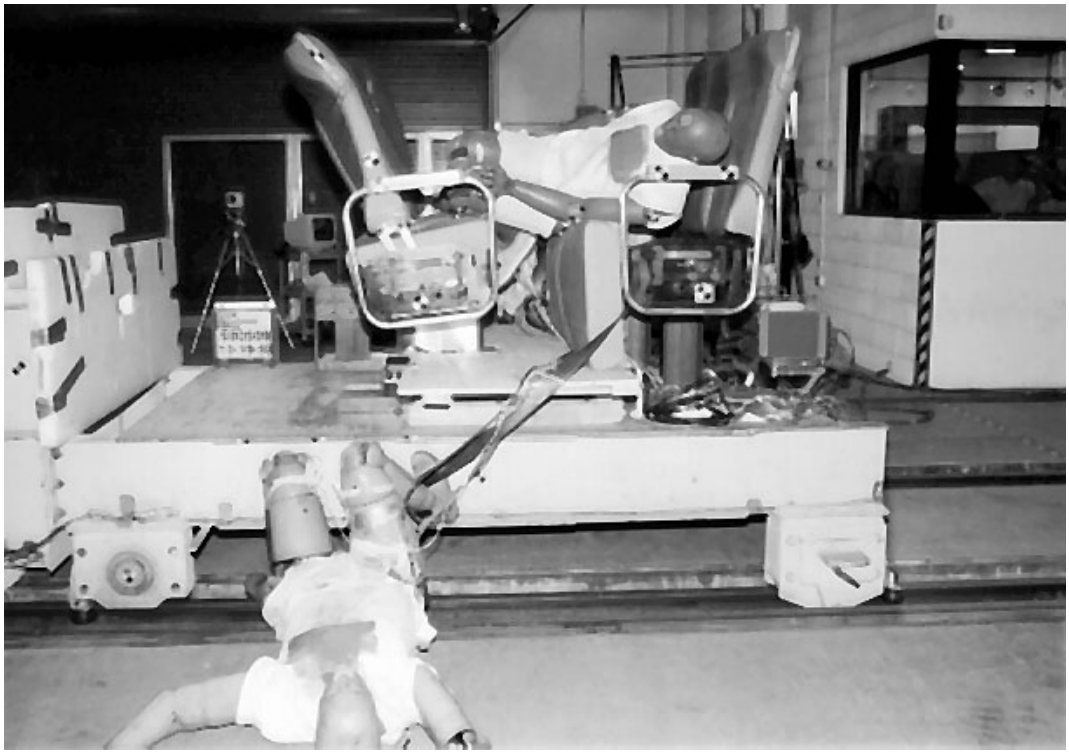

Figure 28. Walkover Seat Post-test - Type 2 Test (98-0509)

6. SEAT/OCCUPANT MODELING RESULTS

6.1 SEAT/OCCUPANT MODELING

The purpose for developing seat/occupant models was to help predict the outcome of the dynamic tests; to help determine the most appropriate dynamic test parameters to incorporate; and to begin devising a useful seat design tool. Predicting the outcome of the tests helped to determine which parameters were most critical, and helped to eliminate concern about some seat/occupant configurations so that more practical configurations could be tested.

6.1.1 MADYMO as the Simulation Tool

Computer simulations of the dynamic testing were developed and implemented using the Mathematical Dynamic Model (MADYMO) analysis program from software supplier TNO, which is based in the Netherlands. MADYMO is a general-purpose program based on the principles of gross body motion and utilizing rigid masses, springs, and dampers. The rigid masses can be connected through the use of joints to allow the creation of complex systems. Ellipsoids and planes are defined to represent contact surfaces such as the seat back and seat cushion in addition to the surfaces of the Hybrid II and Hybrid III ATDs. Contacts between the ATDs and the various seat components were handled with the use of force-deflection characteristics obtained from quasi-static testing.

6.1.2 The Occupant Model

All the occupants modeled in this simulation represented the typical ATDs used by the automotive and airline industries. Specifically, the ATDs modeled were the Hybrid III 5th-percentile female, 50th-percentile male, and 95th-percentile male, and the Hybrid II 50th-percentile male. These ATD computer models were built and validated by TNO. The Hybrid family of ATDs has been designed, simulated, and validated for use in the study of frontal impacts for both restrained and unrestrained conditions. All the ATDs, regardless of size, are configured identically with 32 elements representing the primary body regions and 51 ellipsoids defining the surfaces of the ATD.

6.1.3 The Seat Model

Each seat was modeled to represent the dimensions, stiffnesses, and contact surfaces of the seats that were tested. The most complex of the seats was the Walkover seat, due to the number of moving components it contained. The force-deflection characteristics for each seat were obtained from the quasi-static tests and were incorporated into each respective model.

C-3 seat - The C-3 seat computer model is shown on Figure 29. The contact surfaces of the seat back were broken into two sections to represent the upper and lower contact regions of the seat. The upper portion of the seat back was defined with hyperellipsoids that captured the curvature of the seat, while the lower region was defined with a plane.

M-Style Seat - The M-Style seat computer model is shown on Figure 30. The contact surfaces on the seat back were defined into three sections. The knee contact was defined with one set of planes, while the head/chest contact area was defined with two planes. Two planes also were required for the upper seat back to capture the change of direction created by the crash pad.

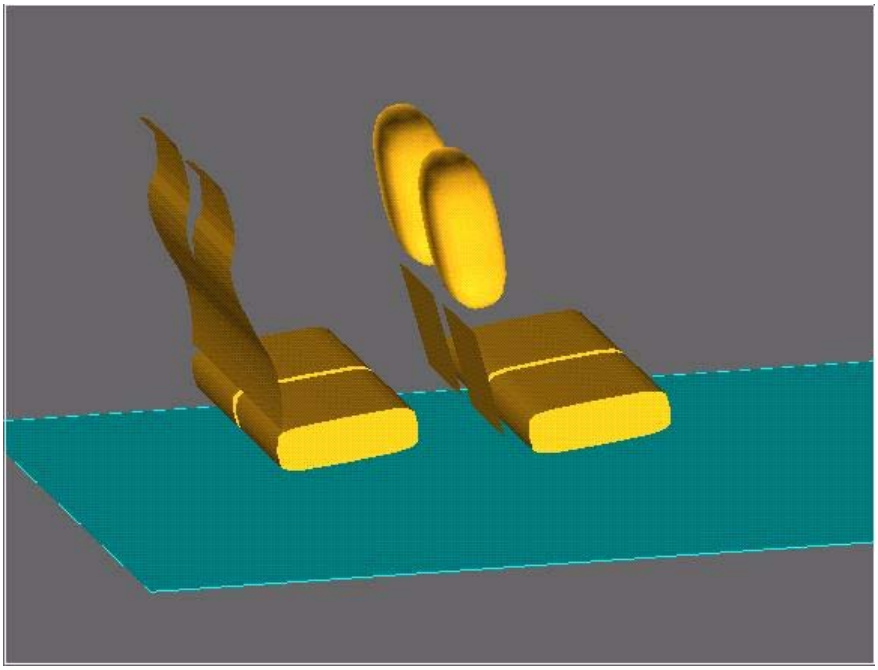

Figure 29. C-3 Seat Computer Model

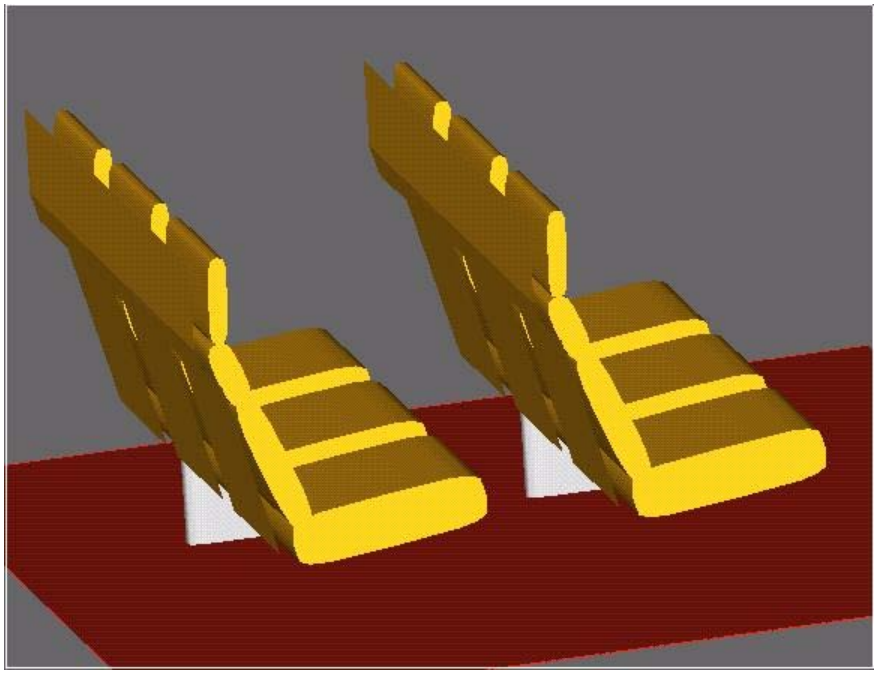

Figure 30. M-Style Seat Computer Model

Walkover Seat - The Walkover seat is shown on Figure 31. The contact surfaces of this seat were defined by several sections. The bottom (seat pan) cushion and the entire middle section of the seat back were defined by hyperellipsoids. The upper and lower sections of the seat back were defined using planes. The

rotation mechanism of the Walkover was defined as a series of one-degree-of-freedom revolute joints. The proper location of each of the single-degree-of-freedom joints was determined from CAD data provided by the seat manufacturer. A torque/rotation resistance was applied to one of these joints (selected for its proper location) to represent the locking mechanism. These torque/rotation resistance data were obtained from the nondestructive static testing on the seat rotation mechanism, which was conducted, in addition to the static tests conducted, on the complete seat to obtain the force-deflection characteristics for the seat back.

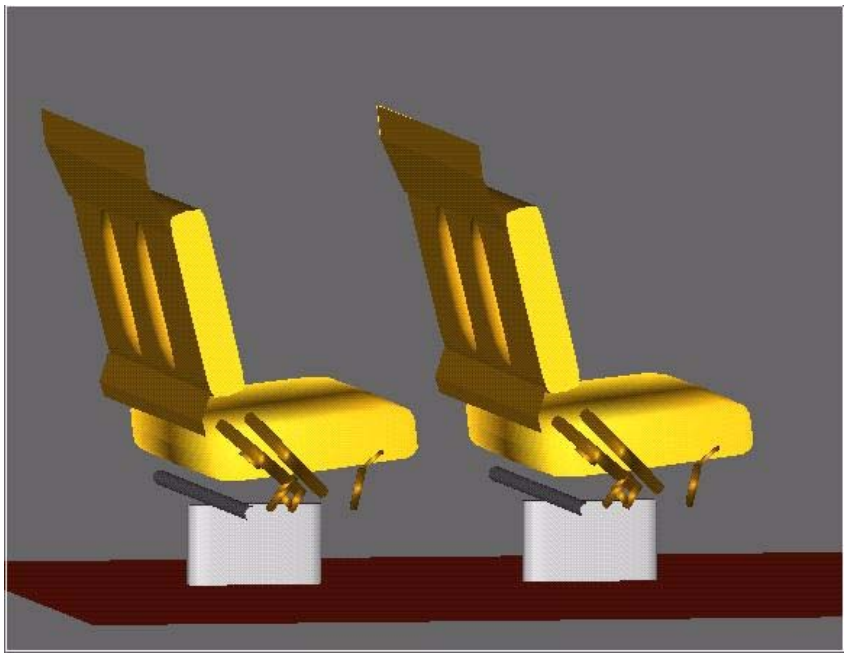

Figure 31. Walkover Seat Computer Model

6.2 PARAMETRIC ANALYSIS - PARAMETERS

Once the initial seat/occupant models were built, a series of computer runs were conducted to help understand the effects of altering specific parameters of the model on the forces and accelerations experienced by the occupant. The goal of this parametric analysis was to help determine which combinations should be considered and incorporated in the dynamic sled tests to ensure adequate occupant protection, under probable seating combinations. The three parameters chosen for evaluation were crash pulse, seat pitch, and ATD size and seating positions.

6.2.1 Crash Pulse

Two crash pulses were evaluated. Both crash pulses were 250-msec, triangular pulses, but one peaked at 7 G and the other peaked at 8 G. The 7-G peak pulse was included in the matrix simply to confirm the logical assumption that the higher crash pulse produced higher injury loads. This assumption was confirmed, and can be observed in the test results presented in Appendix D.

6.2.2 Seat Pitch

The seat pitch is the distance from one point on a seat to the same point on a second seat located in front of the first seat. The distance between any two seat rows affects the impact velocity of the occupant seated in the rear seat row. In any given impact involving a seat and an occupant striking the seat from behind, the kinetic energy absorbed by the seat will vary as a function of the velocity of the occupant relative to the seat. As the seat pitch is decreased, the relative velocity between the occupant and the seat at the time the occupant impacts the seat back will also decrease. Reducing the occupant's velocity change results in less kinetic energy to be dissipated in the secondary impact, as well decreased deceleration levels, force levels, and injury potential. An increase in seat pitch will create the opposite effect: the relative velocity between the occupant and seat will increase causing an increase in kinetic energy to be absorbed by the seat. Higher deceleration/force levels and injury indices result from longer seat pitches. The seat pitches chosen for this parametric analysis were originally set at 34, 37, and 48 inches to evaluate the influence of seat pitch on occupant injury measurements.

6.2.3 Anthropomorphic Test Dummies

ATD size and location were selected to cause the maximum loading on the seat (testing seat strength) or to increase the risk of producing high injury loads. For instance, three 95th-percentile Hybrid III ATDs in an impact will severely test the integrity of the seat, but not likely result in severe occupant injury values due, in part, to the probability of large amounts of seat deformation (and energy-absorption). On the other hand, three 5th-percentile Hybrid IIIs in the same seat may result in high injury values but not test the structural integrity of the seat. For the three-passenger seats, the total number of possible ATD seating combinations, including the possibility of two empty positions, is 63. For the two-passenger seat, the total number of combinations, assuming the possibility of one empty seat, is 15. Rather than conducting a parametric analysis for all 63 combinations for each seat type, a total of 13 conditions were analyzed: seven conditions for the three-place seats and six conditions for the two-place seat.

Occupant sizes and positions for the analysis were chosen to evaluate the following conditions:

- Average, baseline condition (all 50th-percentile ATDs).
- Greater risk to occupant safety, such as a 5th-percentile female loading the stiffest region of the seat, which is typically the window side. No other occupants would be present.
- Greater risk to seat integrity, as created with 95th-percentile males in all seats.

The configuration matrix used for the analysis is shown in Table 10. The complete parametric evaluation consisted of each listing in Table 9 plus the same configurations at seat pitches of 37 inches and 48 inches.

6.3 PARAMETRIC ANALYSIS – RESULTS

The results of the simulations for each seat type are listed in Tables D1, D2, and D3 in Appendix D. These tables list the occupant injury loads for each of the seat/occupant MADYMO models run using the parameters described above. The primary occupant injury criteria that were evaluated include the 36-msec HIC, 3-msec chest deceleration, and axial femur loads. Neck loads were recorded in the models, and are compared to injury thresholds in Appendix E, and to the actual test results in Appendix F.

Table 10. Parametric Analysis Table for 34-In. Seat Pitch

Seat Type	Aisle Occupant	Center Occupant	Window Occupant	Seat Pitch (in.)	Pulse Peak (G)
2-Passenger C-3	50th	-	50th	34	8
	50th	-	50th	34	7
	-	-	5th	34	8
	95th	-	5th	34	8
	95th	-	-	34	8
	95th	-	95th	34	8
3-Passenger M-Style	50th	50th	50th	34	8
	50th	50th	50th	34	7
	-	-	5th	34	8
	95th	50th	5th	34	8
	50th	50th	5th	34	8
	95th	-	-	34	8
	95th	95th	95th	34	8
3-Passenger Walkover	50th	50th	50th	34	8
	50th	50th	50th	34	7
	-	-	5th	34	8
	95th	50th	5th	34	8
	50th	50th	5th	34	8
	95th	-	-	34	8
	95th	95th	95th	34	8

As anticipated, the greater the seat pitch, the more severe the loads imparted to the occupants. This outcome suggested that the 48-inch seat pitch should have been the parameter to incorporate during dynamic testing. However, all three seats in the study are used in commuter cars where the seat pitch is less than 48 inches. Discussions with CCEC, makers of all three seat types, indicated that the typical seat pitch used is between 32 inches and 34 inches.

Based on this information, the decision was made to focus on the modeling produced with the shorter seat pitch for all seats in the study. The results from the longer seat pitch are still of value after the model and sled test are compared. If the model and the actual test correlate well, then the data gained from the larger seat pitches can be used to indicate the ability of the seats to safely restrain the occupants at the increased distances.

The intent of the modeling was to determine which occupant configuration should be tested. In anticipation of the seat standard, occupant configuration(s) representing the greater population were considered in the analysis. To be able to compare results, it was also useful to consider using the same occupant configuration for every seat type. Occupant configurations that addressed the occupant injury potential as well as seat strength (typically two opposing conditions) were desired.

The results of the Walkover seat test in Table D3 indicate all occupant injury values are well below those of the C-3 and M-Series seats. Therefore, the Walkover seat was not used to determine the ATD configuration for dynamic testing.

Unlike the results of dynamic testing, the injury values produced from the seat/occupant modeling with a 34-inch seat pitch suggested that no injury value is exceeded for either the C-3 or the M-Style seats. However, if these data are compared between the C-3 and M-Style seats, the HIC and femur loads for the C-3 seat are greater than they are for the M-Style seat (while the 3-msec chest value is about the same for both seats). Therefore, the C-3 seat was chosen to determine the ATD configuration.

The results from the C-3 and M-Style seat/occupant model with a seat pitch of 34 inches, a 5th-percentile female ATD in the window seat and a 95th-percentile male ATD in the aisle seat (and a 50th-percentile male in the middle seat, if applicable), indicated that the HIC for the female ATD is significantly higher than the other cases where a second occupant is present, while the 3-msec chest values and femur loads are comparable to the others. This condition was chosen as one of the test cases.

When the 5th-percentile female is present with no occupant seated next to her, the results for the female are the same as they are when there is an occupant seated next to her. In reality, the single-occupant condition would likely result in higher injury values, but the seat characteristics of the model were based on the quasi-static testing of the seat in which the loading across the seatback was done simultaneously. When this information is translated to a rigid-body computer model, the results are that occupant reactions into seatbacks are independent of whether or not the other seats are occupied.

For the second C-3 test, the two 50th-percentile ATD's and the two 95th-percentile ATDs provide similar results for the occupant. The HIC of the 50th-percentile ATDs are higher, while the femur loads for the 95th-percentile ATD are greater. The 3-msec chest values are similar. Since use of the 50th-percentile ATDs would provide information regarding "average"-sized occupants in a dynamic test, these were chosen for the second test.

7. COMPARISON OF TEST AND MODELING RESULTS

The results of the dynamic sled tests and the output from the seat/occupant models were compared. Injury threshold comparisons are provided in Appendix E and all data channel outputs are compared to modeling outputs in Appendix F. The differences between the tests and the modeling were addressed, and, in most cases, the seat/occupant model was modified to better represent the test results. In effect, the seat/occupant models have been validated.

Several items are worth noting prior to the comparison discussion:

- The original parametric analysis was conducted with a seat pitch of 34 inches Due to mounting configurations on the test sled, all the dynamic tests were conducted with a seat pitch of 32 inches, which is the lower boundary value for the typical seat pitch in a commuter car. A comparison between the MADYMO results for both the 32-inch and 34-inch seat pitches indicate that there is very little difference in the results.

- The original parametric analysis was conducted with an ideal triangular, 250-msec, 8-G peak crash pulse. After the tests were conducted, the actual sled deceleration pulse for each test was input into the corresponding model and re-run. The deceleration plots for all dynamic tests are shown in Appendix F and compared to the corresponding simulation outputs.

- The original parametric analysis incorporated only Hybrid III 50th-percentile ATDs, whereas a combination of Hybrid II and Hybrid III 50th-percentile ATDs were used during the actual dynamic testing. The computer models and results below represent updated versions of the model with the correct ATDs in the corresponding seat(s).

The occupant injury results from the dynamic testing and the predictions from the modeling output are provided in tables in Appendix E as normalized values with respect to the corresponding injury tolerance value. An injury measurement exceeds the tolerance value if it is greater than 1.0. A relative comparison is made between the test results and the modeling output data. For example, the HIC for the window-side ATD (in both the dynamic test and the model) was normalized with respect to the HIC 1,000 injury limit, and in Test No. 980480, the normalized test and modeling results are 0.55 and 0.51, respectively. The modeling predicted a slightly lower HIC than was produced in the corresponding test, yet both results were below the normalized injury tolerance value of 1.0. Results for the HIC, 3-msec chest G, the neck loads, and the femur loads were all compared and are provided in Appendix E. Since the Hybrid II ATD does not accommodate a neck load cell, the only injury parameters that are compared for the Hybrid II ATD are the HIC, 3-msec chest load, and the femur load.

The following discussion compares the results from the model and the test. The loads recorded by the seat load cells also are discussed.

7.1 C-3 SEAT - TYPE 1 TEST (98-0480) - TWO 50TH-PERCENTILE ATDs

Comparison to injury threshold: The model accurately predicted all values from the aisle-side, Hybrid II 50th-percentile ATD to be below their respective injury thresholds. The model accurately predicted all values (except for the neck moment) for the Hybrid III 50th-percentile window-side occupant to be below their respective injury thresholds, and in the case of the neck shear, to exceed the injury threshold. In the case of the neck moment, there was a discrepancy between the prediction and the test value: the model predicted a moment that exceeds the injury threshold, whereas actual testing produced a moment below the

injury threshold. While both outcomes are below the injury tolerance values, the output from the seat/occupant models (for both the aisle and window-side ATDs) over-predicted the 3-msec chest value by a small margin and under-predicted the HIC. The injury comparisons for the Hybrid II 50th-percentile aisle-side occupant and the Hybrid III 50th-percentile window-side occupant are shown in Figures E1 and E2 (Appendix E).

Comparison between model prediction and test results: In genreal, the time-history curves for both occupants indicate a good correlation in the timing and shape of the curves. However, the X-component of the head acceleration (for both ATDs) in the computer model (Appendix F, Figures F15 and F21) failed to reach the peak levels produced in the test. The vertical component of the chest acceleration in the model was greater than the levels produced in the test (Appendix F, Figures F12 and F18). These differences suggest that, in the model, the chest of the ATDs had a greater role in slowing down the occupant than the chest of the ATDs in the actual test. This phenomenon in the Hybrid III 95th-percentile ATD is further noted by a greater neck bending moment in the model than in the actual test.

Figures F24 and F25 in Appendix F show the neck compressive forces and neck bending moment of the Hybrid III ATD. In the test, the neck compressive forces continue to increase, while the bending moment levels out at approximately 150 msec. In the MADYMO model, however, the head continues to bend backward, causing a greater bending moment and lower neck compressive force. This response in the model results in a slightly lower head deceleration (X comasponent) and a corresponding decrease in HIC.

Seat attachment load comparisons: The predicted and actual loads at the seat attachments are compared in Appendix F. Since the C-3 is an extremely stiff seat structure and is rigidly attached to the test fixture, the fore/aft loading and the vertical loading match well between testing and modeling. The tension/compression of the mounts show a match in trend, but not in peaks. This is due in part to the static data used to simulate the loading into the seat backs. The seat stiffness characteristics were measured during quasi-static testing, which provides data that are typically stiffer than that actually produced during dynamic testing.

7.2 C-3 SEAT - TYPE 2 TEST (98-0481) - 95TH- AND 5TH-PERCENTILE ATDs

Comparison to injury threshold: The Hybrid III 5th-percentile ATD was instrumented with neck and femur load transducers and head and chest accelerometers, while the 95th-percentile ATD lacked the neck transducer. In this test, the Hybrid III 5th-percentile female ATD exceeded the recommended injury criteria for the neck moment, left and right femur loads, and was exactly at the maximum value allowed for the neck shear. The injury comparisons for the Hybrid III 95th-percentile ATD aisle-side occupant and the Hybrid III 5th-percentile ATD window-side occupant are shown in Figures E3 and E4 (Appendix E).

Comparison between model prediction and test results: While the HIC and neck shear for the 5th-percentile ATD match quite well, the model under-predicted the femur loads and over-predicted the neck compression loads and moments. Review of the test film showed that after penetrating the seat with the knees, the 5th-percentile female ATD begins to drop down, as if the knees were driven downward after impact. However, in the model, the knees begin to rebound slightly, which in turn causes the upper body, which is still moving forward, to rotate about the lumbar spine. This causes the chest to have a greater deceleration value in the Z component of the chest (Appendix F, Figure F44) and correspondingly causes a higher 3-msec chest value, as well as larger values for the neck bending moment and neck compressive forces (see Appendix F).

While predicted injury values for the 95th-percentile ATD correlated with the test, the direction of the loading vectors differed slightly. In Figures F36 and F37 in Appendix F, it can be seen that the X

components of the model were slightly less than the test, while the Z components were just higher. Slightly different properties in the ATD's lumbar areas could allow for a difference in the upper body rotation and create the different occupant angles during impact.

Seat attachment load comparisons: The data output for each seat attachment load cell are shown in Appendix F. As with the previous test, the fore/aft and vertical components show reasonable correlation, while the tension/compression loads have a fair amount of variance (For examples, see Figures F28 - F30).

7.3 M-STYLE SEAT - TYPE 1 TEST (98-0507) - ALL 50TH-PERCENTILE ATDs

Comparison to injury threshold: A Hybrid III 50th-percentile ATD was seated in the window seat and was instrumented with neck and femur transducers and head and chest accelerometers. The Hybrid II 50th-percentile male ATDs positioned in the aisle and center seats were instrumented in the same manner as the Hybrid III 50th-percentile ATD, with the exception of the neck transducer. The injury comparisons for Test No. 980507 are shown in Figure E5, E6, and E7 (Appendix E).

Comparison between model prediction and test results: The impact of the occupants into the seat back allows the pedestal to crush and the seat back to deform, rotating about a point below the knees. This deformation causes a decrease in the femur loads in the test, while the rigid body structure of the MADYMO model continues to load the occupants's femurs (Figure F68, Appendix F).

The second impact, the upper body region, is again affected by the seat's deformation. As the seat deforms, the occupants travel farther to impact the seat. As the knees have already made contact, the upper body rotates and allows the head of the occupants to impact in the middle of the seat's crash pad. The model of the seat, which does not deform, does not allow the additional rotation of the upper body so that the chest of the occupants removes more energy from the system. This results in the higher values for the 3-msec chest value for all three occupants.

Seat attachment load comparisons: The results of the load cell comparison are similar to the results for the previous tests. The lateral and fore/aft loads compare well, while the tension/compression forces differ due the dynamic bending of the seat frames and pedestal. The results of the front aisle load cell are provided in Appendix F.

7.4 M-STYLE SEAT - TYPE 2 TEST (98-0506) - 95TH-, 50TH-, AND 5TH-PERCENTILE ATDs

Comparison to injury threshold: Both the 95th-percentile and 5th-percentile ATDs were equipped with neck load cells, while the 50th-percentile ATD in the middle seat was not. All three ATDs were instrumented with head and chest accelerometers, and femur load cells. As can be seen in the graphs, no injury value recorded for any ATD in either the test or the model exceeds 70 percent of the corresponding injury value. However, it also can be seen that there are discrepancies between the computer model's predictions and the test. The primary cause of the difference is due to the greater deformation of the seat back during dynamic impact compared to the generally stiffer response in the model. The injury comparisons for the Hybrid III 95th-percentile ATD aisle-side occupant, the Hybrid III 50th-percentile ATD middle-seat occupant, and the Hybrid III 5th-percentile ATD window-side occupant are shown in Figures E8, E9, and E10 (Appendix E).

Comparison between model prediction and test results: In the dynamic test, as the knees begin impacting the seat back, the seat structure begins to collapse at two points: the location where the frame tubes are bent in order to transition from the seat back to the bottom cushion, and at the pedestal. Since the seat in the MADYMO model is rigid, this deformation does not occur, and the femurs continue to load the seat back (Figure F115, Appendix F). At approximately 115 msec post-impact (for the 5th-percentile and 50th-percentile ATDs), there is a decrease in the femur loads in the test, while the computer model continues to load. Until this time, all three ATDs show good femur correlation with respect to timing and loading.

As the seat structure deforms in the test, the femur loads decrease and the occupants have further to travel until contact with the seat back. For the 5th-percentile female, the delayed impact causes a difference in the body position when comparing the test and model. In the test, the head and neck are the primary components slowing down the occupant, whereas in the model, the chest and femurs play a significant role. The smallest difference between the model and the test appears in the 95th-percentile male, whose initial impact with the seat back begins the deformation.

Seat Attachment load comparisons: The load cell comparisons are shown in Appendix F. As with the previous test, the fore/aft and vertical components show reasonable correlation, while the tension/compression loads have a fair amount of variance.

7.5 WALKOVER SEAT - TYPE 1 TEST (98-0508) - ALL 50TH-PERCENTILE ATDs

Comparison to injury threshold: The testing indicated that no injury tolerance value was exceeded, while MADYMO predicted that the neck would fail in compression. This difference would be due primarily to the inherent increased stiffness of the modeled seat. The injury comparisons for Test No. 980508 are shown in Figures E11, E12, and E13 (Appendix E).

Comparison between model prediction and test results: A review of the test film and modeling kinematics indicate a difference in the way the loading occurs after the knees impact the seat back. In the test, after the knees impact the bottom cushion, the seat clips which hold the cushion in place bend, allowing the cushion to translate forward. The occupants continue to travel forward several inches. At this point, the knees begin to load and the upper body begins to rotate, loading the seatback and causing flexing and deformation near the top edge of the seat. In the MADYMO model, the cushion is fixed to the seat base and the rotation of the upper body begins earlier. The heads of the ATDs strike the forward seat such that loading is more along the vertical axis of the ATDs' heads. This results in the higher predicted neck compression and bending moments seen in Figures F164 and F165 in Appendix F. Although there are differences in the injury values and some peak values, the trend of the curves comparing the test and model indicate a good correlation.

Seat attachment loads comparison: Representative curves for the fore/aft, lateral, and tension/compression direction from the load cells are provided in Appendix F. All the curves match well, up to the point where the Walkover seat reaches the forward stop, at which point the MADYMO model sees a sharp increase in loading. In the dynamic test, after the seat reaches the forward stop, additional energy is removed from the system with the deformation of the seat, the crush of the pedestal, and the torsional rotation about the lateral axis of the aisle side of the seat. While the static data used in the model for the seat back will capture some of this affect, dynamic conditions tend to produce softer load curves; hence the computer model predicts higher loads at the initial impact with the forward stop.

7.6 WALKOVER SEAT - TYPE 2 TEST (98-0509) - 95TH-, 50TH-, AND 5TH-PERCENTILE ATDs

Comparison to injury threshold: The final test of the series, Test No. 980509, consisted of 95th-, 50th-, and 5th-percentile ATDs in the aisle, center, and window position, respectively. As with the M-Style seat, the 95th-percentile and 5th-percentile ATDs were equipped with the neck load cells. In this comparison, no injury values in either the test or model exceed the current recommendations. The chart does indicate that the bending moment for both the 5th-percentile and 95th-percentile are near their current limits, and that there is some difference between the compressive and shear force readings for both ATDs. The injury comparisons for Test No. 980509 are shown in Figures E14, E15, and E16 in Appendix E.

Comparison between model prediction and test results: The variance of the loading values for the head and neck of the 95th-percentile ATD are due to the impact of the head into the seat back. In the test, the upper body of the ATD does not appear to rotate as much as the model. In addition, impact with the head is more along the shear axis of the neck. In the MADYMO model, after the knees impact the seat cushion, the ATD's upper body begins to rotate while continuing to travel forward. Impact between the head and the seat back is primarily along the Z axis of the head. One possible cause of the impact difference could be attributed to the lower seat cushion. This cushion is held in place with a series of metal clips. When the ATD's knees impact the cushion, the forward clips deform and allow the cushion to translate forward. In the model, however, the cushion is fixed to the seat frame and does not move.

The 50th-percentile male ATD in the center seat has a reaction similar to the 95th-percentile male ATD. The motion of the cushion in the test allows more forward translation of the upper body. The difference allows the head to impact at an angle different from the model. This can be seen in Figures F194 and F195 in Appendix F, which shows the X and Z components for the 50th-percentile male. The reaction of the 95th-percentile male is similar in trend.

The large difference in the neck compression and bending moment of the 5th-percentile female ATD is caused by the bending of the seat back. The middle of the seat is softer than either side and as deformation occurs in the test, the seat will bend more in the middle than it will on the sides. During impact between the head of the 5^{th}-percentile female and the seat back, the impact surface is no longer perpendicular to the direction of motion of the head. The angle causes the head and neck to bend about the x-axis of the neck. This reduces both the y-axis bending moment and compressive forces on the ATD. Being a rigid model, the MADYMO plane does not see this deformation and all reactions on the head are applied perpendicular to the seat back plane (See Figures F204 and F205, Appendix F).

Seat attachment loads comparison: The load cells for Test No. 98-0509 compare in the same fashion as those for Test No. 98-0508. The general trend of the curves match up to the point where the seat impacts the forward stop. The data used in the model, recorded from static testing, produce higher spikes than seen in the actual test.

8. CONCLUSIONS

The purpose for conducting these tests was to evaluate the performance of three existing commuter rail seats in terms of both the seat and dummy response, and to validate the seat/occupant models that were developed with MADYMO, an analysis software program. The three seats tested were the C-3 two-place seat, the M-Style three-place seat, and the Walkover three-place seat.

Seat stiffness characteristics were measured using uniform quasi-static loading of the seat back. For the C-3 and M-Style seat static tests, the load was applied uniformly across the upper seat back in the first test, and across the lower seat back in the second test.

All seats were uniformly tested against a triangular crash pulse of 250 msec duration and 8 G peak acceleration. This crash pulse was derived using computer models previously developed and reported in the literature (Reference 4). However, it would be desirable to validate this crash pulse selection through full-scale passenger rail car crash testing.

Each test was composed of two seat rows spaced 32 inches apart, with unrestrained ATDs in the rear seat. Commuter seats in the field are typically attached with a 33- to 34-inch seat pitch. The results from computer seat models run with a 32-inch and a 33-inch seat pitch suggest that the difference between these two seat pitches on occupant injury loads is small. However, computer results did show that as seat pitch increased to 48 inches (more typical of inter-city rail seats) the predicted injury loads increased. Therefore, injury outcomes identified from these tests will likely become worse as the seat pitch increases.

The original seat/occupant computer models were re-run and compared with the actual crash test pulse (rather than the idealized crash pulse), representative ATD sizes and positions, and a 32-inch seat pitch.

In the dynamic testing, lower forces were measured than were predicted by the model. However, it should be noted that the inertial mass of the seat itself causes the seat back to bend forward, thus lowering the forces experienced by the ATDs.

Dynamic test results demonstrated that these dynamic sled tests were repeatable and provided consistent information. Since the seats were rigidly mounted to the test fixture, the effect of the rail car structure on the outcome of the tests was not directly taken into account. To address this issue, seat attachment loads were measured to provide some information regarding seat attachment strength.

Cushion detachment during dynamic testing proved to be the primary source of flying objects. This hazardous response to dynamic loading was especially severe for the M-Style seat, whose cushions detached from the seat and impacted the occupants as they rebounded from the seat in front of them. The exposed metal seat frame became an additional hazard to the occupants rebounding back into the seat.

Occupant compartmentalization was strictly defined in this program as the seat's ability to contain the occupants between the two seat rows tested. Occupants who fell onto the floor during testing, therefore, were not considered to have been compartmentalized. However, because all occupants impacted the seat in front of them before landing on the floor, compartmentalization could be considered to have occurred.

The stiffer C-3 rail seat improved passenger compartmentalization, but it increased the likelihood of neck injuries caused by the occupants impacting the seat in front of them. The more-compliant seats (i.e., the M-Style and Walkover seats) increased the risk of passengers ejecting from the seats, but they reduced the likelihood of neck injuries caused by the occupants impacting the seats in front of them.

The injury criteria used in this program are consistent with accepted standards used in automotive and aviation federal regulations. These injury criteria are directly related to FAA injury standards, to the NHTSA FMVSS 208 injury standards, and to NHTSA's proposed new rule. The newly proposed NHTSA rule includes neck injury criteria and injury criteria for the 5th-percentile female.

Results from this test program indicate that incorporating injury criteria for the 50th-percentile male ATD into the new rail passenger safety standards is technically feasible.

9. RECOMMENDATIONS

Existing commuter rail seats have provided acceptable performance characteristics for passengers in normal operations. However, the performance of these seats in dynamic collision environments has not previously been evaluated scientifically. This program performed controlled dynamic tests on, and analyzed, three commuter rail seats to provide the information needed for assessing the current level of crashworthiness and occupant safety. This approach to obtaining rail seat crashworthiness information is similar to one of the approaches used in the automotive and aviation industries. It is recommended that the rail industry continue to conduct similar research and analysis programs on other seat types to advance rail crashworthiness.

The crash pulse used in this testing needs to be validated through full-scale passenger rail car crash testing.

Full-scale dynamic testing using a commuter rail car is recommended with interior experiments consisting of several seat configurations. The outcome of the full-scale testing should then be correlated to the tests conducted in this program. These tests will only need to be conducted once; thereafter, seats can be certified by modeling or sled testing.

The dynamic sled tests conducted in this program generated reproducible results and useful trends. This testing method is both meaningful and cost-effective. Sled testing should be incorporated into the new FRA Passenger Rail Safety Standards as the primary method for certifying new seat designs.

New interior equipment should be designed to minimize injuries to the full range of occupants. Seat stiffness should be optimized to withstand the dynamic forces of occupants impacting the seats from behind and to keep the occupants compartmentalized, and yet not be so stiff as to inflict injurious forces on the occupants.

To standardize seat certification requirements, the 50th-percentile male Hybrid III ATD is recommended for occupant injury assessment in the new APTA Passenger Rail Equipment Safety Standards because of its wide-spread availability.

A second dynamic sled test using 95th-percentile (by weight) male Hybrid III ATDs is recommended for inclusion in the standards to test seat strength.

One cost-effective change to increase the safety of existing seating would be to improve the method used to attach cushions to the seat frame. Strengthening the seat cushion attachments is recommended to prevent them from detaching in a collision.

10. REFERENCES

1. Melvin, J. W., and A.M. Nahum, Ed., *Accidental Injury, Biomechanics and Prevention*, Springer-Verlag, NY, 1993.

2. Department of Transportation, National Highway Traffic Safety Administration, 49 CFR Parts 571, 585, 587, and 595, Docket No. NHTSA 98-4405; Notice 1, RIN 2127-AG70, Federal Motor Vehicle Safety Standards; Occupant Crash Protection, September 18, 1998.

3. Department of Transportation, Federal Aviation Administration, 14 CFR Part 25, Airworthiness Standards: Transport Category Airplanes.

4. Tyrell, D.C., K.J. Severson, and B.P. Marquis, *Analysis of Occupant Protection Strategies in Train Collisions*, ASME International Mechanical Engineering Congress and Exposition, AMD-Vol. 210, BED-Vol. 30, pp. 539-557, 1995.

APPENDIX A. DETAILED SEAT DESCRIPTION

C-3 Seat

The C-3 seat is manufactured by Coach and Car Equipment Corporation (CCEC) and is designed to be cantilever-mounted in the C-3 cars currently being placed in revenue service. Under the designation Model 992, the seat also is scheduled to be supplied to Nippon Sharyo for double-level Gallery cars for the Caltrain line in San Francisco and to Kawasaki for double-level cars for the Virginia Railway Express (VRE) in Washington, D.C. The Caltrain and VRE seats will be pedestal-mounted versions rather than the cantilever-mounted C-3 version.

The C-3 seats are mounted in the car transversely, typically facing in the same direction (see Figure A1). The seats are supplied mainly in two-passenger versions, with small quantites of one-passenger versions used in the C-3 cars.

As tested, the C-3 seat consists of a welded tubular carbon-steel frame, a molded fiberglass back shell, two molded fiberglass armrest shells, two neoprene-covered armrest caps, a cast aluminum grab handle, a bottom cushion, and a back cushion.

The C-3 seat is mounted to the car using a three-point cantilever mounting system (see Figure A2) consisting of studs, shims and nuts. This hardware is supplied by the rail car builder. The studs attach to the seat frame though holes in steel blocks at the lower front and upper rear seat mounting points. The blocks are an integral part of the seat frame weldment.

The bottom and back cushions (not shown in the figures) attach to the seat frame by means of spring clips that engage the seat frame's tubing. These cushions are designed to be readily removed without the use of tools for rapid repair or replacement.

The C-3 seat is fitted with armrests on both the aisle and wall sides of the seat. The armrest structure is an integral part of the seat frame and is covered with a molded plastic armrest shell which, in turn, is covered with a stainless steel cap. On the seat tested, the cast aluminum grab handle is located on the aisle side of the seat.

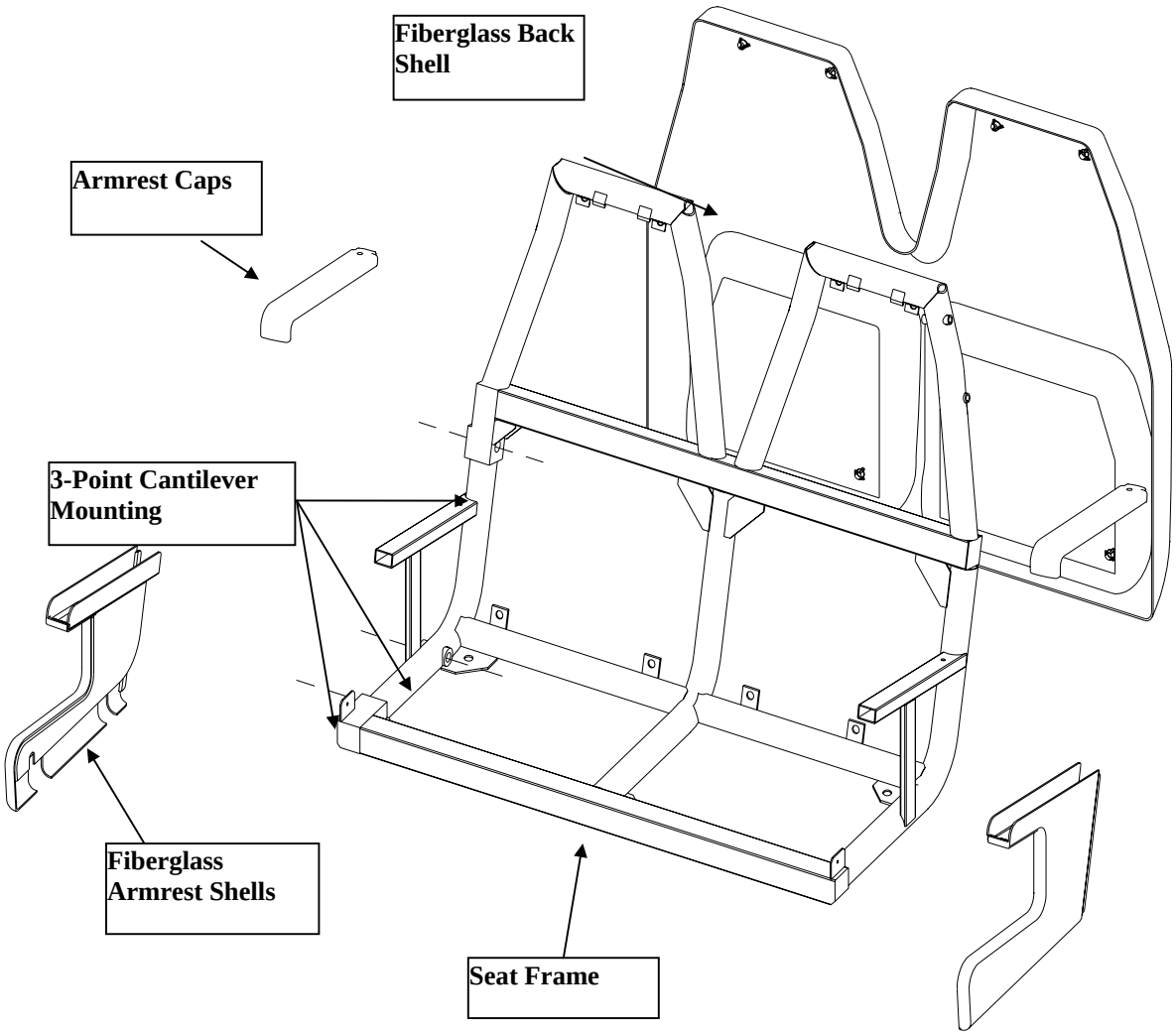

Figure A1. C-3 Seat (Cushions not shown)

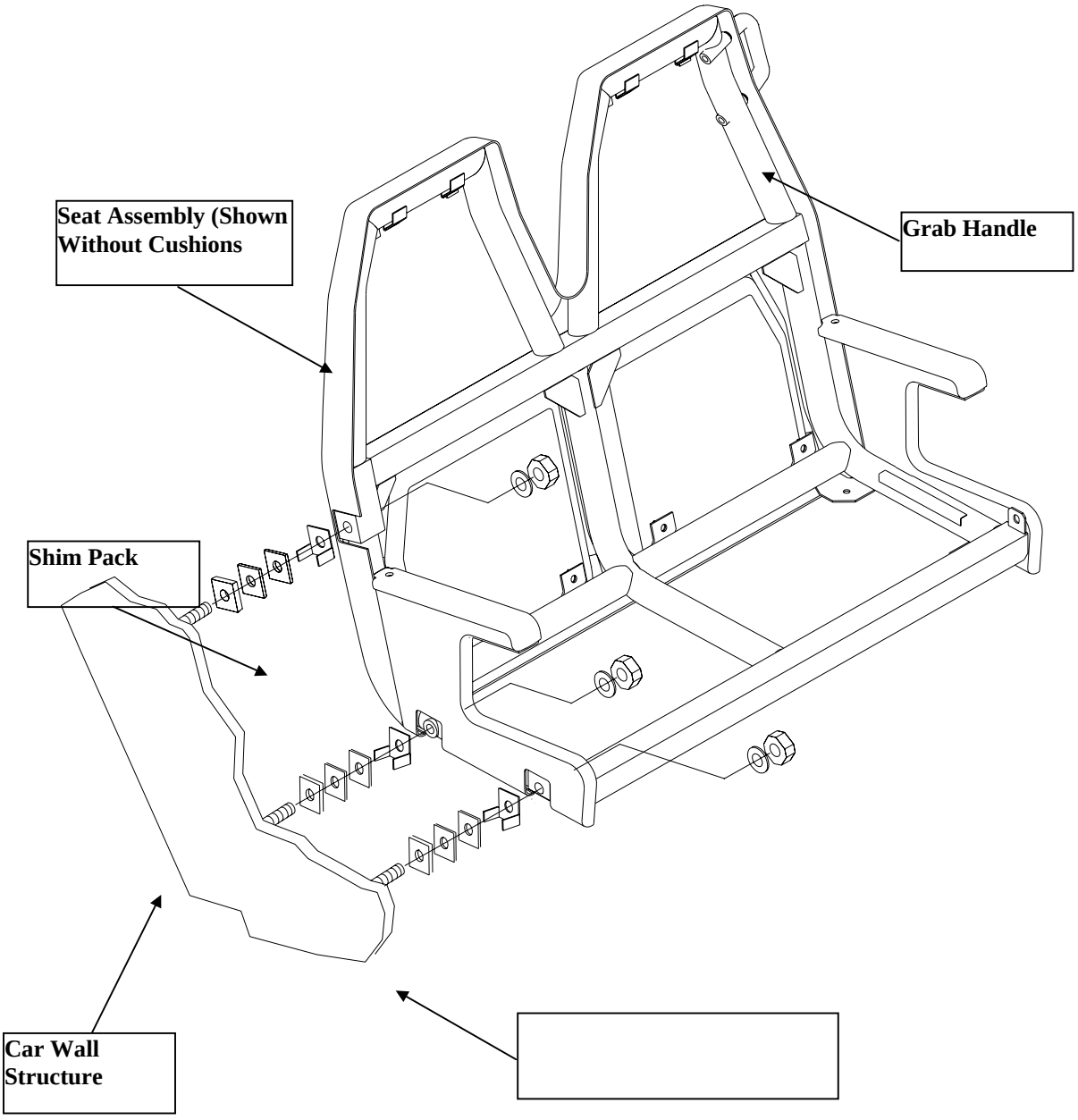

Figure A2. C-3 Seat Cantilever Mounting

M-Style Seat

The M-Style seat assembly tested is a three-passenger seat supplied by Artcraft Industries to Bombardier for use in Metro-North cars. This seat style is, in various configurations, the most prevalent commuter seat used in the US.

The M-Style seat is so named because it is the "standard" seat supplied by several seat manufacturers (including CCEC, Tenyru of Japan, AMI of Colorado Springs, and U.S. Seating of Philadelphia) for use in M1, M2, M3, M3A, M4, and M6 cars. These cars form the bulk of the fleets of both the LIRR and Metro-North and have been manufactured by several car builders, including General Electric, Morrison-Knudsen, Tokyo Car, and others. The seat is also known as the Model 429 and 429A seat as supplied by CCEC.

Besides the Metro-North and LIRR M-Series cars, the seat has been used by many other transit authorities, including Massachusetts Bay Transit Authority (MBTA), Maryland Area Rail Commuter System, (MARC), Northern Indiana, Southeastern Pennsylvania Transportation Authority, (SEPTA), New Jersey Transit (NJT), and others. It is supplied in one-, two-, and three-passenger versions, with most supplied in three-by-two configurations in single-level cars. The MBTA uses a modified version of the seat in double-level cars supplied by Kawasaki (the 700/1700 Series) and in recently renovated single-level Pullman cars.

The three-passenger version tested consists of a welded carbon-steel tubular frame, a thermoformed plastic back shell, a thermoformed plastic armrest shell, a crash pad cushion, a bottom cushion, a back cushion, and a headrest cushion (see Figure A3). Each of these cushions is of one-piece construction, generally consisting of an aluminum pan, foam, and a sewn upholstery cover.

The M-Style seat is supported on the aisle side by a fully enclosed welded stainless steel pedestal and on the wall side by means of brackets on the seat frame that are bolted to the top of floor heaters. The pedestal is mounted to the car structure with two 0.50-inch bolts, and the frame is mounted to the wall side heater with two 0.375-inch bolts. The pedestal is bolted to the seat frame with two 0.375-inch mounting bolts.

The M-Style seat is fitted with an armrest on the aisle side only. The armrest structure is an integral part of the seat frame and is covered with a molded plastic armrest shell which, in turn, is covered with a stainless steel cap. A cast aluminum grab handle is located on the aisle side of the seat.

The seat's bottom cushion of the M-style sest is mounted to the seat frame by means of spring-steel clips engaging the seat frame tubing. The clips are mounted to the underside of the bottom cushion pan structure. The back and headrest cushions also are mounted with clips. These cushions are designed to be readily removed without the use of tools for rapid repair or replacement.

The crashpad cushion mounts to the top of the seat back shell and is secured to the back shell along the lower edge of the cushion with retention pins and push nuts.

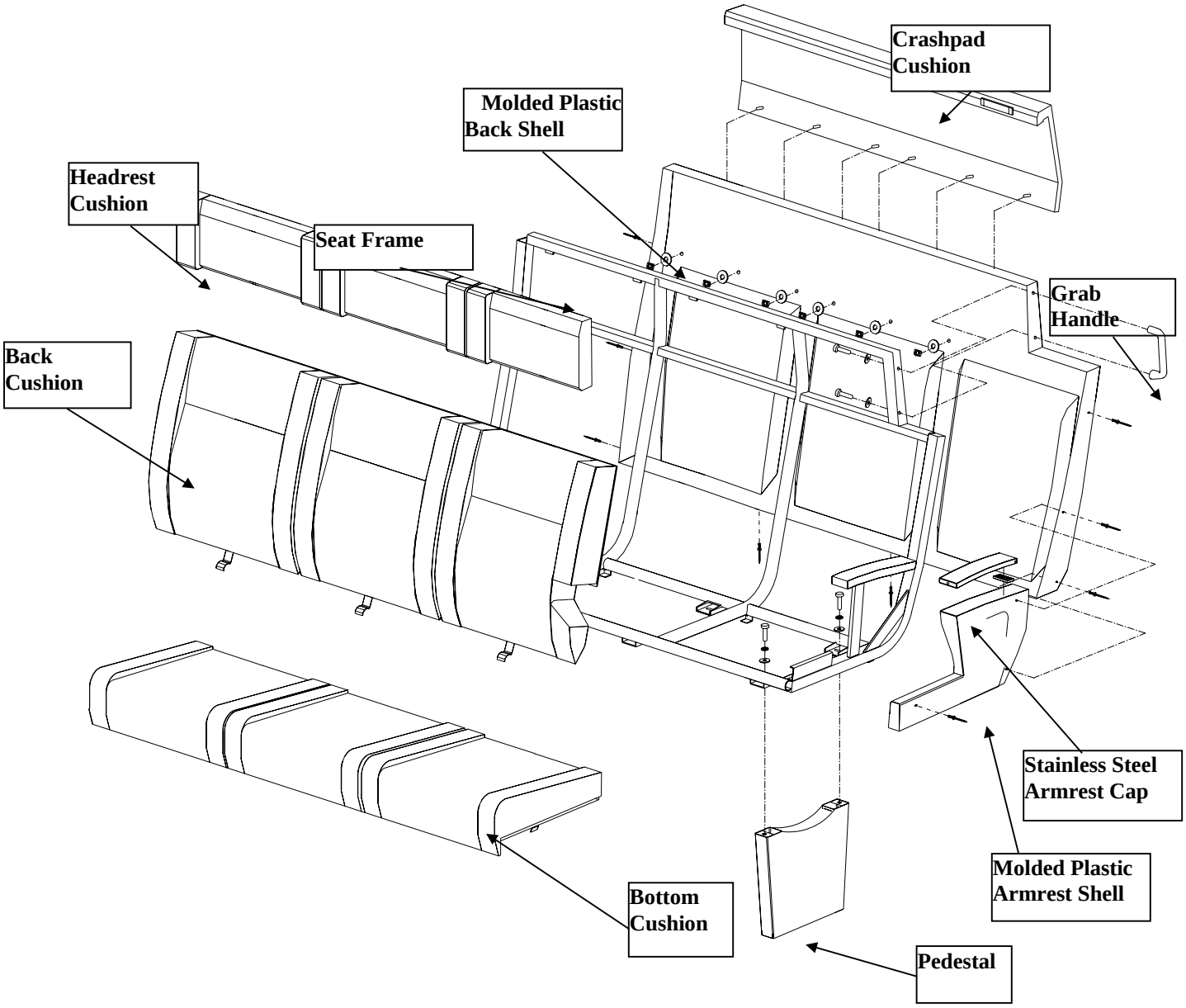

Figure A3. M-Style Seat

Walkover Seat

The Walkover seat tested is a three-passenger version of the CCEC Model 500 with a Coach and Car Safe Stop ™ inertial locking mechanism. The seat is identical to those three-passenger seats supplied to Bombardier for the NJT Comet IV rail cars.

Walkover seats are intended to be mounted in the rail car transversely and are designed to be reversible; i.e., the seat can be made to face in either direction by simply moving the back cushion to the desired position. Walkover seats are typically supplied in one-, two-, and three- passenger versions. Some transit authorities, such as NJT, use a two-by-three arrangement in a single-level car. Others, such as Northeast Illinois Regional Commuter Railroad Corporation, which operates the Metra Commuter Rail Service, and the Peninsula Corridor Joint Powers Board, which operates the Caltrain Commuter Rail Service, use walkover seats in a double-level car with a two-by-two arrangement in the lower level and single-passenger transversely mounted seats in the upper level.

The Walkover seat consists of a bottom cushion, a back cushion, a welded and painted carbon steel seat frame, and a stainless steel pedestal (see Figure A4). The seat frame includes a full walkover mechanism, a rocking cradle mechanism, and an inertial lock mechanism. The Walkover mechanism is a four-bar link arrangement located on the aisle and wall sides of the seat that is designed to ensure that the seat back is properly angled in both seating positions. The rocking cradle mechanism is connected to the four-bar link Walkover mechanism by means of linkages.

The seat has stainless-steel tubular armrests with molded plastic caps on both the aisle and wall sides. The top of the seat back is straight all the way across with a diagonal slope at the aisle side for the mounting of a padded hand grip.

The latest versions of the Walkover seats include an inertial locking mechanism that is designed to restrain the seat back during deceleration of the vehicle with the seat in either seated position.

The seat frame is mounted to the car structure by means of a fully enclosed, welded stainless-steel pedestal on the aisle side and a wall bracket that is attached to the heater guard on the wall side. Mounting bolts consist of two 0.50-inch bolts at the pedestal-to-car-floor attachment points and two 0.375-inch bolts at the heater guard. The hardware for mounting the seats to the cars is typically supplied by the car builder, rather than the seat manufacturer. The pedestal is fastened to the seat frame by means of two 0.375-inch bolts typically supplied by the seat manufacturer.

The bottom cushions for the Walkover seats are mounted on a rocking cradle mechanism that is designed to move the bottom cushion from one seating position to the opposite direction automatically by means of a linkage as the back cushion is moved from one position to the other.

The bottom seat cushion assembly is mounted into the seat frame cradle assembly with spring-steel clips which are attached to the seat bottom surfaces. When the cushions are installed to the seat frame cradle/tubing structure, these clips engage with that structure and thereby hold the bottom seat cushion assembly in place.

The seat back cushion consists of a welded steel frame covered with padding and upholstery. The foam is contoured for each side of the seat back. In this case, “Side” means the front and back surfaces of the seat-back cushion when the seat is locked in one position. The front and back surfaces are identical, so that each can perform the intended function of a seat back with the seat positioned in either direction.

The seat bottom and seat back cushion assemblies are designed to be readily removable without the use of tools for rapid repair or replacement.

The inertial locking mechanism is accessible from the aisle side of the seat and located so as not to be a hazard to aisle passage. The inertial locking mechanism is located below and behind the aisle side close-off panel and does not engage during the normal use of the Walkover seat mechanism, i.e., when the back is cycled from one position to the other.

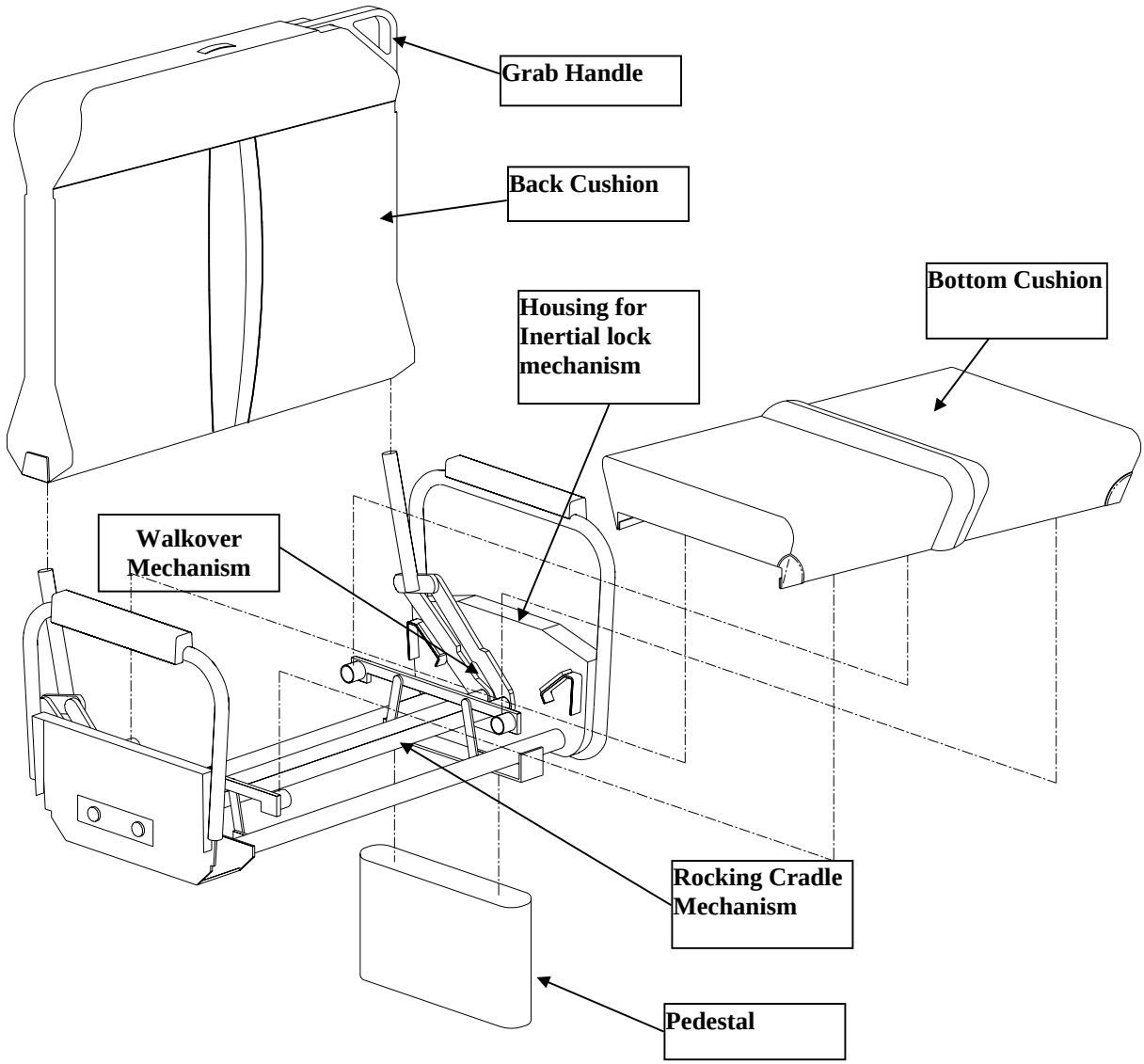

Figure A4. Two-Passenger Version of the Walkover Seat

APPENDIX B. STATIC TEST RESULTS: SEAT STIFFNESS CURVES AND SEAT ATTACHMENT LOADS

SEAT STIFFNESS CURVES (FROM STATIC TESTING)

High Test

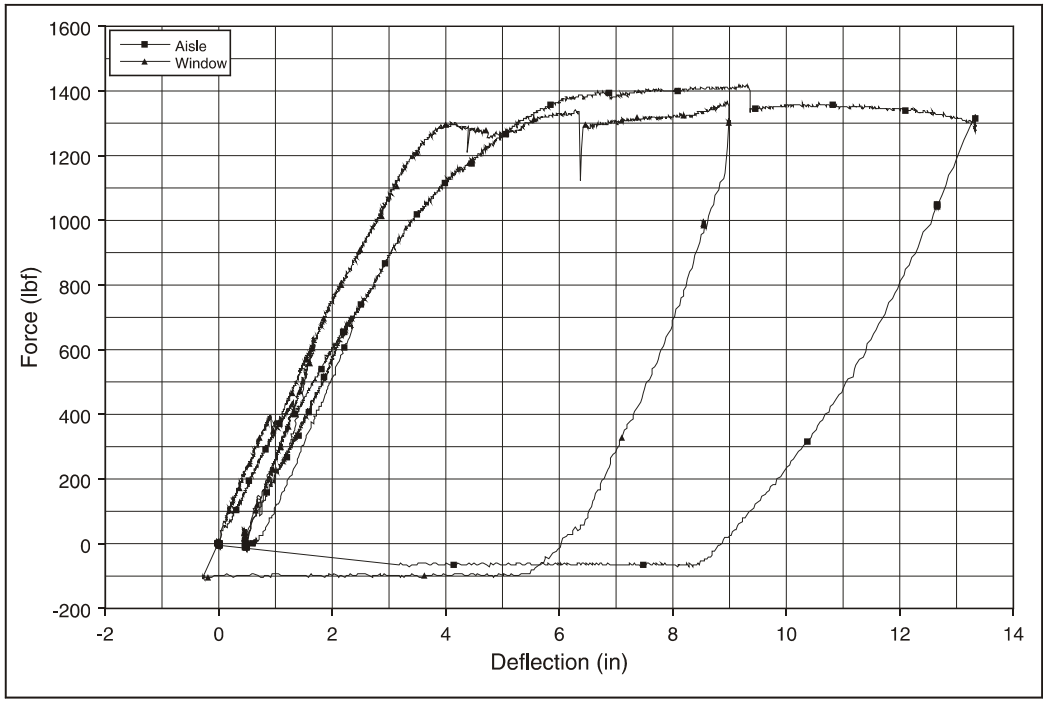

Figure B1. C-3 Upper Seat Back Stiffness Curves

Low Test

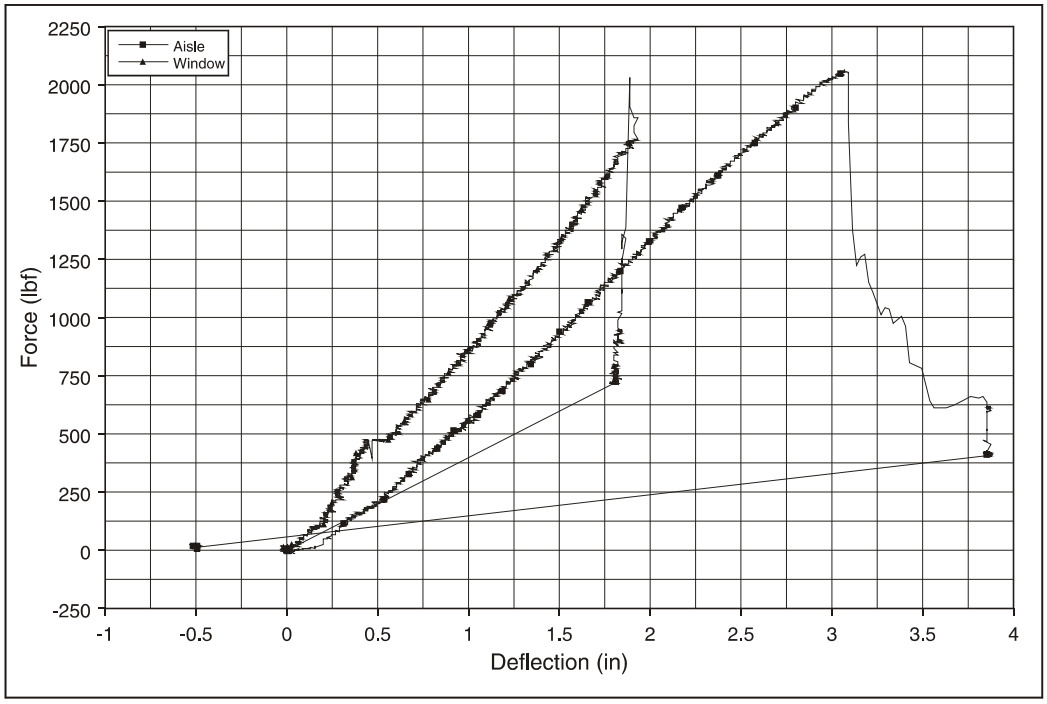

Figure B2. C-3 Lower Seat Back Stiffness Curves

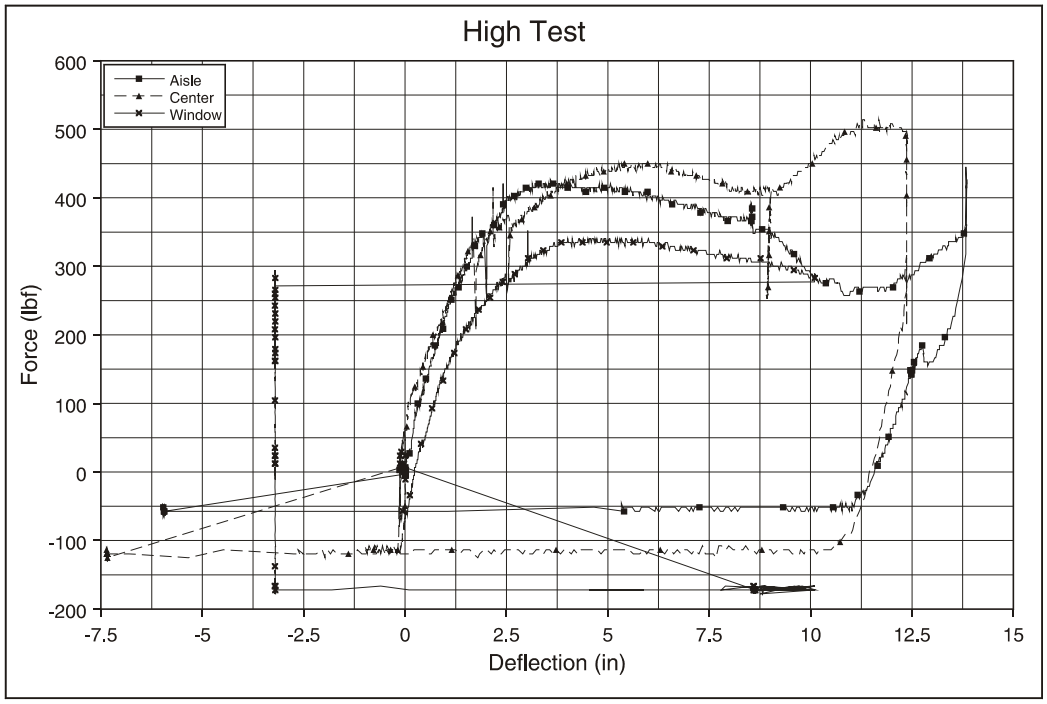

Figure B3. M-Style Upper Seat Back Stiffness Curves

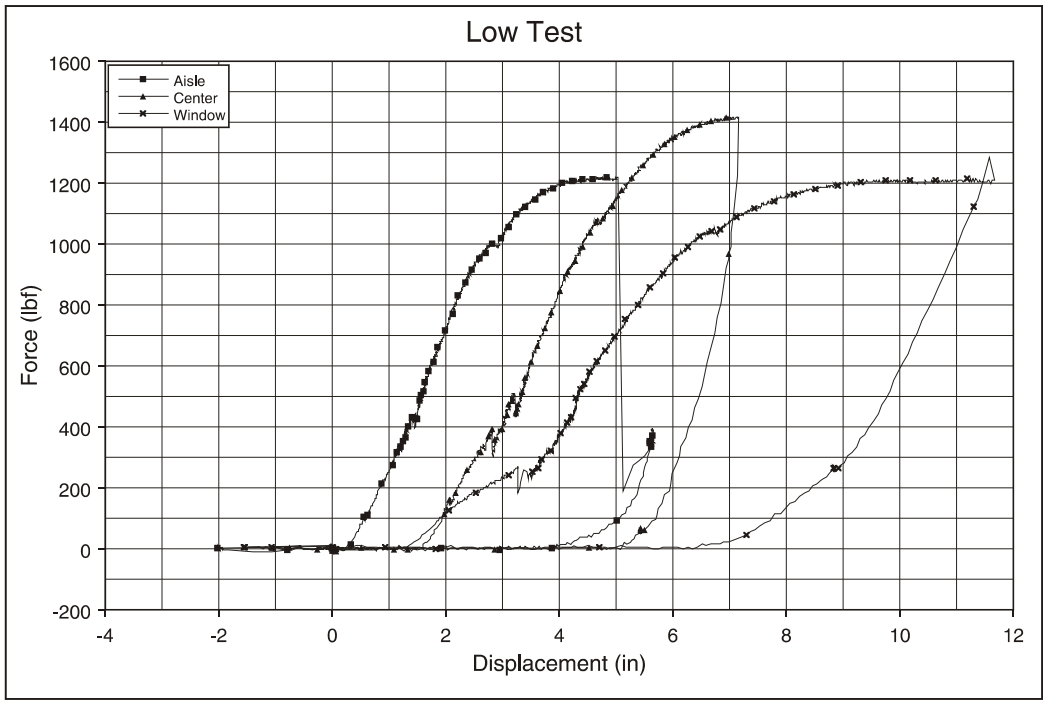

Figure B4. M-Style Lower Seat Back Stiffness Curves

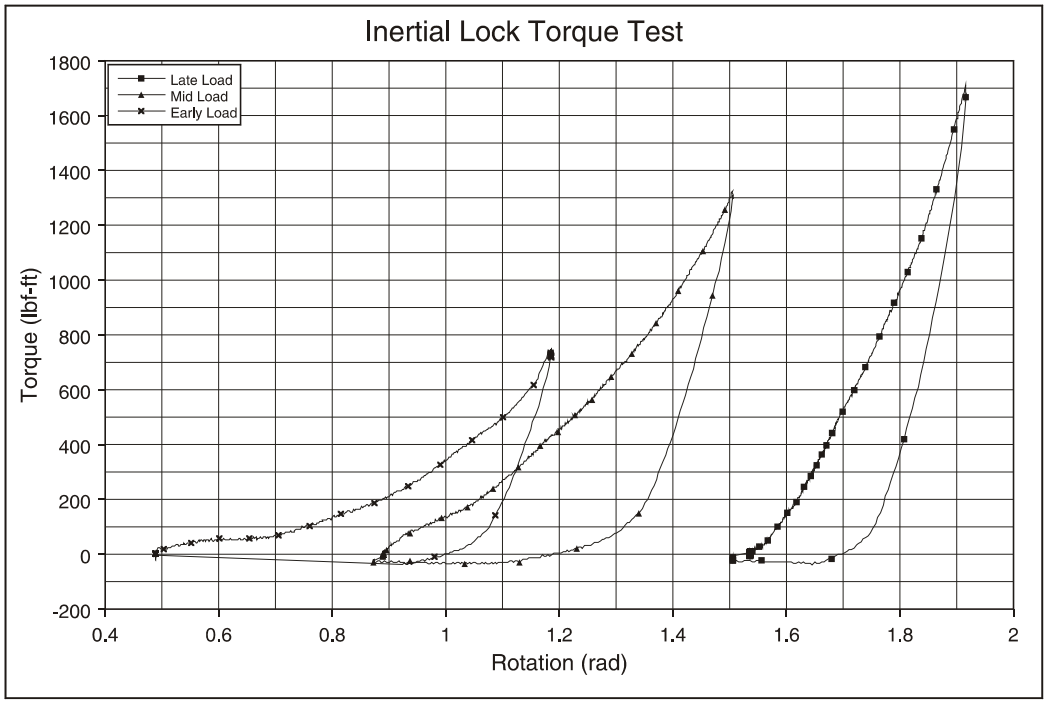

Figure B5. Walkover Seat Torsion Bar Lock Stiffness Curves

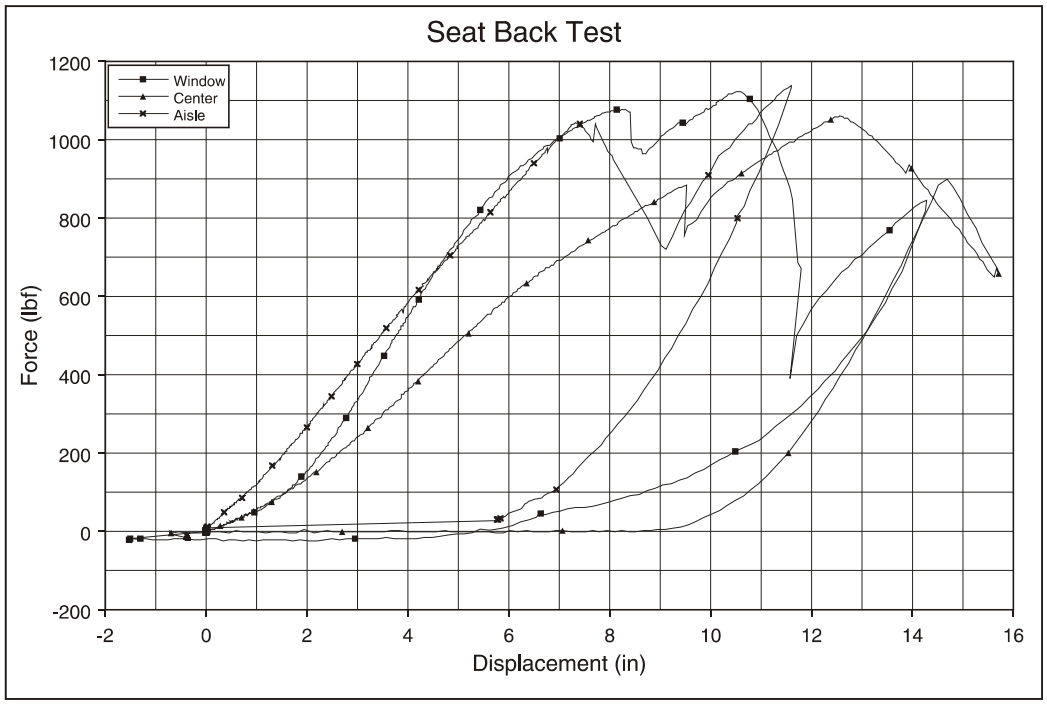

Figure B6. Walkover Seat Back Stiffness Curves

SEAT ATTACHMENT LOADS (FROM STATIC TESTING)

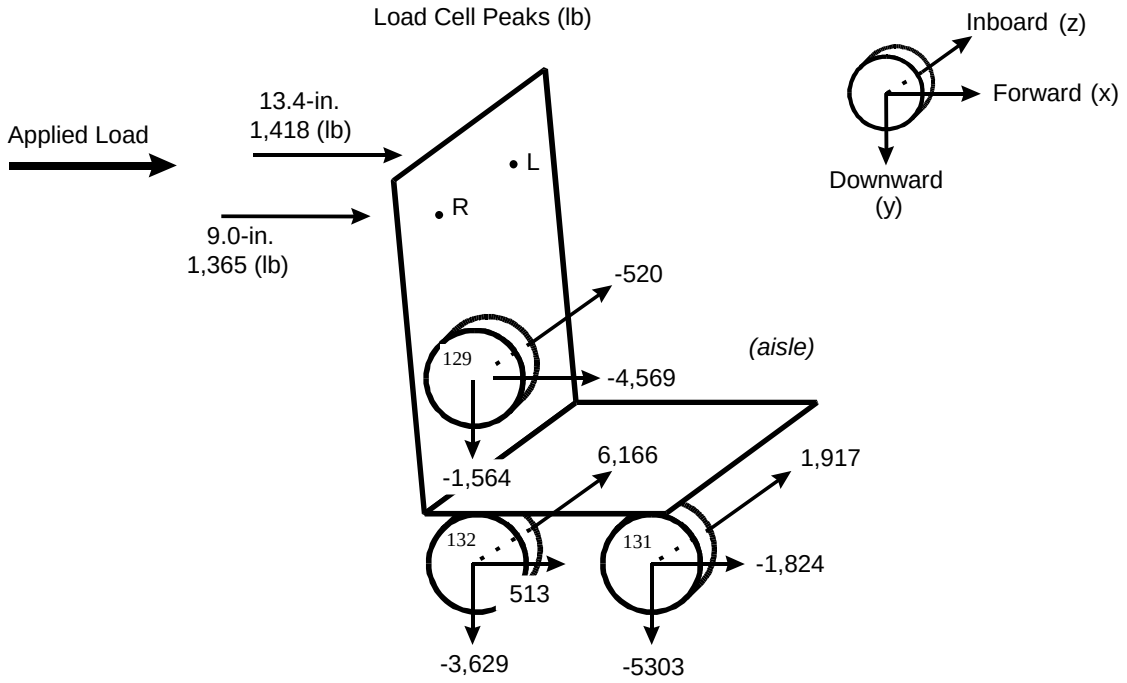

Figure B7. C-3 Static Test (Upper Load), Peak Seat Attachment Loads

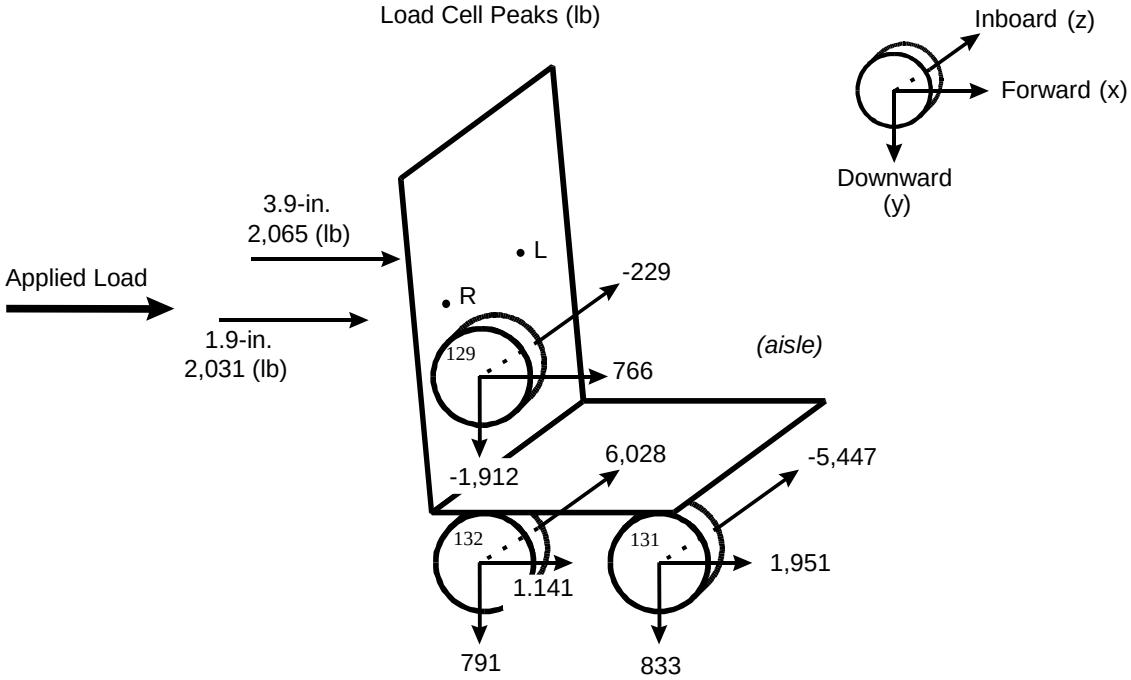

Figure B8. C-3 Static Test (Lower Load), Peak Seat Attachment Loads

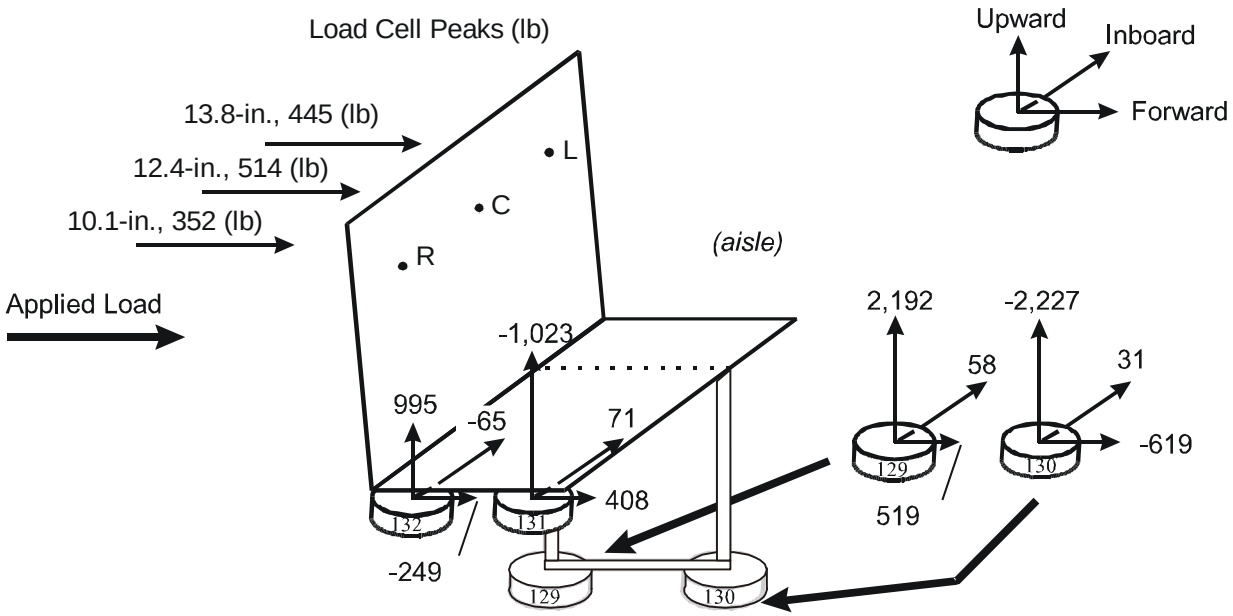

Figure B9. M-Style Static Test (Upper Load), Peak Seat Attachment Loads

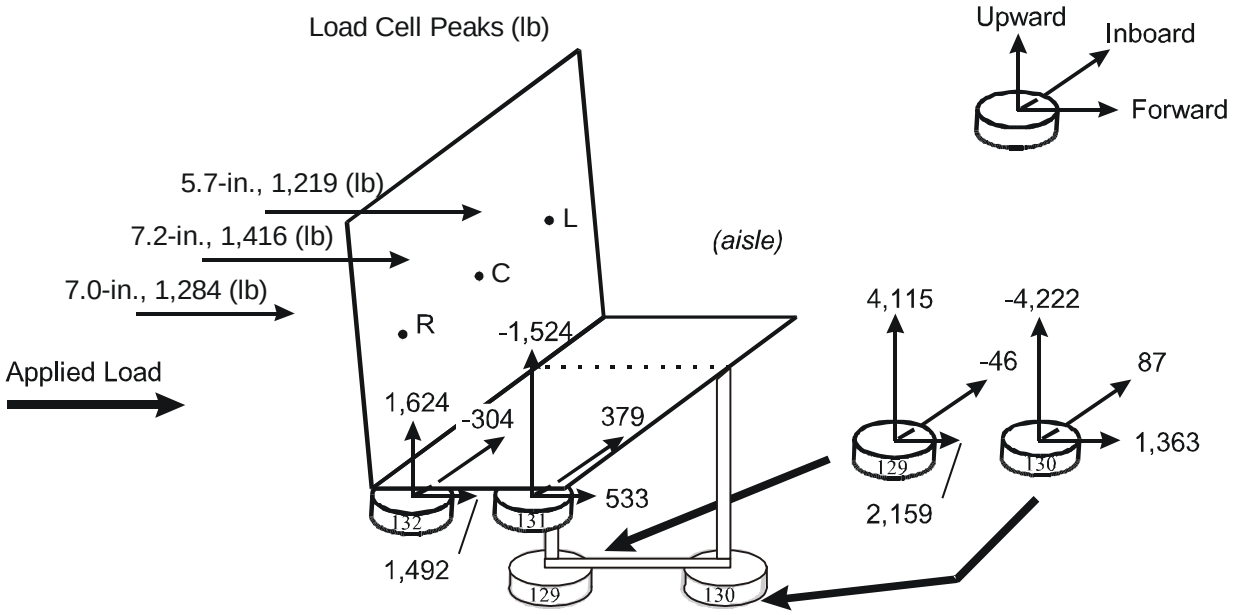

Figure B10. M-Style Static Test (Lower Load), Peak Seat Attachment Loads

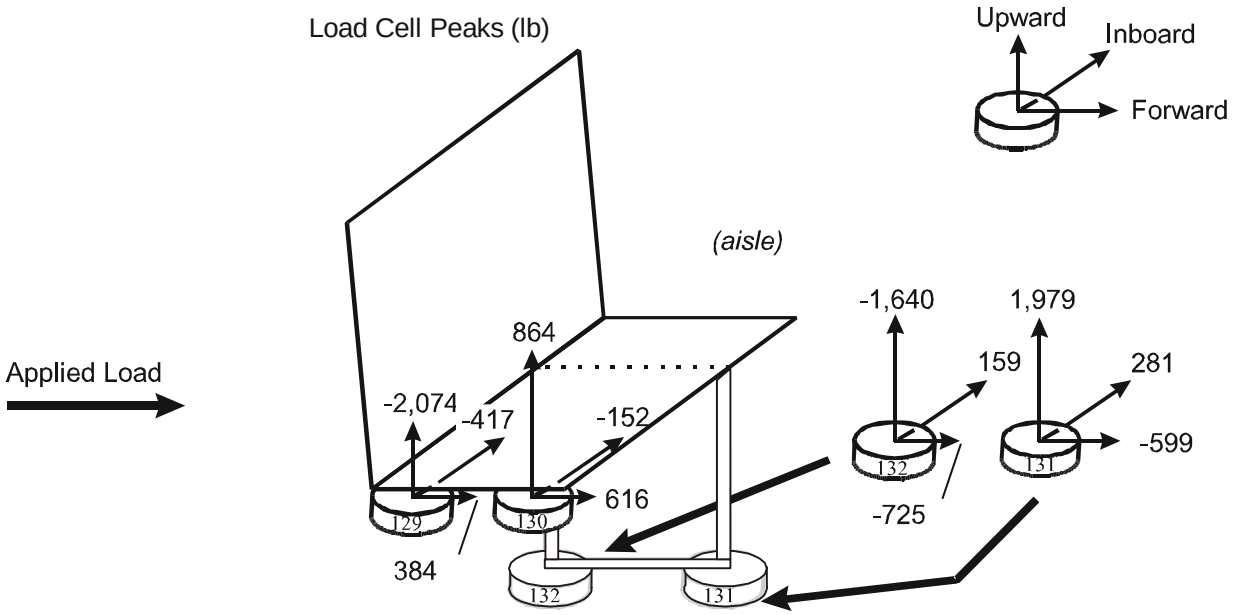

Figure B11. Walkover Static Test (Torsion Bar - Early), Peak Seat Attachment Loads

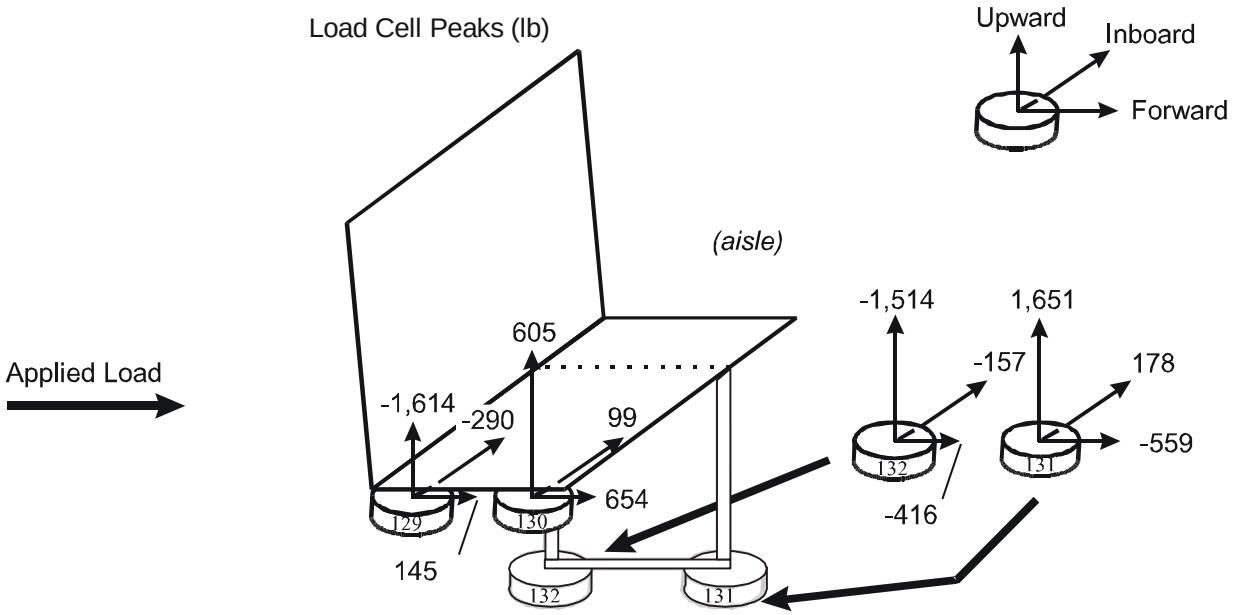

Figure B12. Walkover Static Test (Torsion Bar - Mid), Peak Seat Attachment Loads

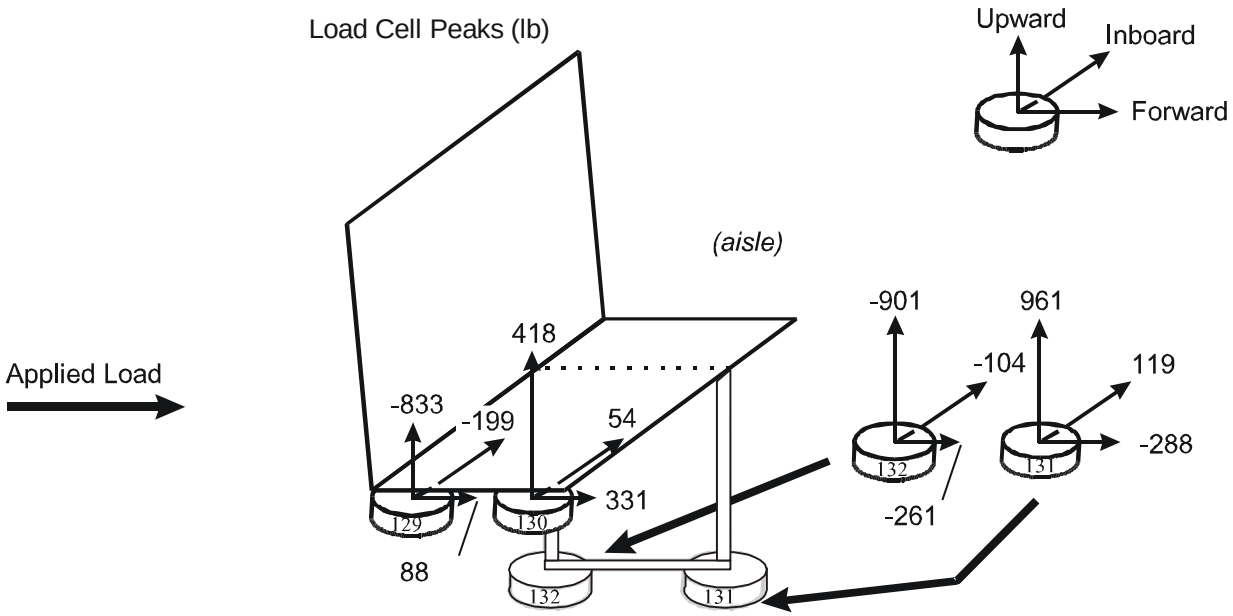

Figure B13. Walkover Static Test (Torsion Bar - Late), Peak Seat Attachment Loads

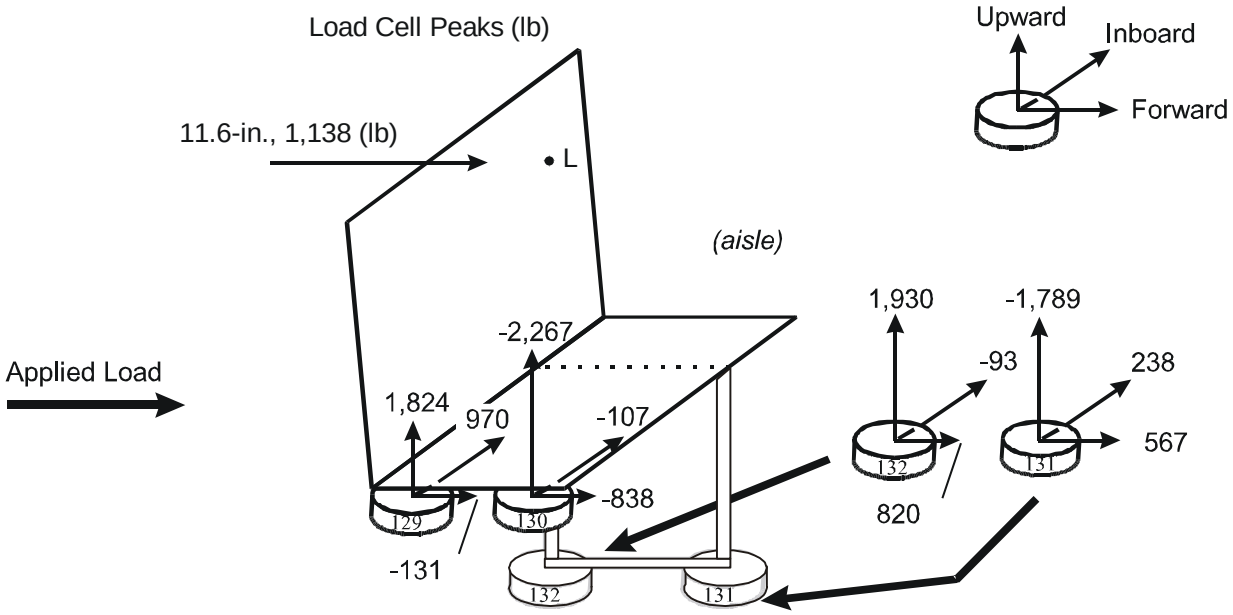

Figure B14. Walkover Static Test (Aisle Seat), Peak Seat Attachment Loads

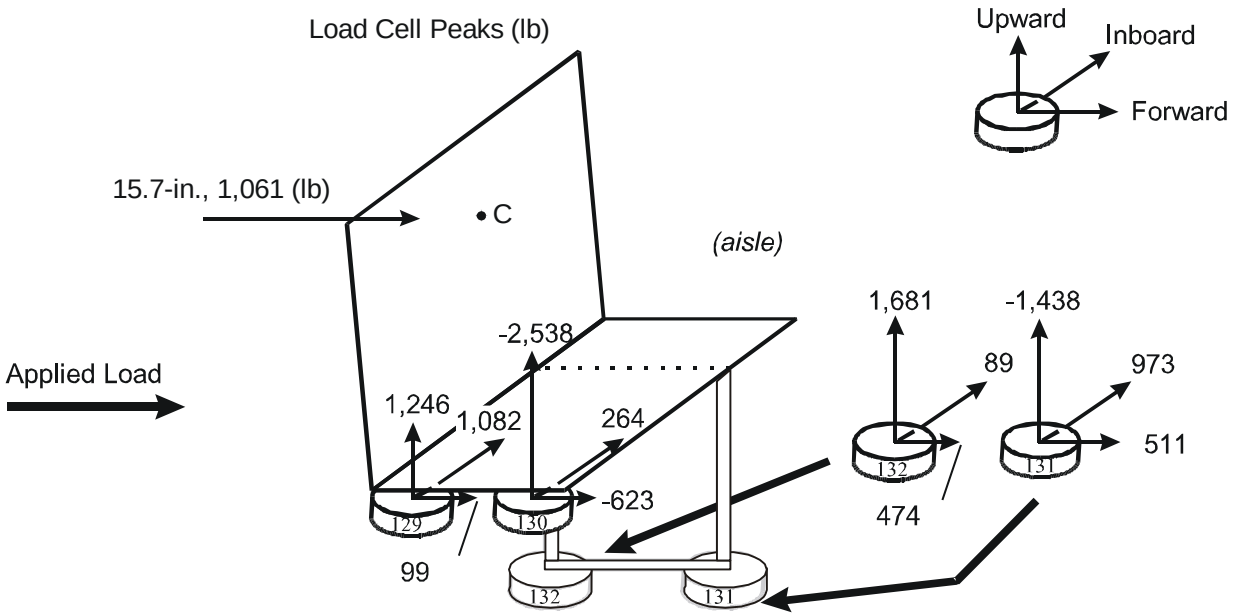

Figure B15. Walkover Static Test (Middle Seat), Peak Seat Attachment Loads

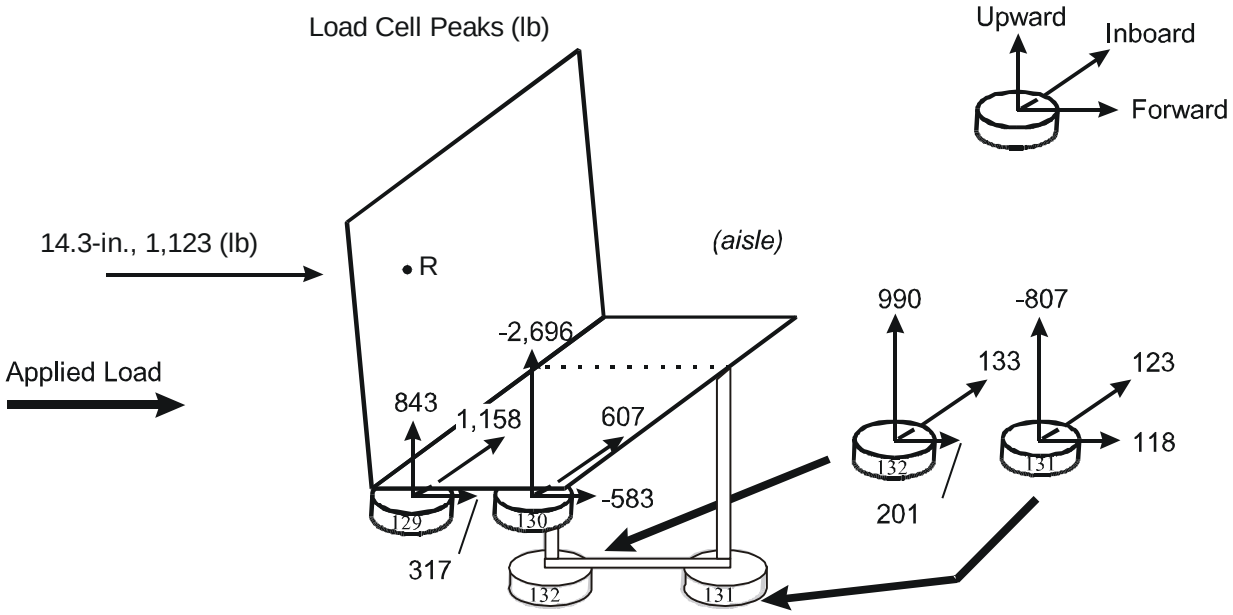

Figure B16. Walkover Static Test (Window Seat), Peak Seat Attachment Loads

APPENDIX C. DYNAMIC TEST RESULTS: DYNAMIC CRASH PULSES AND SEAT ATTACHMENT LOADS

DYNAMIC CRASH PULSES

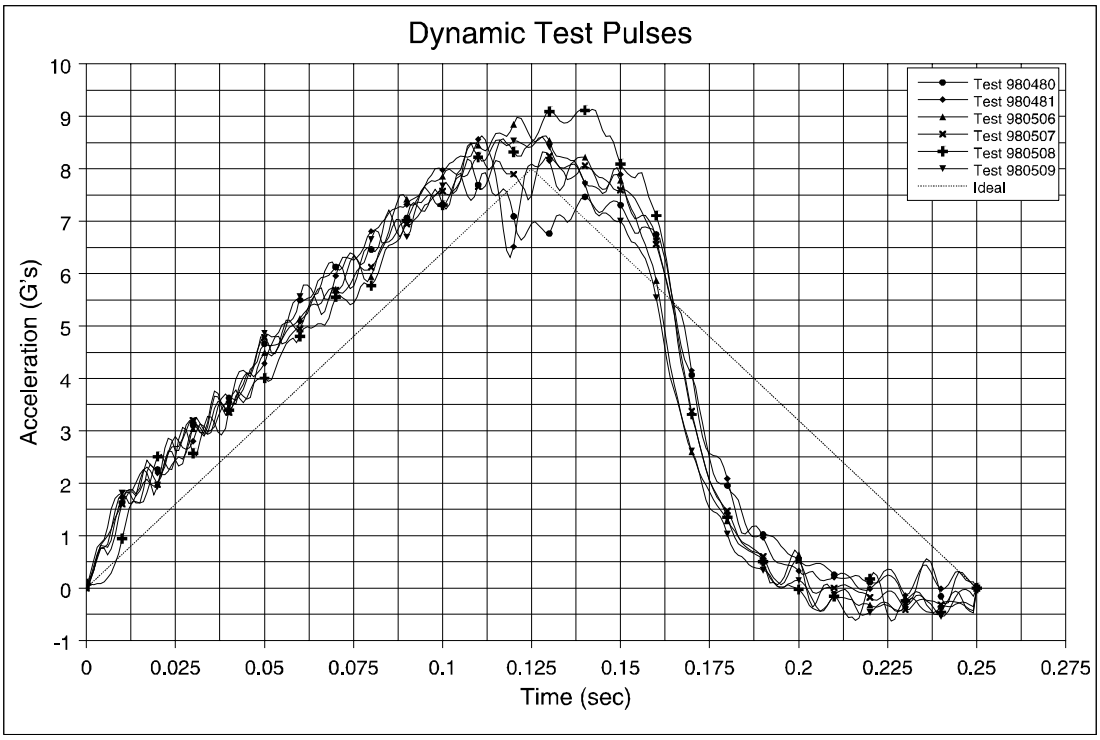

Figure C1. Crash Pulses for Each Dynamic Seat Test

SEAT ATTACHMENT LOADS (FROM DYNAMIC TESTING)

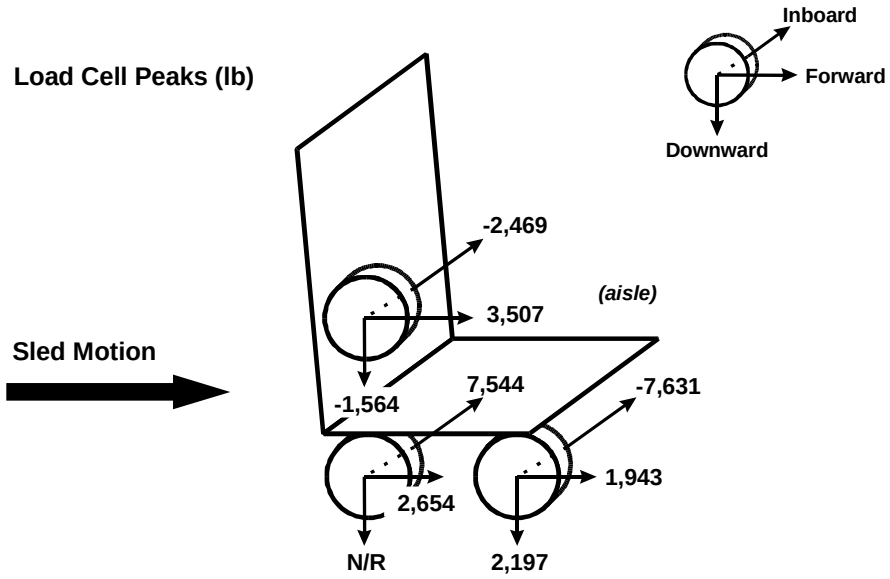

Figure C2. C-3 Seat Attachment Peak Loads, Type 1 Test (98-0480)

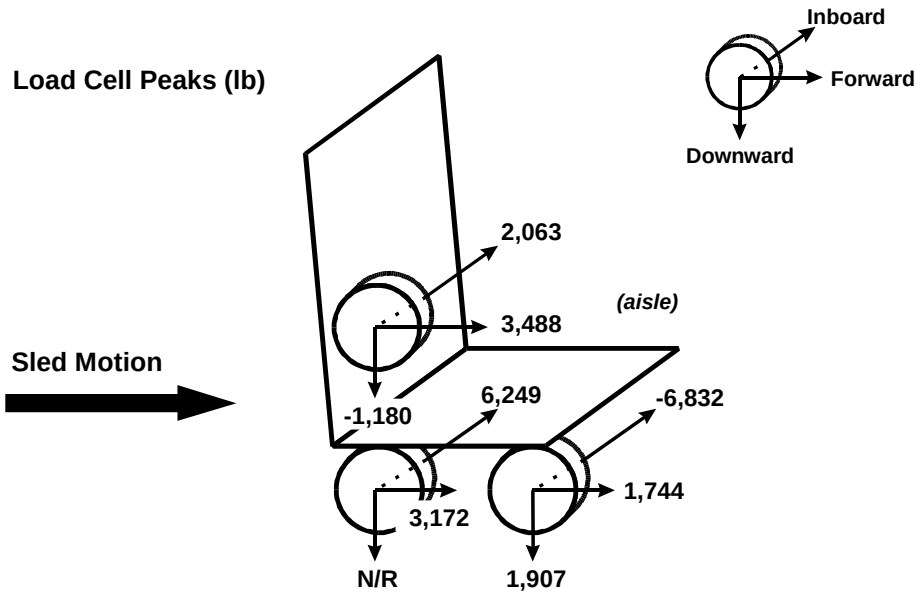

Figure C3. C-3 Seat Attachment Peak Loads, Type 2 Test (98-0481)

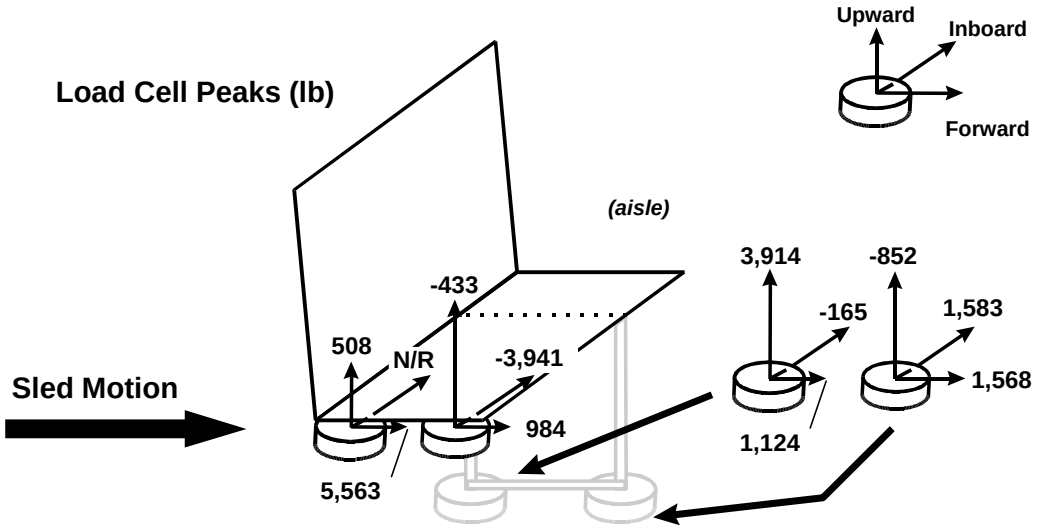

Figure C4. M-Style Seat Attachment Peak Loads, Type 1 Test (98-0507)

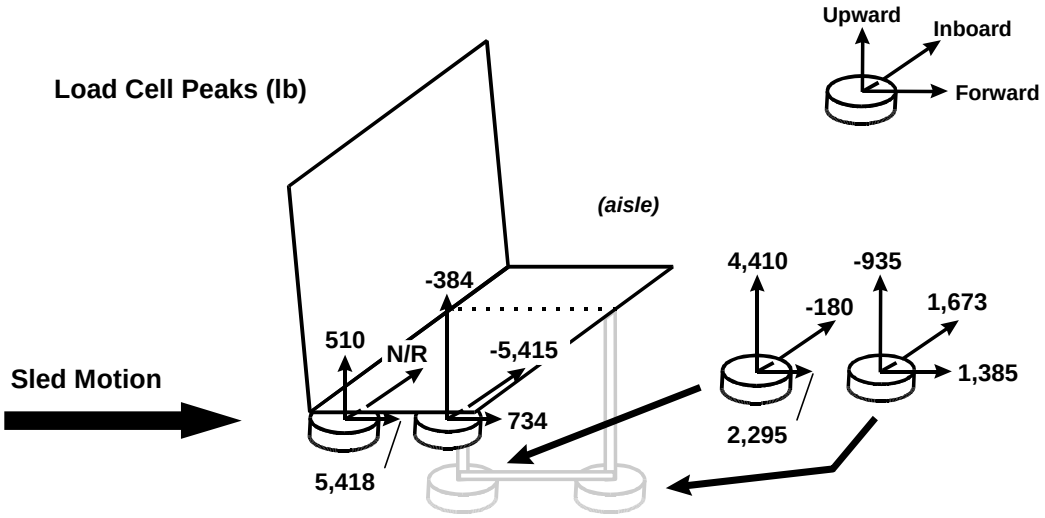

Figure C5. M-Style Seat Attachment Peak Loads, Type 2 Test (98-0506)

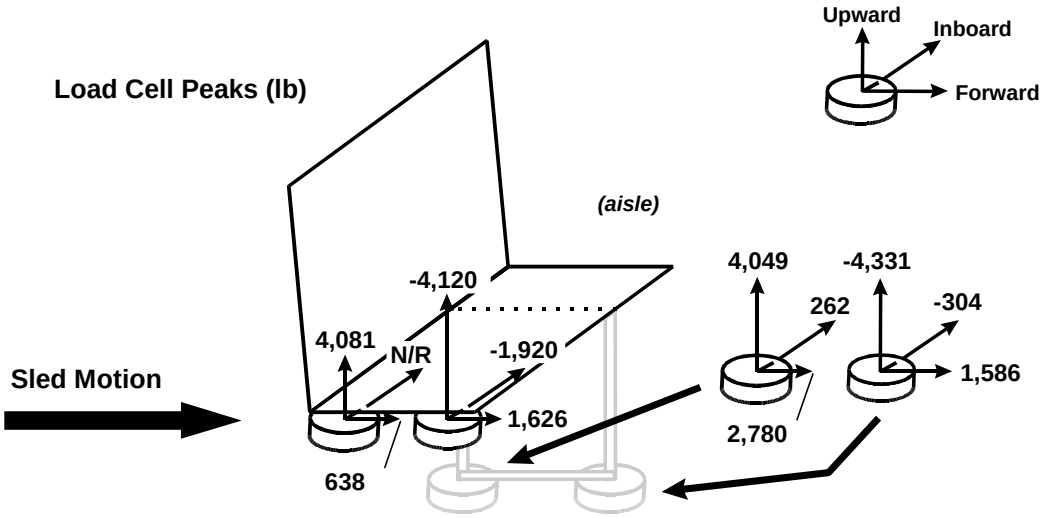

Figure C6. Walkover Seat Attachment Peak Loads, Type 1 Test (98-0508)

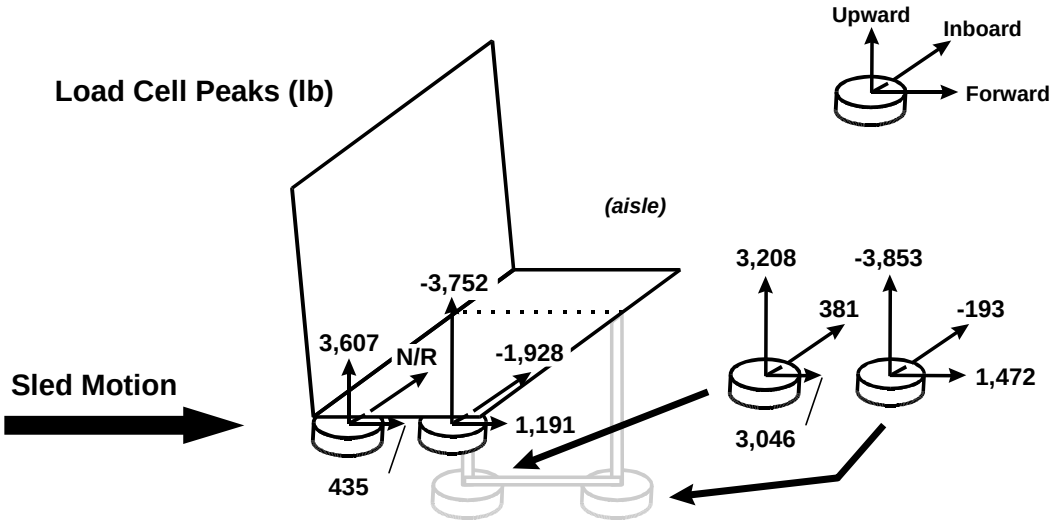

Figure C7. Walkover Seat Attachment Peak Loads, Type 2 Test (98-0509)

APPENDIX D. SIMULATION MODELING RESULTS

Table D1. 2 Passenger C-3 Seat

	HIC		3MS (G's)		F E M U R L O A D S (lbs)			
					Aisle Occupant		Window Occupant	
	Aisle	Wndw	Aisle	Wndw	L	R	L	R
34" Pitch								
50 50	396.7	517	31.04	28.02	-1.47E+03	-1.42E+03	-1.64E+03	-1.57E+03
50 50	339.2	435.7	26.19	21.95	-1.38E+03	-1.33E+03	-1.55E+03	-1.49E+03
0 5		664.1		34.15			-1.57E+03	-1.45E+03
95 5	358	664.1	34.17	34.15	-1.58E+03	-1.52E+03	-1.57E+03	-1.45E+03
95 0	358		34.17		-1.58E+03	-1.52E+03		
95 95	358	450.7	34.17	32.12	-1.58E+03	-1.52E+03	-1.74E+03	-1.66E+03
37" Pitch								
50 50	435.8	541	41.17	36.03	-1.89E+03	-1.82E+03	-2.13E+03	-2.05E+03
50 50	368.4	474.3	32.28	28.2	-1.70E+03	-1.63E+03	-1.93E+03	-1.84E+03
0 5		807.1		38.92			-1.80E+03	-1.68E+03
95 5	369.3	807.1	36.39	38.92	-2.16E+03	-2.08E+03	-1.80E+03	-1.68E+03
95 0	369.3		36.39		-2.16E+03	-2.08E+03		
95 95	369.3	444.6	36.39	35.1	-2.16E+03	-2.08E+03	-2.44E+03	-2.34E+03
48" Pitch								
50 50	537	642.9	55.56	52.05	-2.58E+03	-2.48E+03	-2.93E+03	-2.81E+03
50 50	429.9	541.5	41.03	38.03	-2.26E+03	-2.17E+03	-2.58E+03	-2.47E+03
0 5		879.2		48.99			-2.18E+03	-2.05E+03
95 5	408	879.2	48.8	48.99	-3.15E+03	-3.03E+03	-2.18E+03	-2.05E+03
95 0	408		48.8		-3.15E+03	-3.03E+03		
95 95	408	531.1	48.8	49.36	-3.15E+03	-3.03E+03	-3.65E+03	-3.50E+03

Note: All tests run at 8G, 250 msec pulse except the second 50 50 50 of each pitch which was run at 7G, 250 msec.

Table D2. 3 Passenger M-Style Seat

	HIC			3MS (G's)			F E M U R L O A D S (lbs)					
							Aisle Occupant		Middle Occupant		Window Occupant	
	Aisle	Middle	Wndw	Aisle	Middle	Wndw	L	R	L	R	L	R
34" Pitch												
50 50 50	218.8	219	218.9	35.8	35.8	35.8	-1.26E+03	-1.22E+03	-1.25E+03	-1.22E+03	-1.26E+03	-1.22E+03
50 50 50	155.6	155.3	155.6	31.6	31.5	31.6	-1.14E+03	-1.11E+03	-1.14E+03	-1.11E+03	-1.14E+03	-1.11E+03
0 0 5			214.5			42.8					-9.19E+02	-9.02E+02
95 50 5	197.9	219	214.5	25.2	35.8	42.8	-1.33E+03	-1.33E+03	-1.25E+03	-1.22E+03	-9.19E+02	-9.02E+02
50 50 05	218.8	219	214.5	35.8	35.8	42.8	-1.26E+03	-1.22E+03	-1.25E+03	-1.22E+03	-9.19E+02	-9.02E+02
95 0 0	197			24.9			-8.69E+02	-8.69E+02				
95 95 95	197	196.9	196.9	24.9	24.9	24.9	-8.69E+02	-8.69E+02	-8.69E+02	-8.68E+02	-8.69E+02	-8.69E+02
37" Pitch												
50 50 50	247.9	248.2	248	41.6	41.6	41.6	-1.43E+03	-1.41E+03	-1.43E+03	-1.41E+03	-1.43E+03	-1.41E+03
50 50 50	176.4	175.9	176.3	38.4	38.4	38.4	-1.33E+03	-1.31E+03	-1.33E+03	-1.31E+03	-1.33E+03	-1.31E+03
0 0 5			237			46.5					-1.26E+03	-1.23E+03
95 50 5	218.7	248.2	237	31.8	41.6	46.5	-1.67E+03	-1.67E+03	-1.43E+03	-1.41E+03	-1.26E+03	-1.23E+03
50 50 05	247.9	248.2	237	41.6	41.6	46.5	-1.43E+03	-1.41E+03	-1.43E+03	-1.41E+03	-1.26E+03	-1.23E+03
95 0 0	202.6			27.6			-1.50E+03	-1.50E+03				
95 95 95	202.6	202.5	202.3	27.6	27.6	27.6	-1.50E+03	-1.50E+03	-1.50E+03	-1.50E+03	-1.50E+03	-1.50E+03
48" Pitch												
50 50 50	237.9	237.9	237.9	45.5	45.5	45.5	-1.69E+03	-1.68E+03	-1.69E+03	-1.68E+03	-1.69E+03	-1.68E+03
50 50 50	153	153	152.9	40.6	40.6	40.6	-1.64E+03	-1.62E+03	-1.64E+03	-1.62E+03	-1.64E+03	-1.62E+03
0 0 5			262.2			52.8					-1.43E+03	-1.41E+03
95 50 5	236.8	237.9	262.2	37.7	45.5	52.8	-1.85E+03	-1.85E+03	-1.69E+03	-1.68E+03	-1.43E+03	-1.41E+03
50 50 05	237.9	237.9	262.2	45.5	45.5	52.8	-1.69E+03	-1.68E+03	-1.69E+03	-1.68E+03	-1.43E+03	-1.41E+03
95 0 0	236.8			37.7			-1.85E+03	-1.85E+03				
95 95 95	236.8	236.7	236.6	37.7	37.7	37.7	-1.85E+03	-1.85E+03	-1.85E+03	-1.85E+03	-1.85E+03	-1.85E+03

Note: All tests run at 8G, 250 msec pulse except the second 50 50 50 of each pitch which was run at 7G, 250 msec

Table D3. 3 Passenger Walkover Seat – Mid Lock Position

	HIC			3MS (G's)			FEMUR LOADS (lbs)					
							Aisle Occupant		Middle Occupant		Window Occupant	
	Aisle	Middle	Wndw	Aisle	Middle	Wndw	L	R	L	R	L	R
34" Pitch												
50 50 50	158.1	158.1	185.3	15.4	16.6	17.9	-5.41E+02	-5.63E+02	-5.42E+02	-5.30E+02	-5.81E+02	-5.28E+02
50 50 50	125.1	125.1	127.3	10.3	14.7	12.3	-4.96E+02	-5.19E+02	-5.12E+02	-4.86E+02	-5.31E+02	-4.86E+02
0 0 5			96.9			20.7					-7.37E+02	-7.64E+02
95 50 5	214.8	187.1	54.7	17.5	17.7	18.3	-6.30E+02	-6.27E+02	-5.27E+02	-5.30E+02	-7.64E+02	-7.84E+02
50 50 05	207	334.6	48.1	15.4	18.6	18.9	-5.57E+02	-5.95E+02	-5.61E+02	-5.31E+02	-7.63E+02	-7.85E+02
95 0 0	271.7			17.1			-6.29E+02	-6.41E+02				
95 95 95	188.6	214.4	209.7	20.7	16.3	21.8	-6.71E+02	-5.47E+02	-6.20E+02	-6.16E+02	-5.67E+02	-5.49E+02
37" Pitch												
50 50 50	213.7	213.7	214.1	19.5	15.8	16.2	-6.26E+02	-7.05E+02	-7.01E+02	-6.98E+02	-7.07E+02	-6.19E+02
50 50 50	170.6	170.6	193.6	12.9	13.5	14.5	-5.89E+02	-6.56E+02	-6.54E+02	-6.53E+02	-6.59E+02	-5.84E+02
0 0 5			109.2			33.4					-7.91E+02	-8.07E+02
95 50 5	258.3	277.4	41.3	17.3	17.9	21.4	-7.17E+02	-8.50E+02	-7.00E+02	-6.97E+02	-8.13E+02	-8.15E+02
50 50 05	296.7	277.4	46	12.3	20.1	23.7	-6.55E+02	-7.07E+02	-7.03E+02	-7.00E+02	-8.13E+02	-8.16E+02
95 0 0	249.5			18.3			-7.17E+02	-8.43E+02				
95 95 95	292.1	249.9	261.2	22.8	23.2	23.2	-7.61E+02	-8.20E+02	-7.11E+02	-7.19E+02	-8.30E+02	-8.07E+02
48" Pitch												
50 50 50	249.3	249.3	249.7	13.3	17.1	17.4	-9.11E+02	-8.86E+02	-9.02E+02	-8.89E+02	-9.05E+02	-8.95E+02
50 50 50	169.5	169.5	170.4	13.3	14.5	16.8	-8.49E+02	-8.33E+02	-8.35E+02	-8.36E+02	-8.39E+02	-8.42E+02
0 0 5			61.1			35.8					-8.91E+02	-9.13E+02
95 50 5	176.9	196.7	43.7	17.9	17.9	23.3	-7.32E+02	-9.08E+02	-9.01E+02	-8.88E+02	-9.03E+02	-9.25E+02
50 50 05	262	246.8	43.7	18.3	18.9	25.0	-9.12E+02	-8.87E+02	-9.03E+02	-8.90E+02	-9.02E+02	-9.24E+02
95 0 0	178.4			21.2			-7.27E+02	-9.08E+02				
95 95 95	227.7	350.8	222.1	24.6	21.1	22.4	-7.41E+02	-9.06E+02	-8.83E+02	-8.98E+02	-8.88E+02	-9.08E+02

Note: All tests run at 8G, 250 msec pulse except the second 50 50 50 of each pitch which was run at 7G, 250 msec

APPENDIX E. INJURY THRESHOLD COMPARISON TABLES FOR DYNAMIC TEST AND MODELING RESULTS

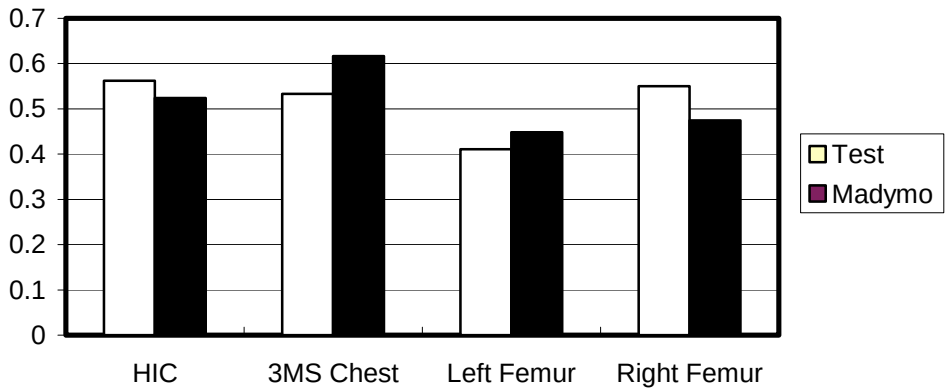

Figure E1. C-3 Seat - Type 1 Test Aisle Occupant - 50th-Percentile Hybrid II Male ATD

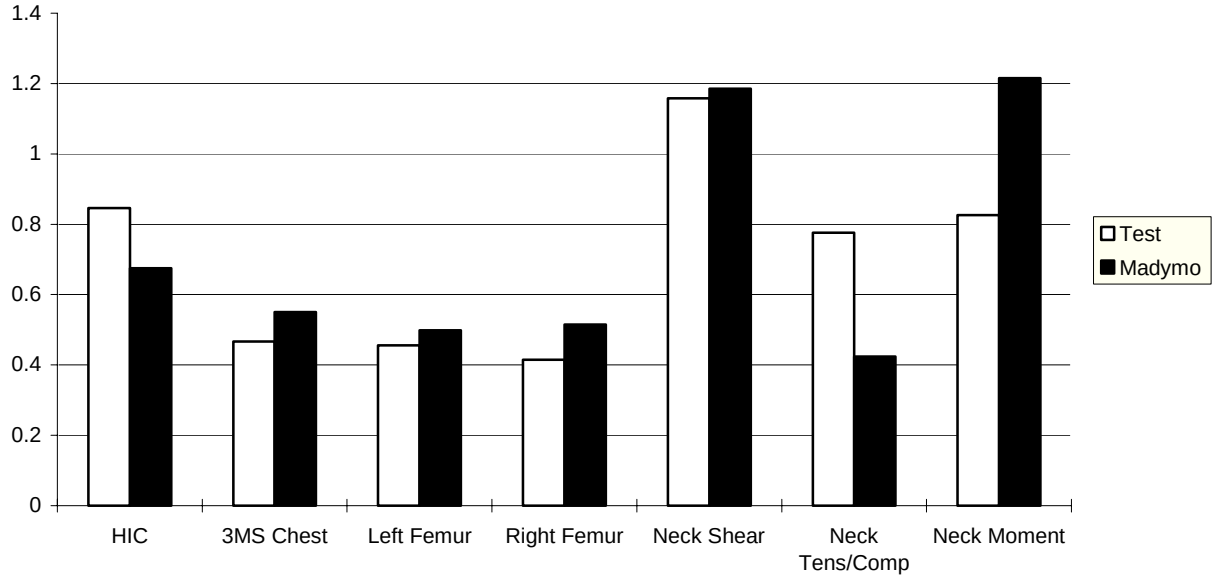

Figure E2. C-3 Seat – Type 1 Test Window Occupant - 50th-Percentile Hybrid III Male ATD

Figure E3. C-3 Seat – Type 2 Test Aisle occupant - 95th-Percentile Hybrid III Male ATD

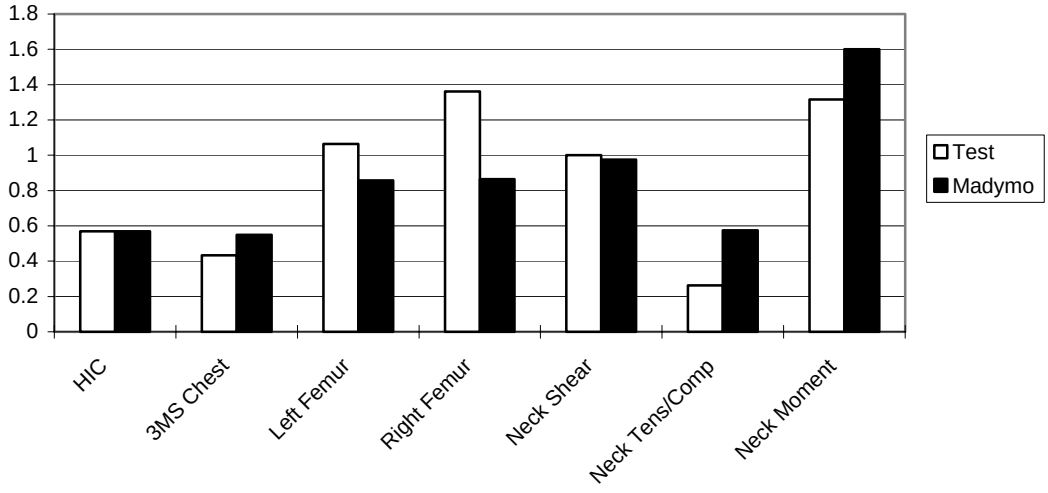

Figure E4. Window Occupant - 5th-Percentile Hybrid III Female ATD

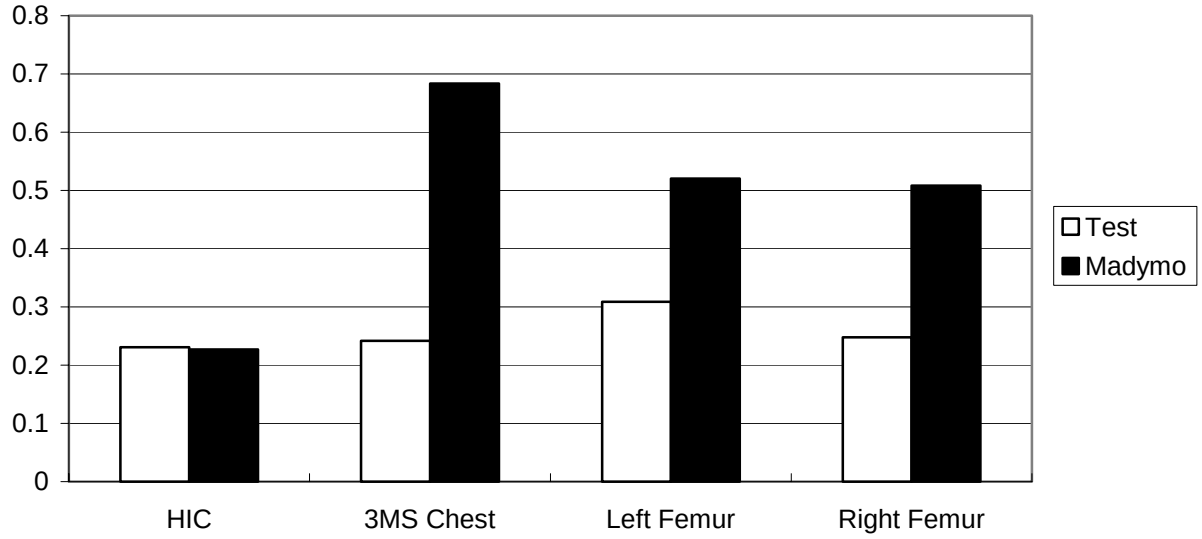

Figure E5. M-Style Seat -Type 1 Test Aisle Occupant - 50th-Percentile Hybrid II Male ATD

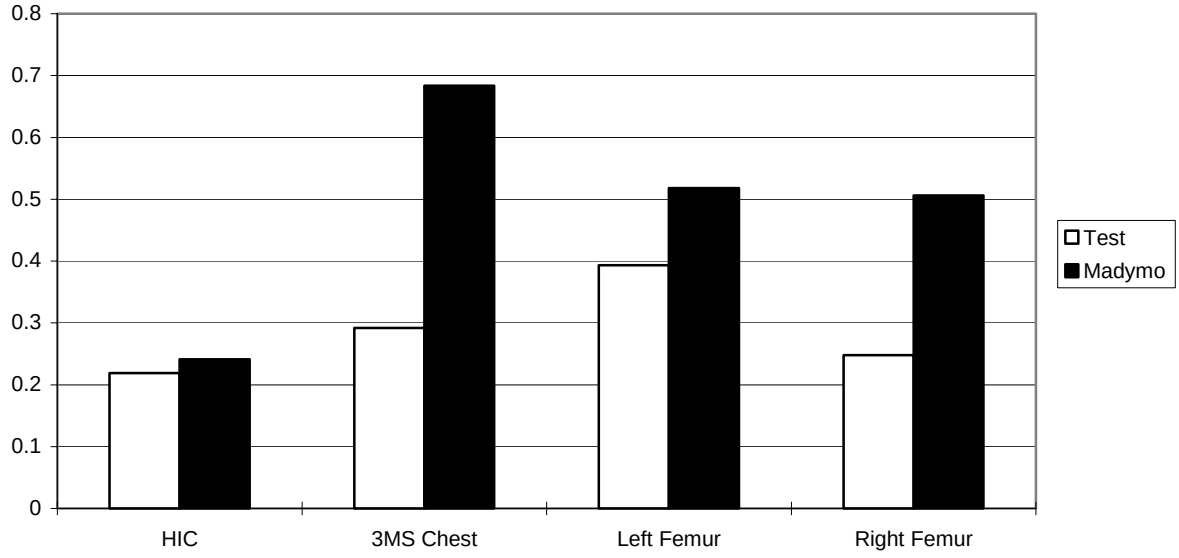

Figure E6. Center Occupant - 50th-Percentile Hybrid II Male ATD

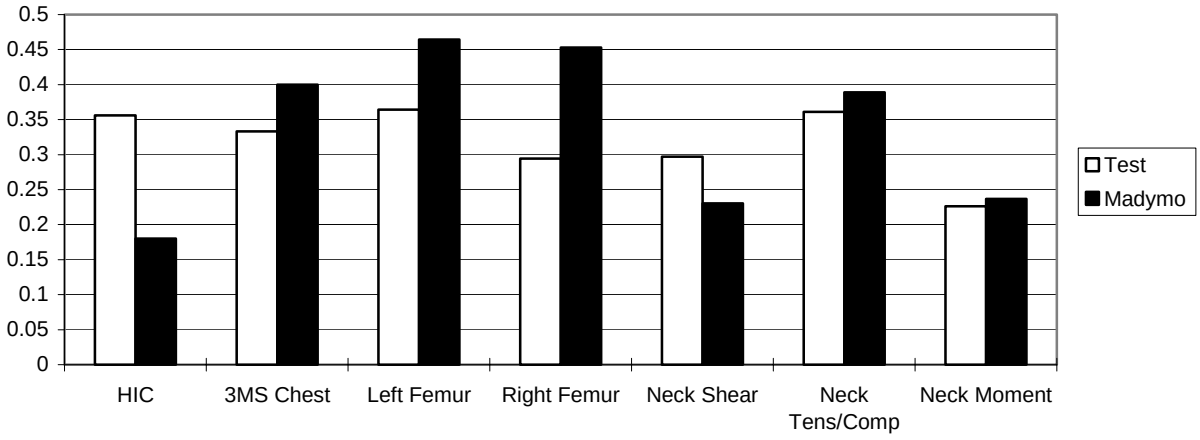

Figure E7. Window Occupant - 50th-Percentile Hybrid III Male ATD

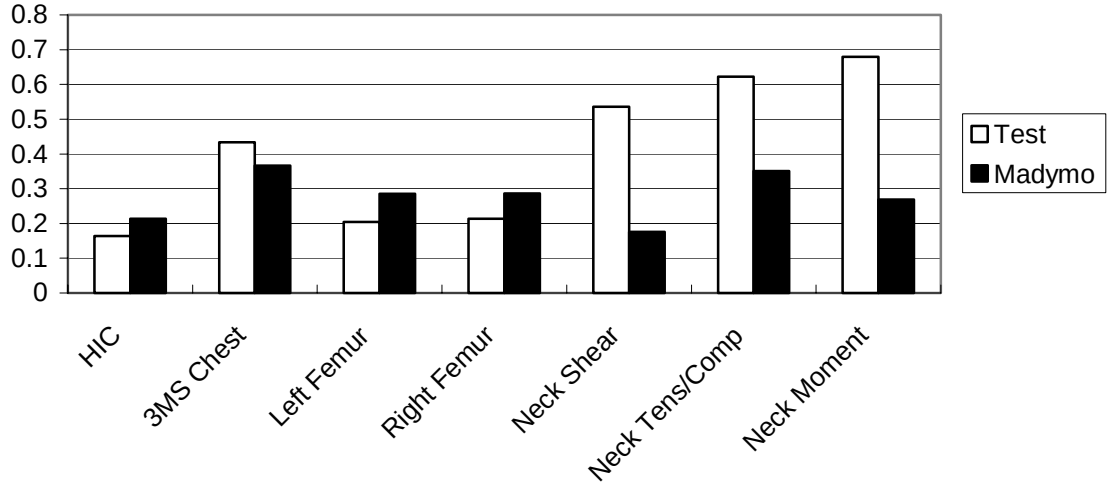

Figure E8. M-Style Seat - Type 2 Test Aisle Occupant - 95th-Percentile Hybrid III Male ATD

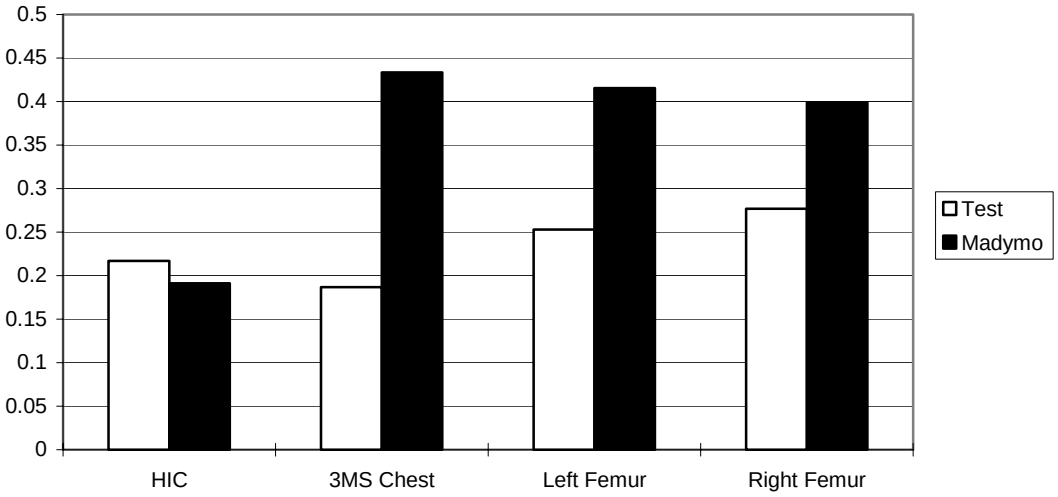

Figure E9. Center Occupant - 50th-Percentile Hybrid III Male ATD

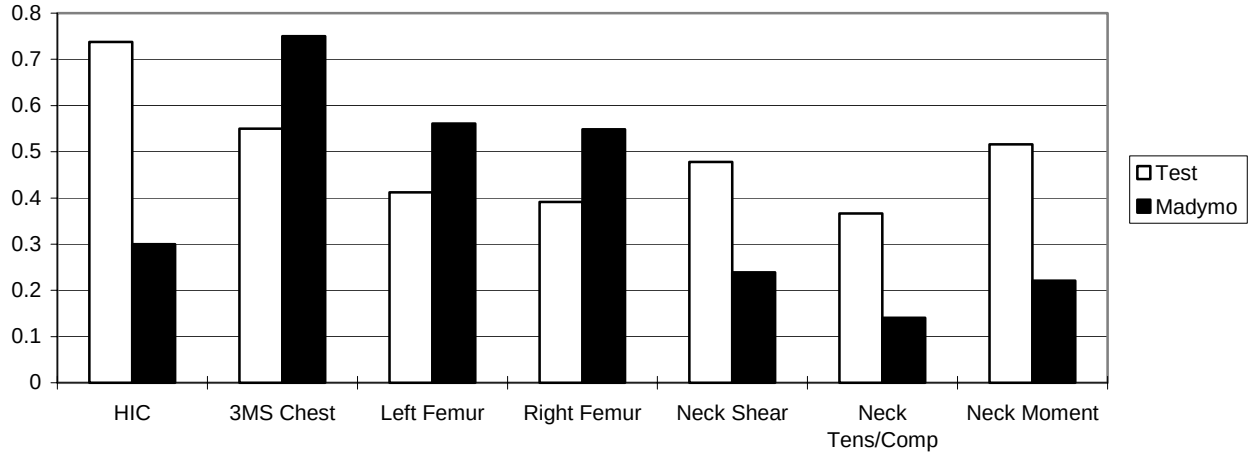

Figure E10. Window Occupant - 5th-Percentile Hybrid III Male ATD

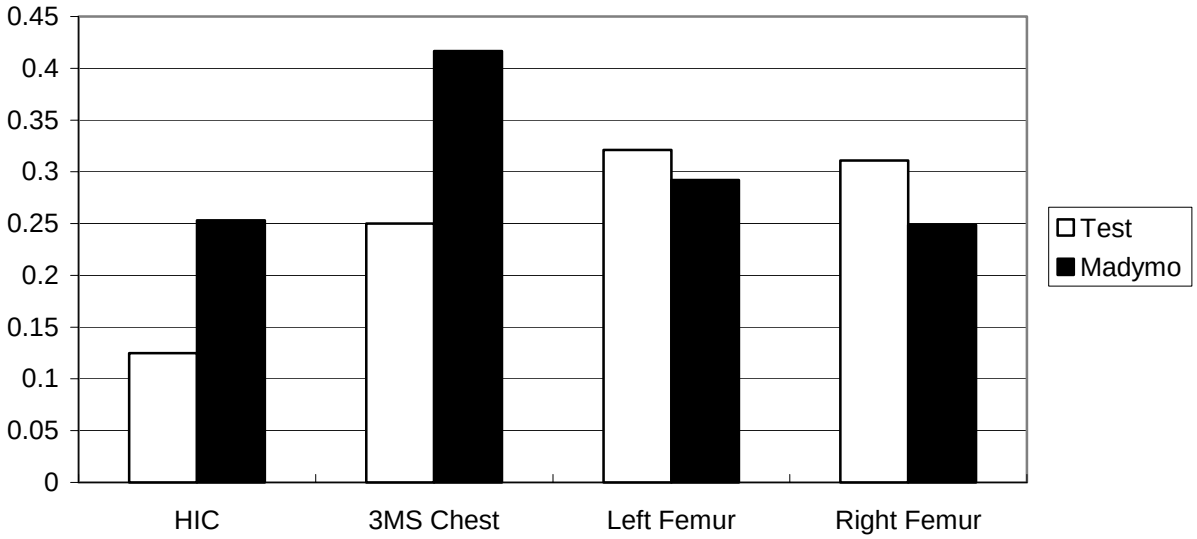

Figure E11. Walkover Seat - Type 1 Test Aisle Occupant - 50th-Percentile Hybrid II Male ATD

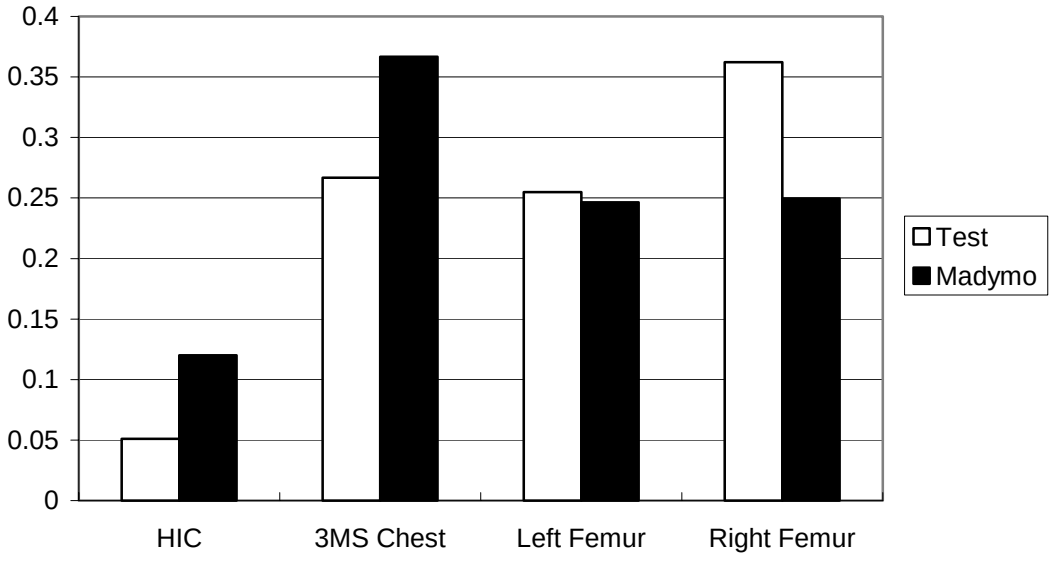

Figure E12. Center Occupant - 50th-Percentile Hybrid II Male ATD

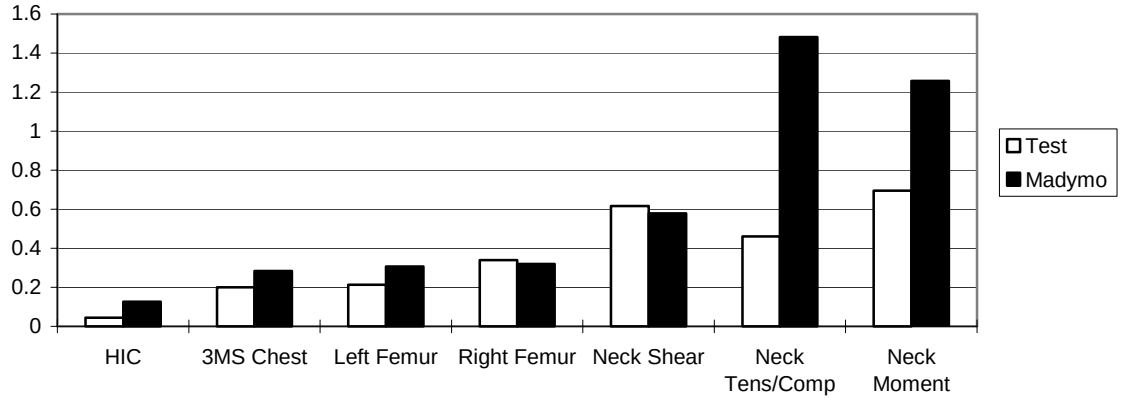

Figure E13. Window Occupant - 50th-Percentile Hybrid III Male ATD

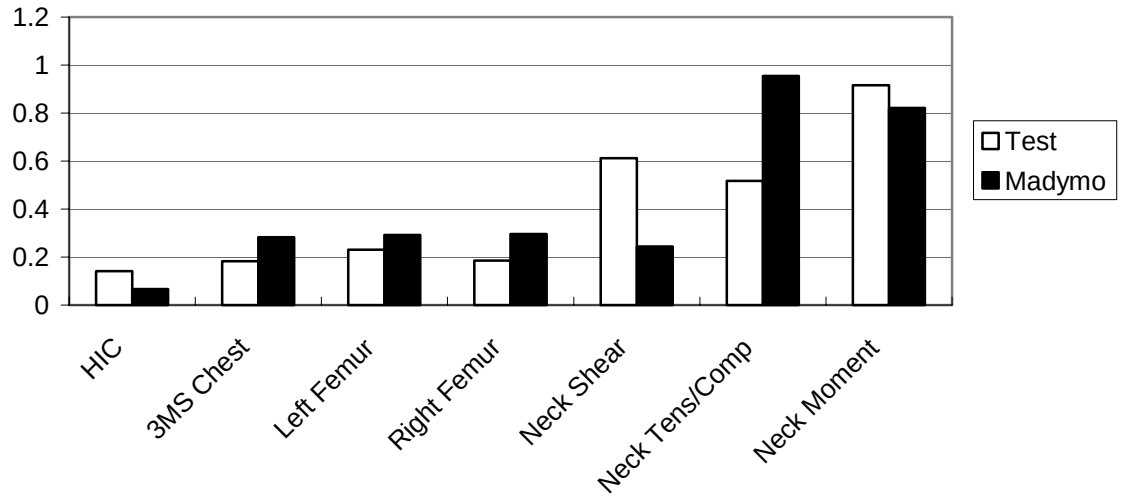

Figure E14. Walkover Seat - Type 2 Test Aisle Occupant - 95th-Percentile Hybrid III Male ATD

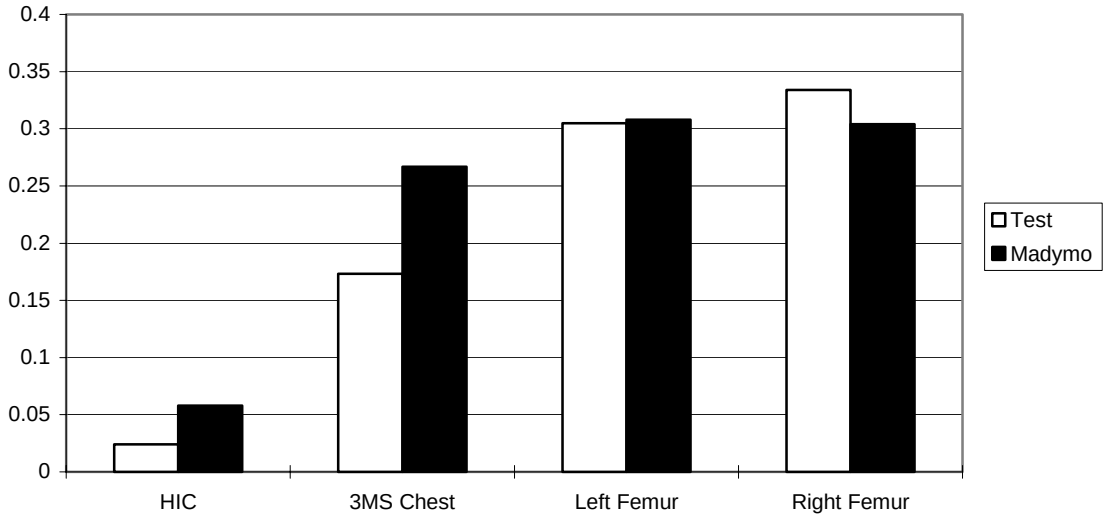

Figure E15. Center Occupant - 50th-Percentile Hybrid III Male ATD

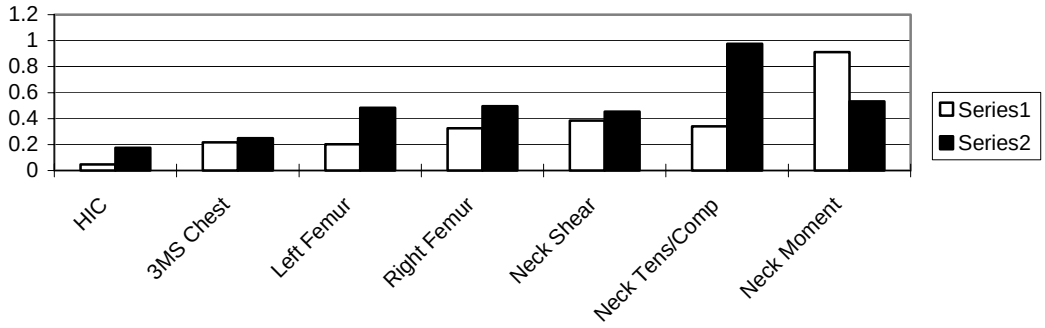

Figure E16. Window Occupant - 5th-Percentile Hybrid III Female ATD

APPENDIX F. CURVES OF TEST AND MODELING DATA FOR EACH DATA CHANNEL

(NOTE: For all graphs shown - Solid Line = Test, Dashed or Dotted Line = Model)

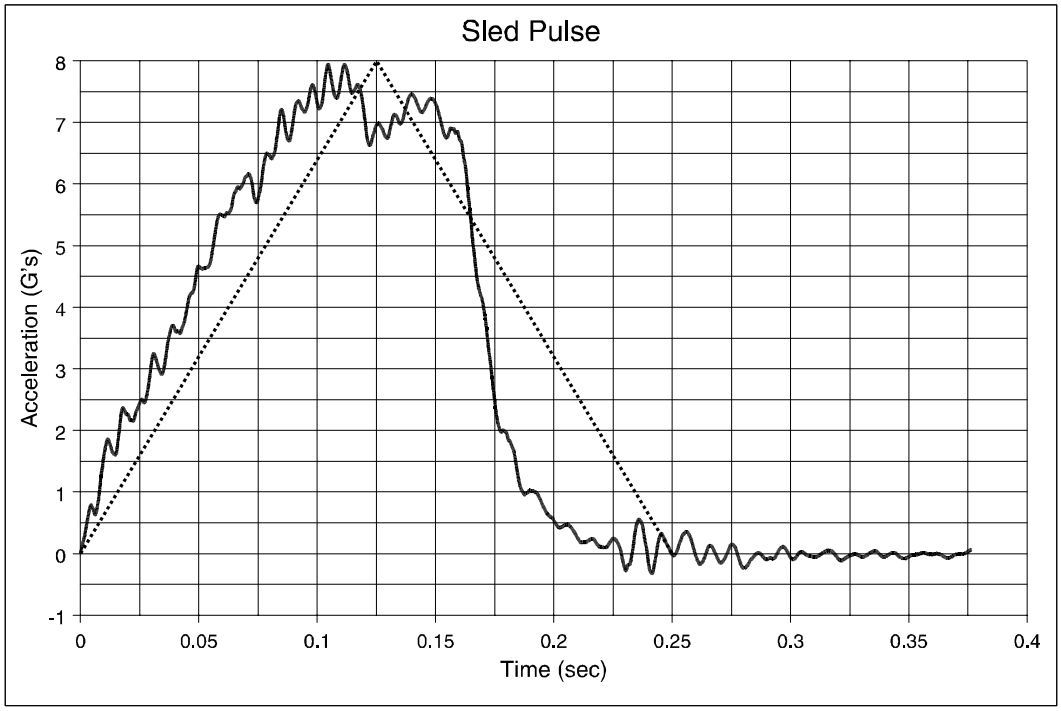

Figure F1. C-3 Seat, Type 1 Test, All 50th-Percentile ATDs: Sled Pulse

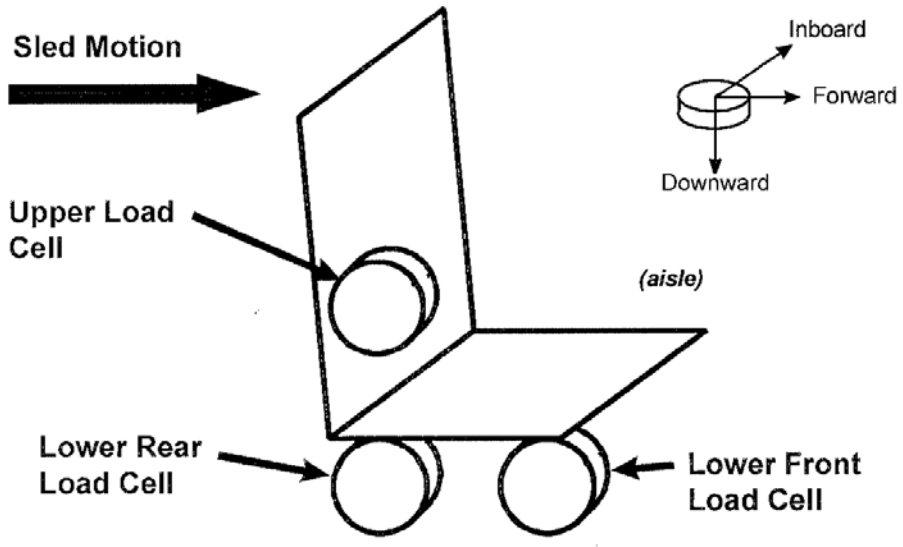

Figure F2. C-3 Seat, Type 1 Test, Seat Attachment Loads: Load Cell Orientation

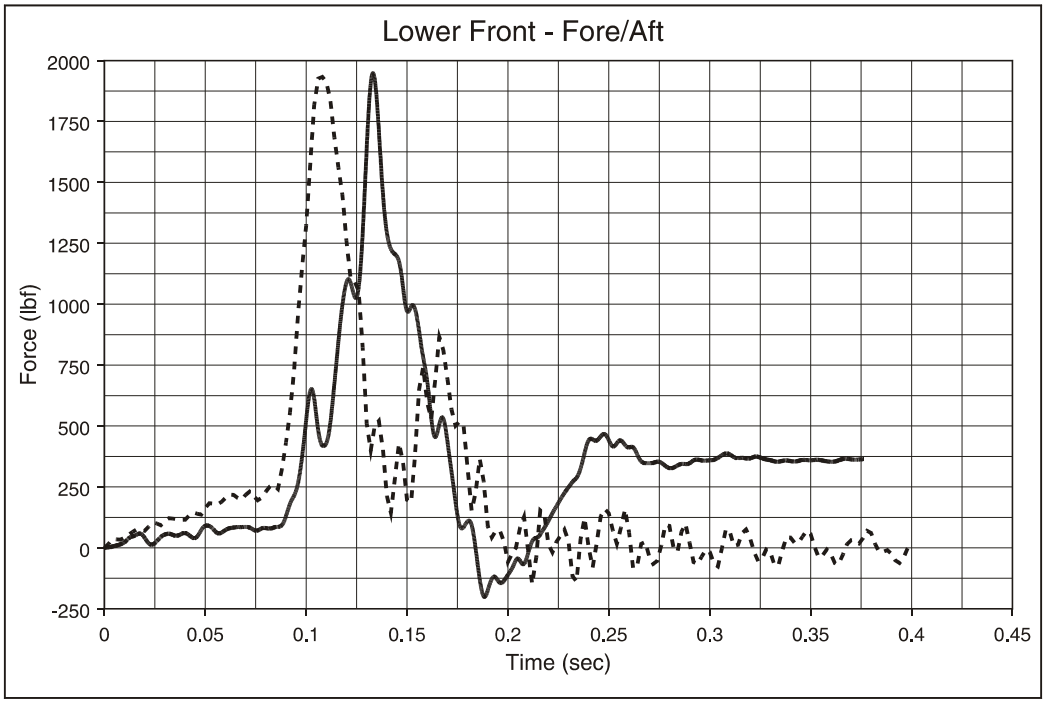

Figure F3. C-3 Seat, Type 1 Test, Seat Attachment Loads: Lower Front Load Cell, x Direction

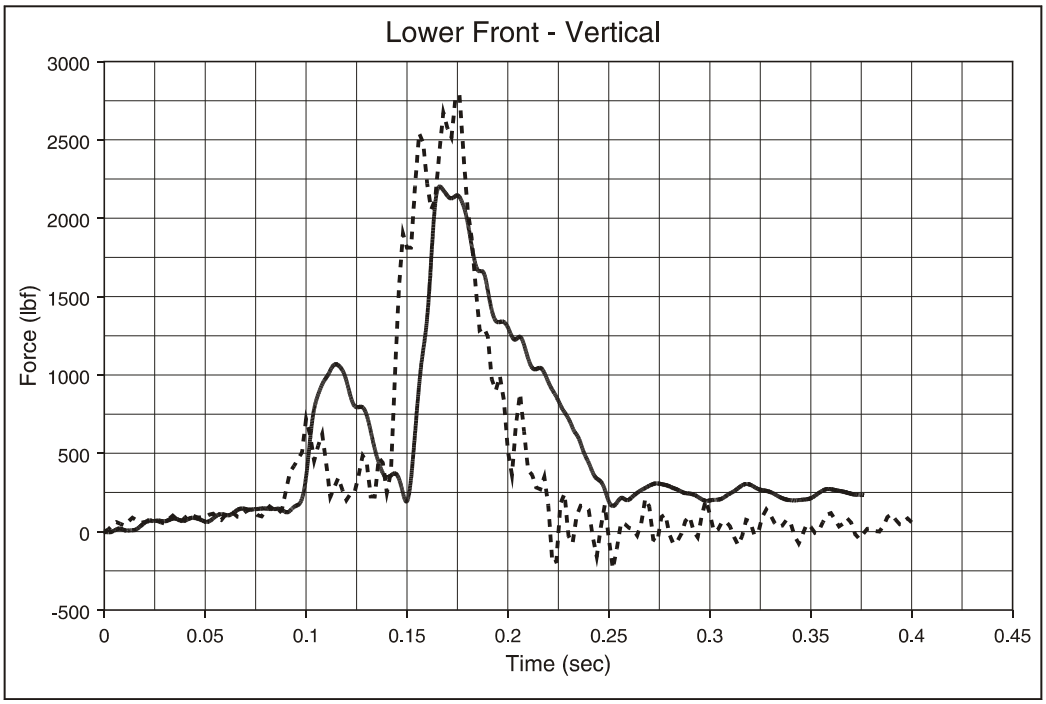

Figure F4. C-3 Seat, Type 1 Test, Seat Attachment Loads: Lower Front Load Cell, y Direction

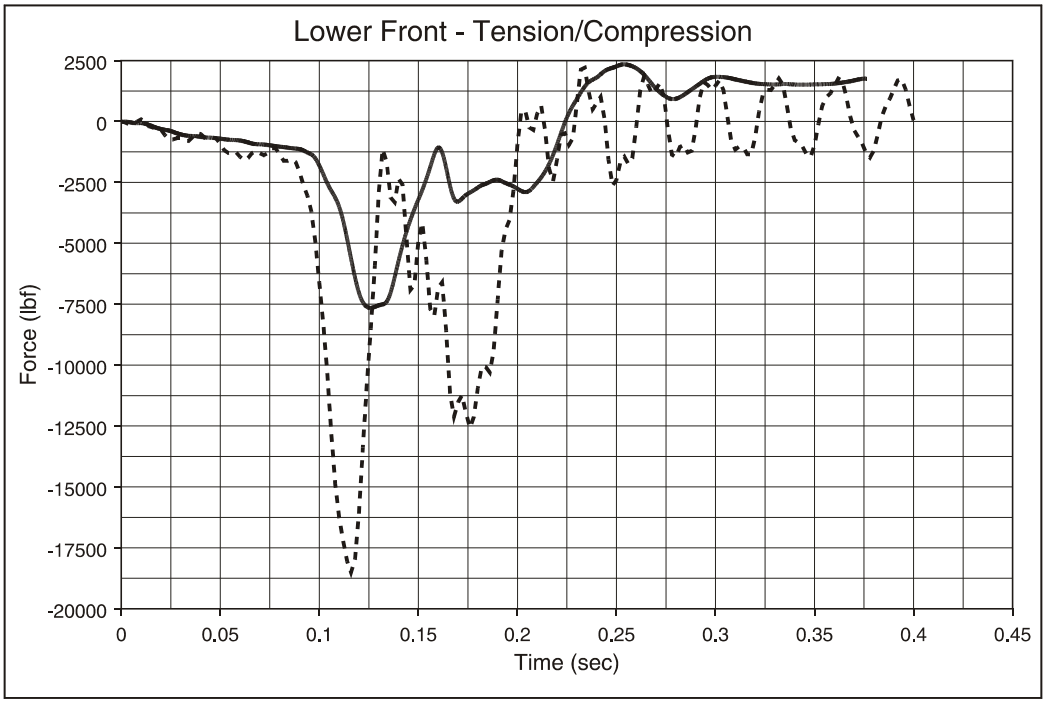

Figure F5. C-3 Seat, Type 1 Test, Seat Attachment Loads: Lower Front Load Cell, z Direction

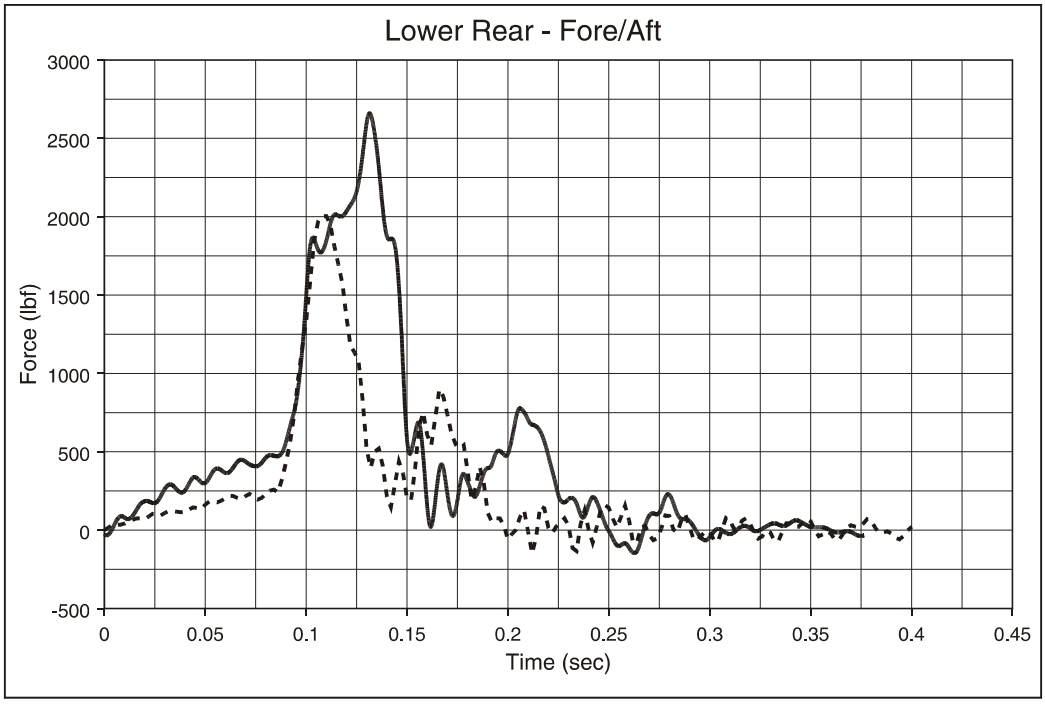

Figure F6. C-3 Seat, Type 1 Test, Seat Attachment Loads: Lower Rear Load Cell, x Direction

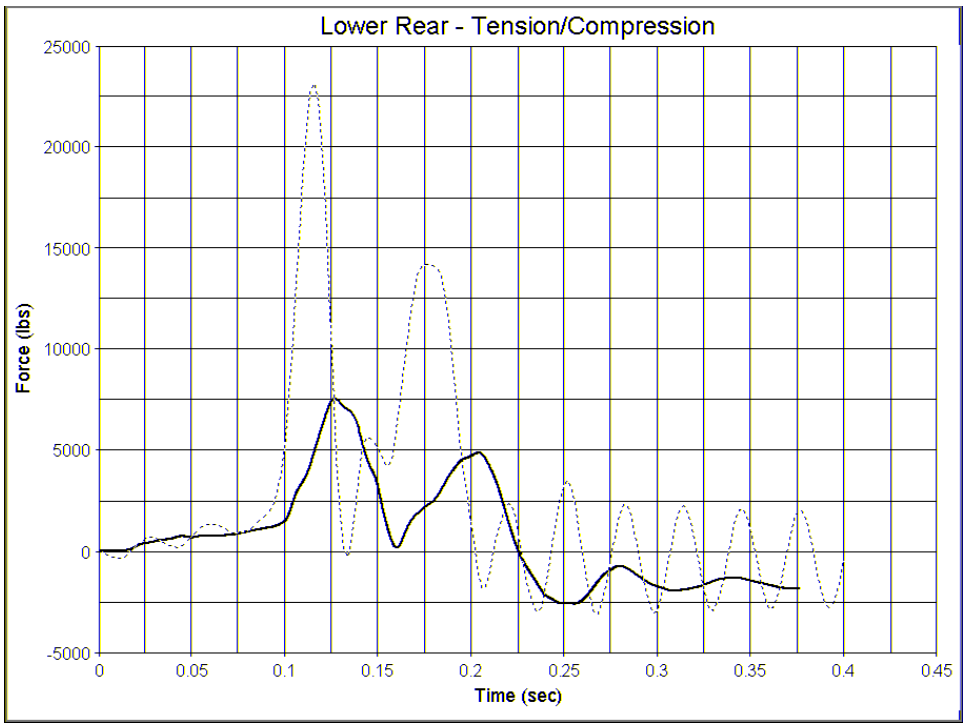

Figure F7. C-3 Seat, Type 1 Test, Seat Attachment Loads: Lower Rear Load Cell, z Direction

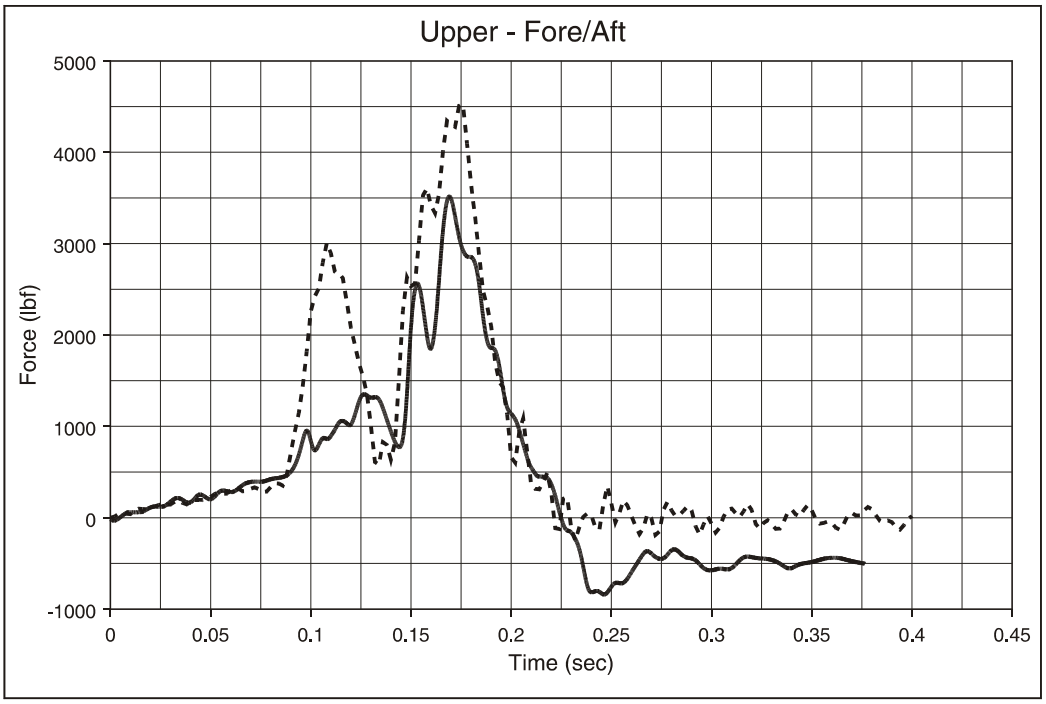

Figure F8. C-3 Seat, Type 1 Test, Seat Attachment Loads: Upper Load Cell, x Direction

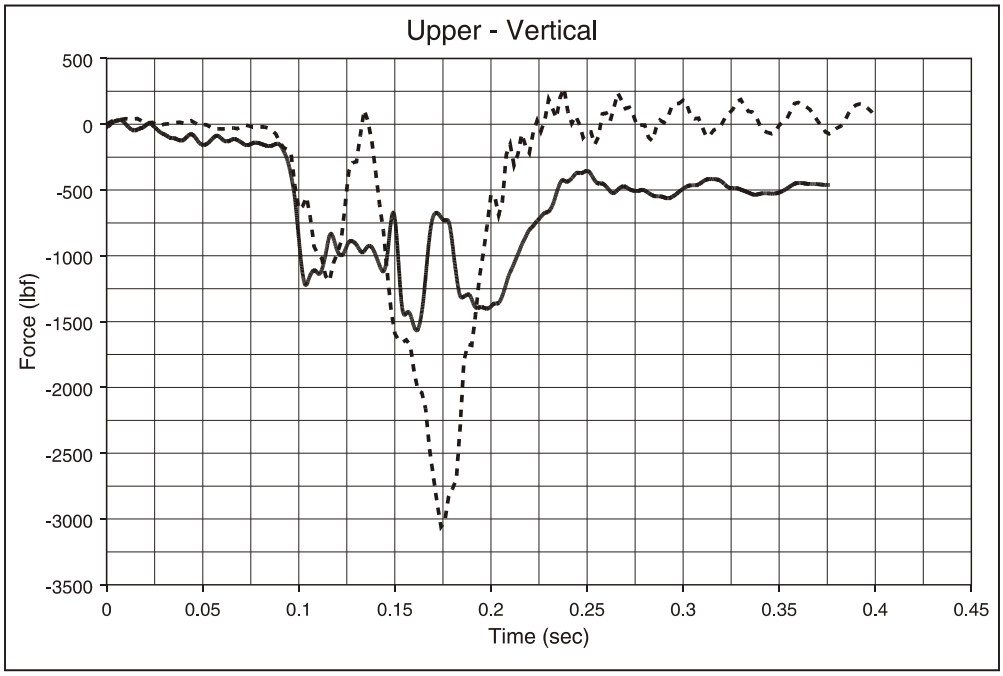

Figure F9. C-3 Seat, Type 1 Test, Seat Attachment Loads: Upper Load Cell, y Direction

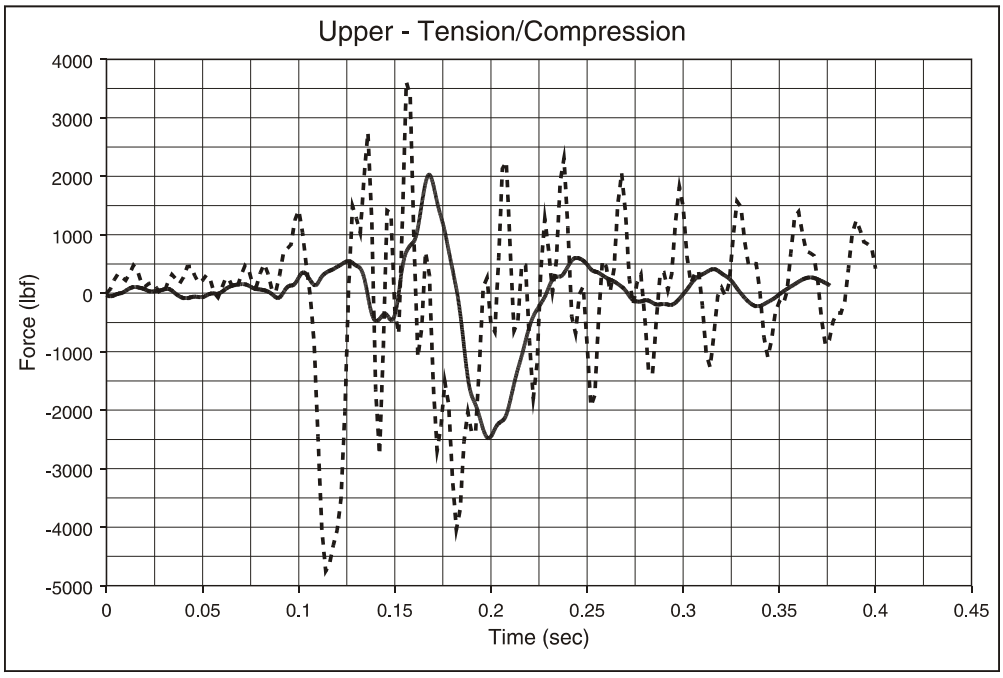

Figure F10. C-3 Seat, Type 1 Test, Seat Attachment Loads: Upper Load Cell, z Direction

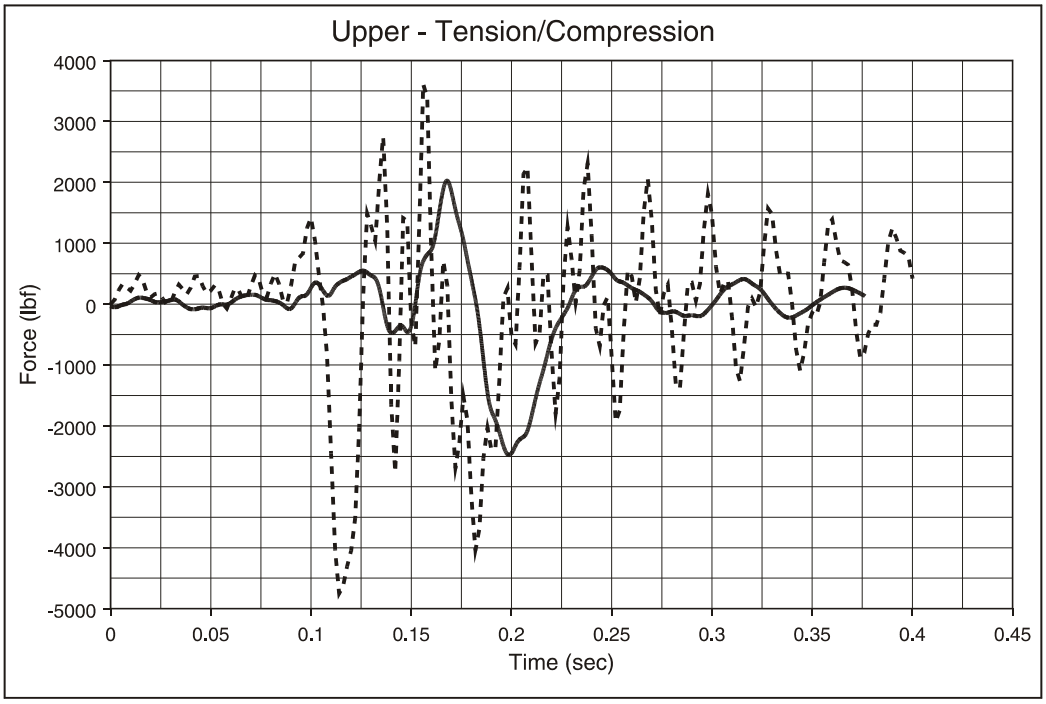

Figure F11. C-3 Seat, Type 1 Test, 50th-Percentile Hybrid II Male ATD, Aisle Seat: Chest Acceleration, x Direction

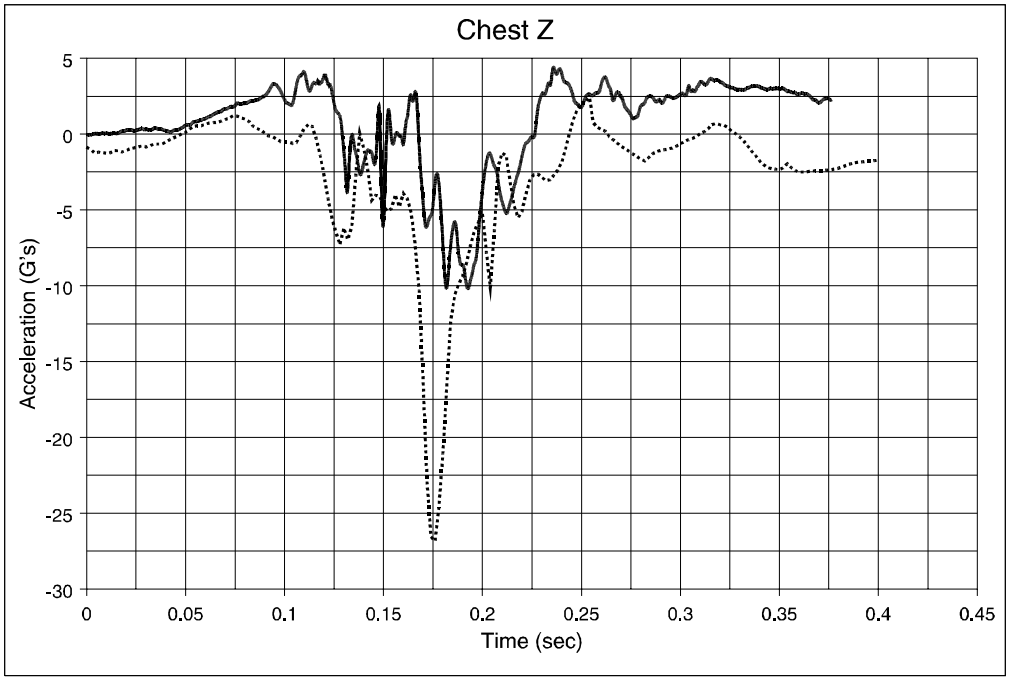

Figure F12. C-3 Seat, Type 1 Test, 50th-Percentile Hybrid II Male ATD, Aisle Seat: Chest Acceleration, y Direction (Left Occupant)

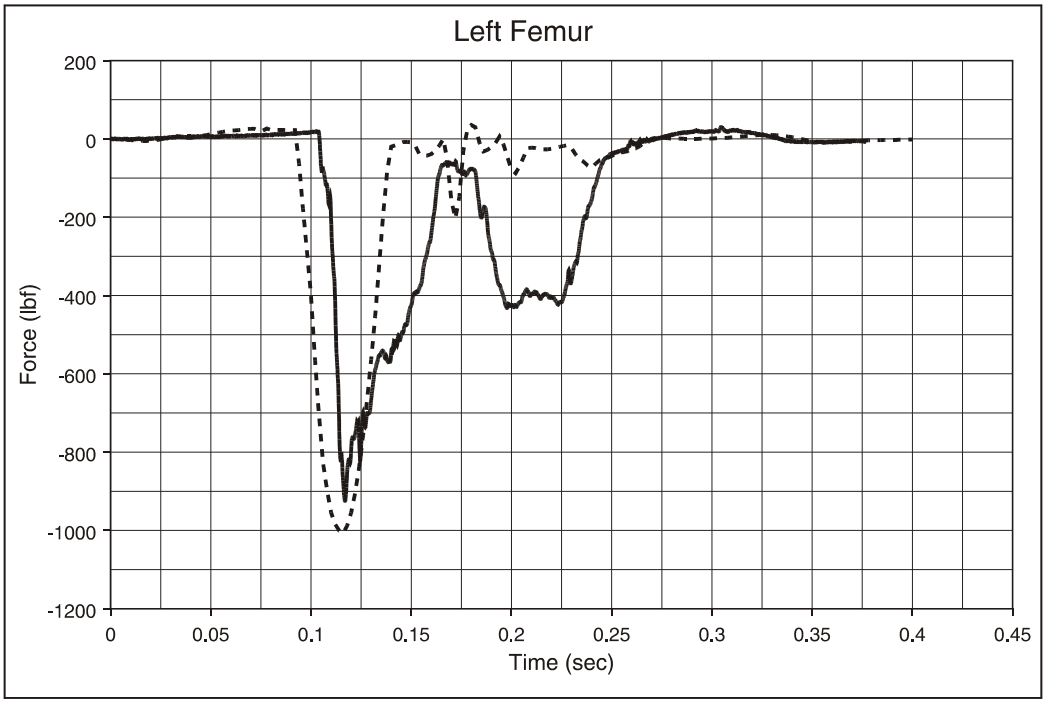

Figure F13. C-3 Seat, Type 1 Test, 50th-Percentile Hybrid II Male ATD, Aisle Seat: Left Femur Load (Left Occupant)

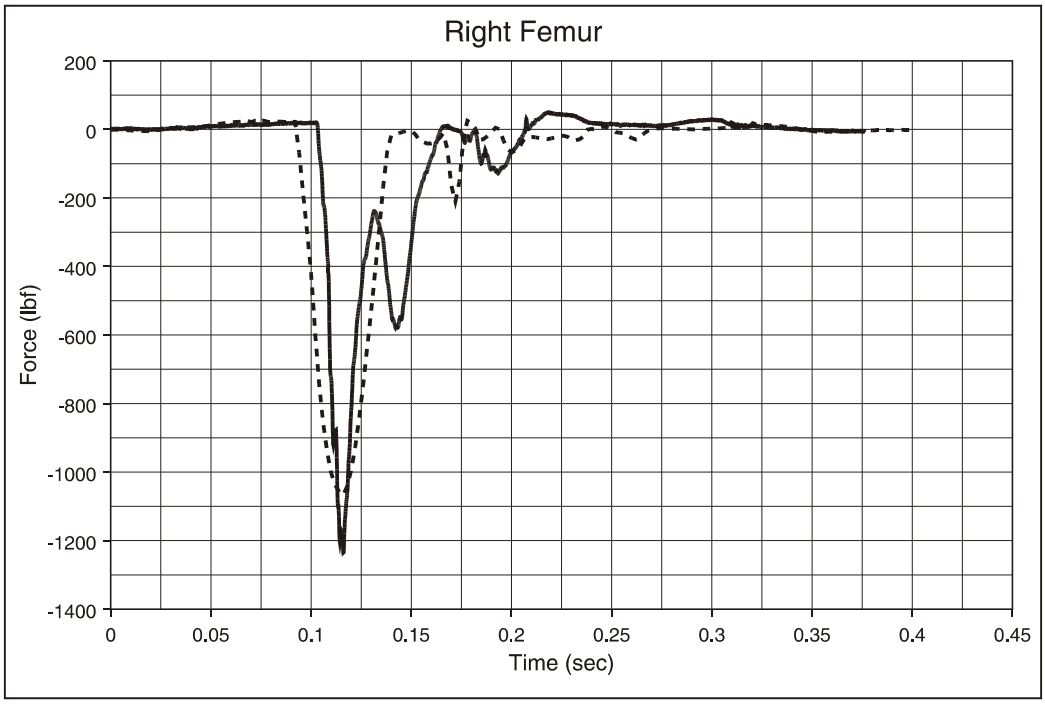

Figure F14. C-3 Seat, Type 1 Test, 50th-Percentile Hybrid II Male ATD, Aisle Seat: Right Femur Load (Left Occupant)

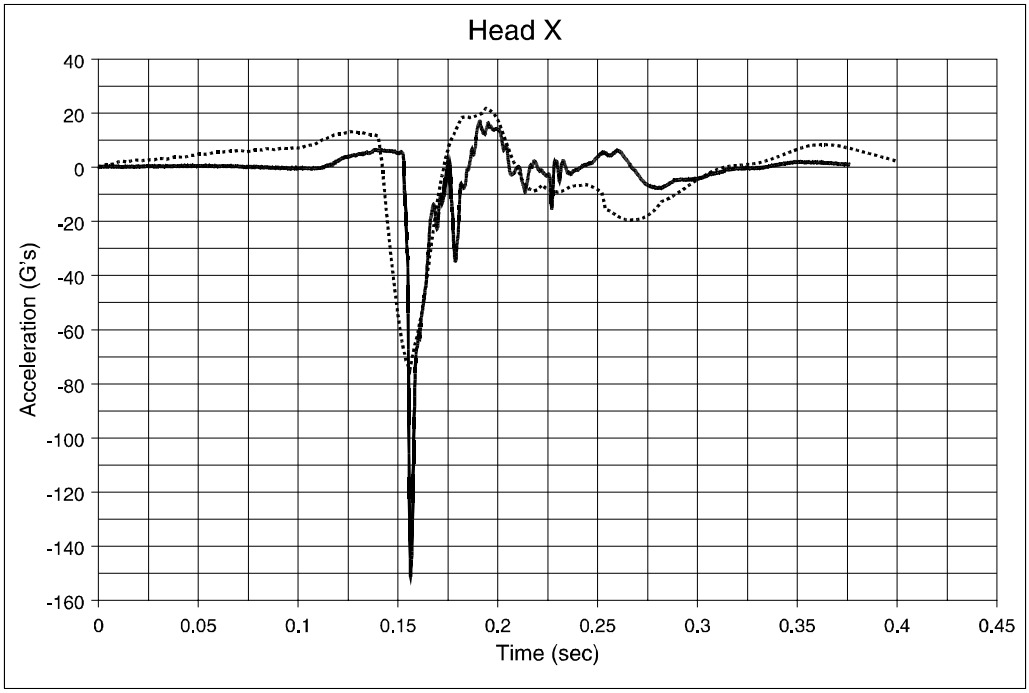

Figure F15. C-3 Seat, Type 1 Test, 50th-Percentile Hybrid II Male ATD, Aisle Seat: Head Acceleration, x Direction (Left Occupant)

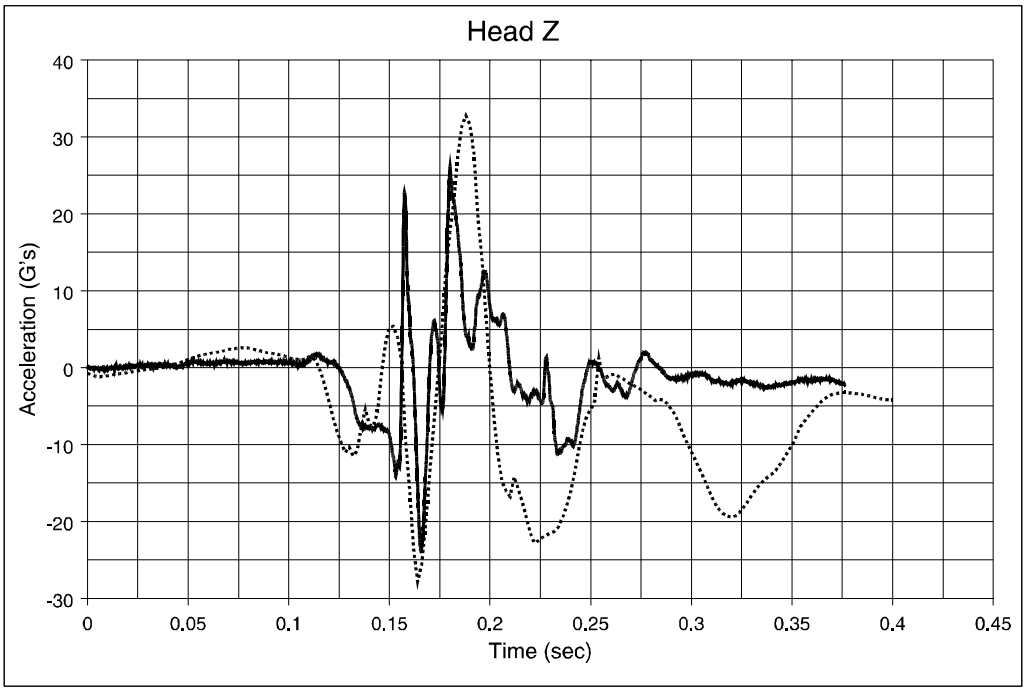

Figure F16. C-3 Seat, Type 1 Test, 50th-Percentile Hybrid II Male ATD, Aisle Seat: Head Acceleration, z Direction (Left Occupant)

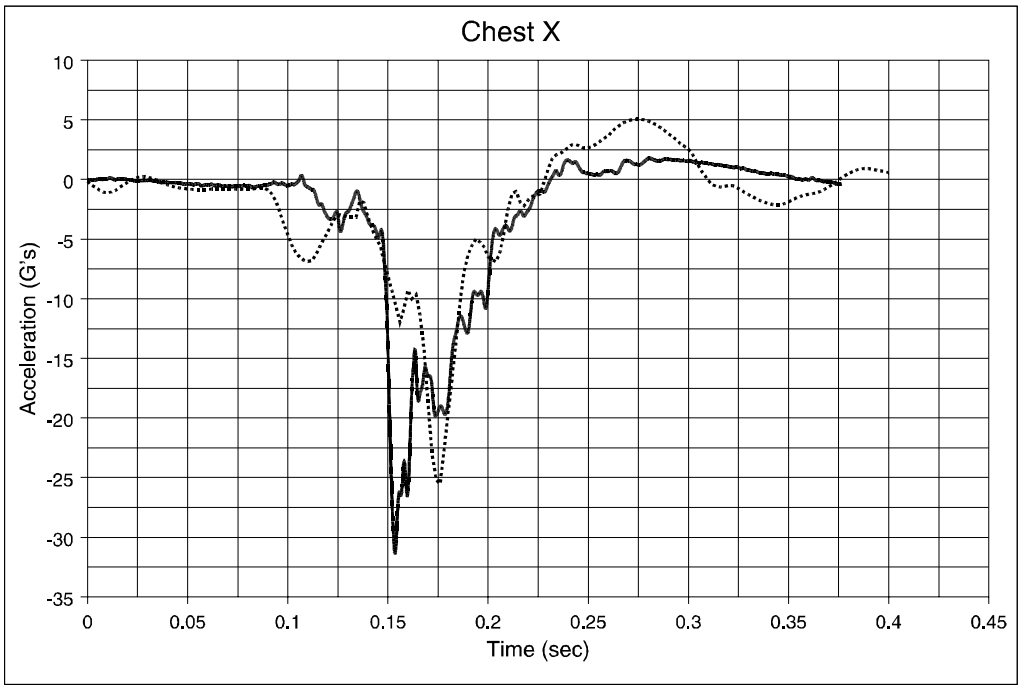

Figure F17. C-3 Seat, Type 1 Test, 50th-Percentile Hybrid III Male ATD, Window Seat: Chest Acceleration, x Direction (Right Ocupant)

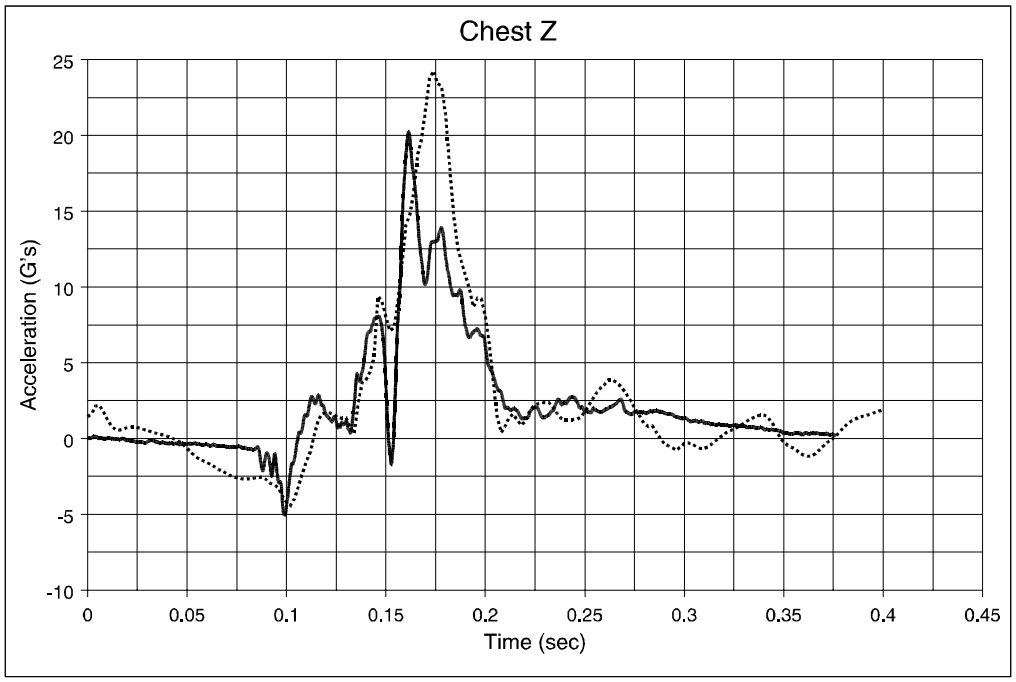

Figure F18. C-3 Seat, Type 1 Test, 50th-Percentile Hybrid III Male ATD, Window Seat: Chest Acceleration, z Direction (Right Occupant)

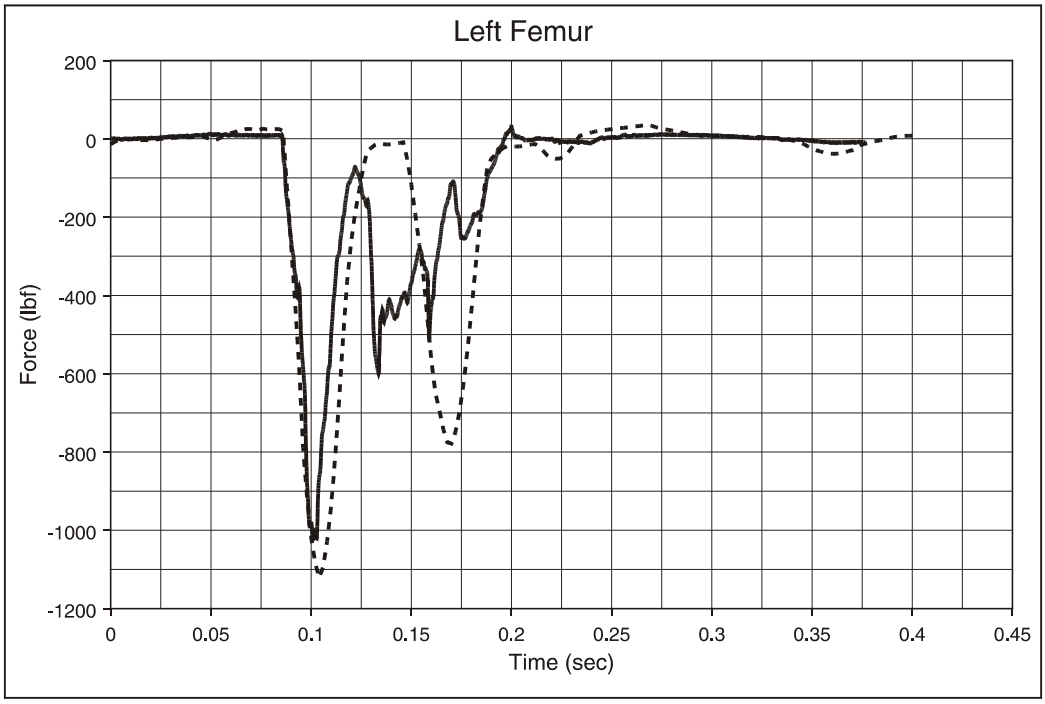

Figure F19. C-3 Seat, Type 1 Test, 50th-Percentile Hybrid III Male ATD, Window Seat: Left Femur Load (Right Occupant)

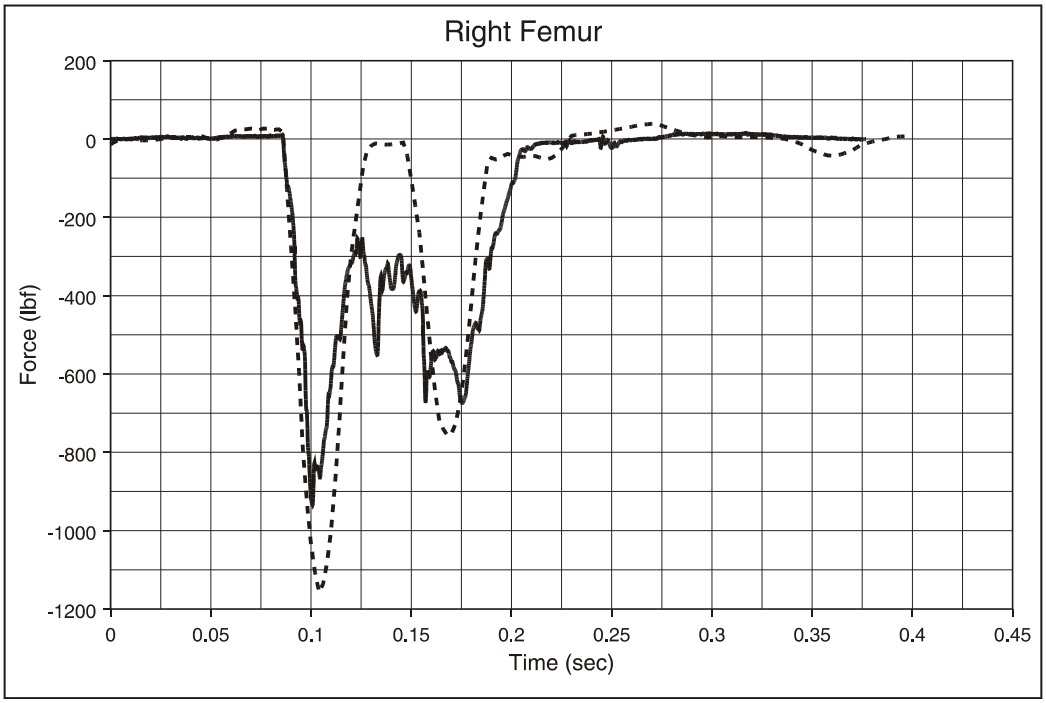

Figure F20. C-3 Seat, Type 1 Test, 50th-Percentile Hybrid III Male ATD, Window Seat: Right Femur Load (Right Occupant)

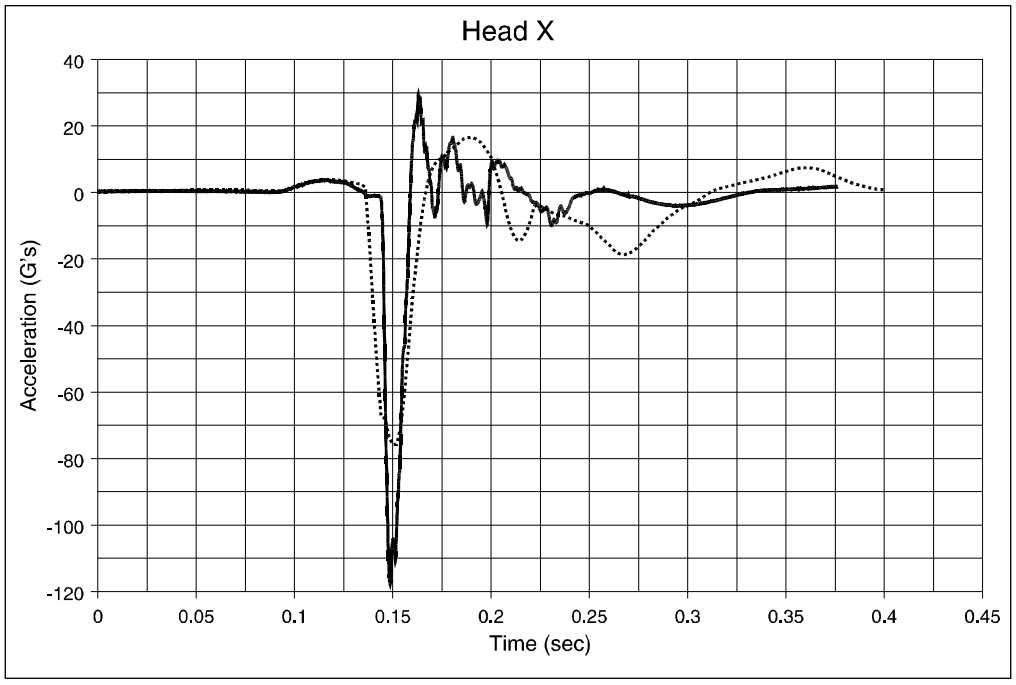

Figure F21. C-3 Seat, Type 1 Test, 50th-Percentile Hybrid III Male ATD, Window Seat: Head Acceleration, x Direction (Right Occupant)

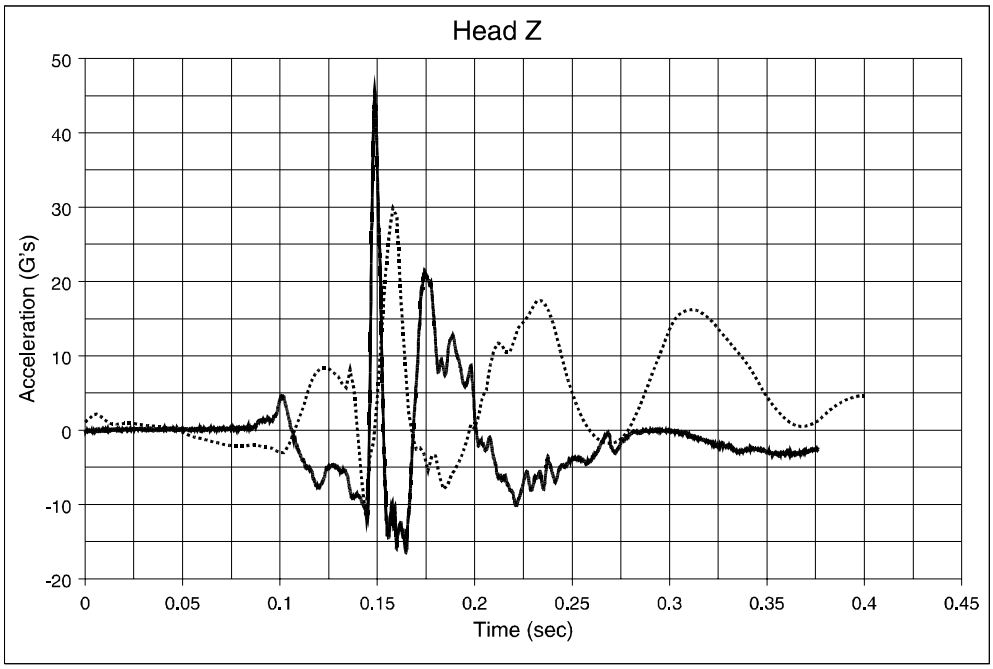

Figure F22. C-3 Seat, Type 1 Test, 50th-Percentile Hybrid III Male ATD, Window Seat: Head Acceleration, z Direction (Right Occupant)

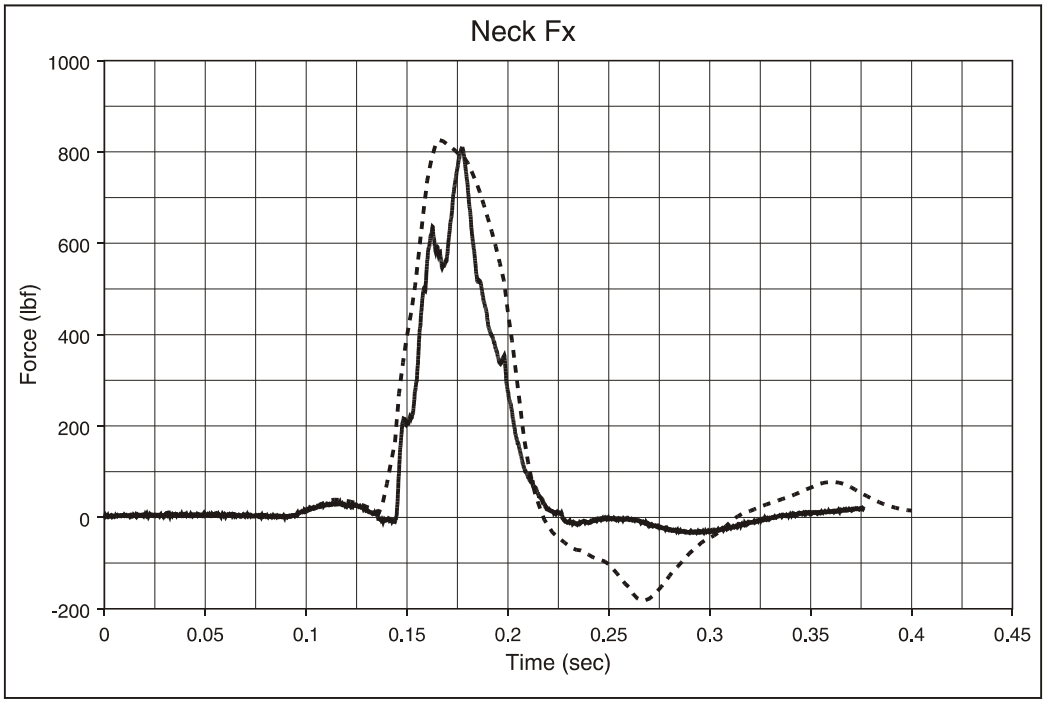

Figure F23. C-3 Seat, Type 1 Test, 50th-Percentile Hybrid III Male ATD, Window Seat: Neck Shear Load (Right Occupant)

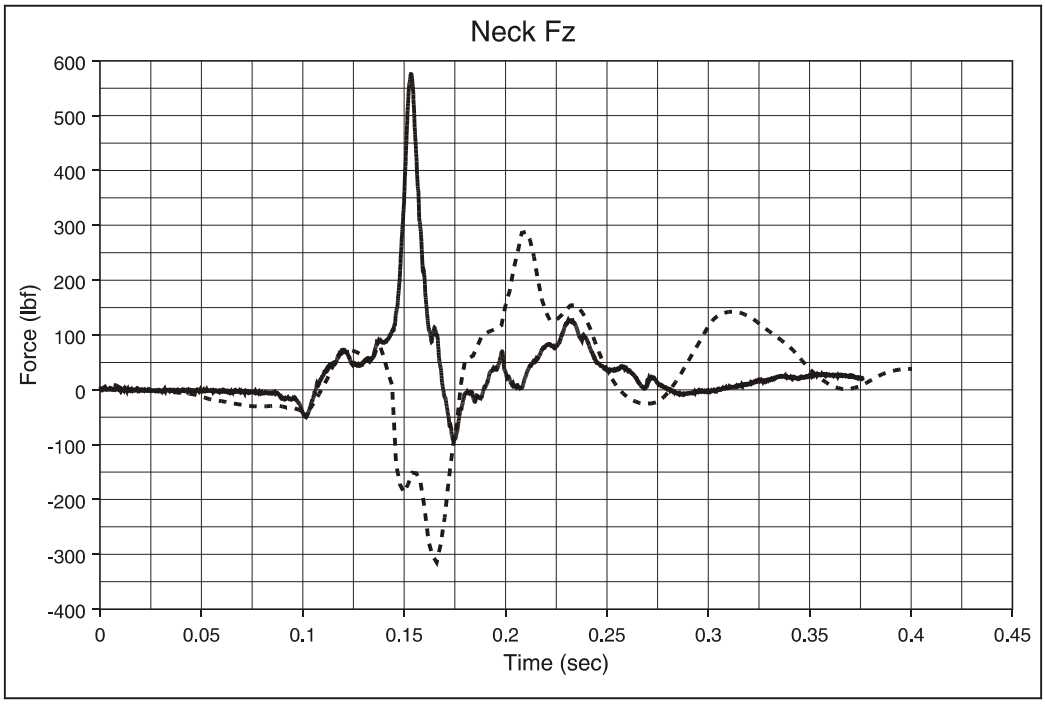

Figure F24. C-3 Seat, Type 1 Test, 50th-Percentile Hybrid III Male ATD, Window Seat: Neck Compression/Tension Load (Right Occupant)

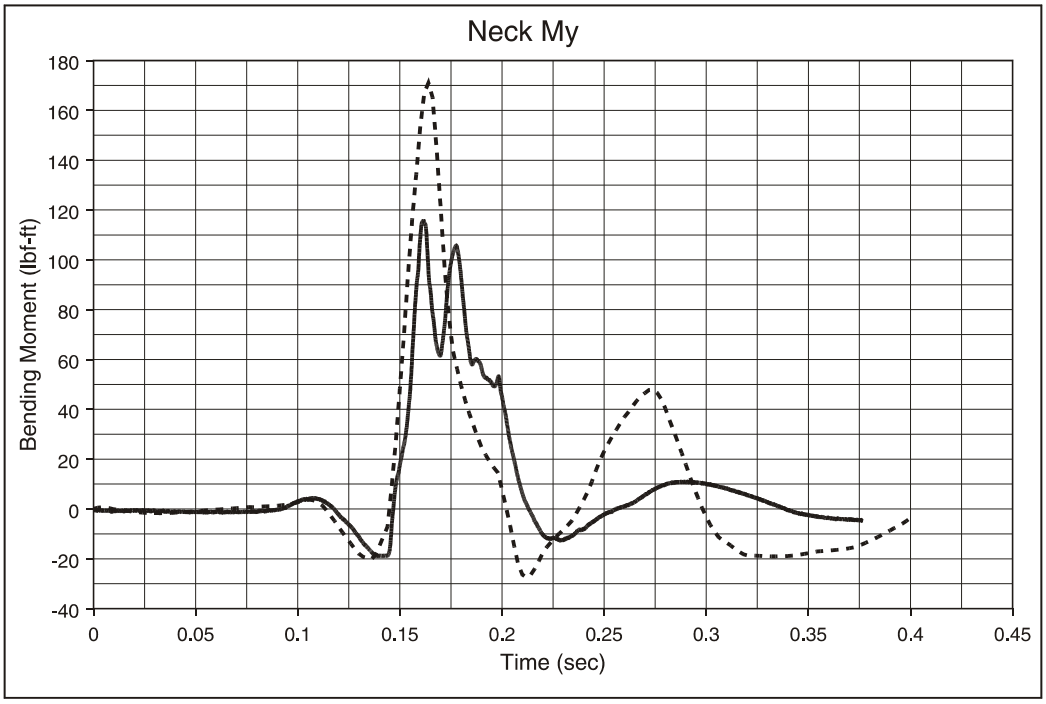

Figure F25. C-3 Seat, Type 1 Test, 50th-Percentile Hybrid III Male ATD, Window Seat: Neck Flexion/Extension Moments (Right Occupant)

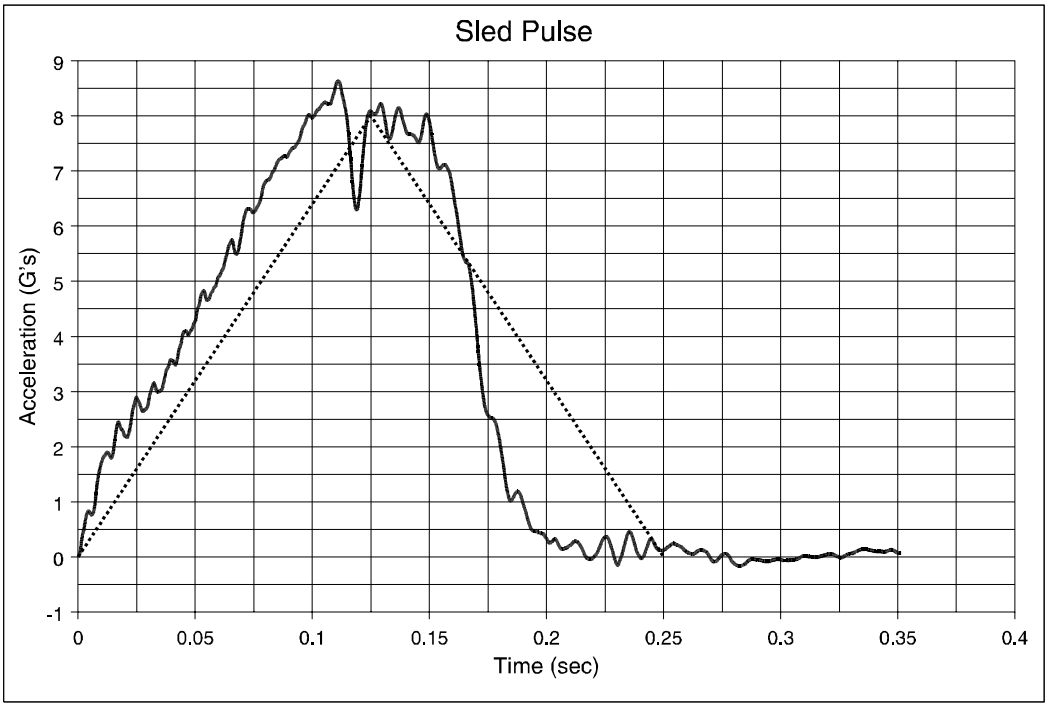

Figure F26. C-3 Seat, Type 2 Test, 95th- and 5th-Percentile ATDs: Sled Pulse

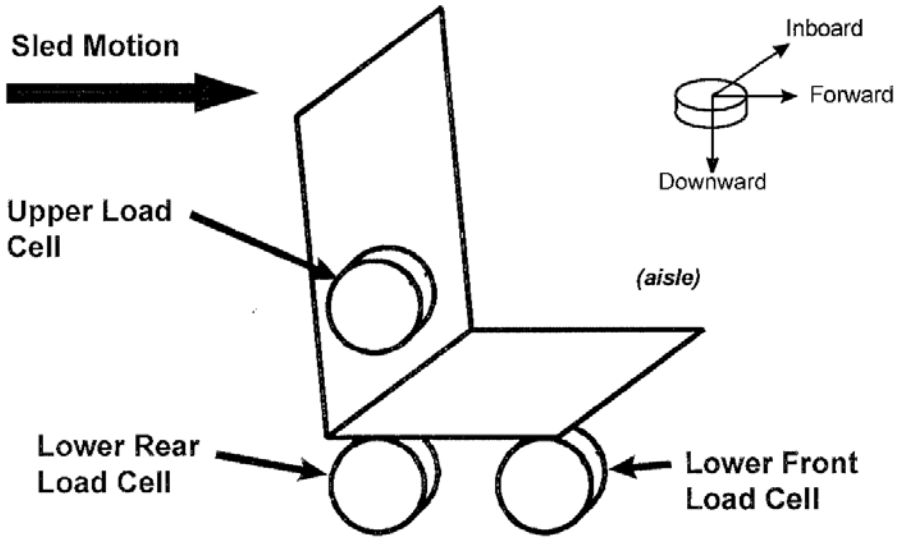

Figure F27. C-3 Seat, Type 2 Test, Seat Attachment Loads, C-3 Seat Load Cell Orientation

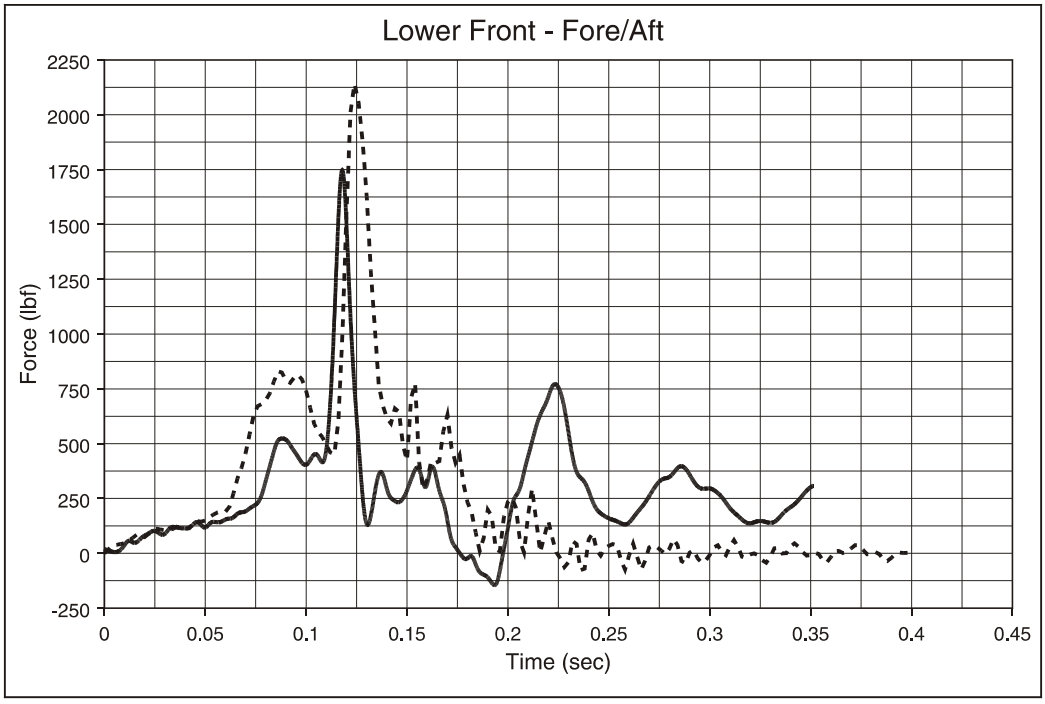

Figure F28. C-3 Seat, Type 2 Test, Seat Attachment Loads, Lower Front Load Cell, x Direction

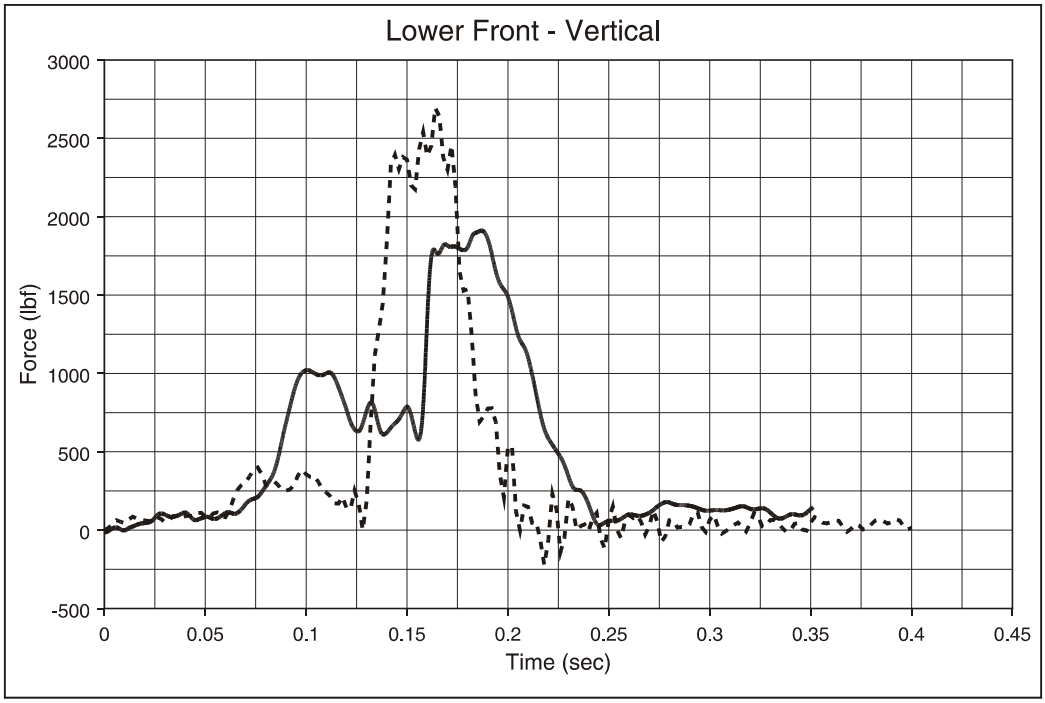

Figure F29. C-3 Seat, Type 2 Test, Seat Attachment Loads, Lower Front Load Cell, y Direction

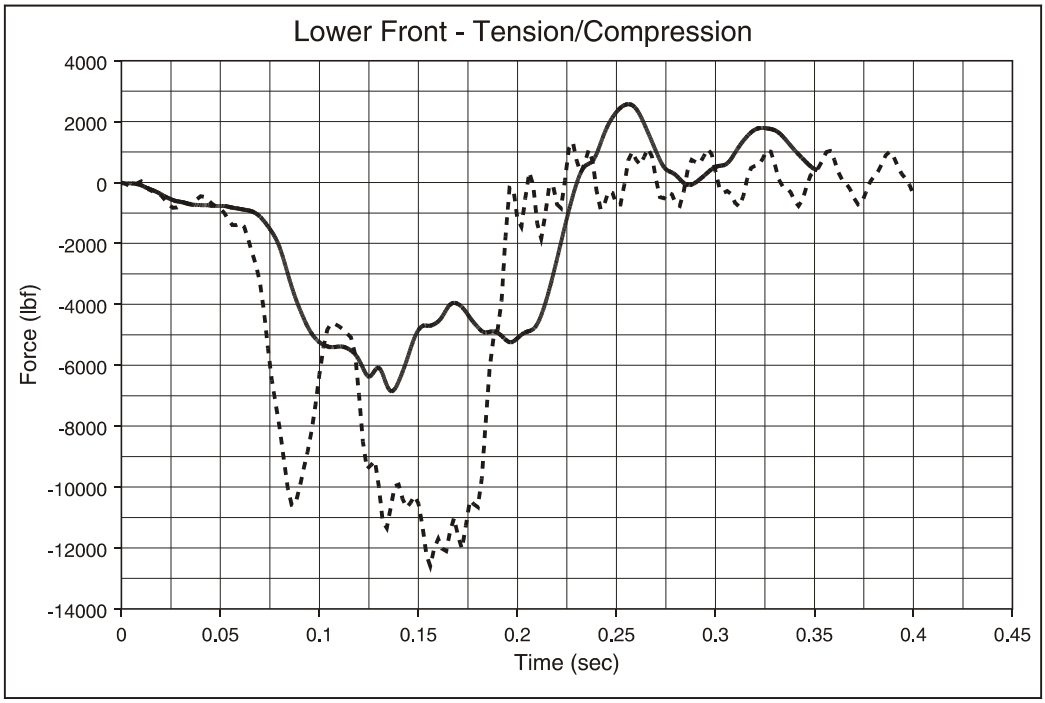

Figure F30. C-3 Seat, Type 2 Test, Seat Attachment Loads, Lower Front Load Cell, z Direction

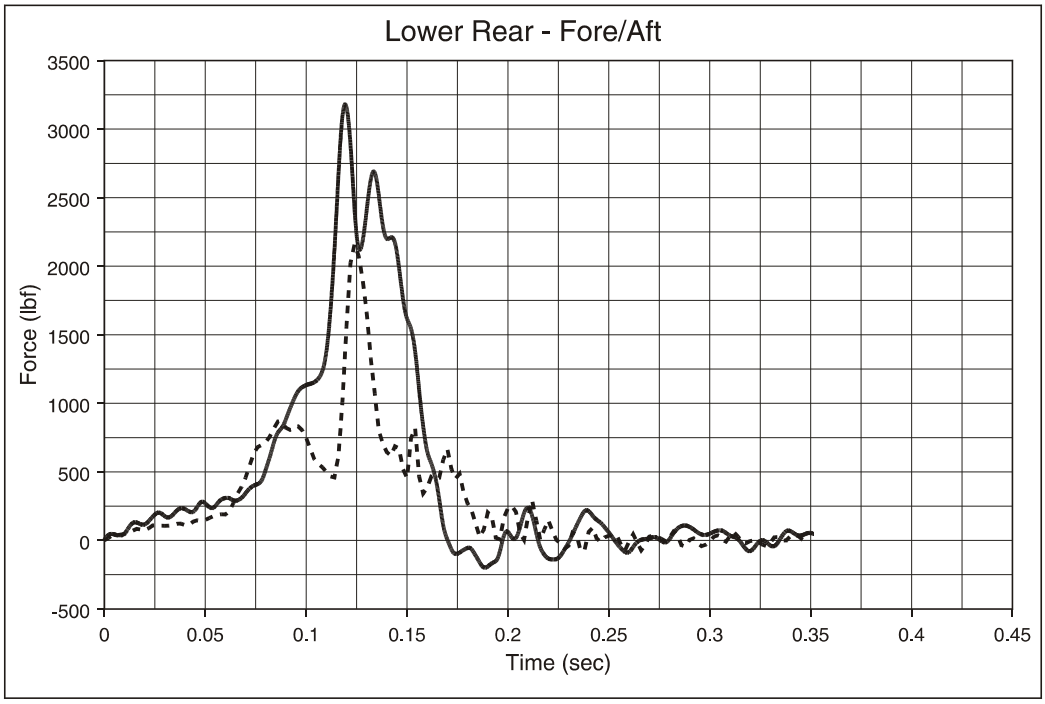

Figure F31. C-3 Seat, Type 2 Test, Seat Attachment Loads, Lower Rear Load Cell, x Direction

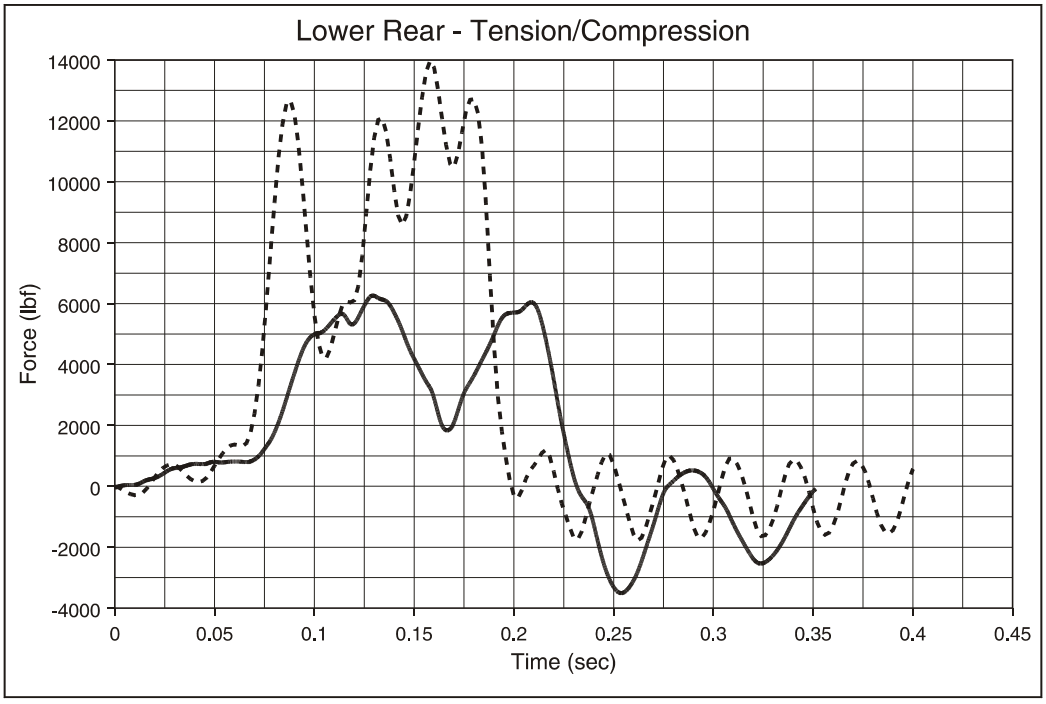

Figure F32. C-3 Seat, Type 2 Test, Seat Attachment Loads, Lower Rear Load Cell, z Direction

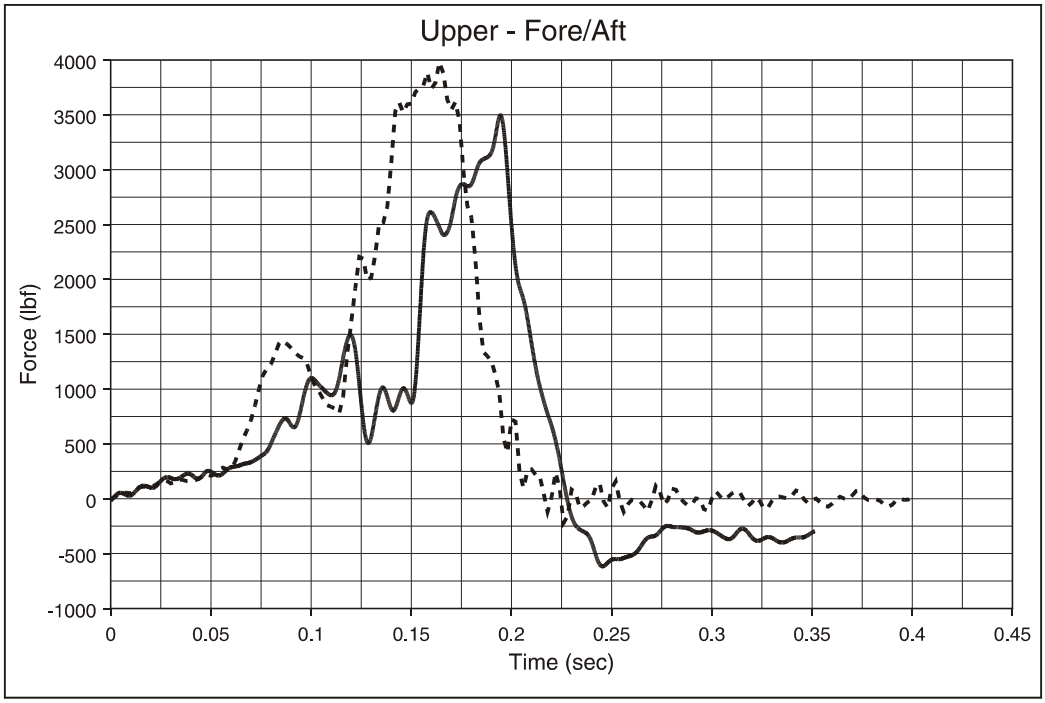

Figure F33. C-3 Seat, Type 2 Test, Seat Attachment Loads, Upper Load Cell, x Direction

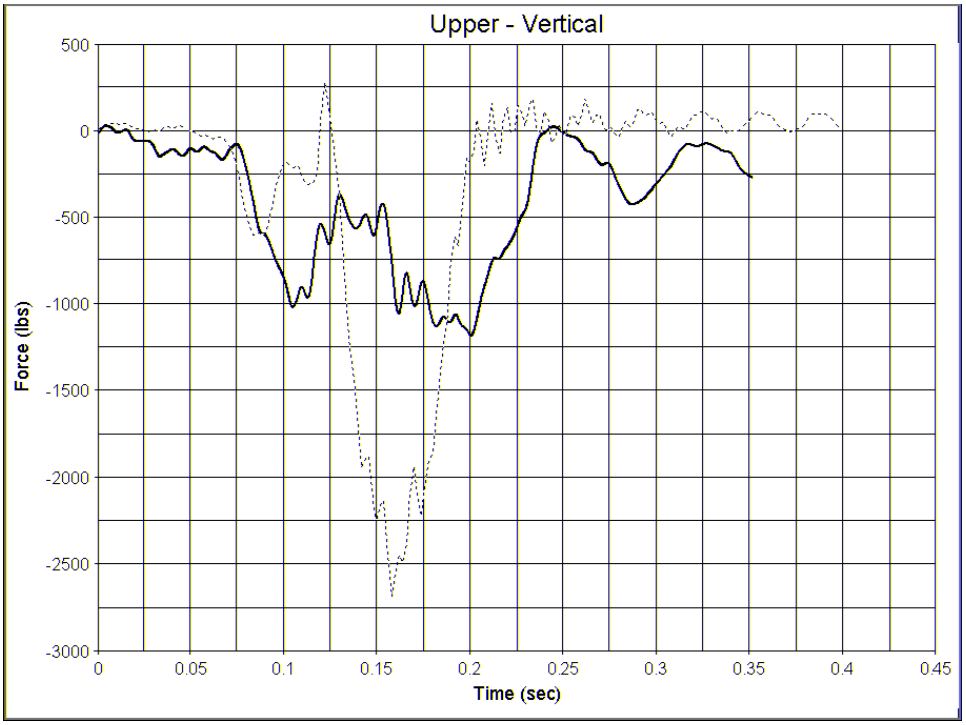

Figure F34. C-3 Seat, Type 2 Test, Seat Attachment Loads, Upper Load Cell, y Direction

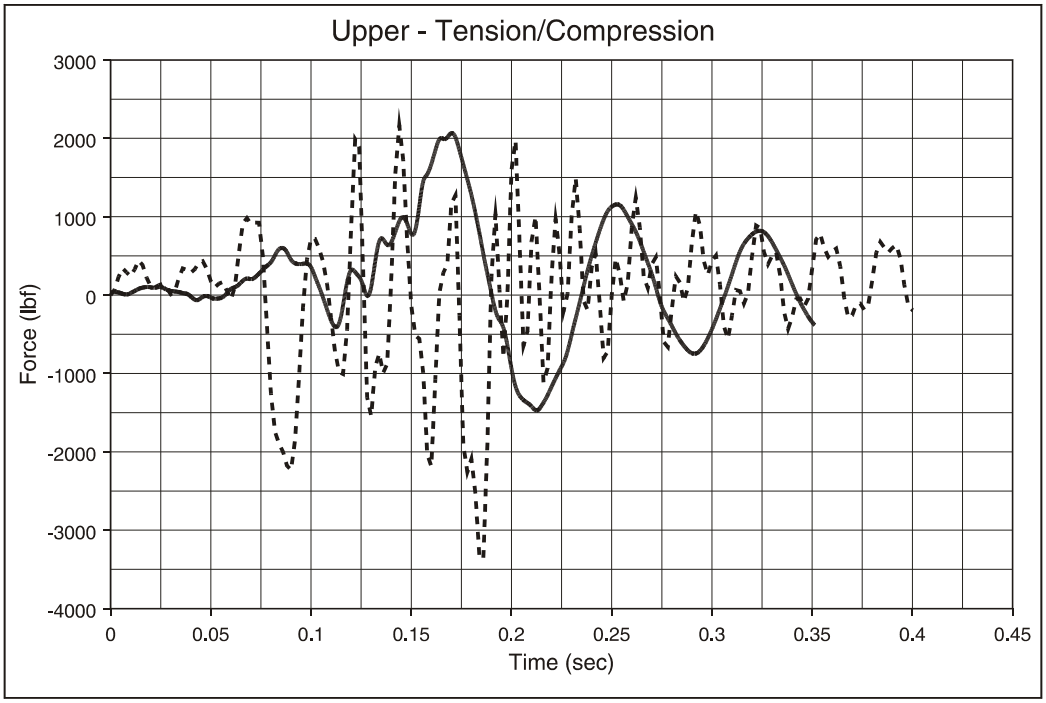

Figure F35. C-3 Seat, Type 2 Test, Seat Attachment Loads, Upper Load Cell, z Direction

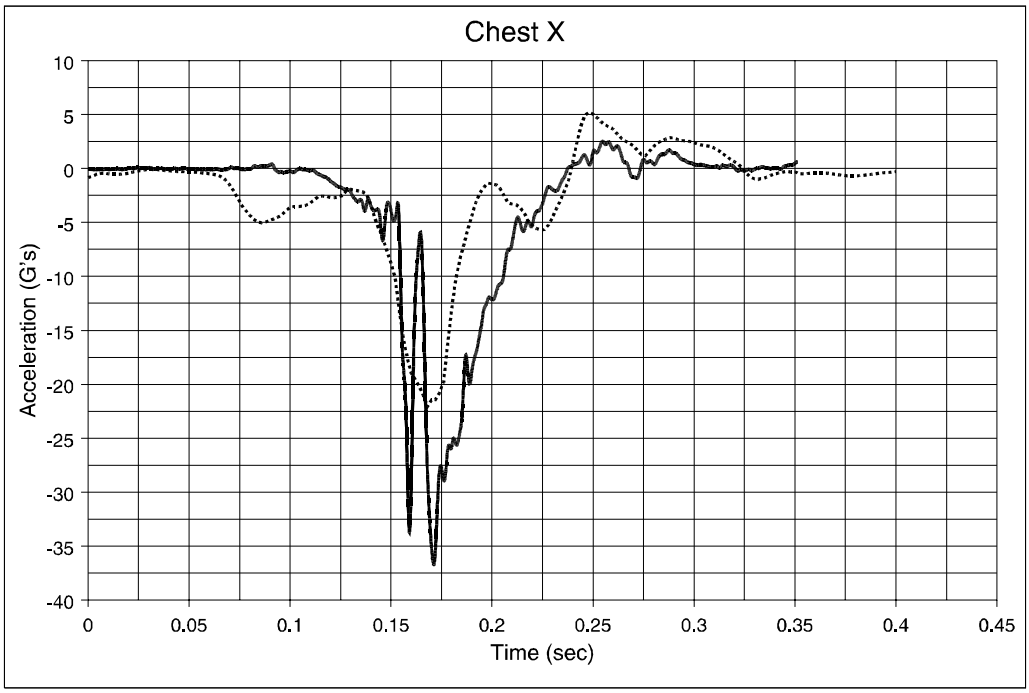

Figure F36. C-3 Seat, Type 2 Test, 95th-Percentile Hybrid III Male ATD, Aisle Seat: Chest Acceleration, x Direction (Left Occupant)

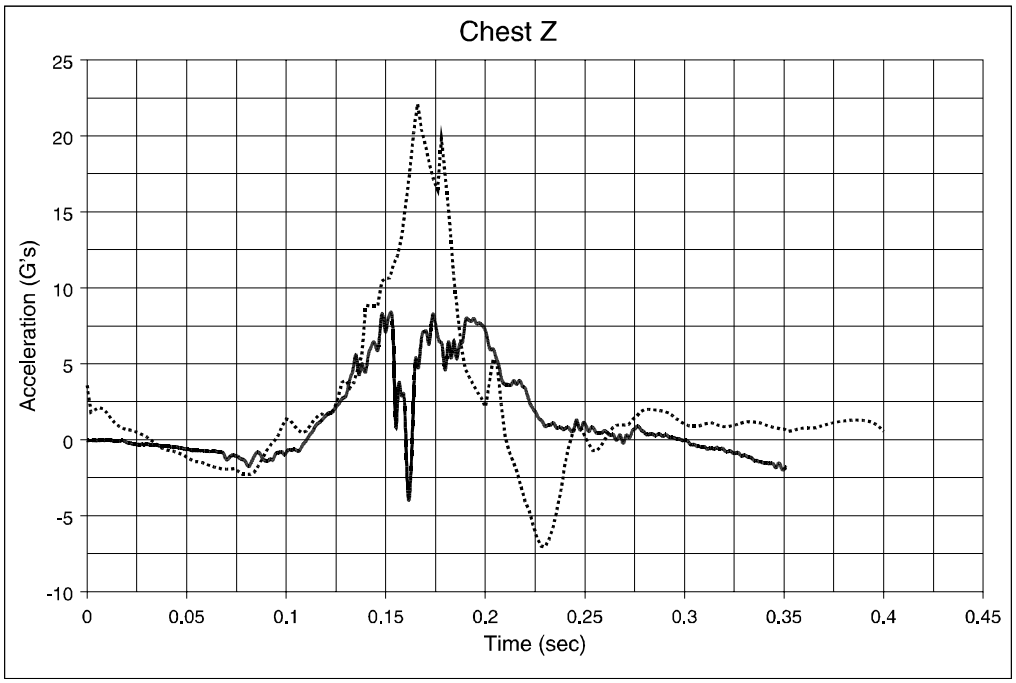

Figure F37. C-3 Seat, Type 2 Test, 95th-Percentile Hybrid III Male ATD, Aisle Seat: Chest Acceleration, z Direction (Left Occupant)

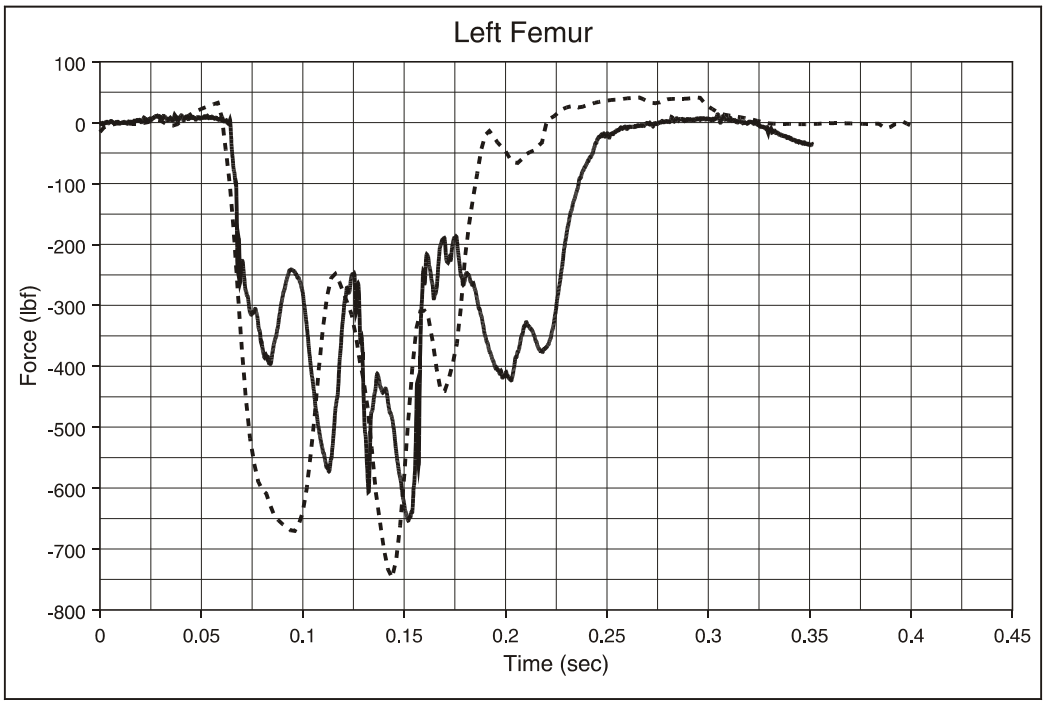

Figure F38. C-3 Seat, Type 2 Test, 95th-Percentile Hybrid III Male ATD, Aisle Seat: Left Femur Load (Left Occupant)

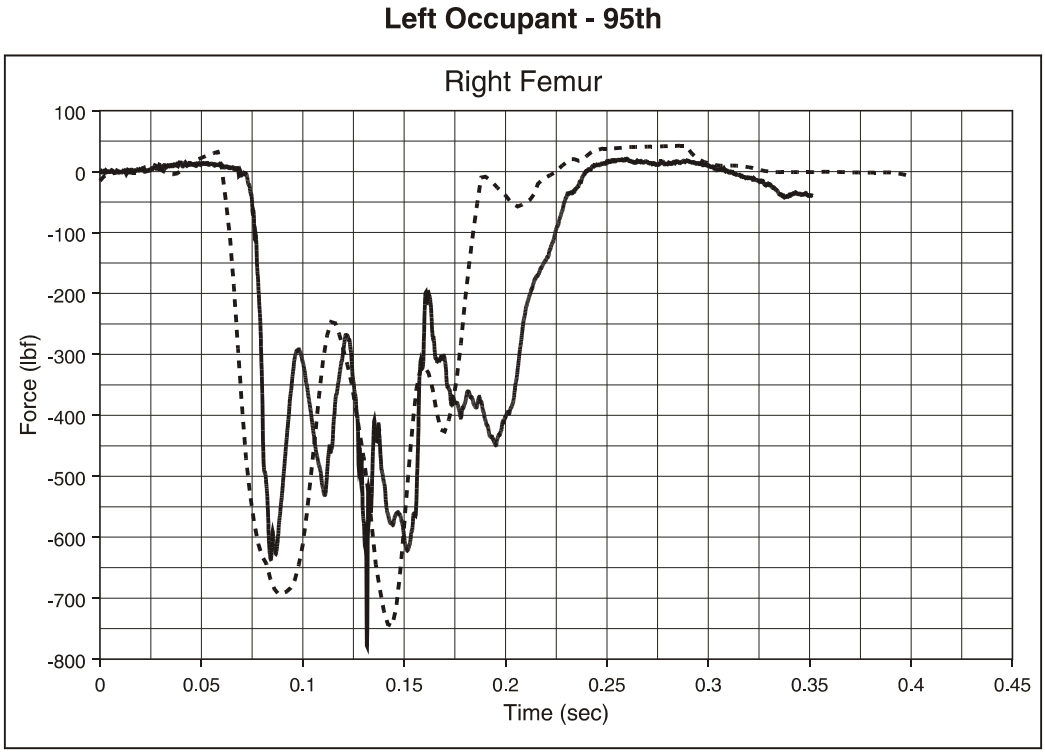

Figure F39. C-3 Seat, Type 2 Test, 95th-Percentile Hybrid III Male ATD, Aisle Seat: Right Femur Load (Left Occupant)

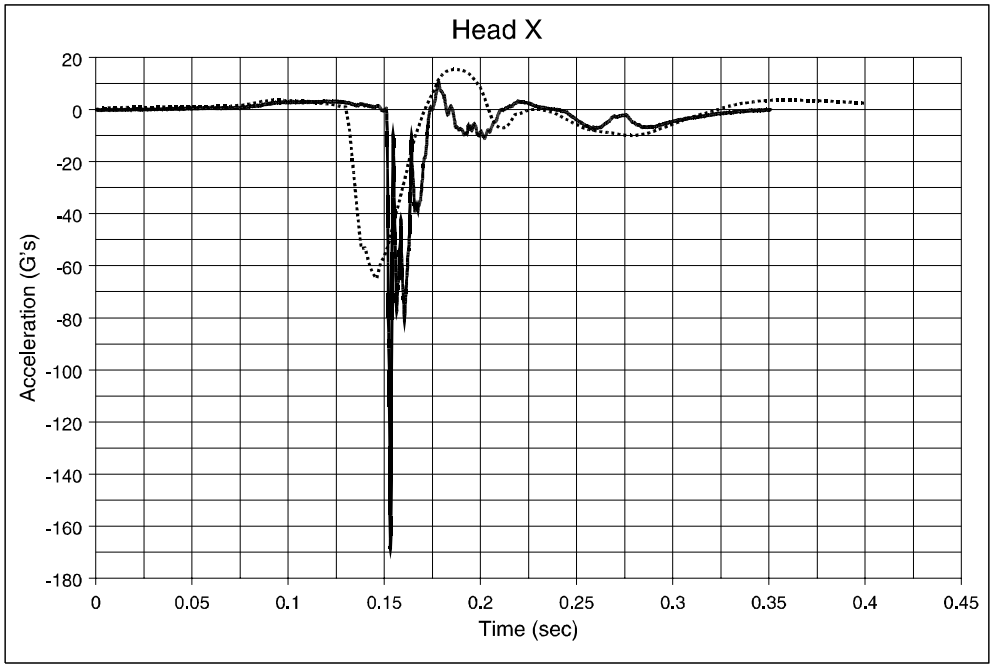

Figure F40. C-3 Seat, Type 2 Test, 95th-Percentile Hybrid III Male ATD, Aisle Seat: Head Acceleration, x Direction (Left Occupant)

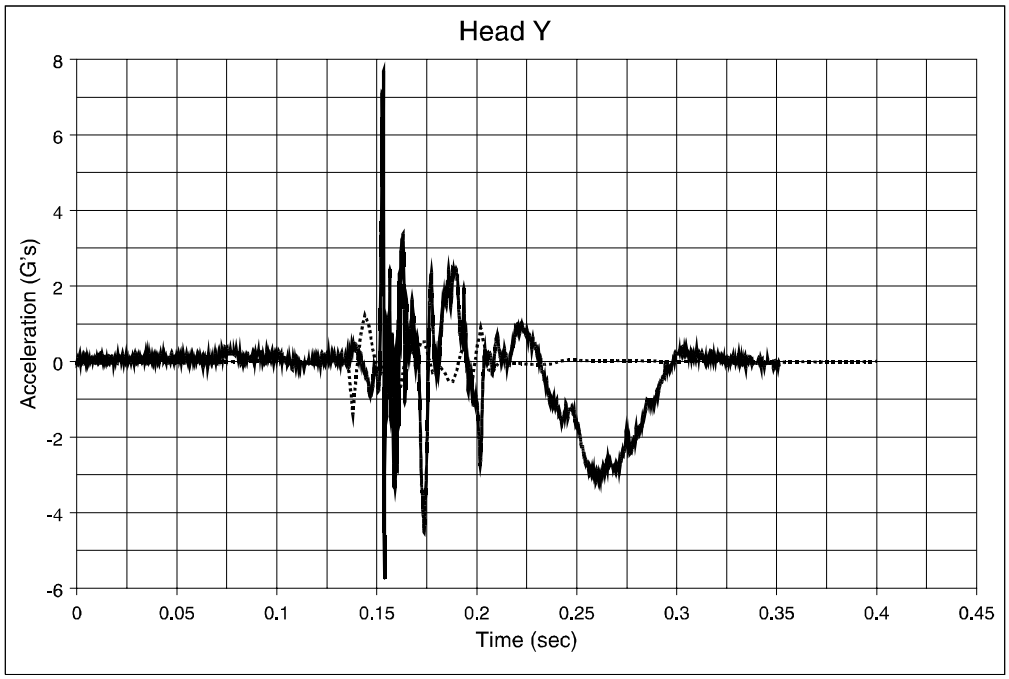

Figure F41. C-3 Seat, Type 2 Test, 95th-Percentile Hybrid III Male ATD, Aisle Seat: Head Acceleration, y Direction (Left Occupant)

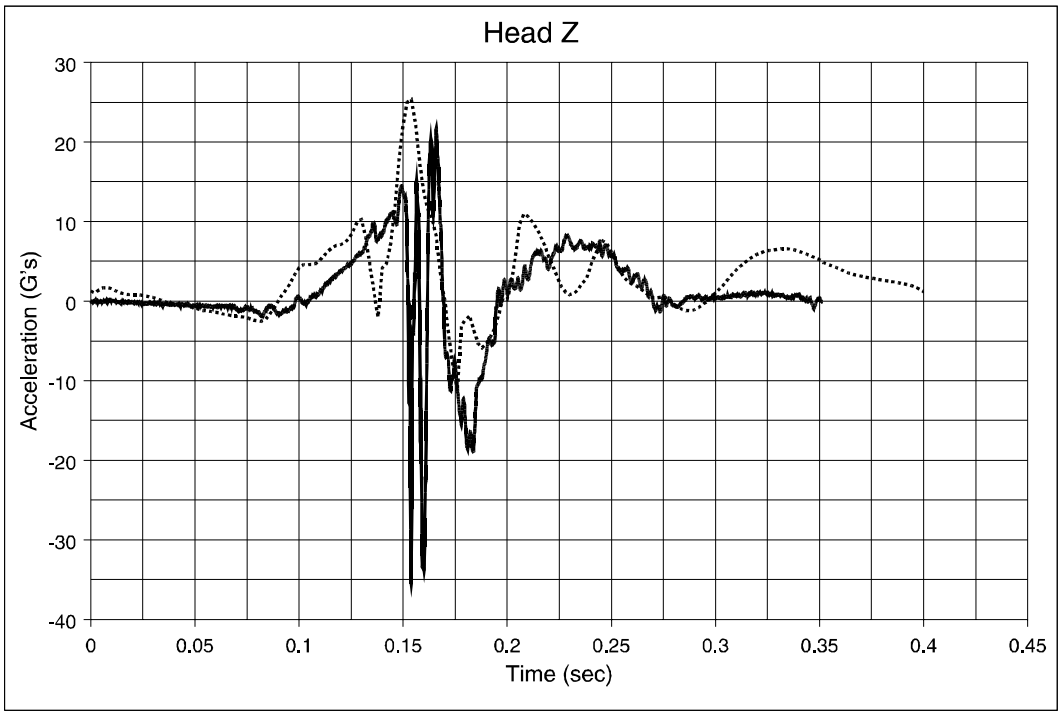

Figure F42. C-3 Seat, Type 2 Test, 95th-Percentile Hybrid III Male ATD, Aisle Seat: Head Acceleration, z Direction (Left Occupant)

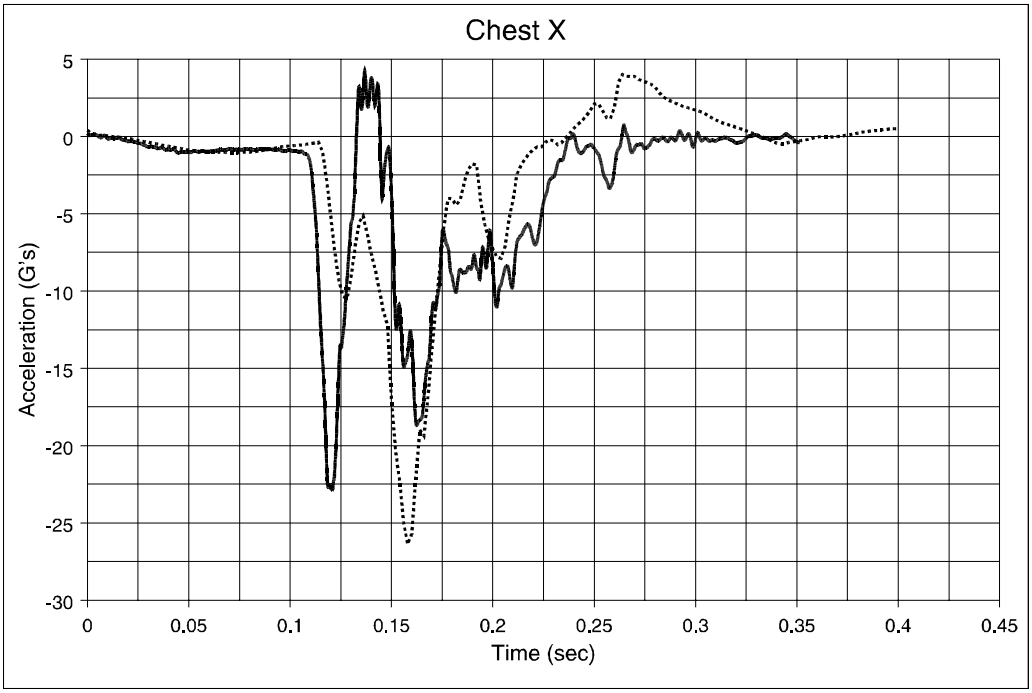

Figure F43. C-3 Seat, Type 2 Test, 5th-Percentile Hybrid III Female ATD, Window Seat: Chest Acceleration, x Direction (Right Occupant)

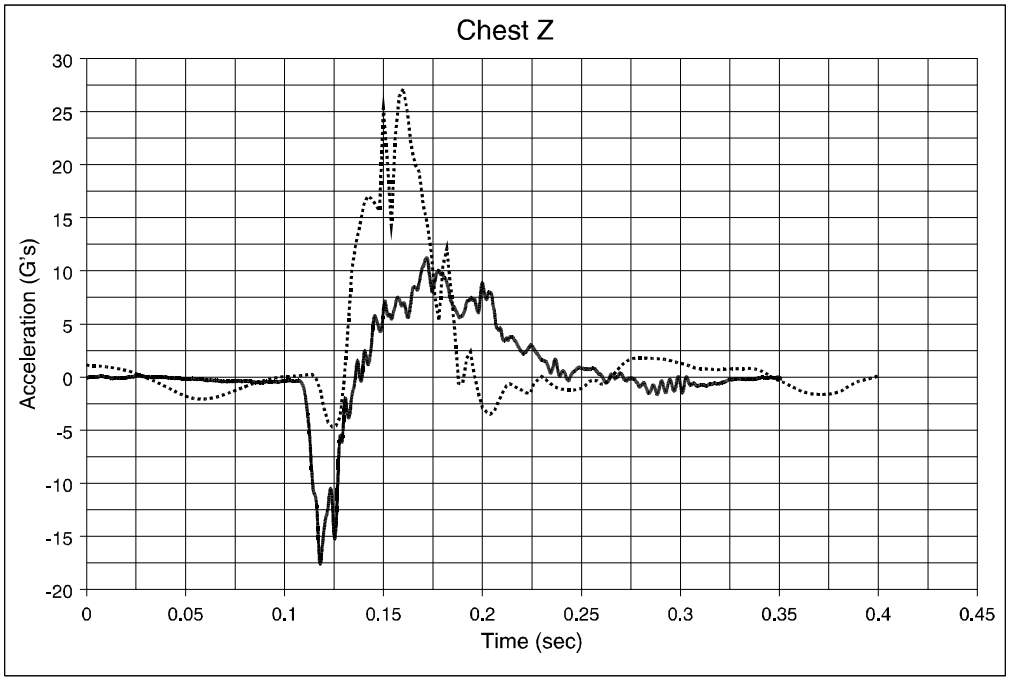

Figure F44. C-3 Seat, Type 2 Test, 5th-Percentile Hybrid III Female ATD, Window Seat: Chest Acceleration, z Direction (Right Occupant)

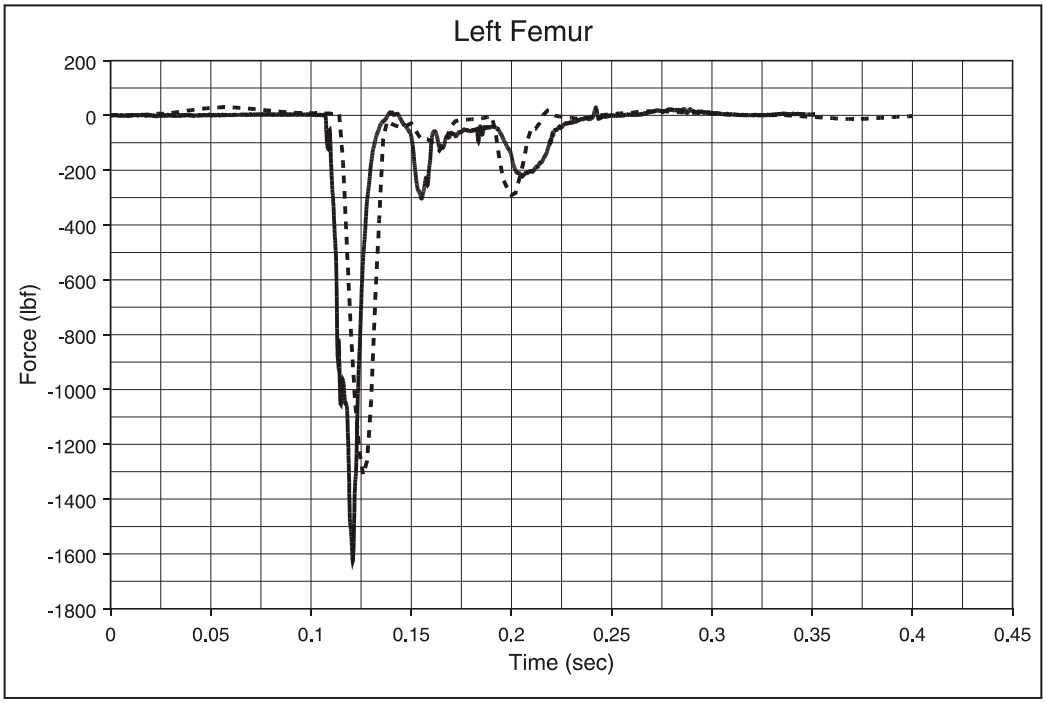

Figure F45. C-3 Seat, Type 2 Test, 5th-Percentile Hybrid III Female ATD, Window Seat: Left Femur Load (Right Occupant)

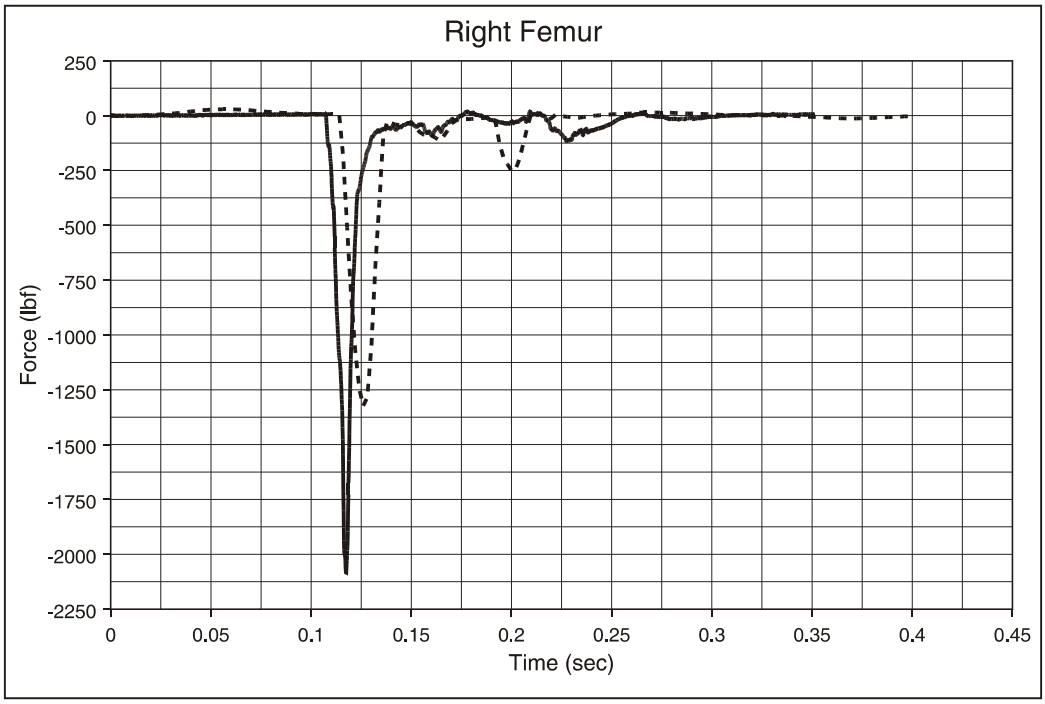

Figure F46. C-3 Seat, Type 2 Test, 5th-Percentile Hybrid III Female ATD, Window Seat: Right Femur Load (Right Occupant)

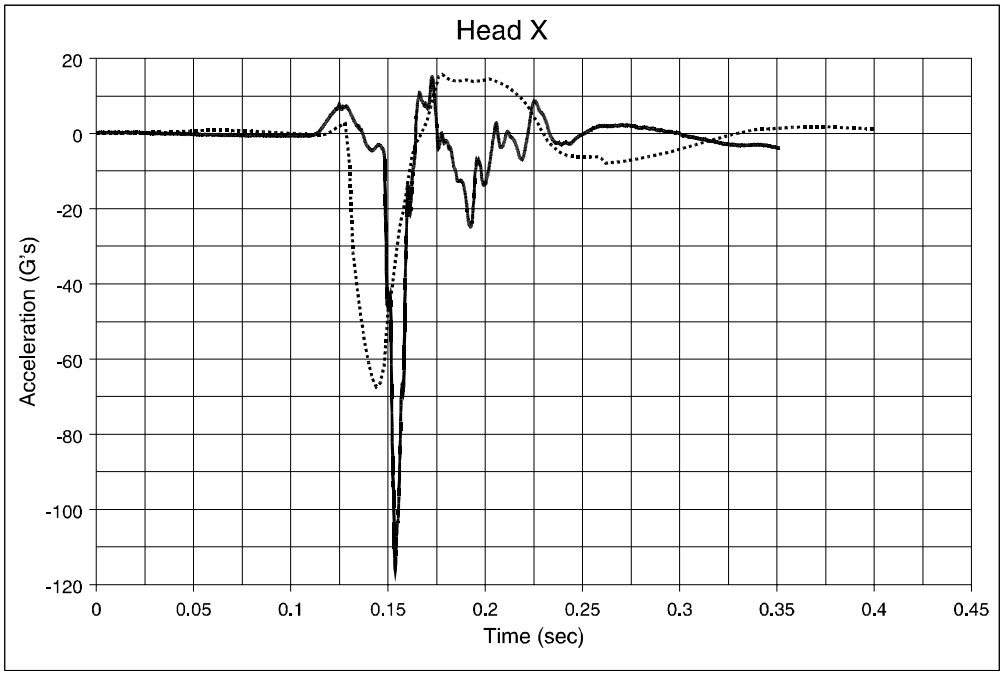

Figure F47. C-3 Seat, Type 2 Test, 5th-Percentile Hybrid III Female ATD, Window Seat: Head Acceleration, x Direction (Right Occupant)

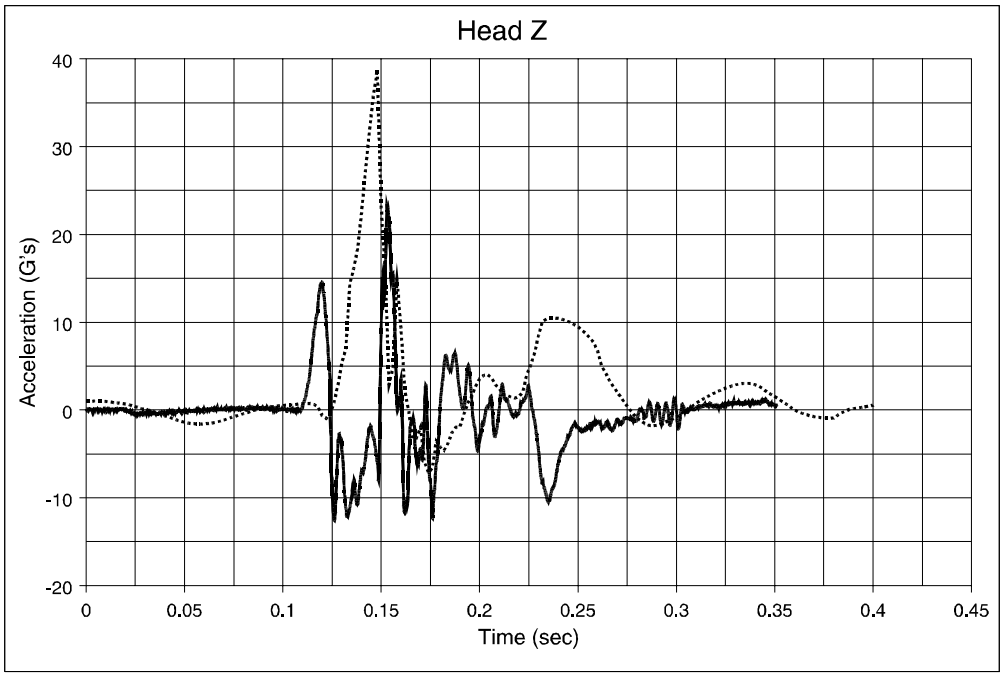

Figure F48. C-3 Seat, Type 2 Test, 5th-Percentile Hybrid III Female ATD, Window Seat: Head Accelerations, z Direction (Right Occupant)

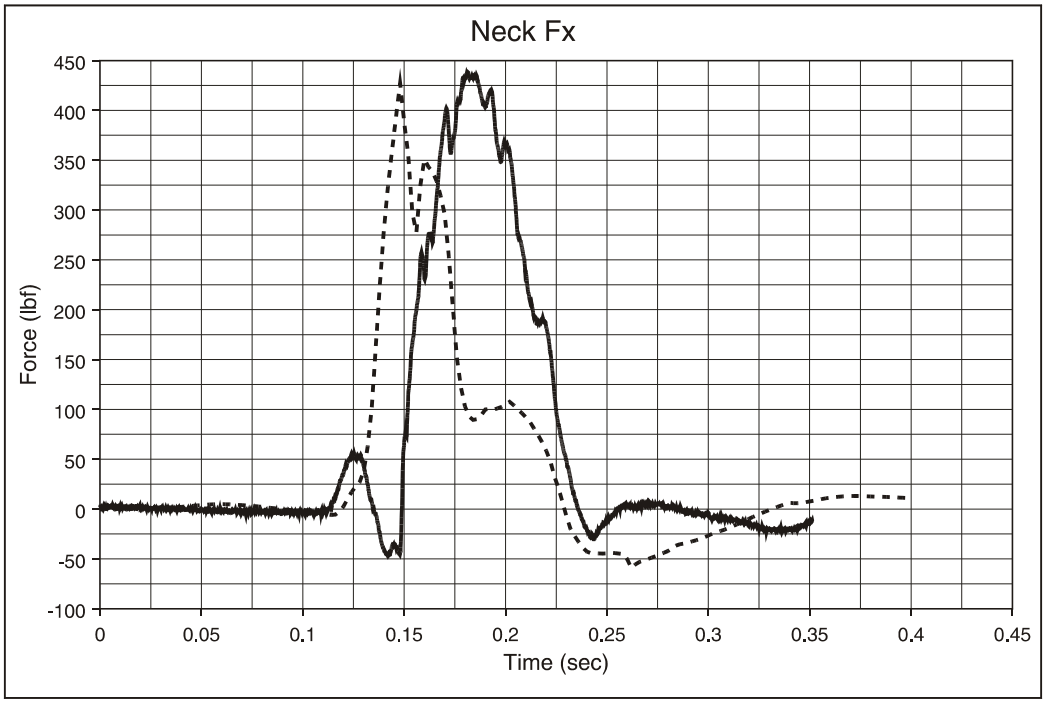

Figure F-49. C-3 Seat, Type 2 Test, 5th-Percentile Hybrid III Female ATD, Window Seat: Neck Shear Load (Right Occupant)

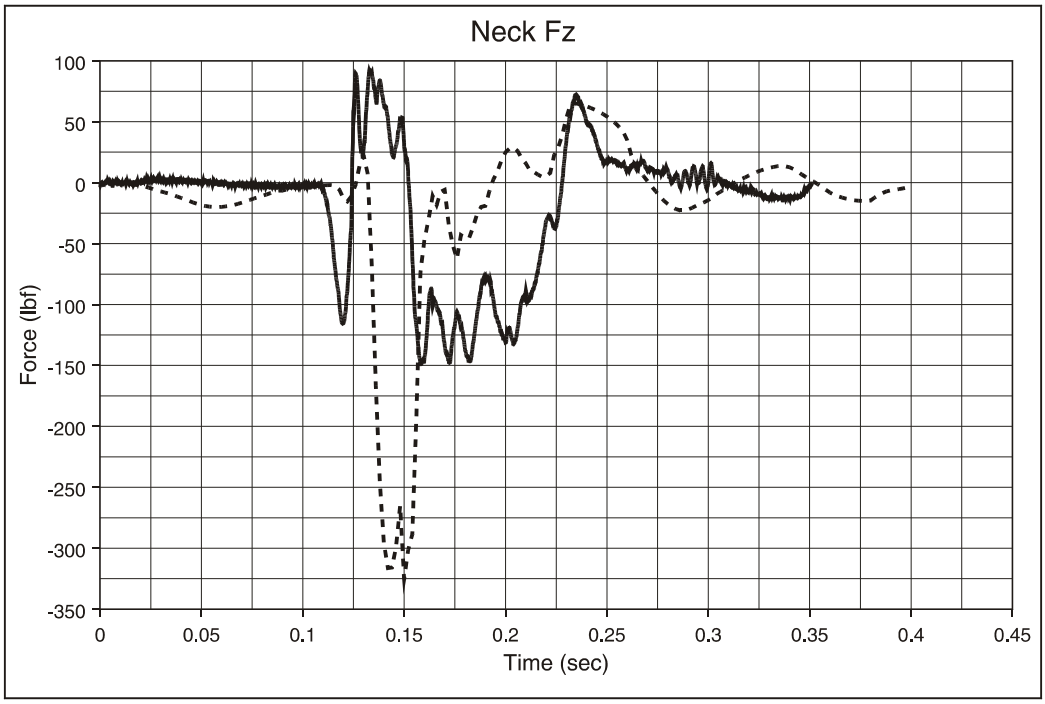

Figure F50. C-3 Seat, Type 2 Test, 5th-Percentile Hybrid III Female ATD, Window Seat: Neck Compression/Tension Load (Right Occupant)

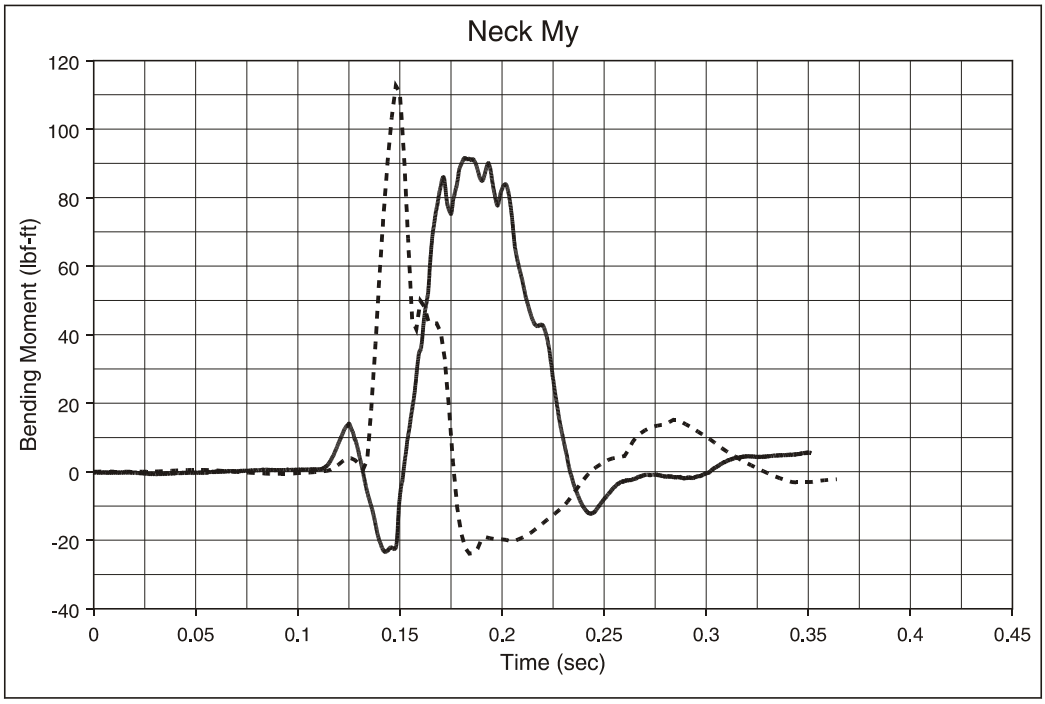

Figure F-51. C-3 Seat, Type 2 Test, 5th-Percentile Hybrid III Female ATD, Window Seat: Neck Flexion/Extension Moment (Right Occupant)

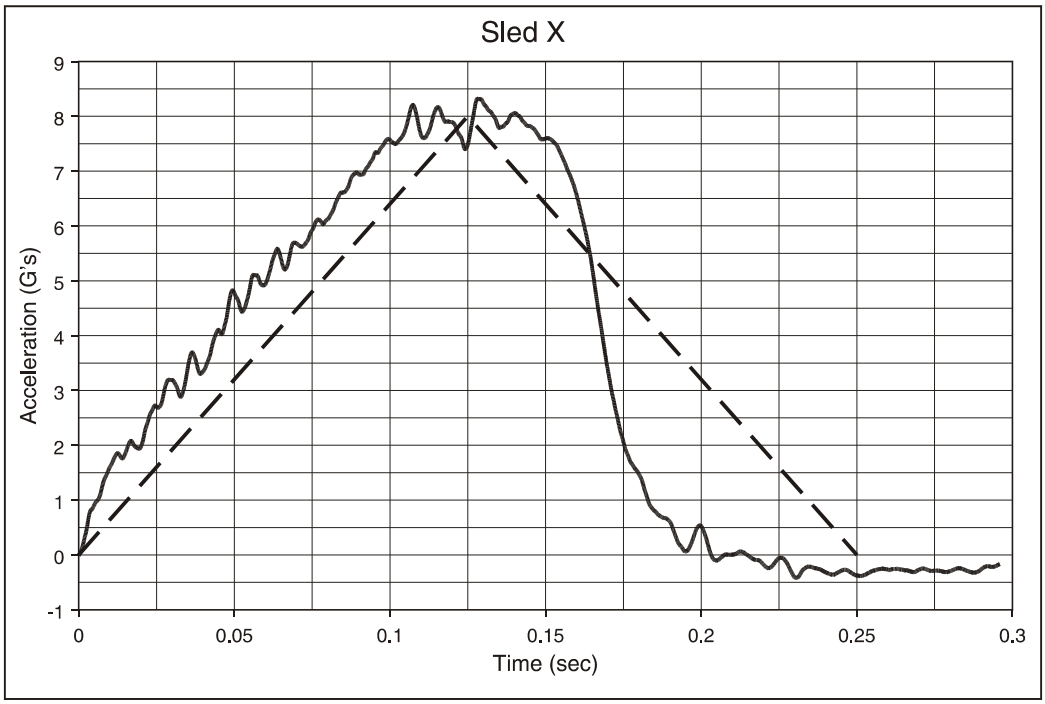

Figure F52. M-Style Seat, Type 1 Test, All 50th-Percentile ATDs: Sled Pulse

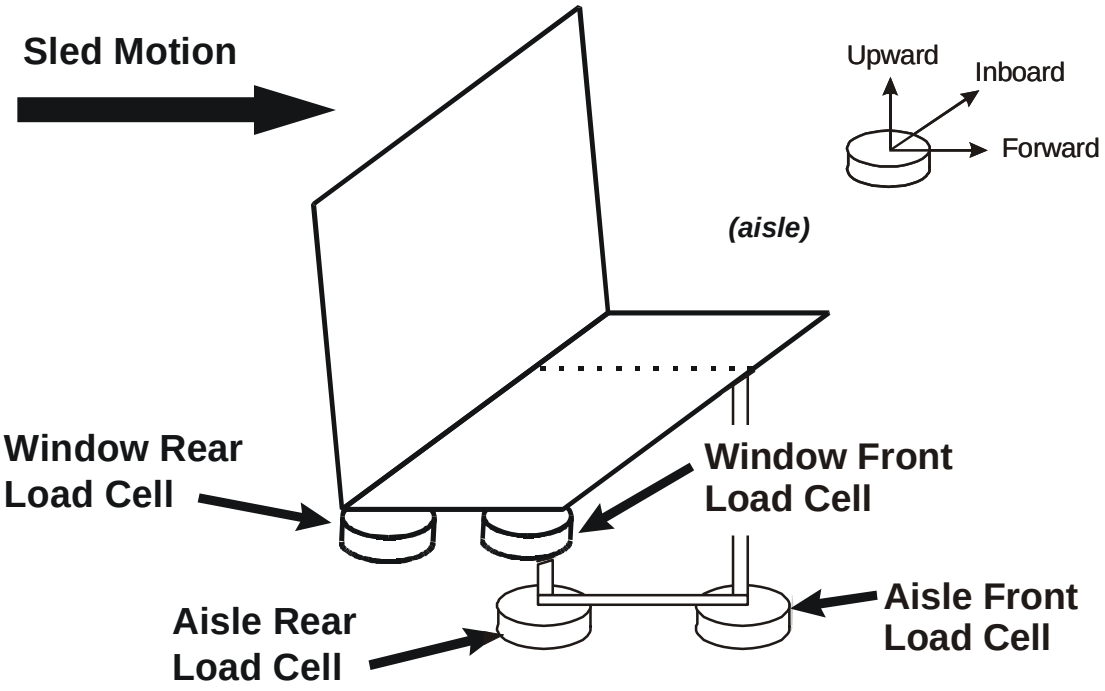

Figure F-53. M-Style Seat, Type 1 Test, Seat Attachment Loads: Load Cell Orientation

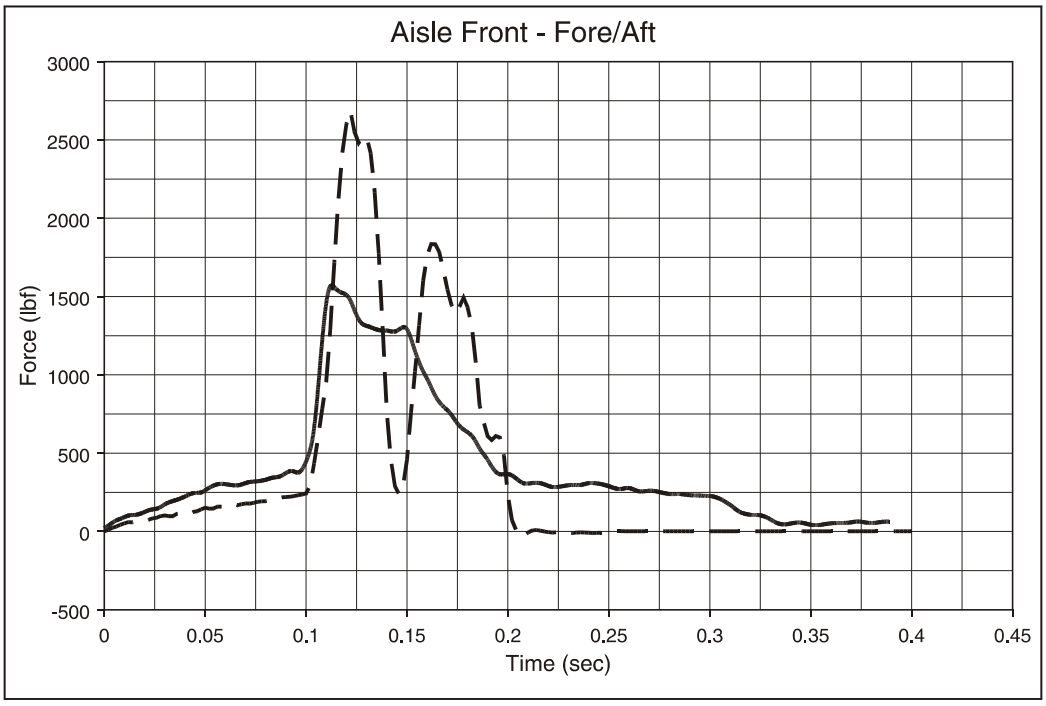

Figure F54. M-Style Seat, Type 1 Test, Seat Attachment Loads: Aisle Front Load Cell, x Direction

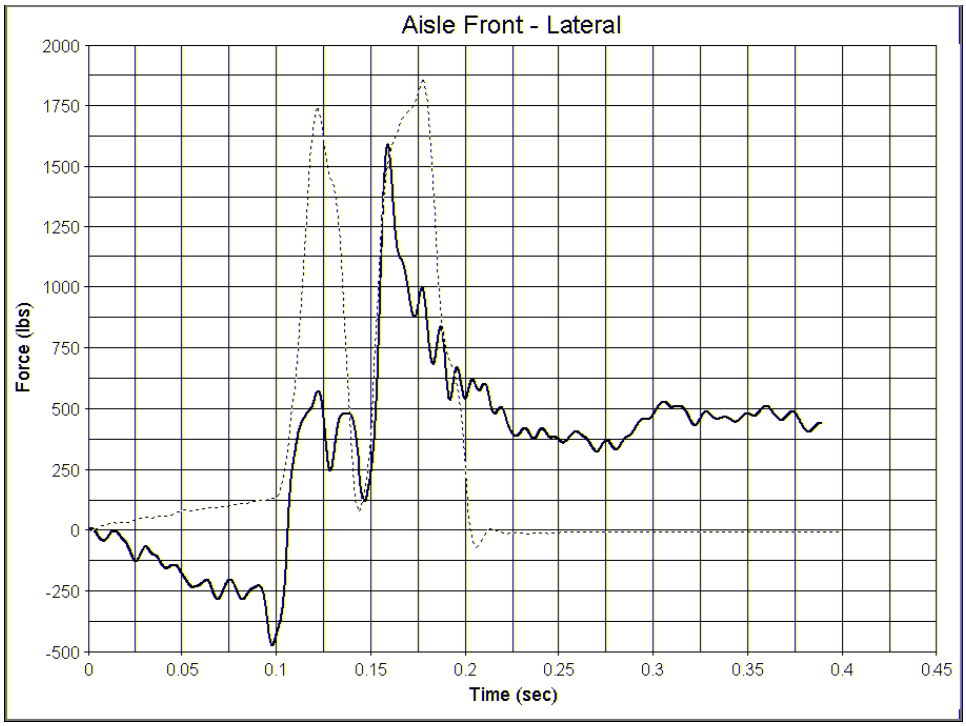

Figure F55. M-Style Seat, Type 1 Test, Seat Attachment Loads: Aisle Front Load Cell, y Direction

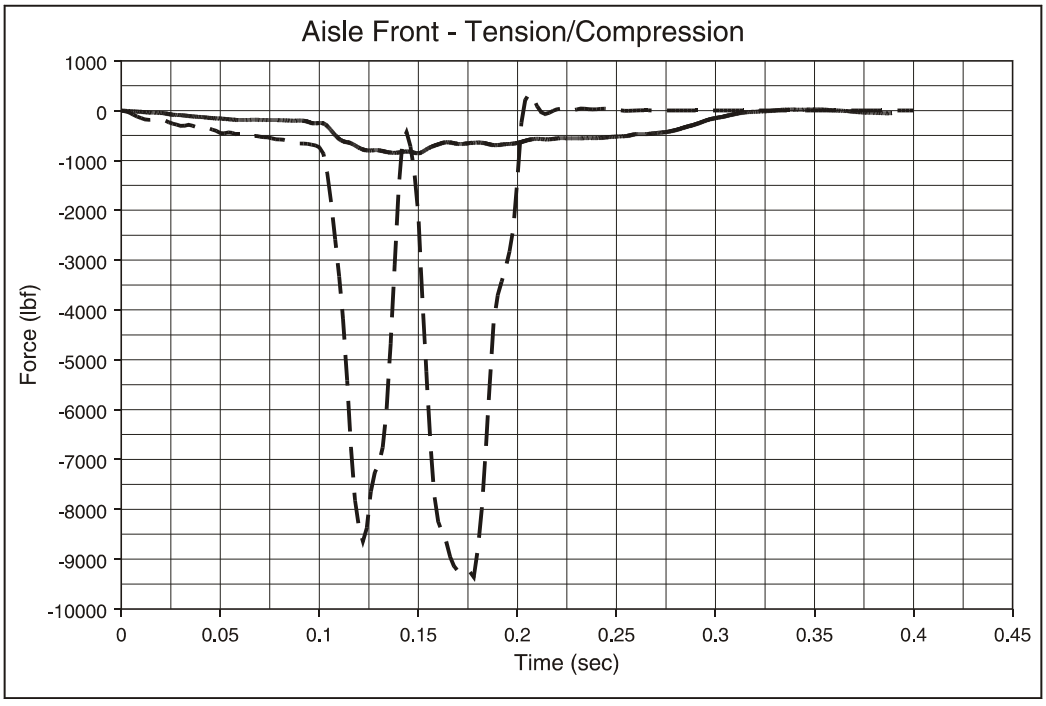

Figure F56. M-Style Seat, Type 1 Test, Seat Attachment Loads: Aisle Front Load Cell, z Direction

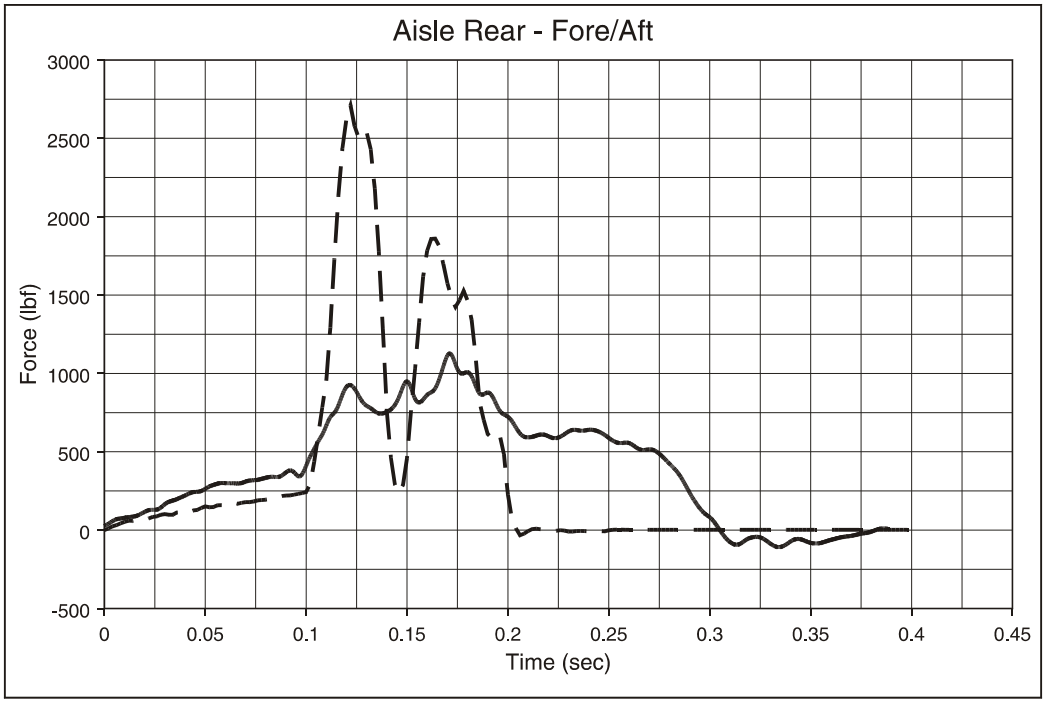

Figure F57. M-Style Seat, Type 1 Test, Seat Attachment Loads: Aisle Rear Load Cell, x Direction

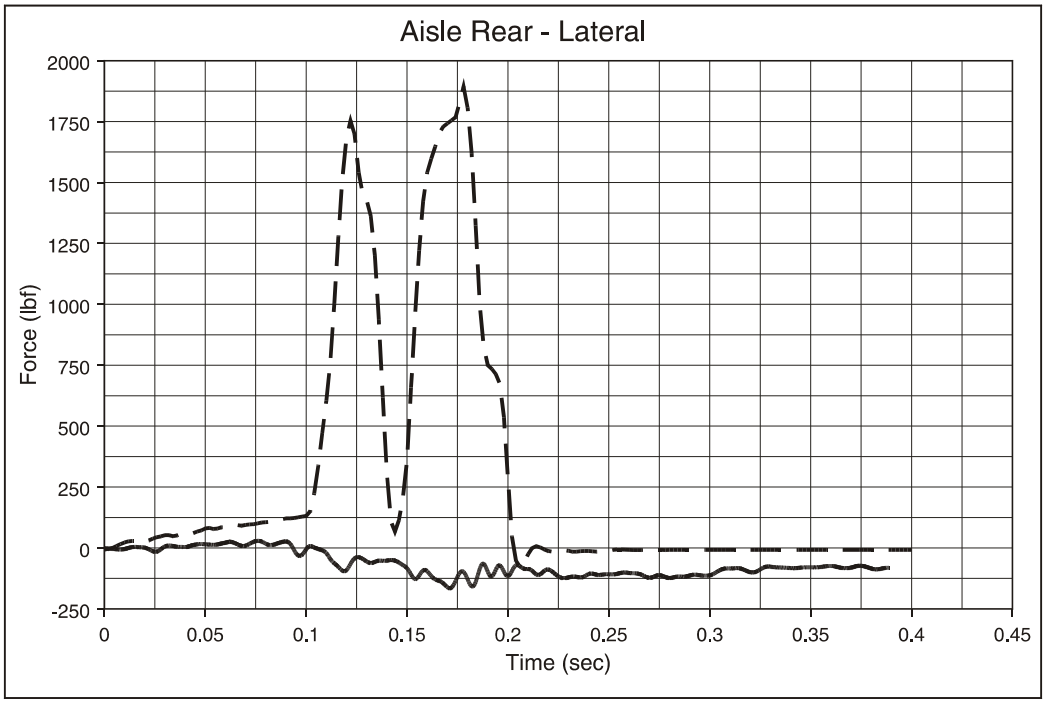

Figure F-58. M-Style Seat, Type 1 Test, Seat Attachment Loads: Aisle Rear Load Cell, y Direction

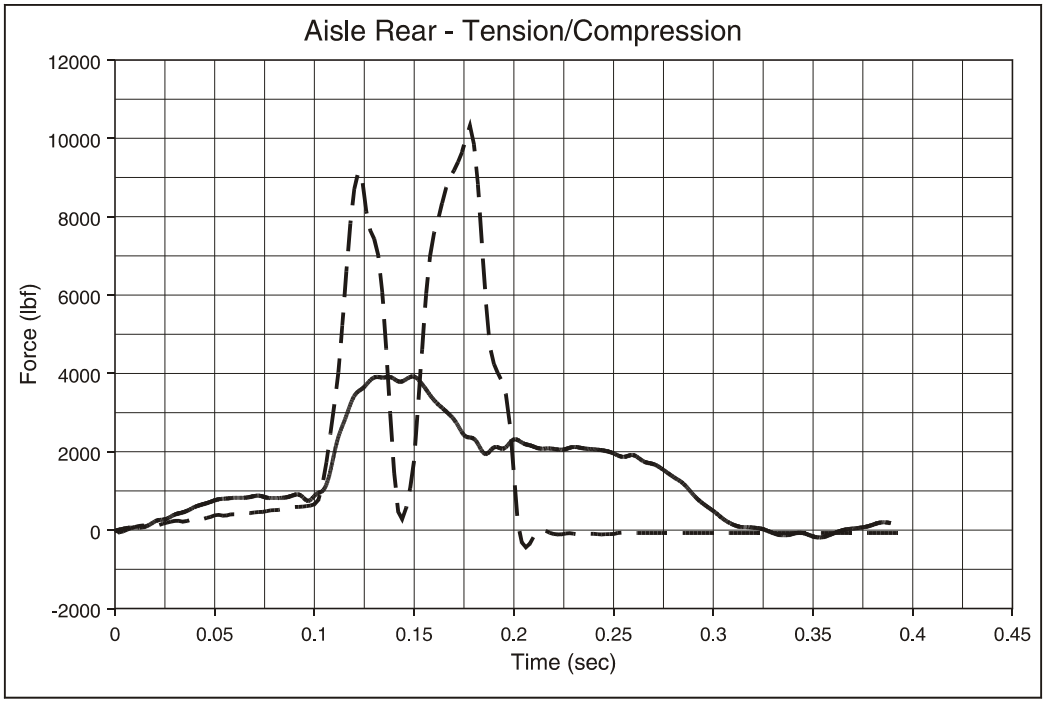

Figure F59. M-Style Seat, Type 1 Test, Seat Attachment Loads: Aisle Rear Load Cell, z Direction

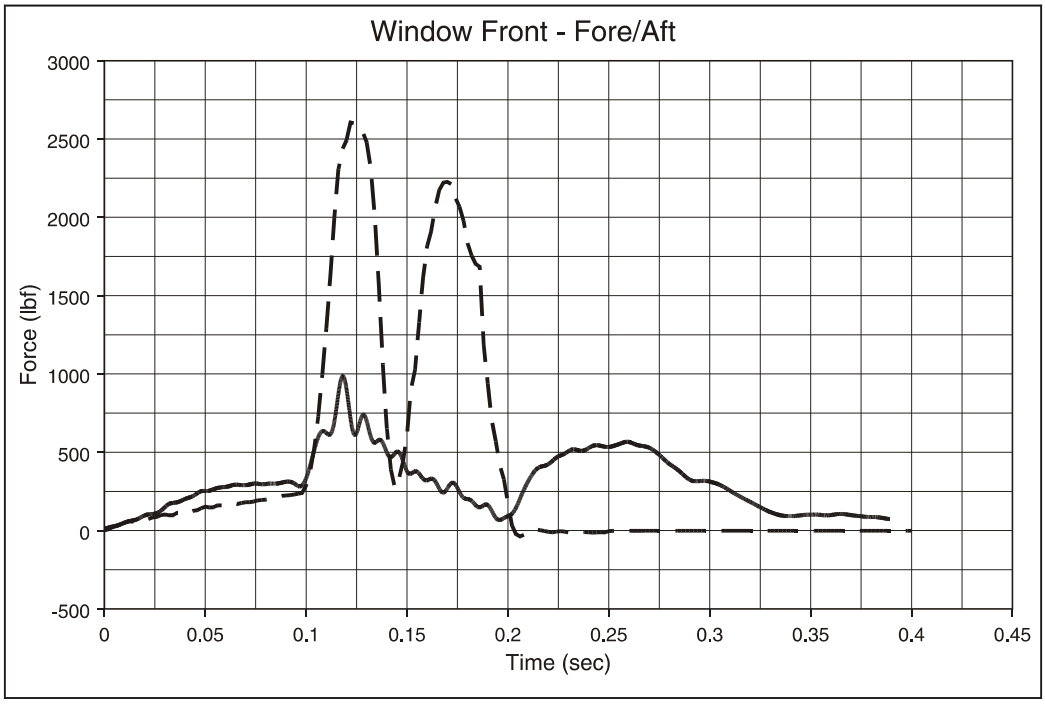

Figure F60. M-Style Seat, Type 1 Test, Seat Attachment Loads: Window Front Load Cell, x Direction

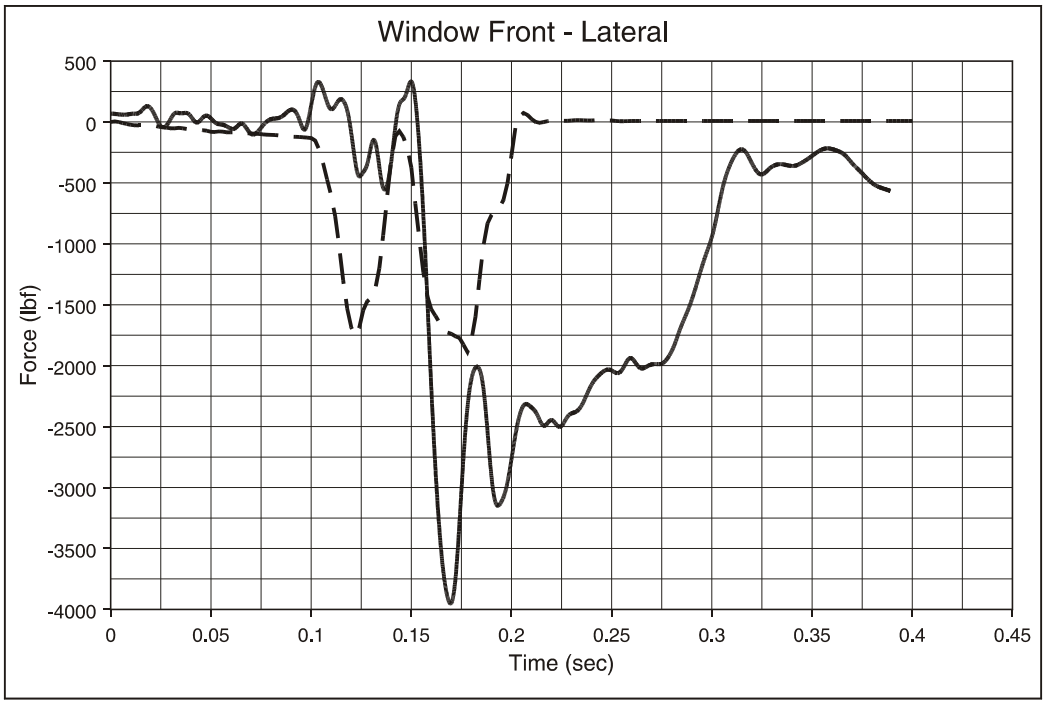

Figure F61. M-Style Seat, Type 1 Test, Seat Attachment Loads: Window Front Load Cell, y Direction

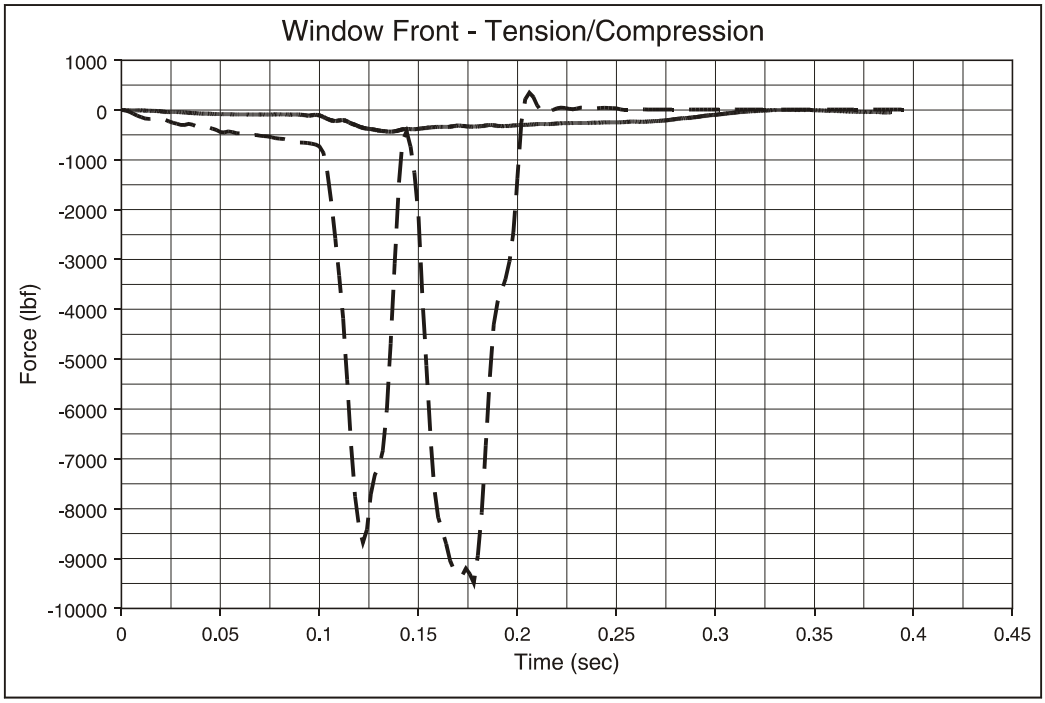

Figure F62. M-Style Seat, Type 1 Test, Seat Attachment Loads: Window Front Load Cell, z Direction

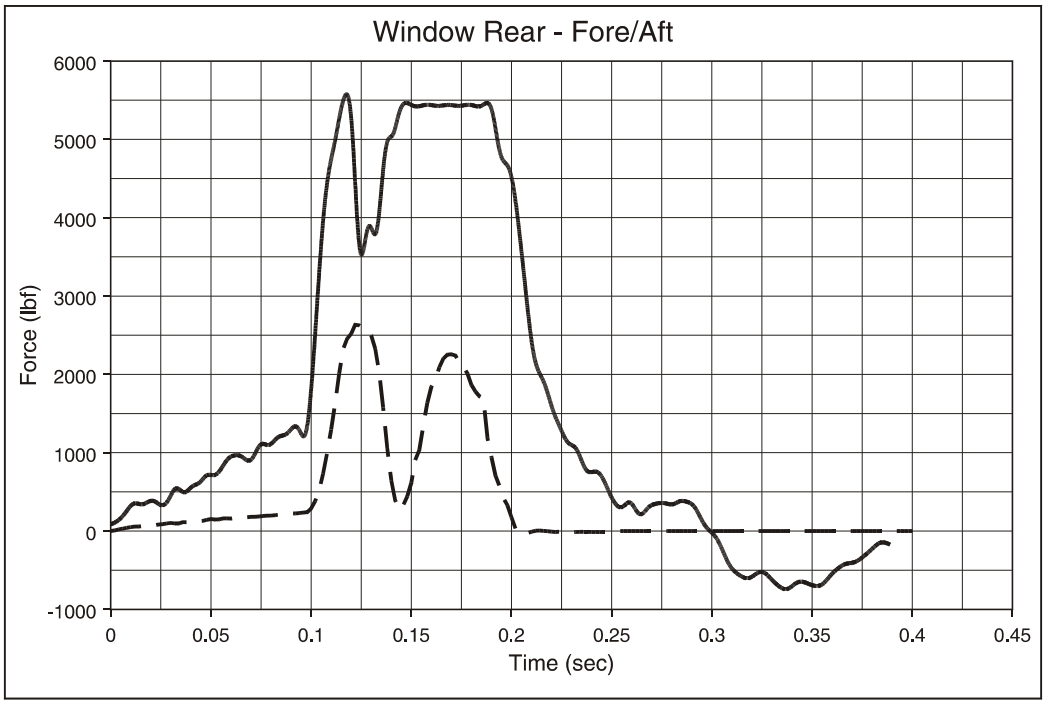

Figure F63. M-Style Seat, Type 1 Test, Seat Attachment Loads: Window Rear Load Cell, x Direction

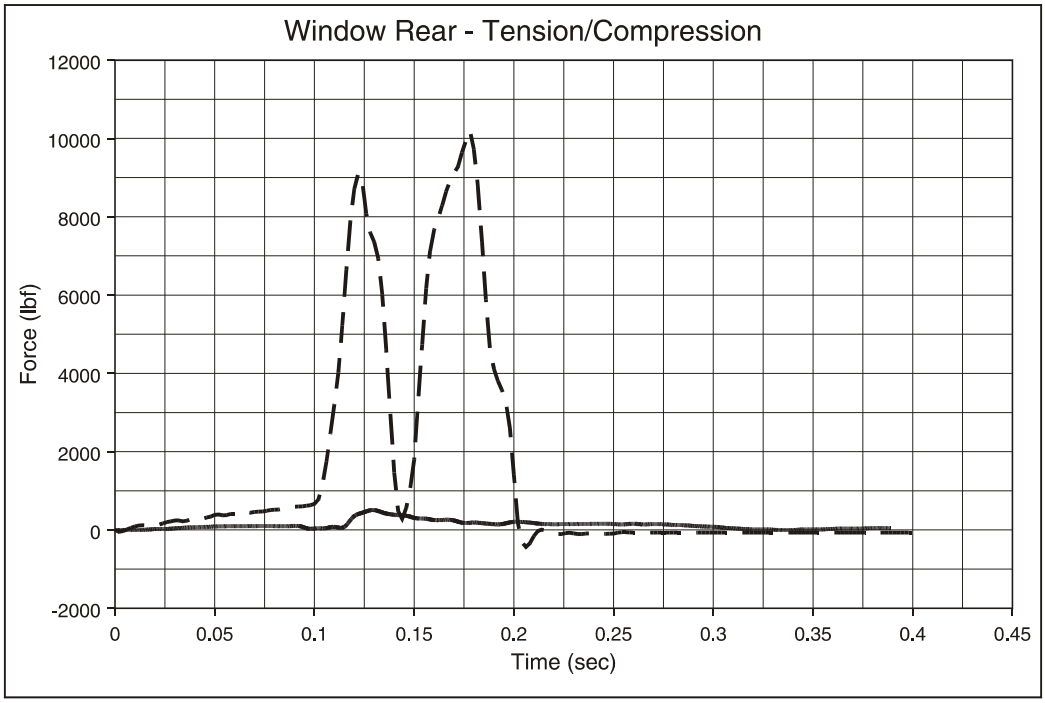

Figure F64. M-Style Seat, Type 1 Test, Seat Attachment Loads: Window Rear Load Cell, z Direction

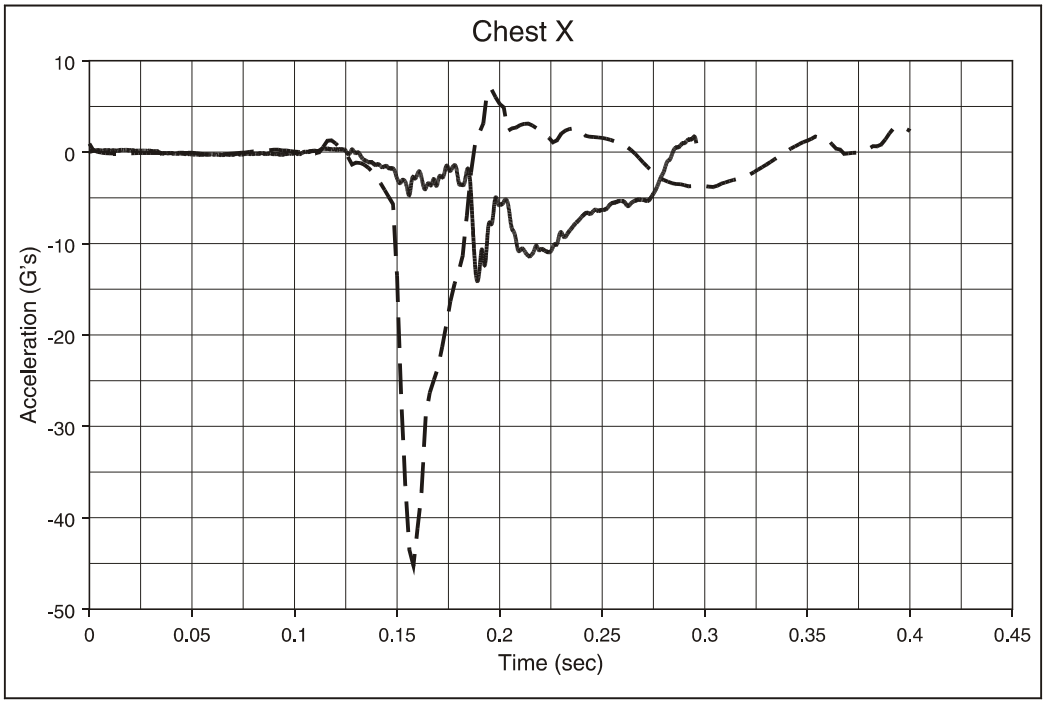

Figure F65. M-Style Seat, Type 1 Test, 50th-Percentile Hybrid II Male ATD, Aisle Seat; Chest Acceleration, x Direction

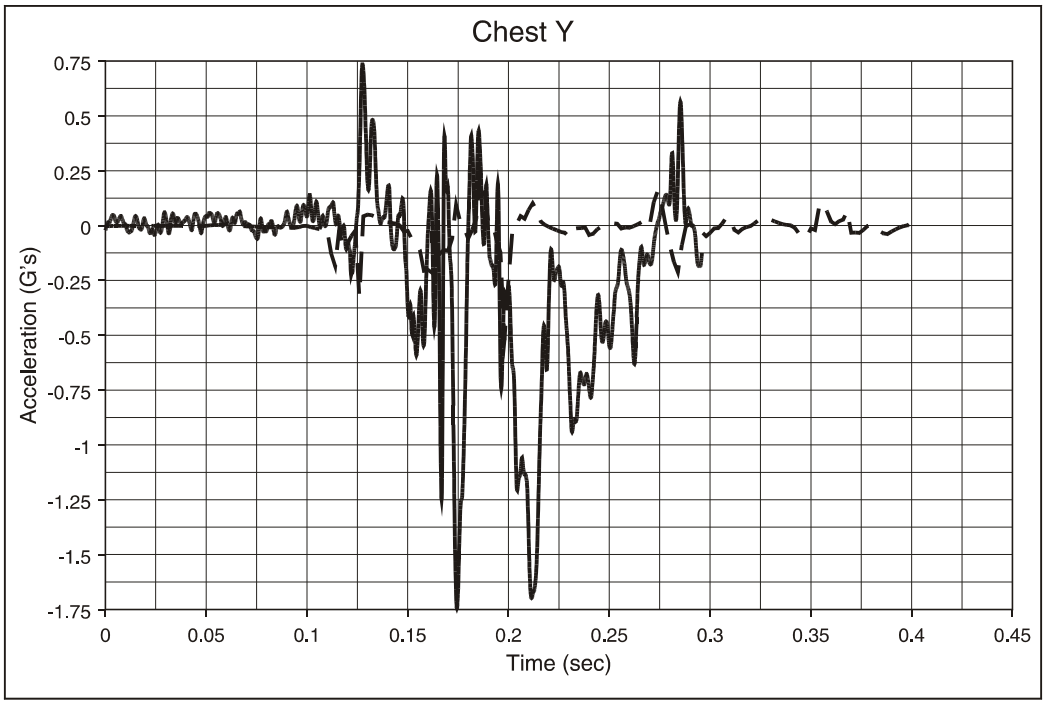

Figure F66. M-Style Seat, Type 1 Test, 50th-Percentile Hybrid II Male ATD, Aisle Seat; Chest Acceleration, y Direction

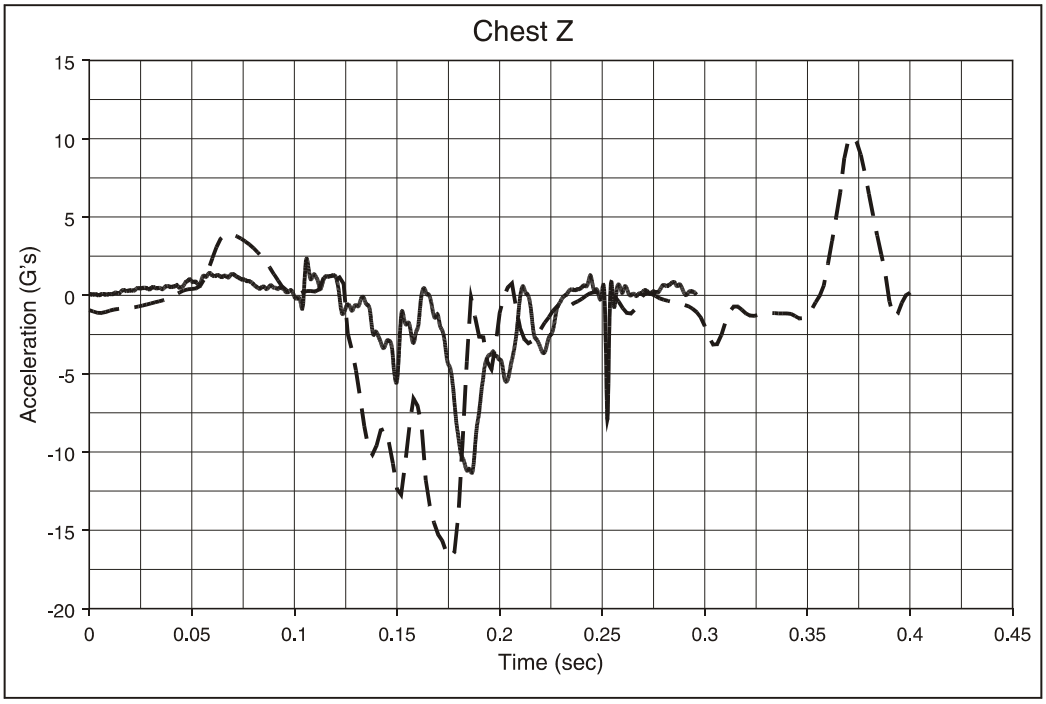

Figure F67. M-Style Seat, Type 1 Test, 50th-Percentile Hybrid II Male ATD, Aisle Seat; Chest Acceleration, z Direction

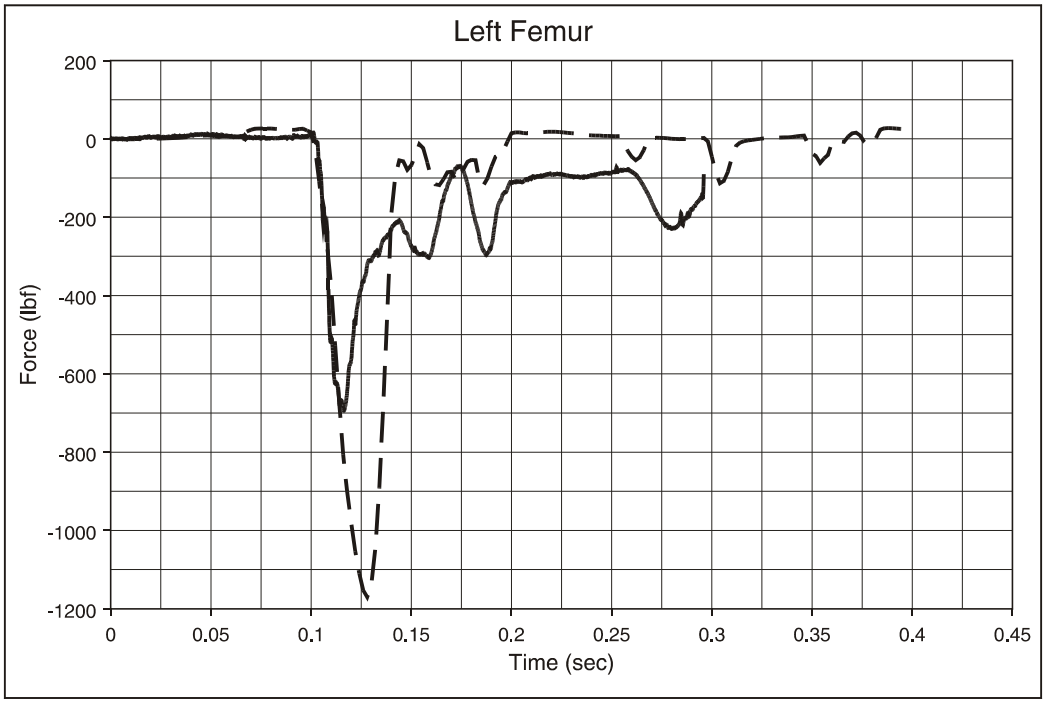

Figure F68. M-Style Seat, Type 1 Test, 50th-Percentile Hybrid II Male ATD, Aisle Seat; Left Femur Load

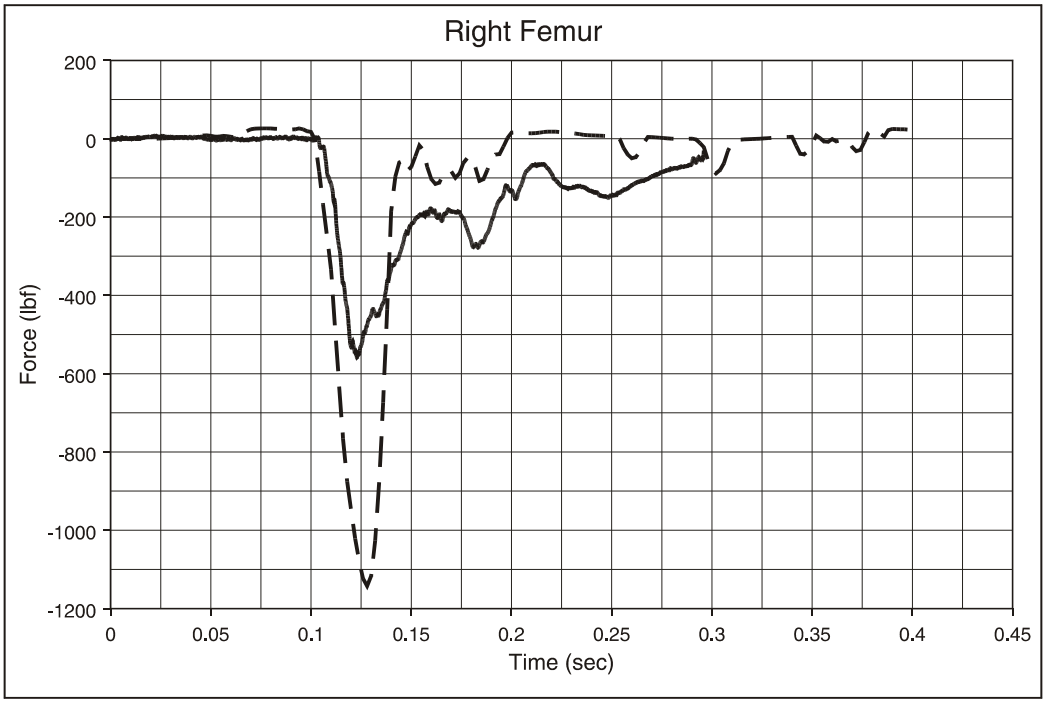

Figure F69. M-Style Seat, Type 1 Test, 50th-Percentile Hybrid II Male ATD, Aisle Seat; Right Femur Load

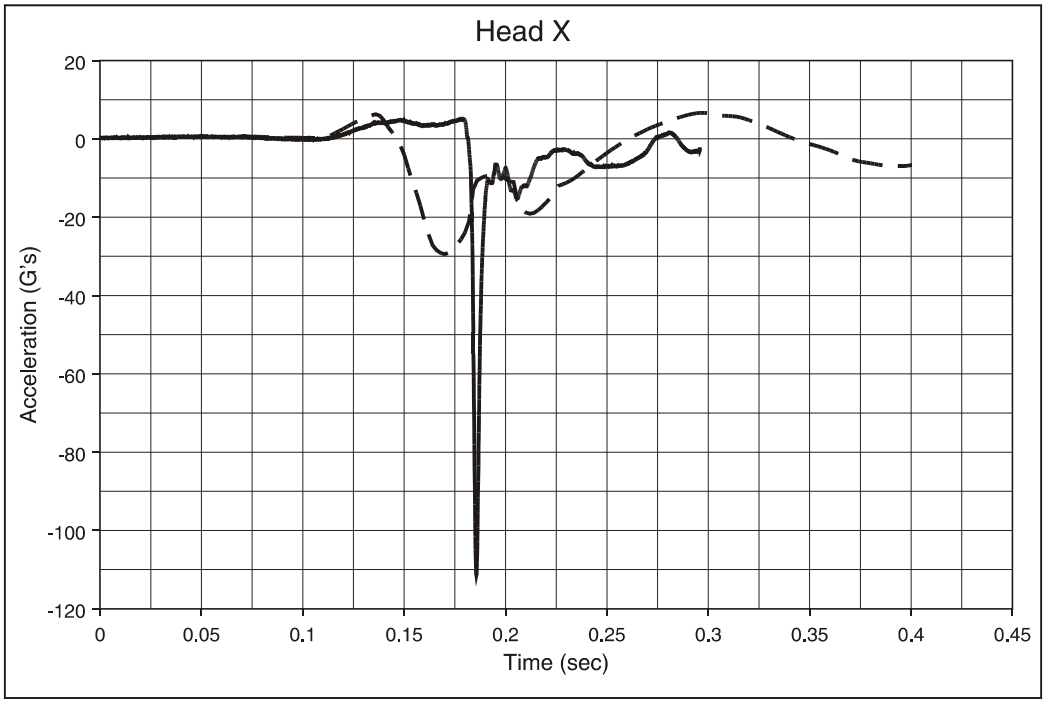

Figure F70. M-Style Seat, Type 1 Test, 50th-Percentile Hybrid II Male ATD, Aisle Seat; Head Acceleration, x Direction

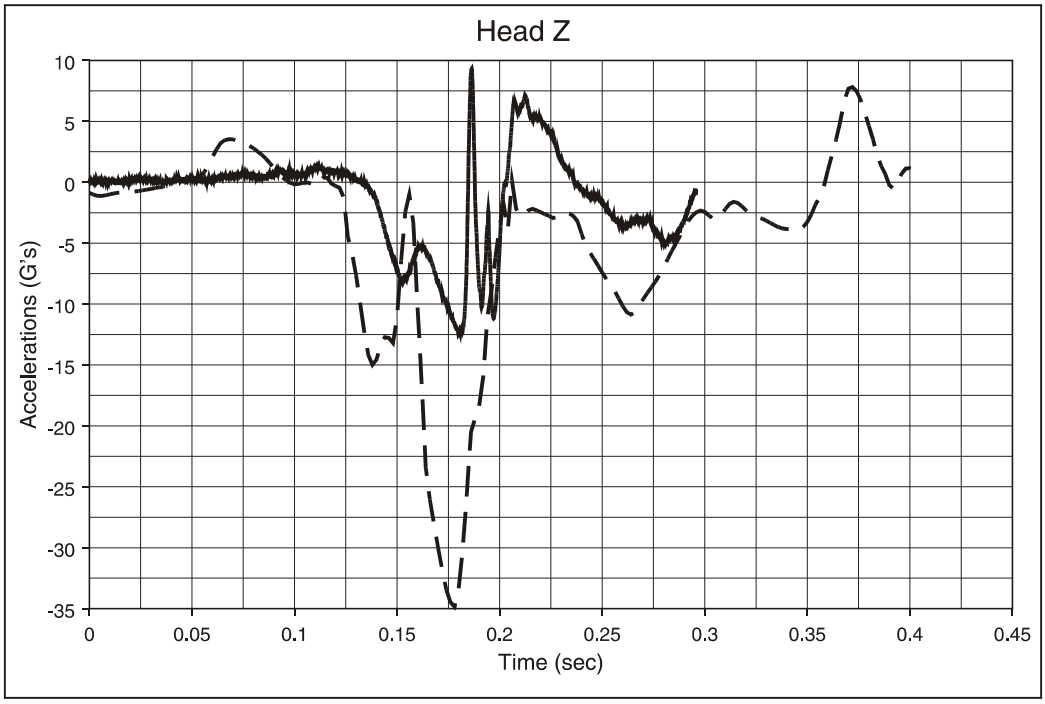

Figure F71. M-Style Seat, Type 1 Test, 50th-Percentile Hybrid II Male ATD, Aisle Seat; Head Acceleration, z Direction

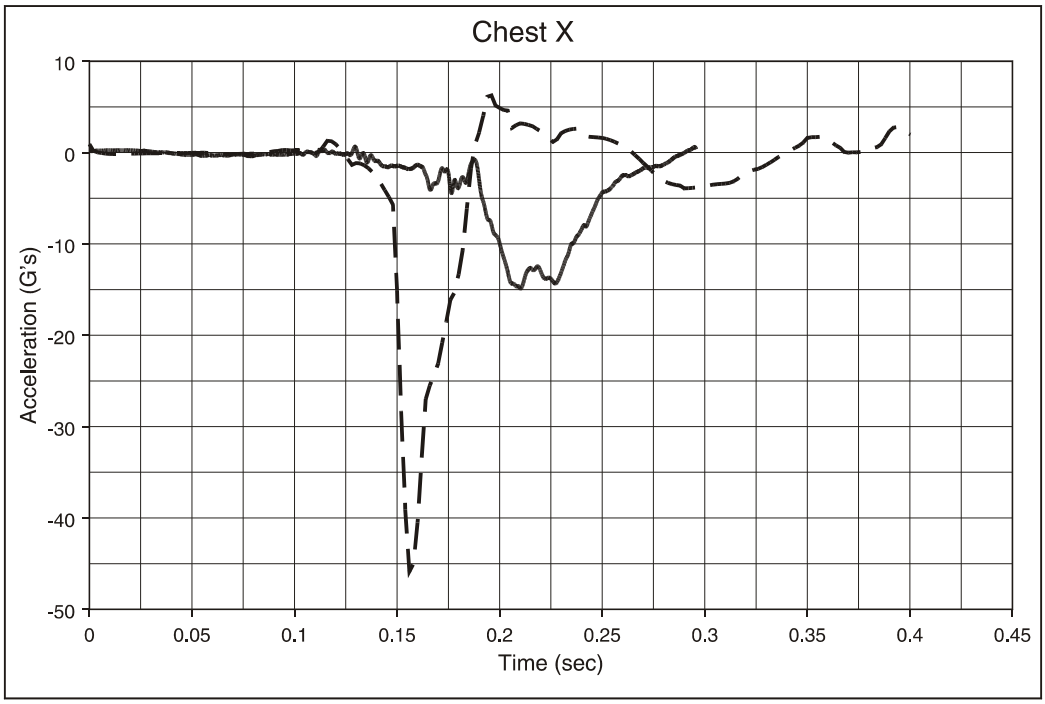

Figure F72. M-Style Seat, Type 1 Test, 50th-Percentile Hybrid II Male ATD, Center Seat; Chest Acceleration, x Direction

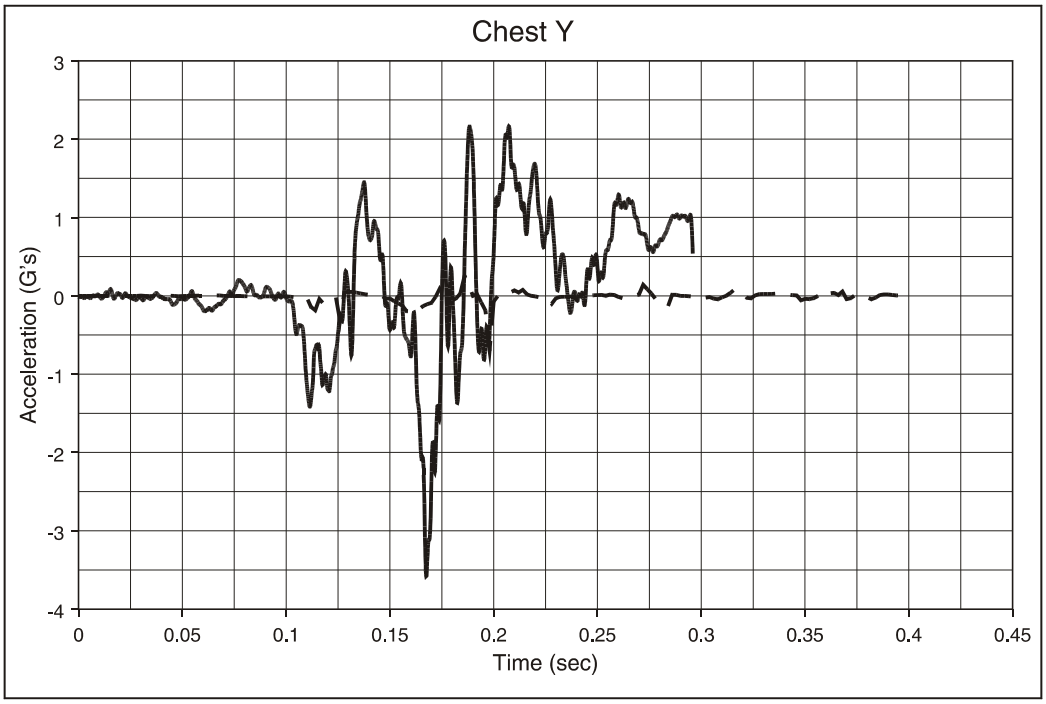

Figure F73. M-Style Seat, Type 1 Test, 50th-Percentile Hybrid II Male ATD, Center Seat; Chest Acceleration, y Direction

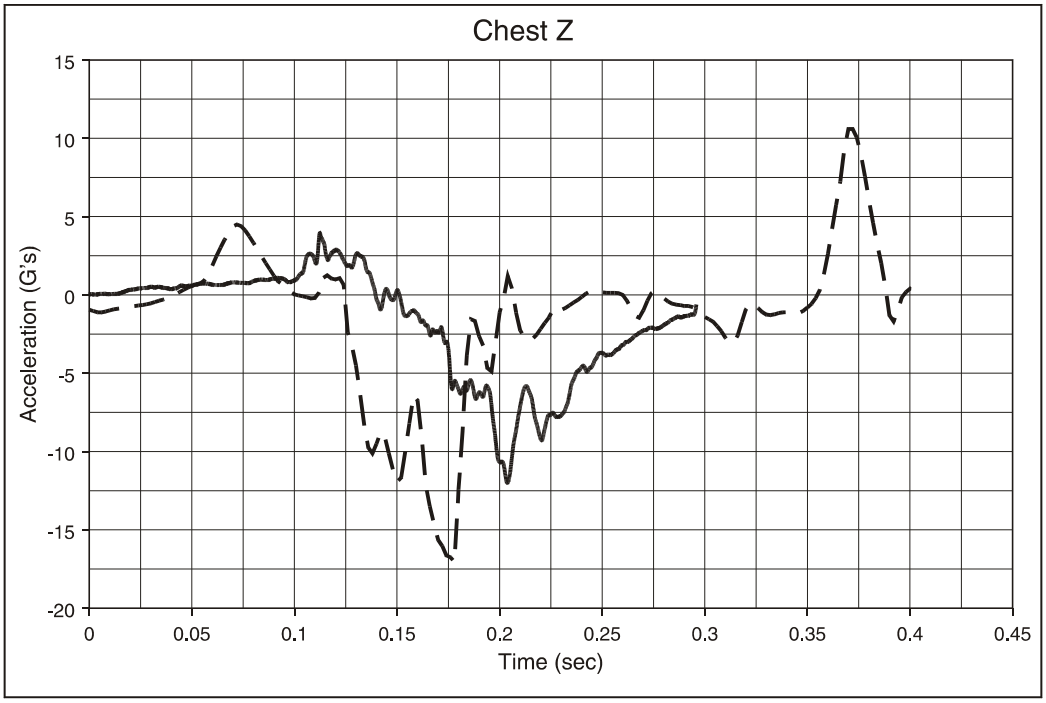

Figure F74. M-Style Seat, Type 1 Test, 50th-Percentile Hybrid II Male ATD, Center Seat; Chest Acceleration, z Direction

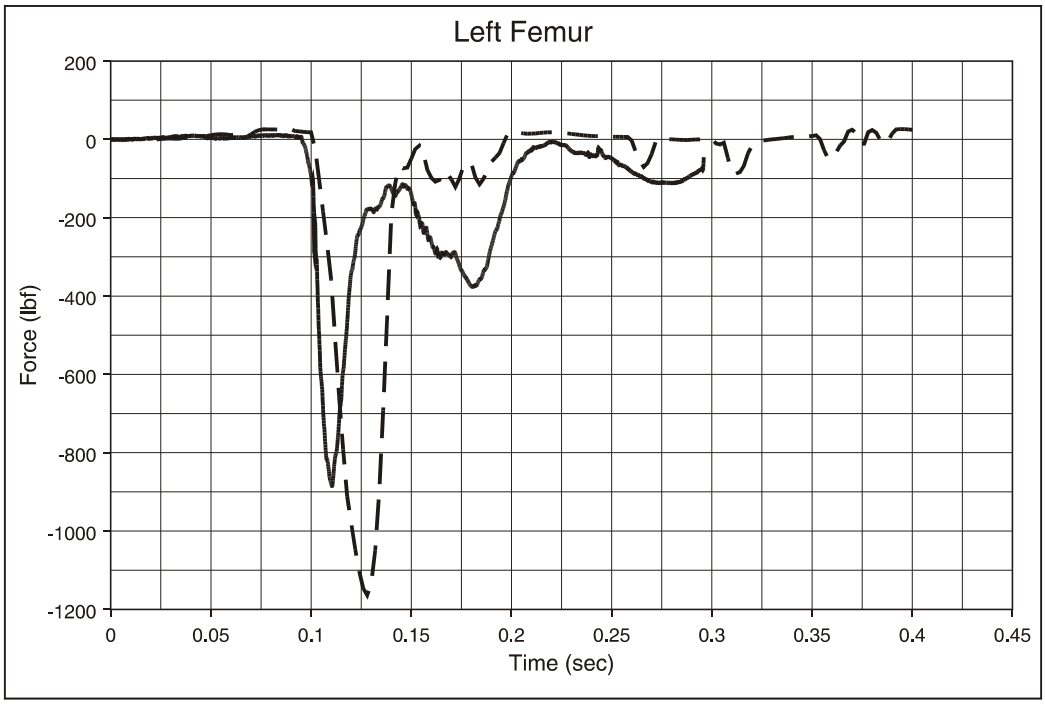

Figure F75. M-Style Seat, Type 1 Test, 50th-Percentile Hybrid II Male ATD, Center Seat; Left Femur Load

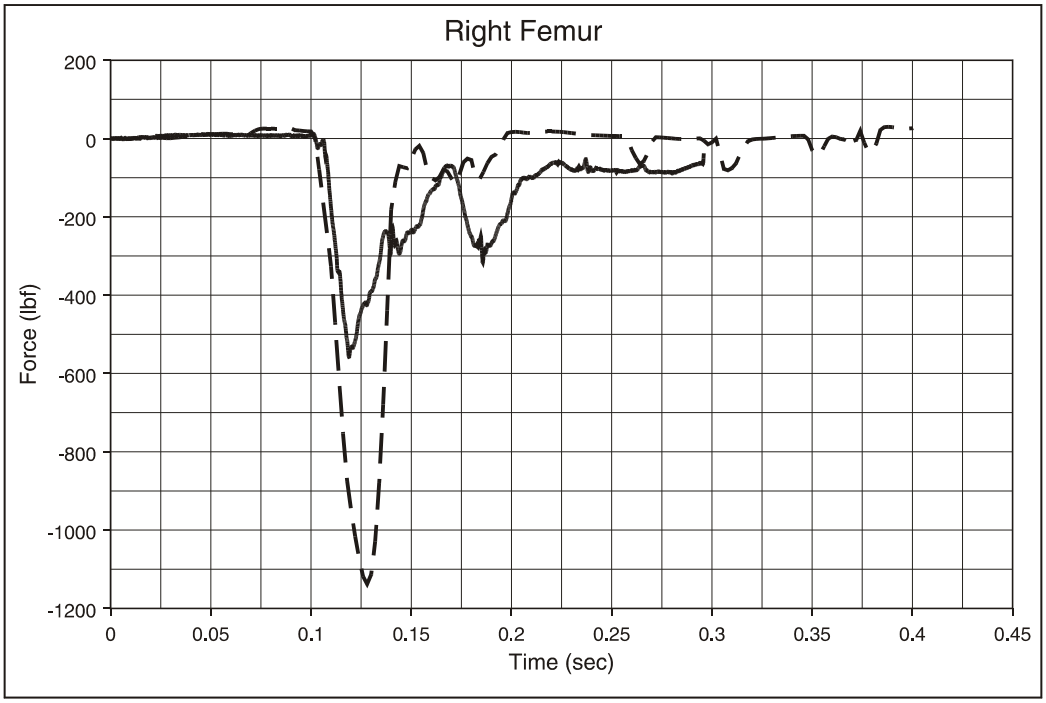

Figure F76. M-Style Seat, Type 1 Test, 50th-Percentile Hybrid II Male ATD, Center Seat; Right Femur Load

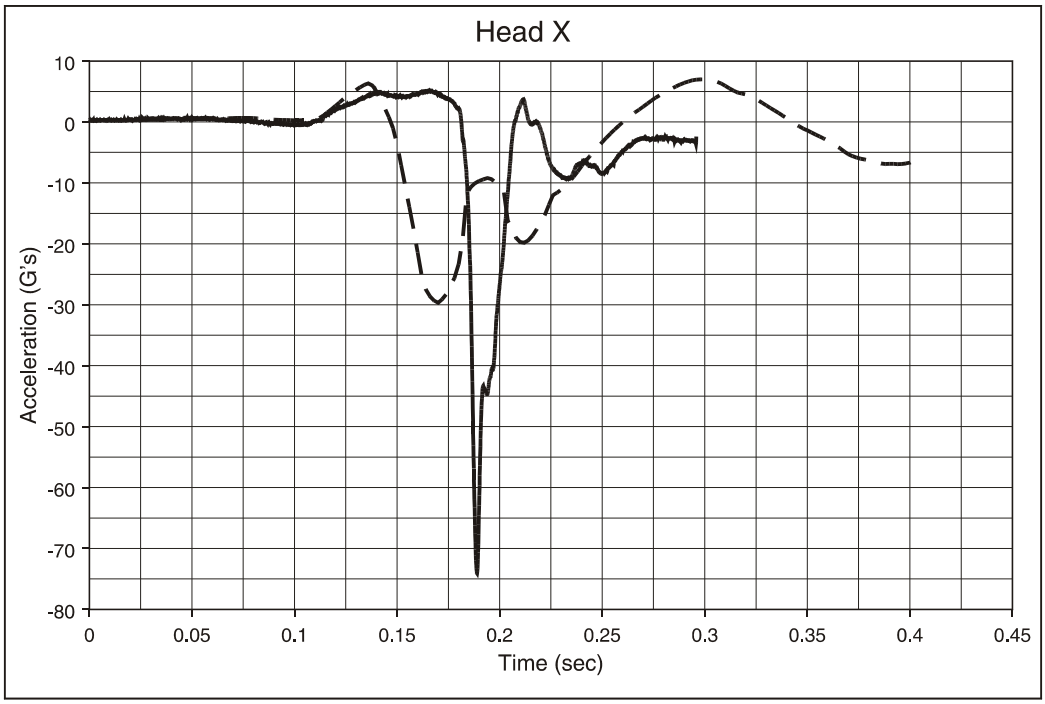

Figure F77. M-Style Seat, Type 1 Test, 50th-Percentile Hybrid II Male ATD, Center Seat; Head Acceleration, x Direction

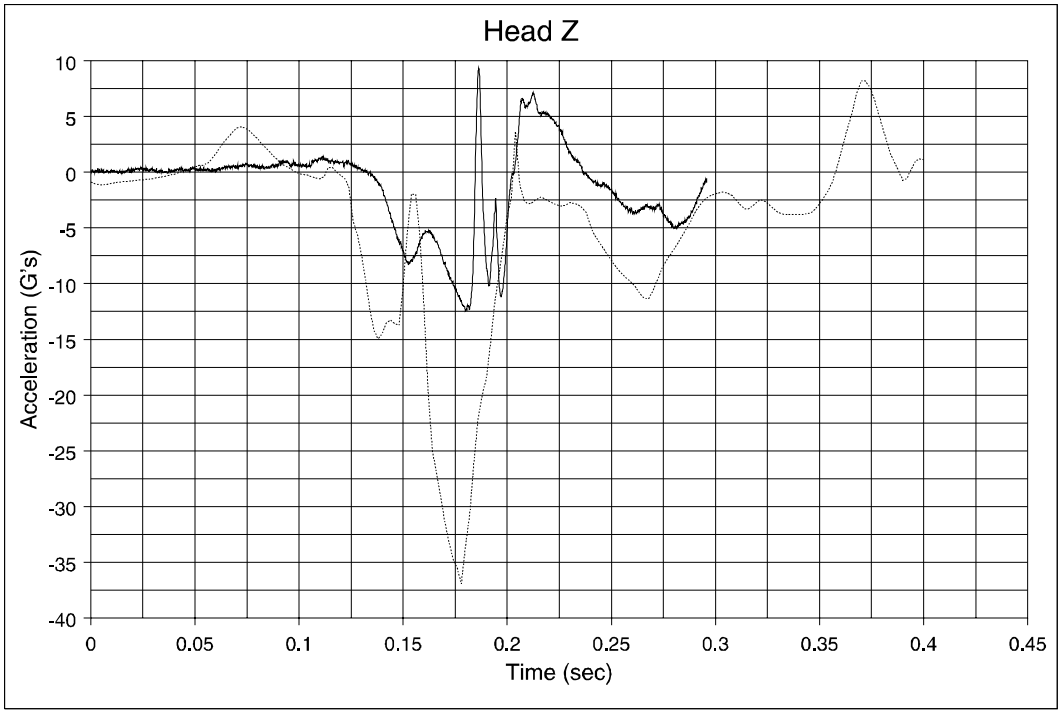

Figure F78. M-Style Seat, Type 1 Test, 50th-Percentile Hybrid II Male ATD, Center Seat; Head Acceleration, z Direction

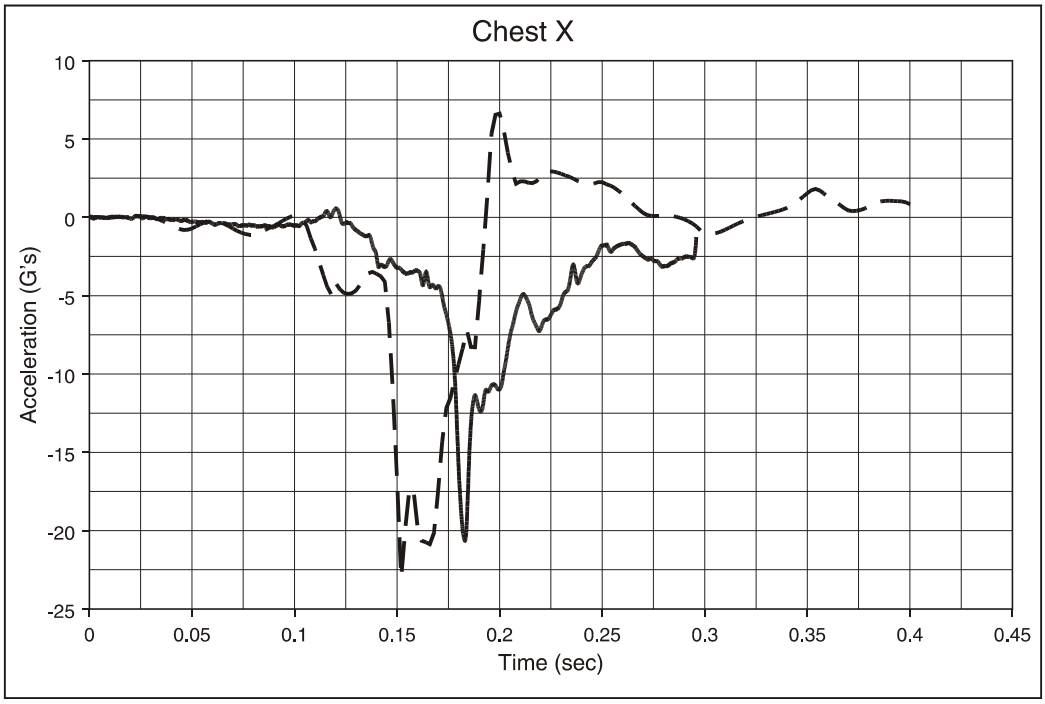

Figure F79. M-Style Seat, Type 1 Test, 50th-Percentile Hybrid III Male ATD, Window Seat; Chest Acceleration, x Direction

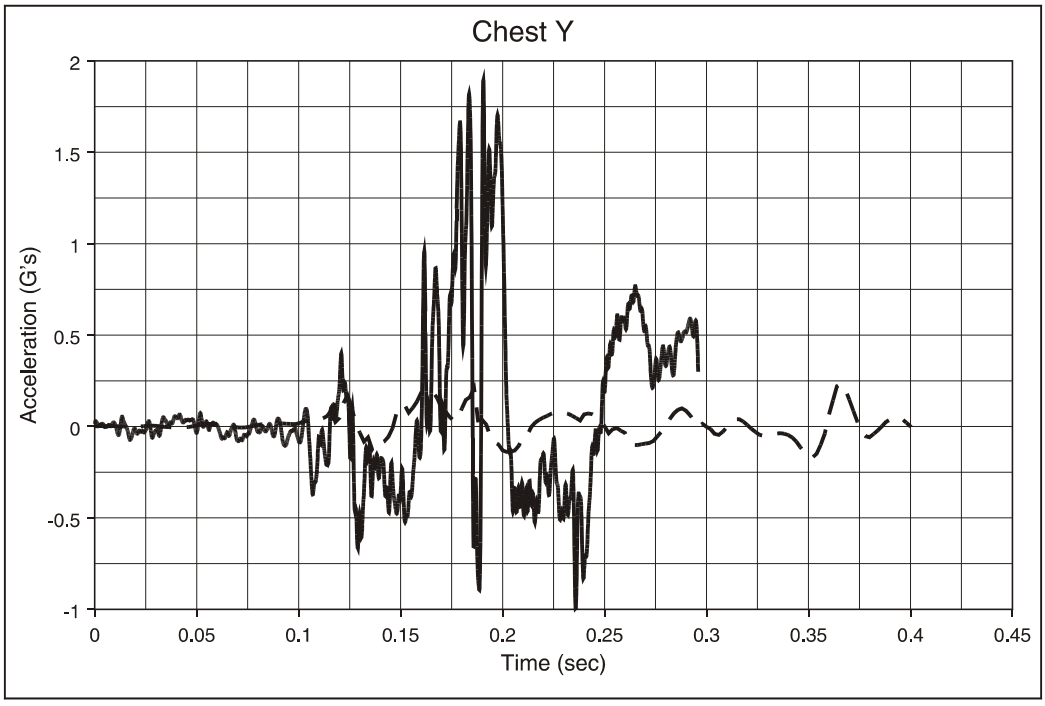

Figure F80. M-Style Seat, Type 1 Test, 50th-Percentile Hybrid III Male ATD, Window Seat; Chest Acceleration, y Direction

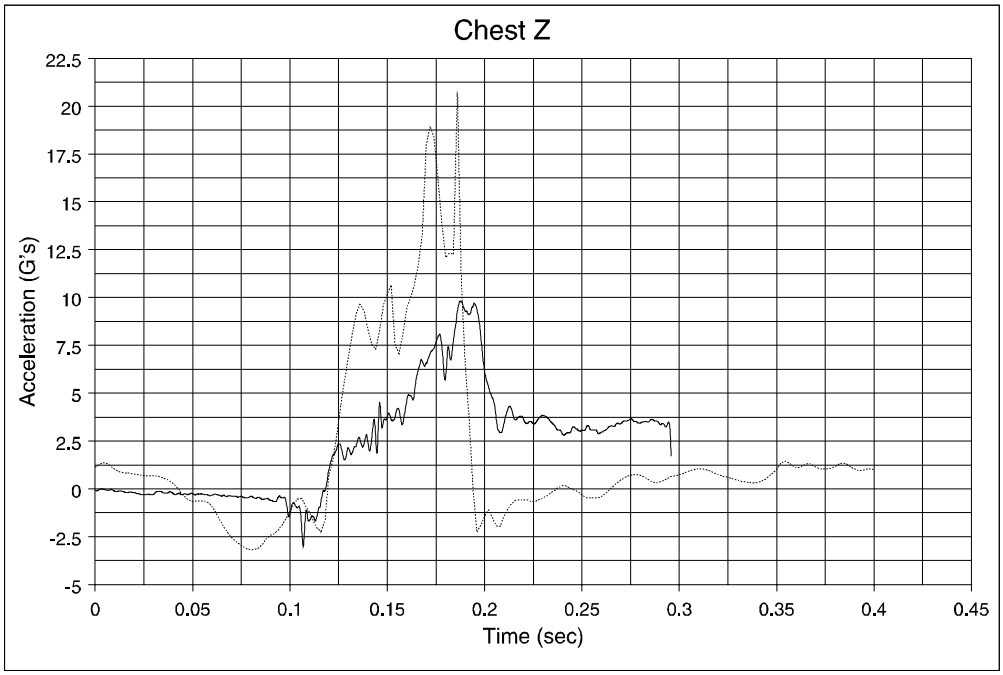

Figure F81. M-Style Seat, Type 1 Test, 50th-Percentile Hybrid III Male ATD, Window Seat; Chest Acceleration, z Direction

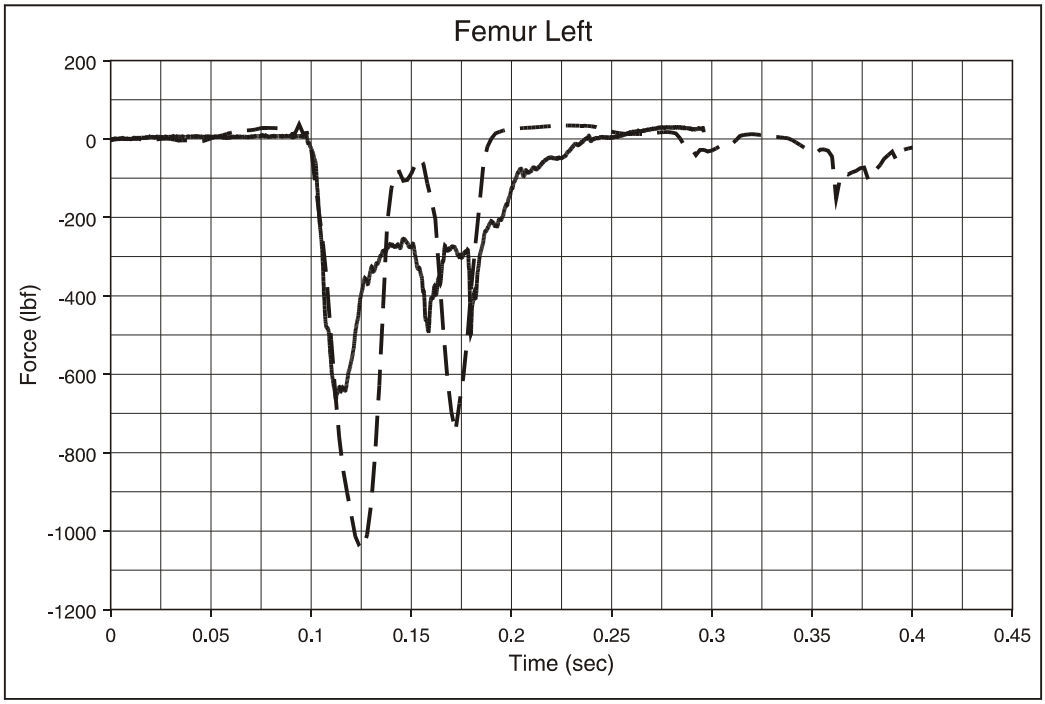

Figure F82. M-Style Seat, Type 1 Test, 50th-Percentile Hybrid III Male ATD, Window Seat; Left Femur Load

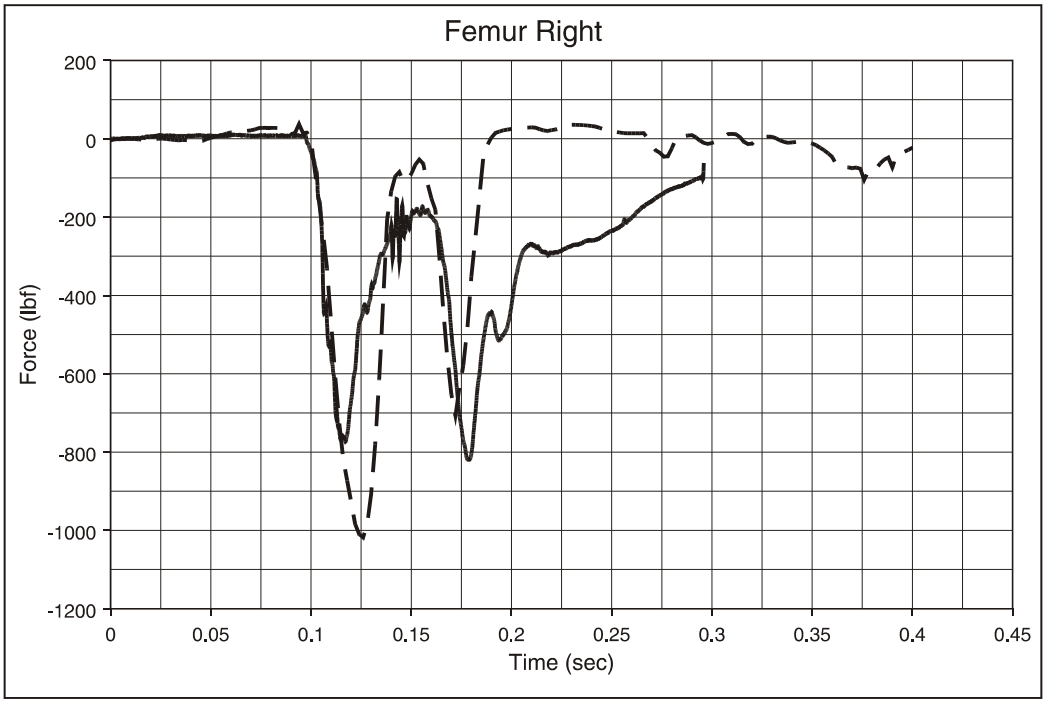

Figure F83. M-Style Seat, Type 1 Test, 50th-Percentile Hybrid III Male ATD, Window Seat; Right Femur Load

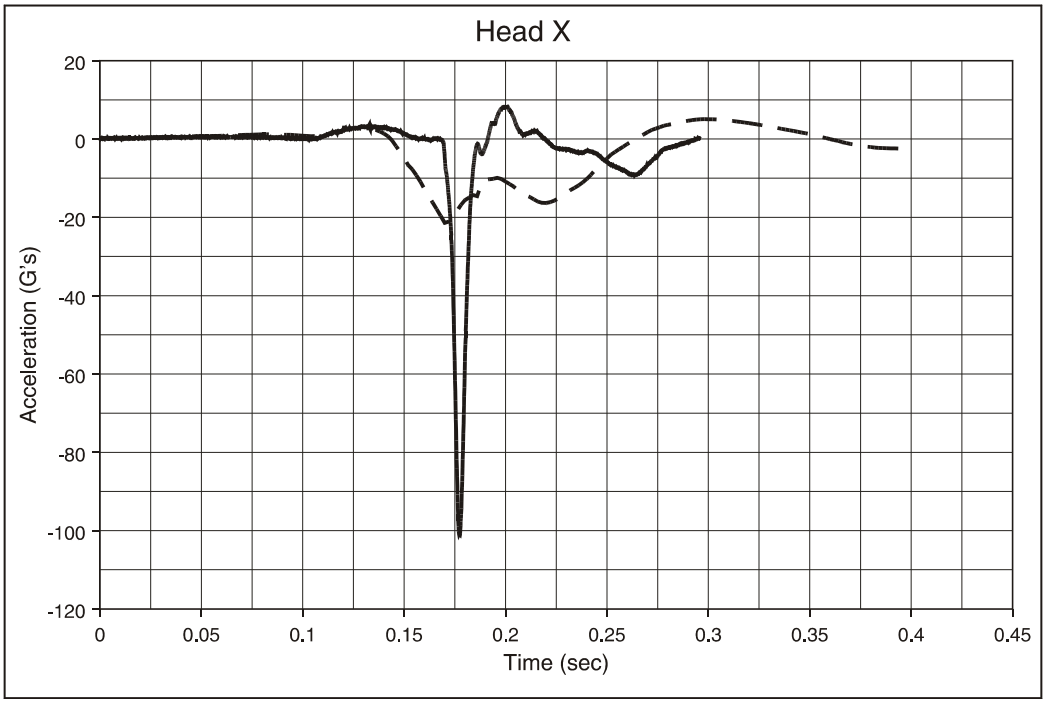

Figure F84. M-Style Seat, Type 1 Test, 50th-Percentile Hybrid III Male ATD, Window Seat; Head Acceleration, x Direction

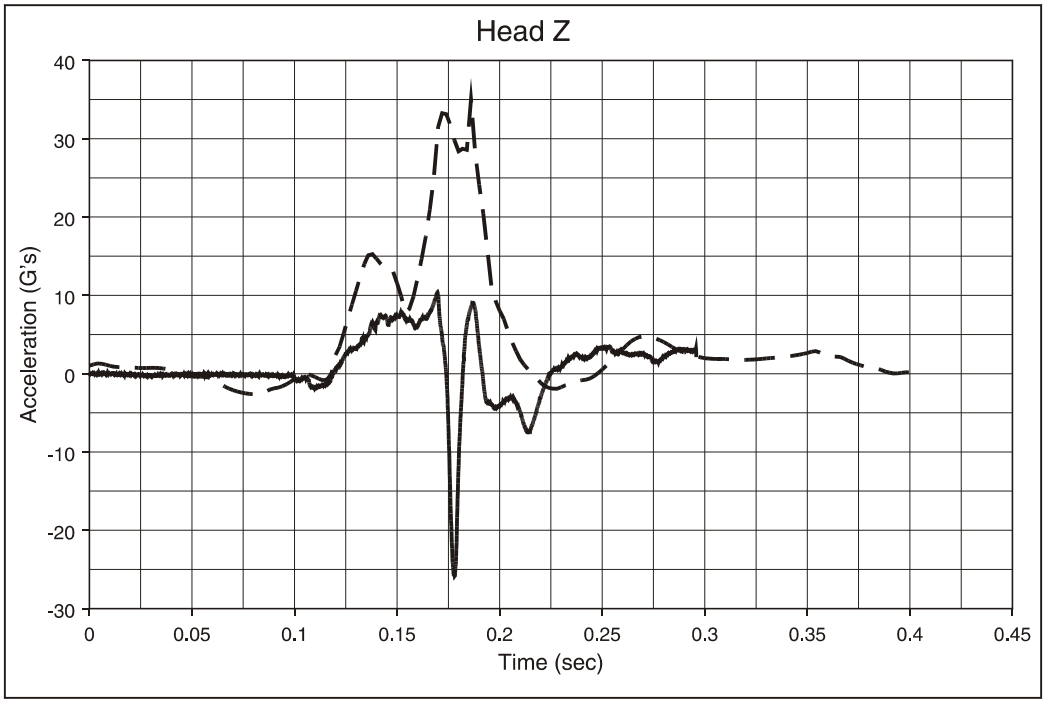

Figure F85. M-Style Seat, Type 1 Test, 50th-Percentile Hybrid III Male ATD, Window Seat; Head Acceleration, z Direction

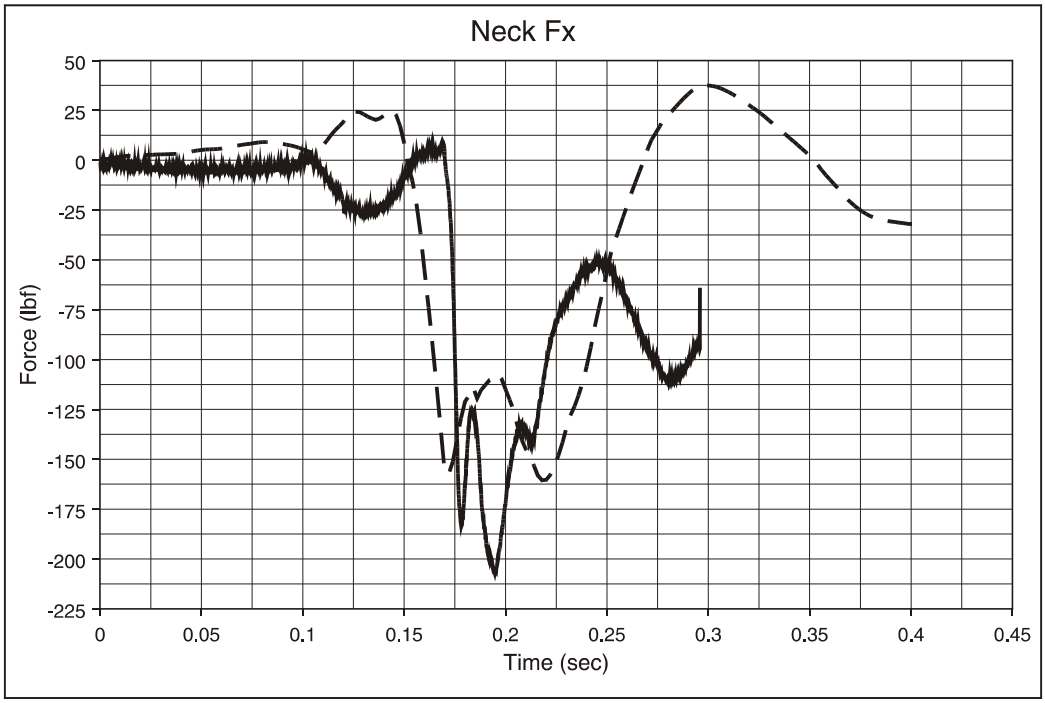

Figure F86. M-Style Seat, Type 1 Test, 50th-Percentile Hybrid III Male ATD, Window Seat; Neck Shear Load

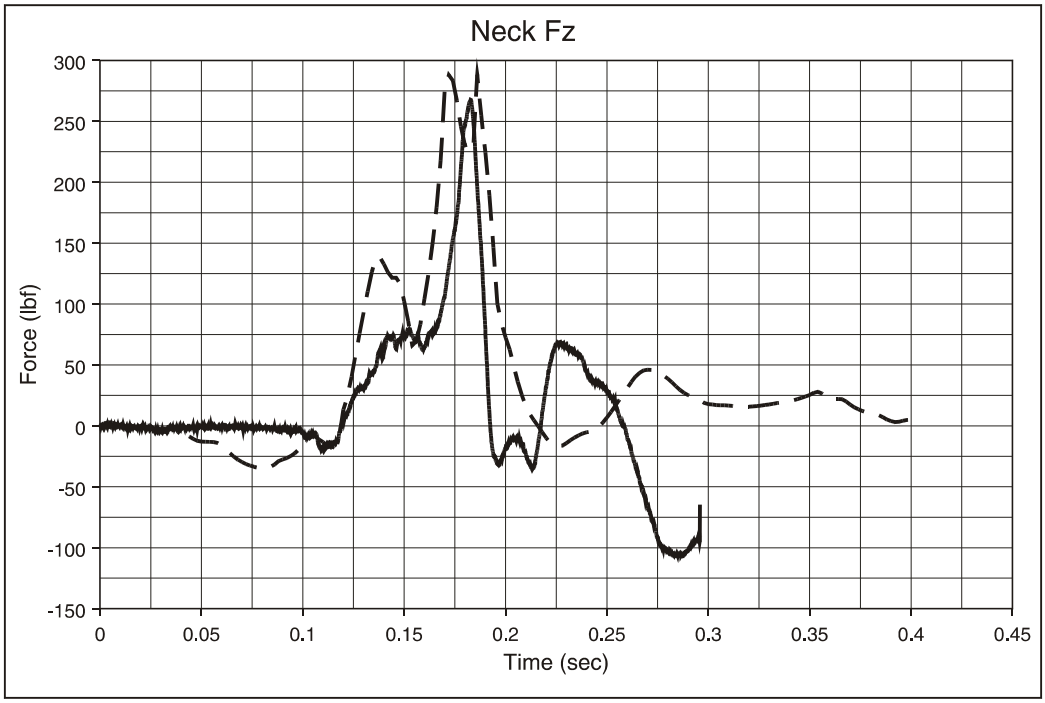

Figure F87. M-Style Seat, Type 1 Test, 50th-Percentile Hybrid III Male ATD, Window Seat; Neck Compression/Tension Load

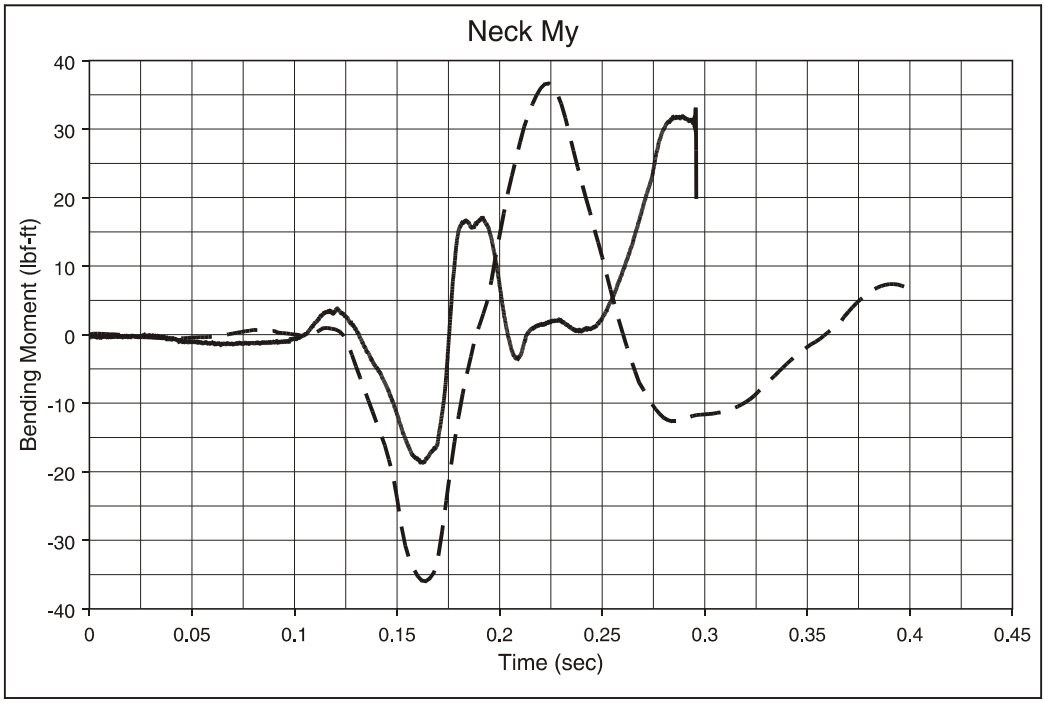

Figure F88. M-Style Seat, Type 1 Test, 50th-Percentile Hybrid III Male ATD, Window Seat; Neck Flexion/Extension Moment

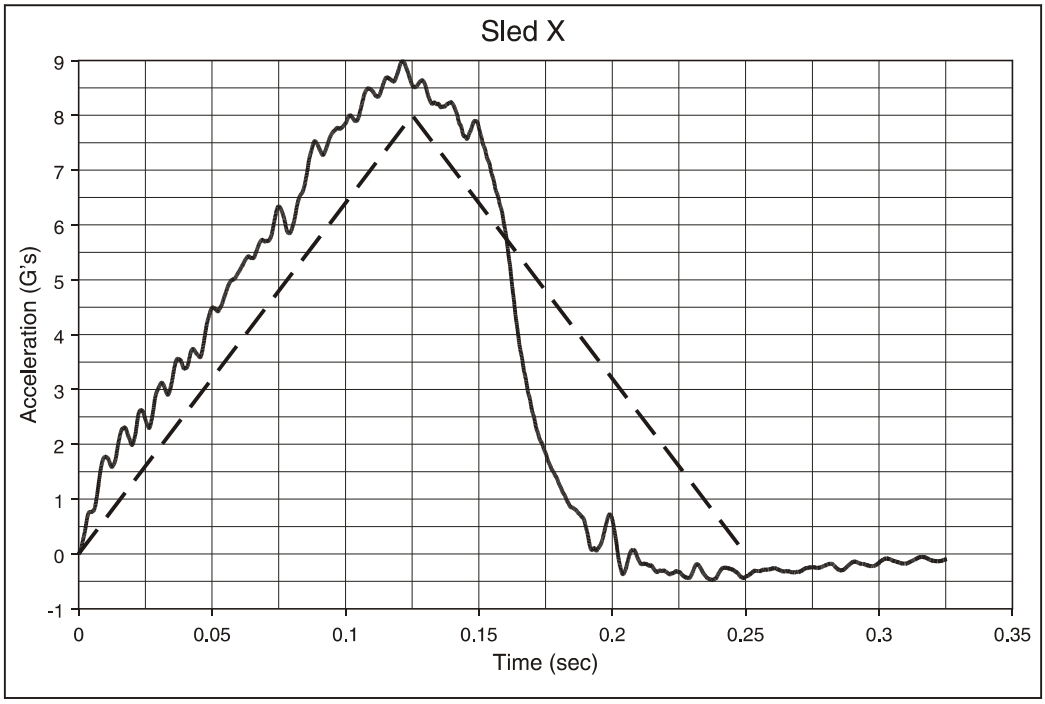

Figure F89. M-Style Seat, Type 2 Test, 95th-, 50th- and 5th-Percentile ATDs: Sled Pulse

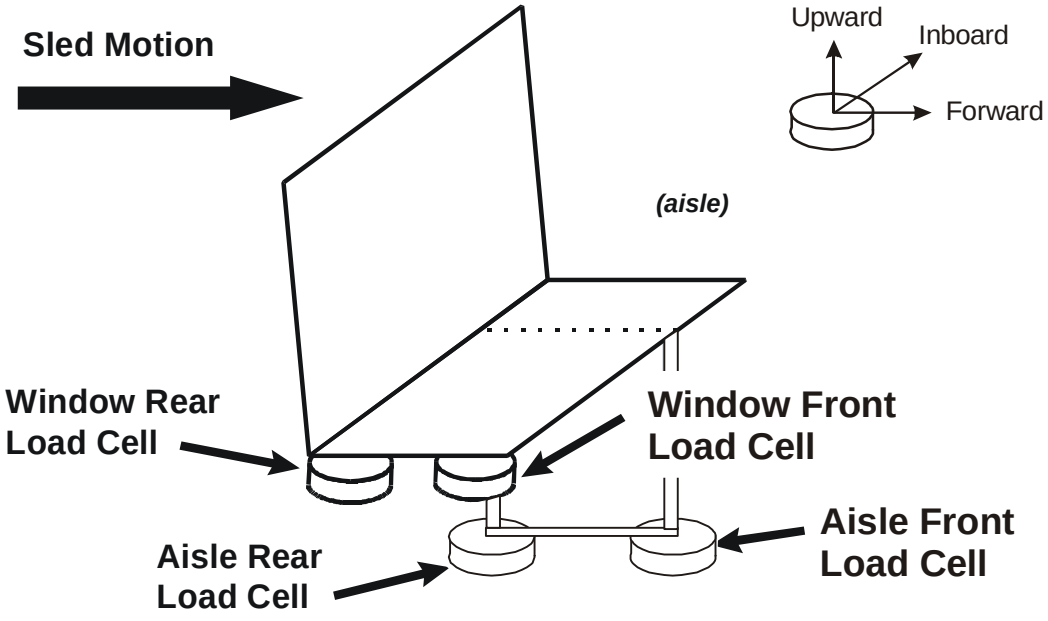

Figure F90. M-Style Seat, Type 2 Test, Seat Attachment Loads: M-Style Seat Load Cell Orientation

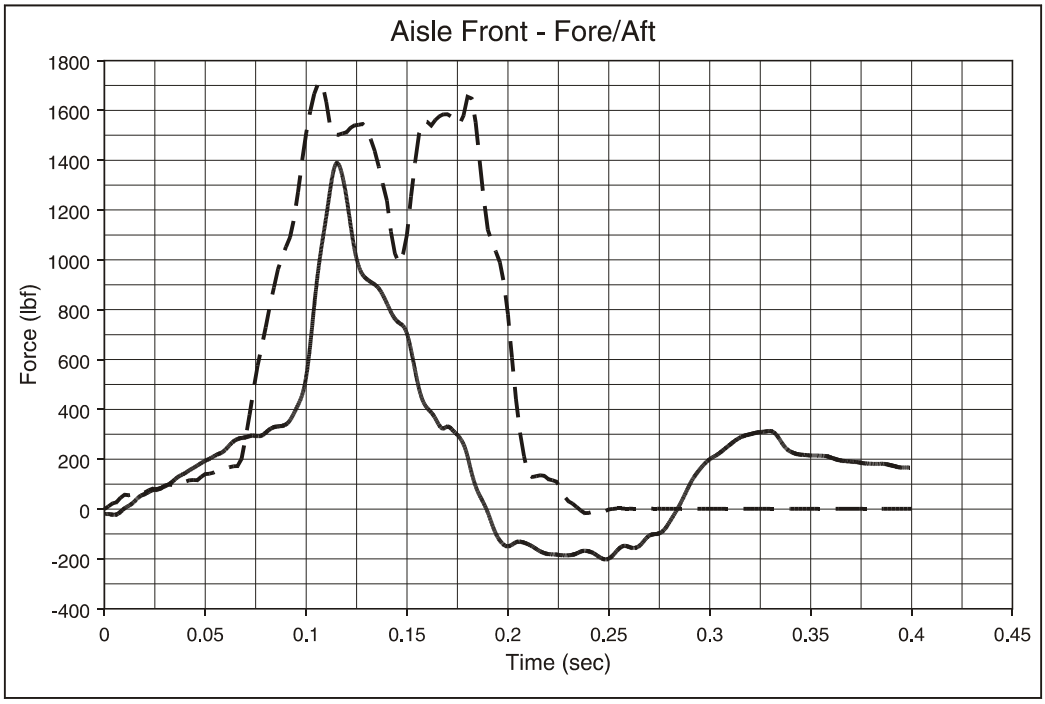

Figure F91. M-Style Seat, Type 2 Test, Seat Attachment Loads: Aisle Front Load Cell, x Direction

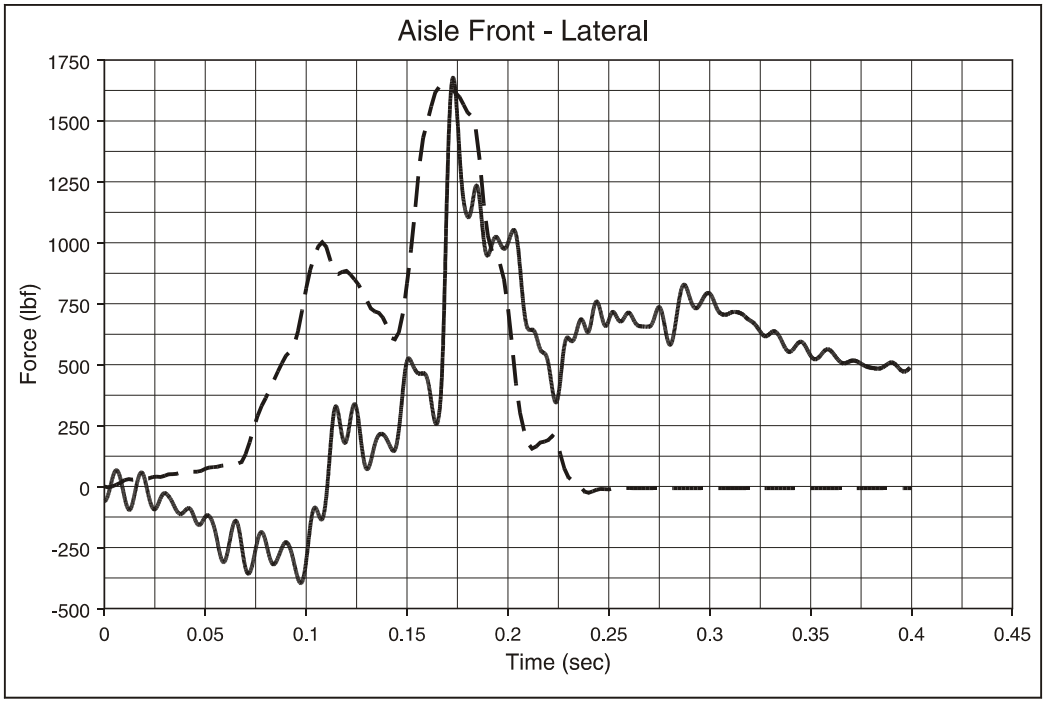

Figure F92. M-Style Seat, Type 2 Test, Seat Attachment Loads: Aisle Front Load Cell, y Direction

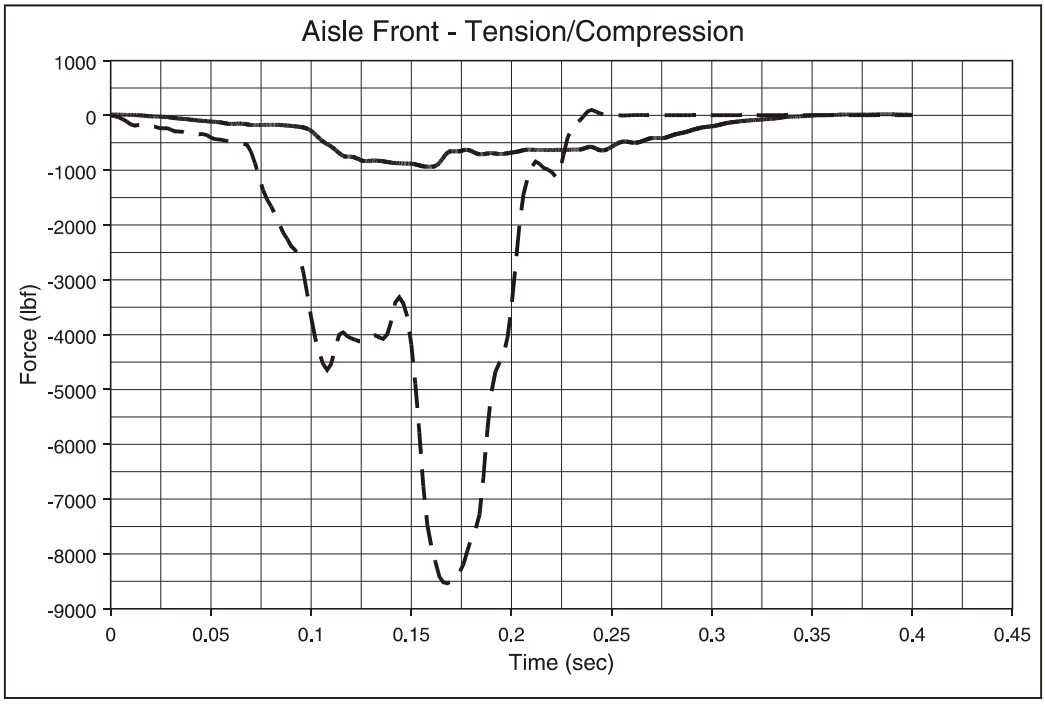

Figure F93. M-Style Seat, Type 2 Test, Seat Attachment Loads: Aisle Front Load Cell, z Direction

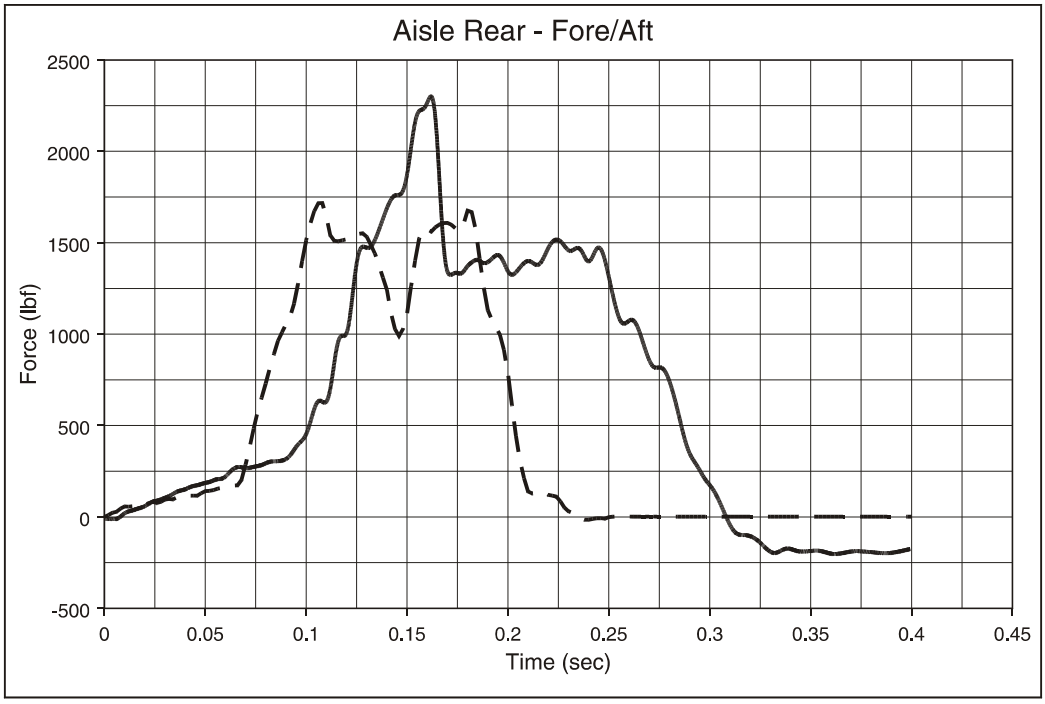

Figure F94. M-Style Seat, Type 2 Test, Seat Attachment Loads: Aisle Rear Load Cell, x Direction

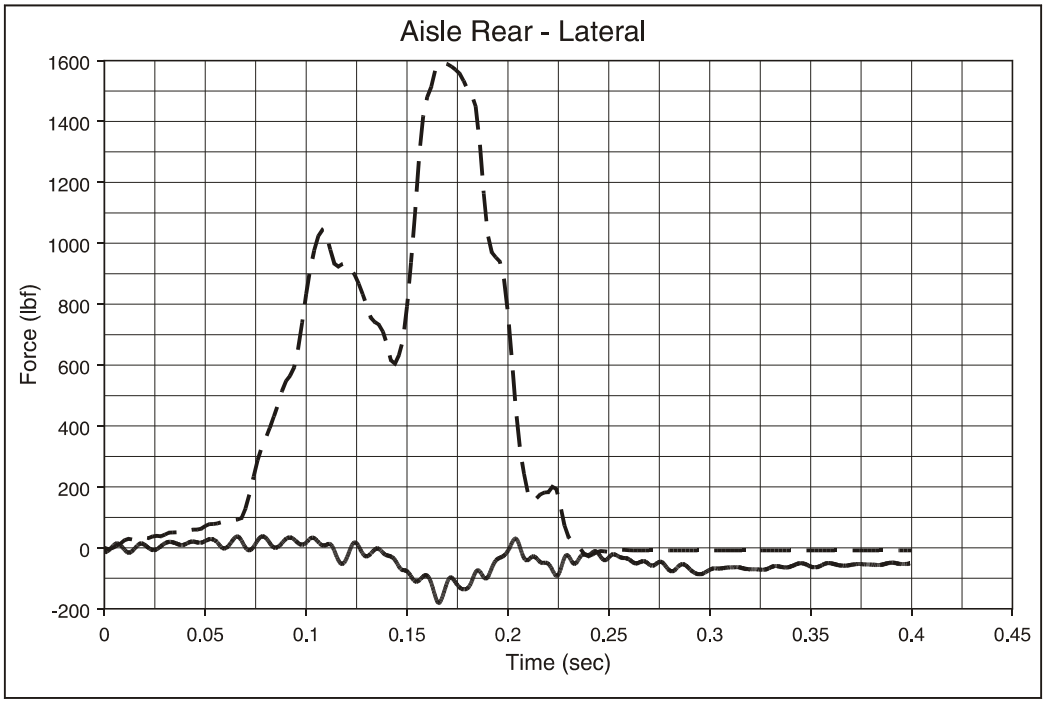

Figure F95. M-Style Seat, Type 2 Test, Seat Attachment Loads: Aisle Rear Load Cell, y Direction

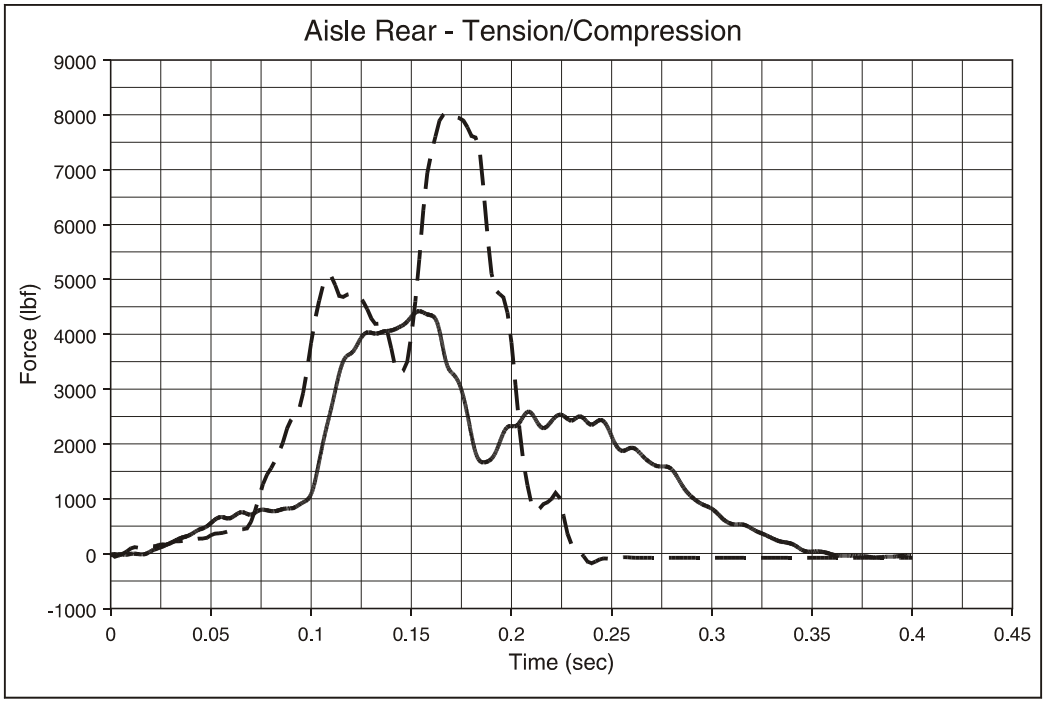

Figure F96. M-Style Seat, Type 2 Test, Seat Attachment Loads: Aisle Rear Load Cell, z Direction

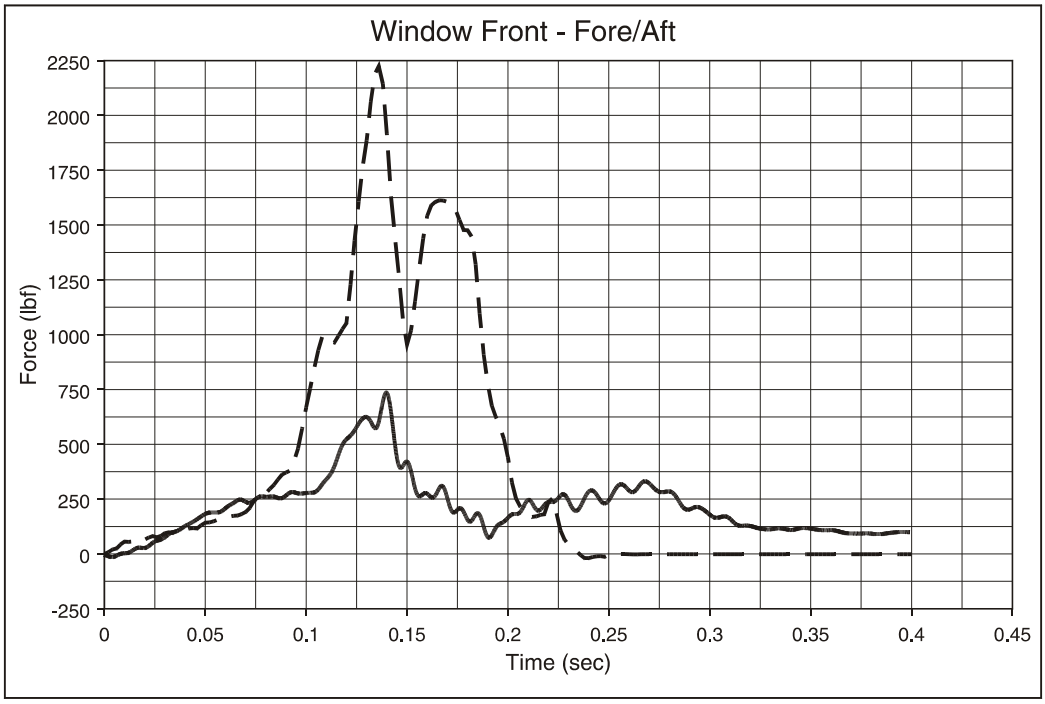

Figure F97. M-Style Seat, Type 2 Test, Seat Attachment Loads: Window Front Load Cell, x Direction

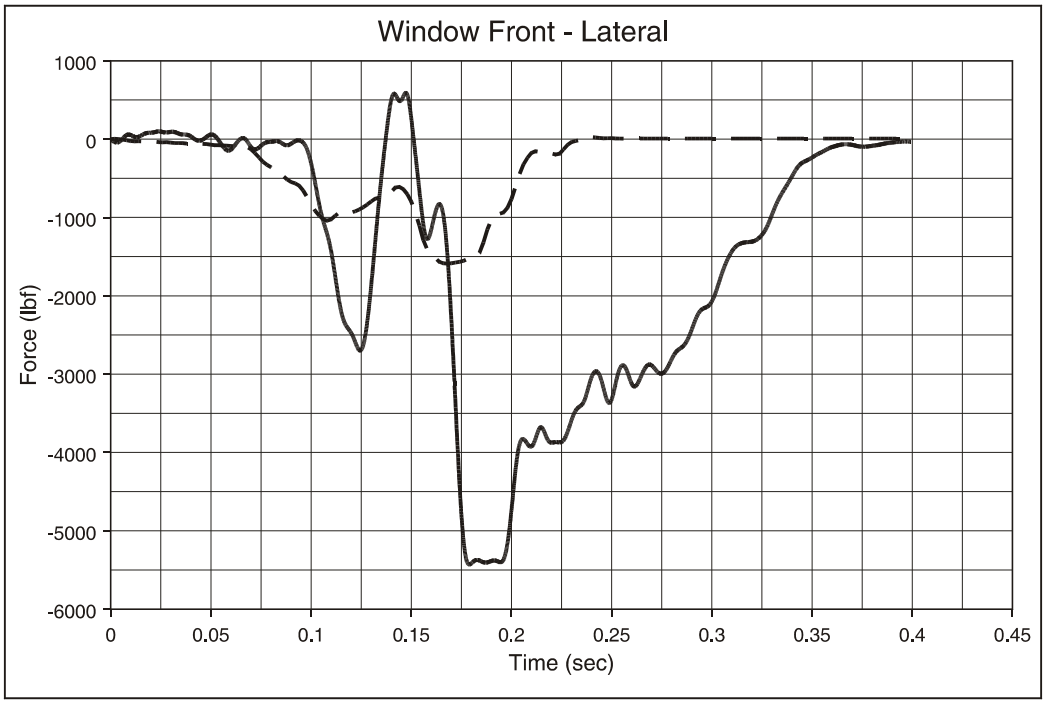

Figure F98. M-Style Seat, Type 2 Test, Seat Attachment Loads: Window Front Load Cell, y Direction

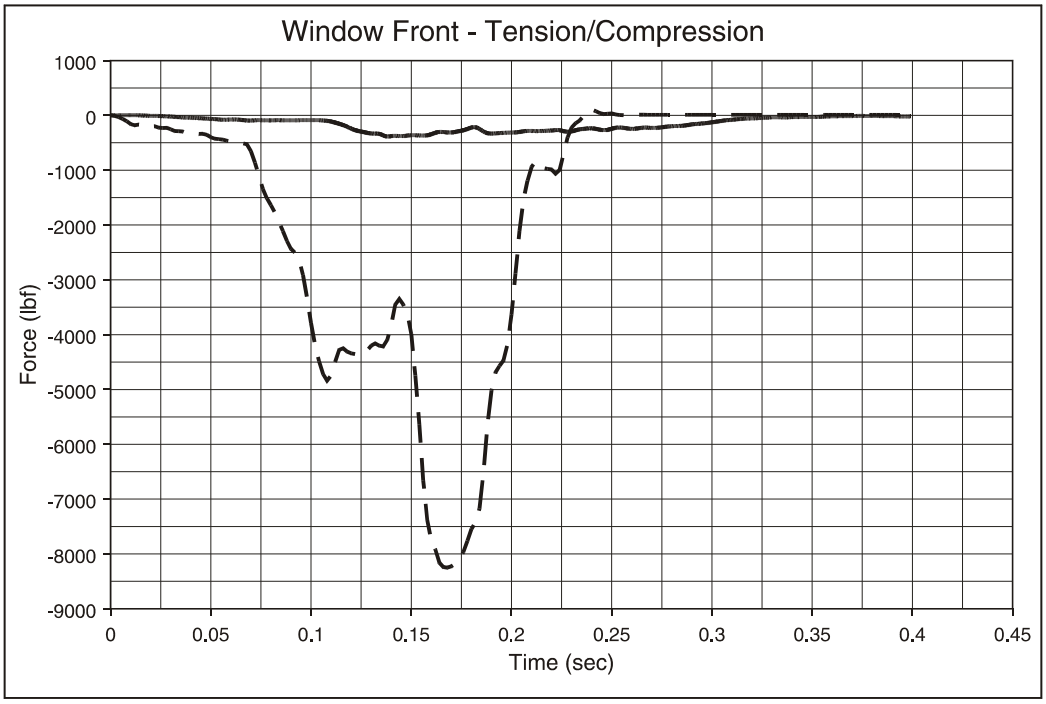

Figure F99. M-Style Seat, Type 2 Test, Seat Attachment Loads: Window Front Load Cell, z Direction

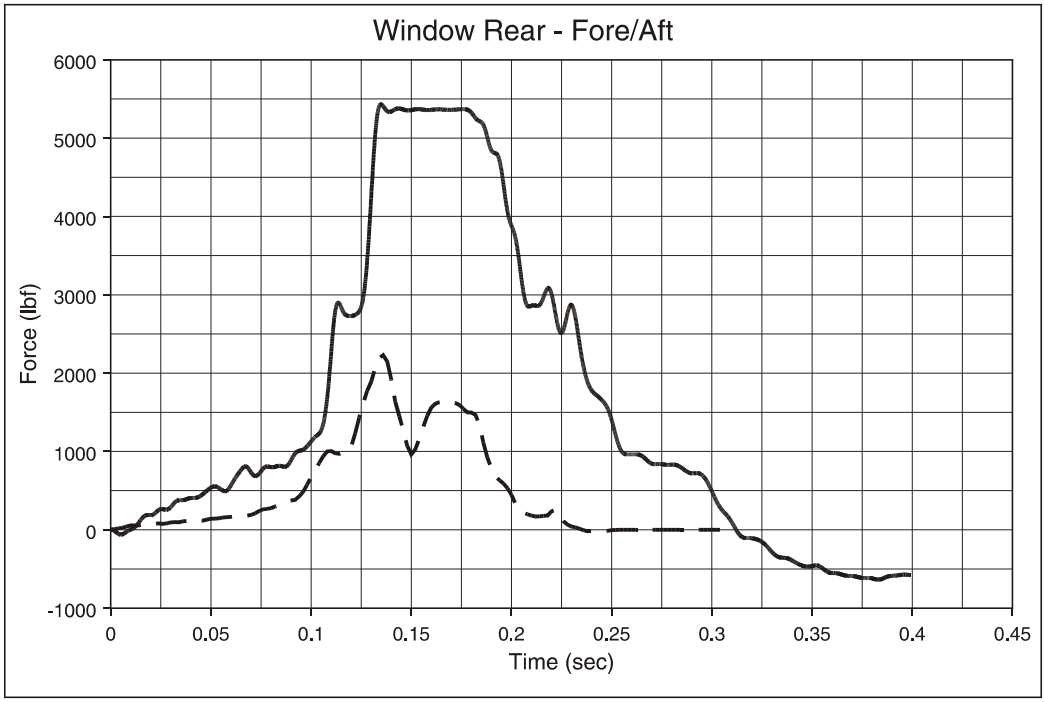

Figure F100. M-Style Seat, Type 2 Test, Seat Attachment Loads: Window Rear Load Cell, x Direction

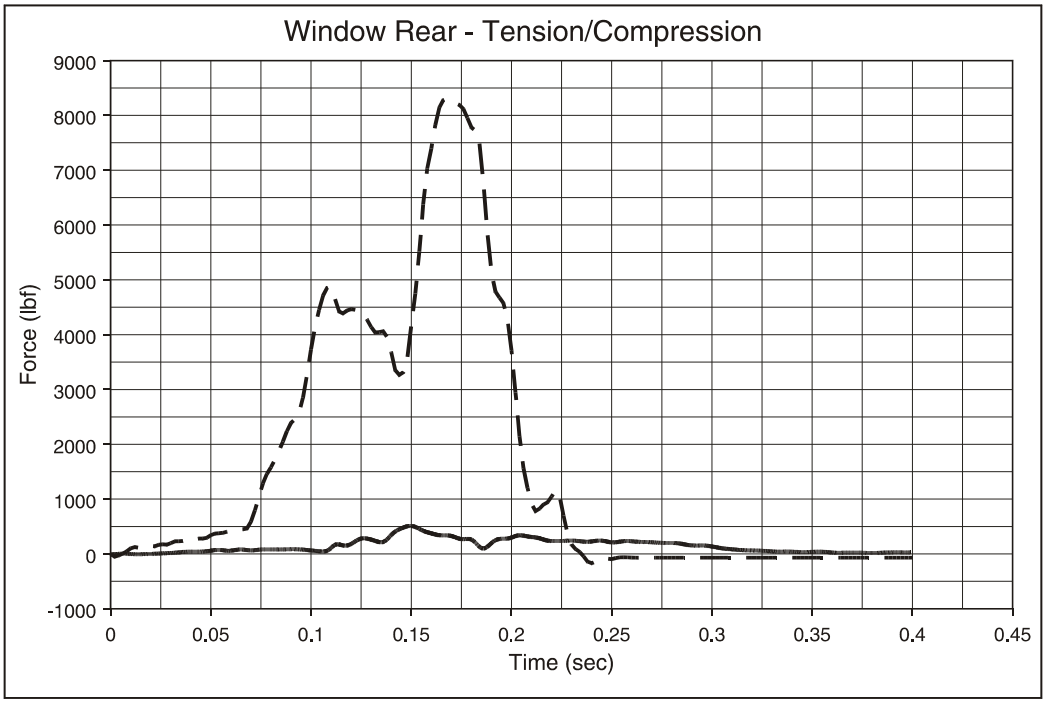

Figure F101. M-Style Seat, Type 2 Test, Seat Attachment Loads: Window Rear Load Cell, z Direction

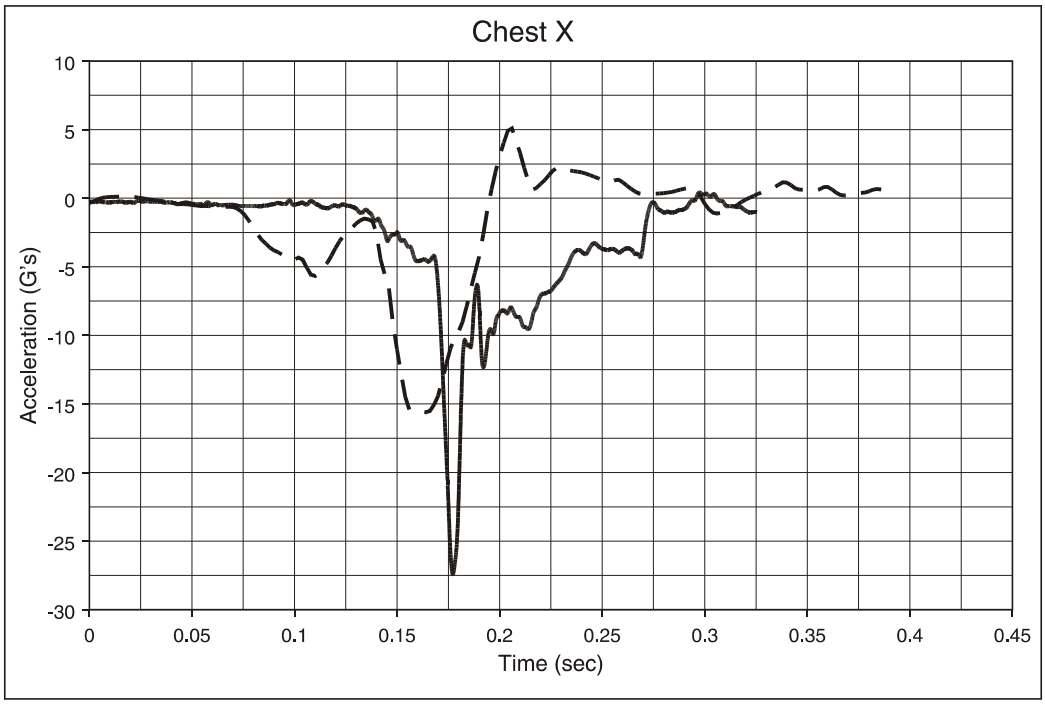

Figure F102. M-Style Seat, Type 2 Test, 95th-Percentile Hybrid III Male ATD, Aisle Seat; Chest Acceleration, x Direction

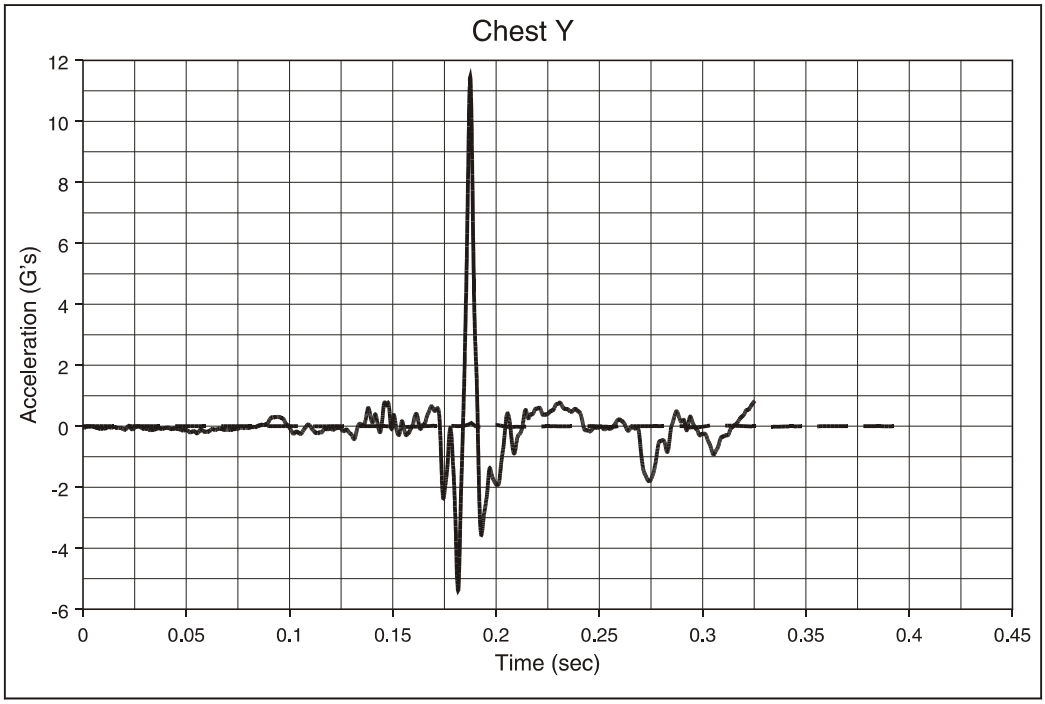

Figure F103. M-Style Seat, Type 2 Test, 95th-Percentile Hybrid III Male ATD, Aisle Seat; Chest Acceleration, y Direction

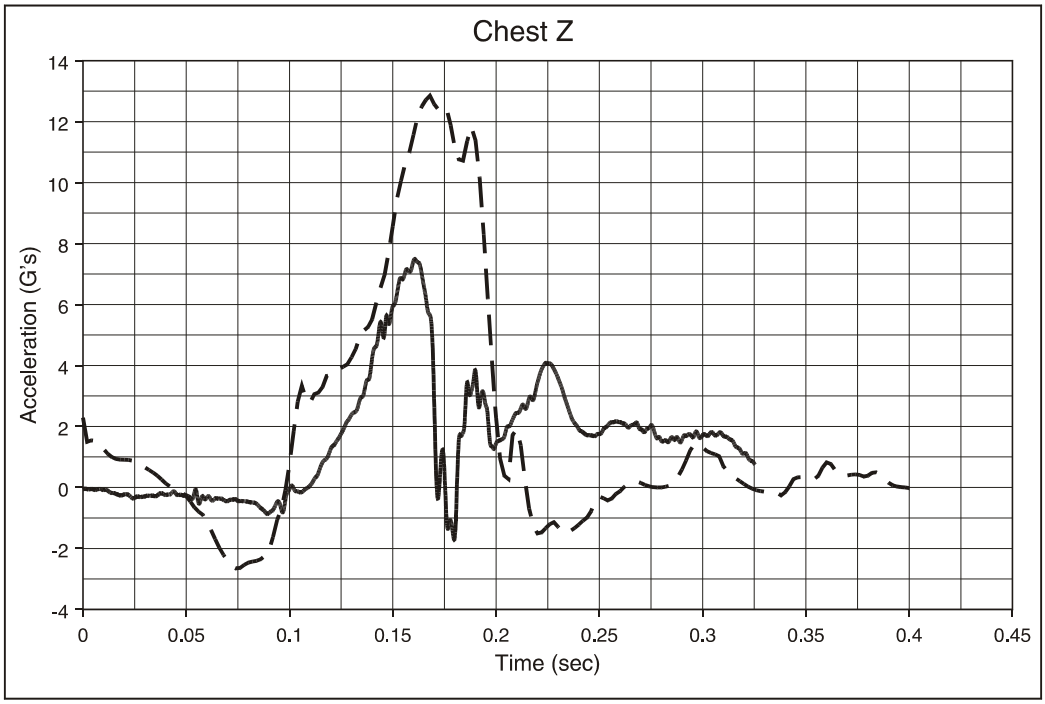

Figure F104. M-Style Seat, Type 2 Test, 95th-Percentile Hybrid III Male ATD, Aisle Seat; Chest Acceleration, z Direction

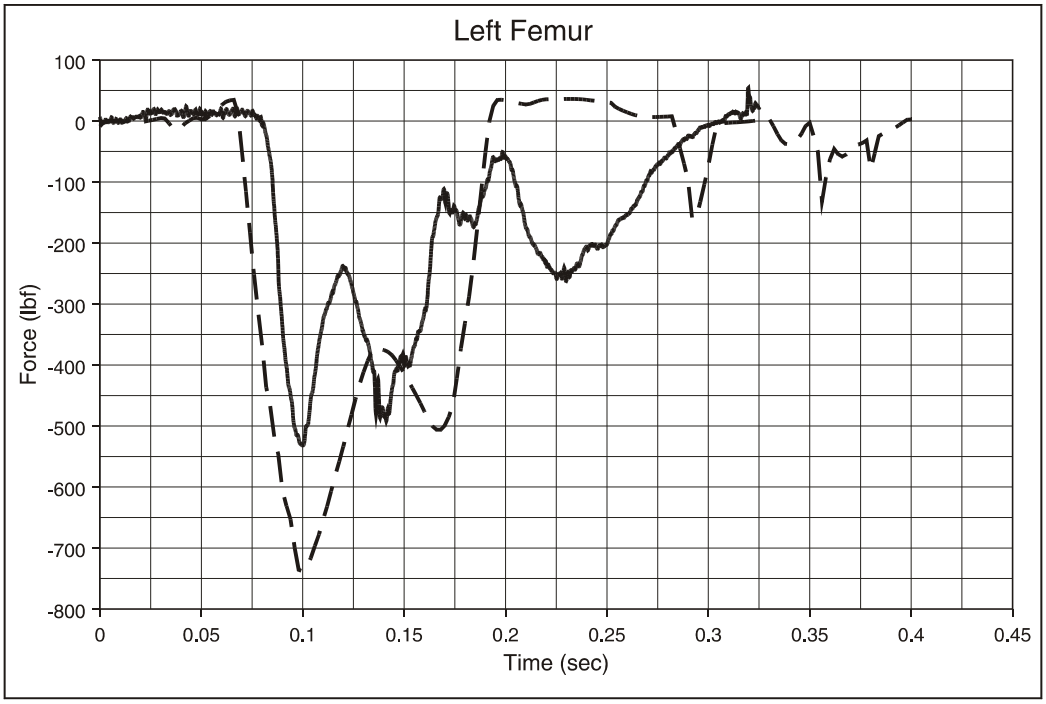

Figure F105. M-Style Seat, Type 2 Test, 95th-Percentile Hybrid III Male ATD, Aisle Seat; Left Femur Load

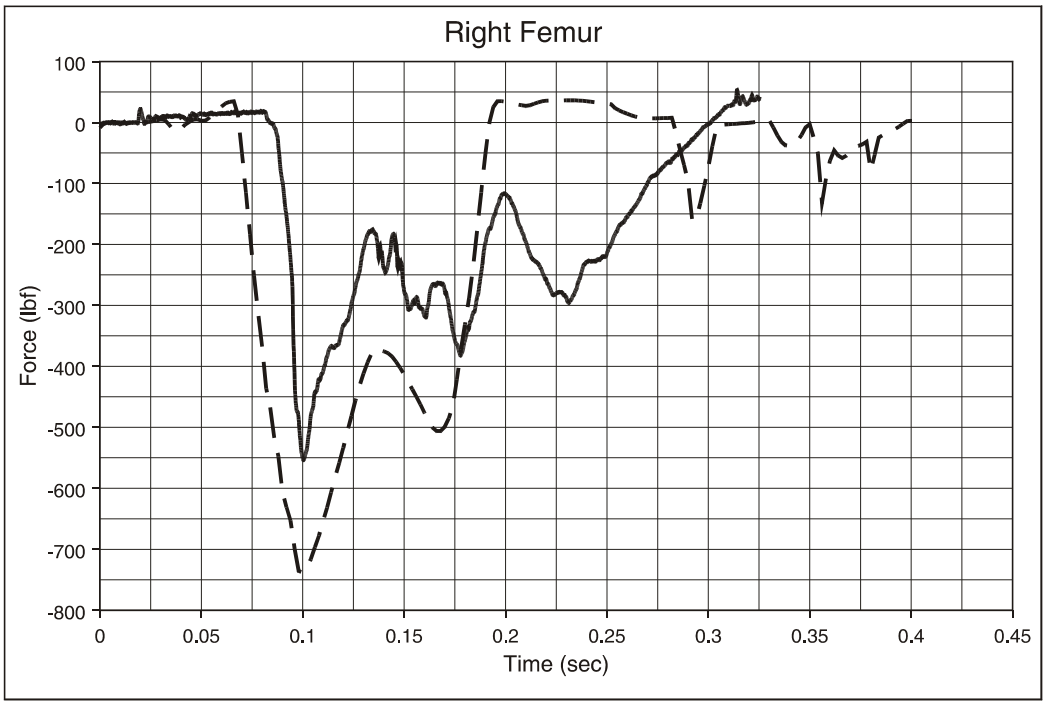

Figure F106. M-Style Seat, Type 2 Test, 95th-Percentile Hybrid III Male ATD, Aisle Seat; Right Femur Load

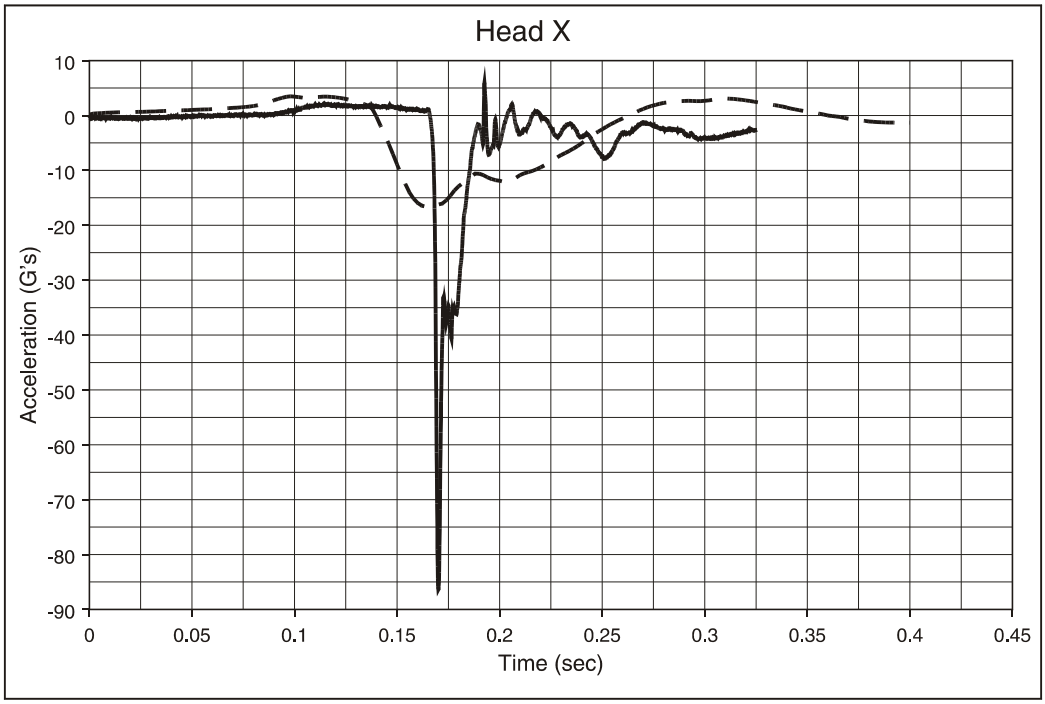

Figure F107. M-Style Seat, Type 2 Test, 95th-Percentile Hybrid III Male ATD, Aisle Seat; Head Acceleration, x Direction

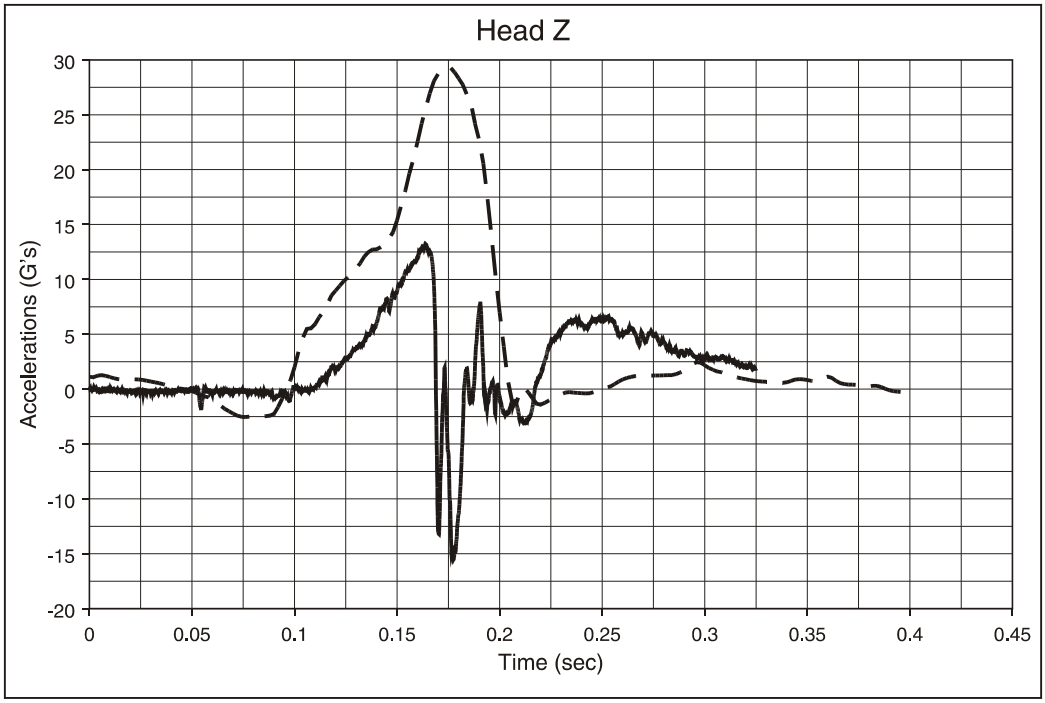

Figure F108. M-Style Seat, Type 2 Test, 95th-Percentile Hybrid III Male ATD, Aisle Seat; Head Acceleration, z Direction

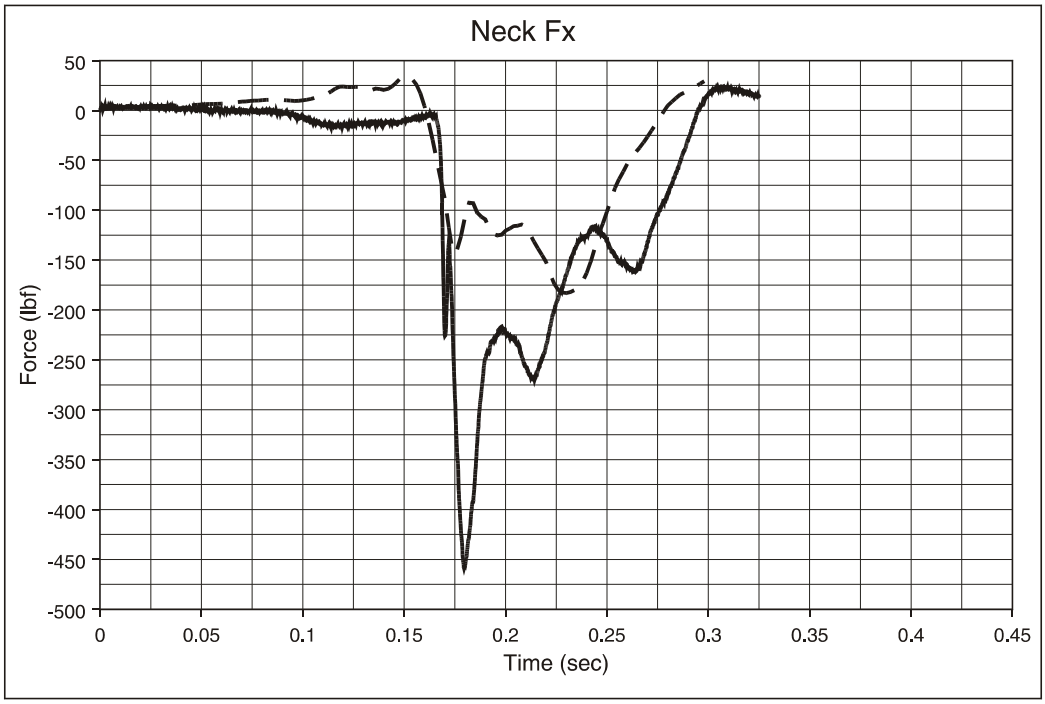

Figure F109. M-Style Seat, Type 2 Test, 95th-Percentile Hybrid III Male ATD, Aisle Seat; Neck Shear Load

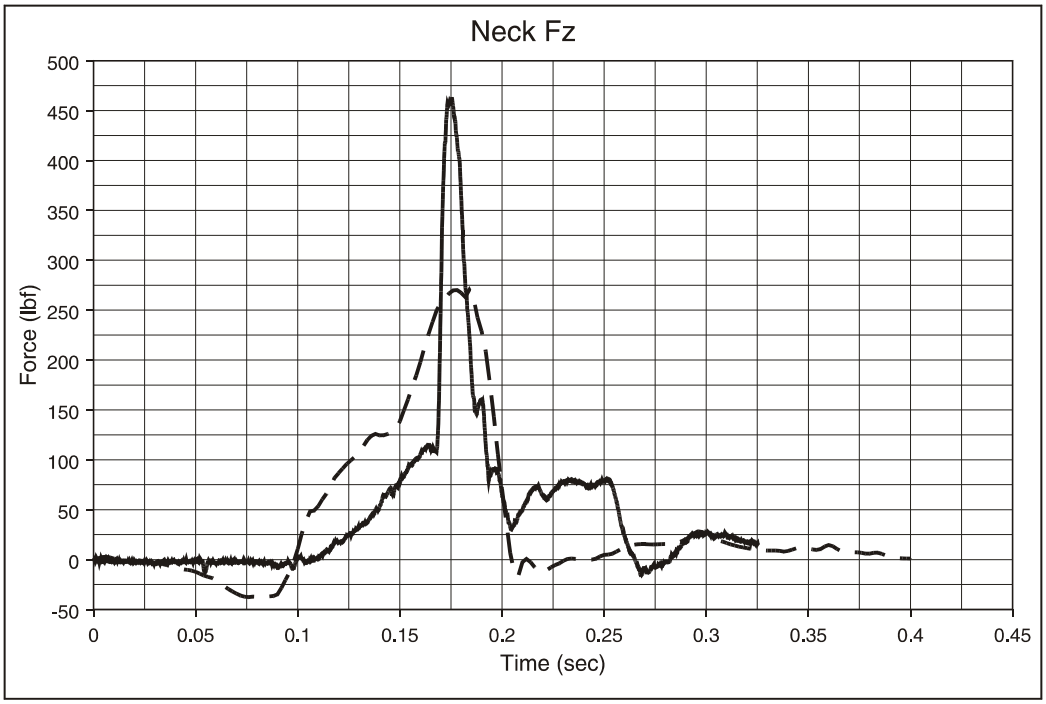

Figure F110. M-Style Seat, Type 2 Test, 95th-Percentile Hybrid III Male ATD, Aisle Seat; Neck Compression/Tension Load

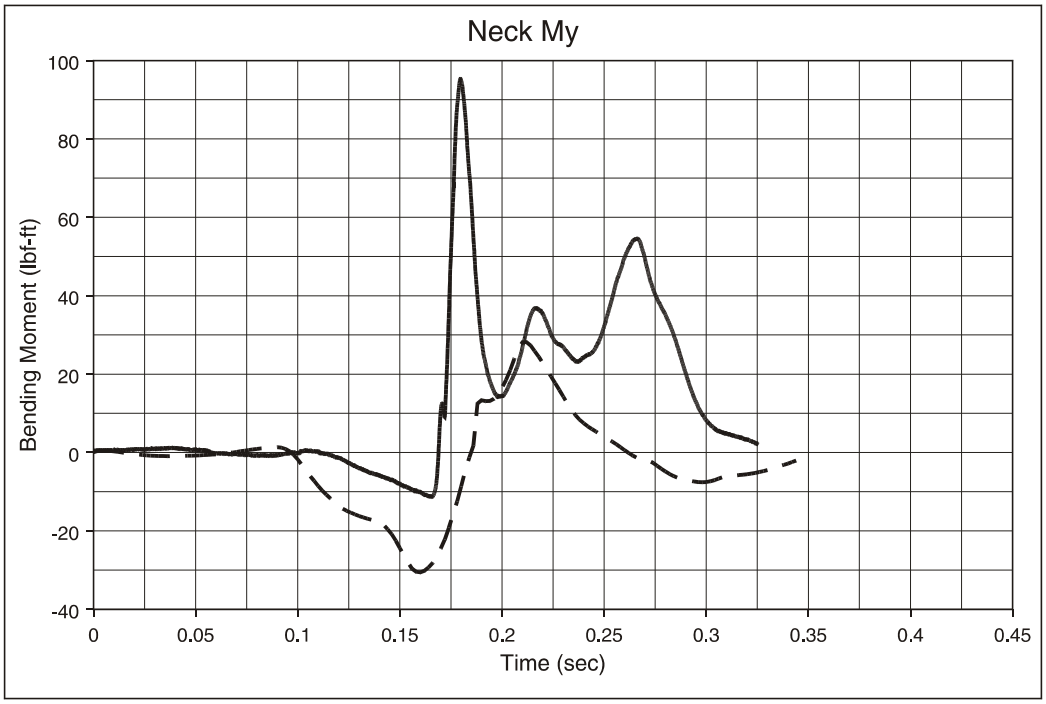

Figure F111. M-Style Seat, Type 2 Test, 95th-Percentile Hybrid III Male ATD, Aisle Seat; Neck Flexion/Extension Moment

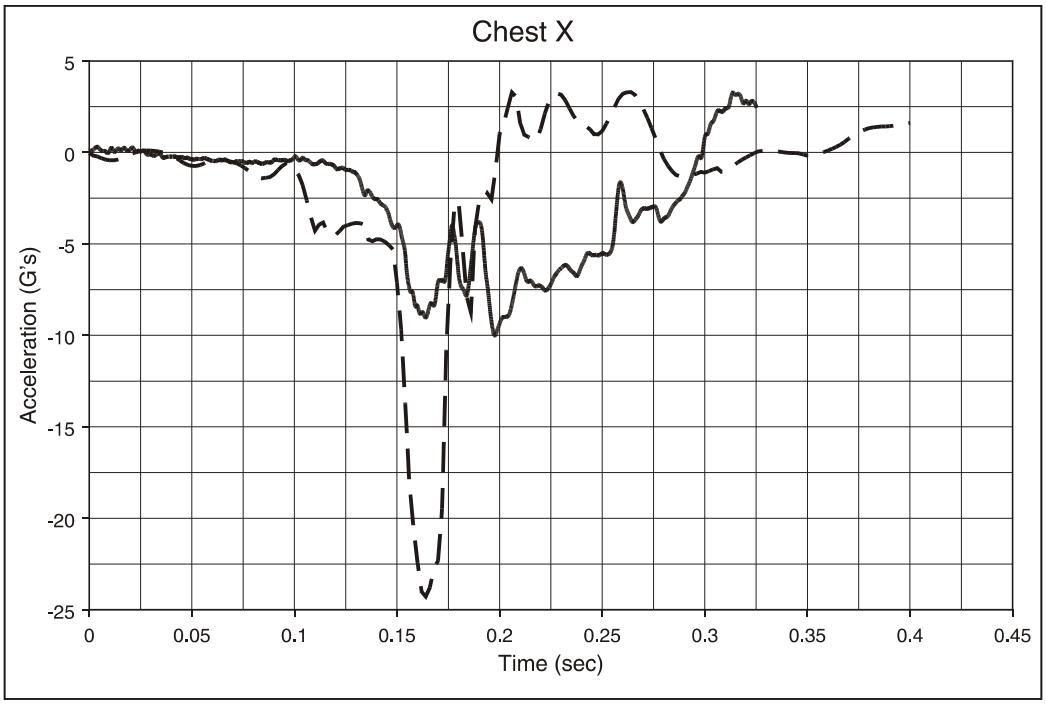

Figure F112. M-Style Seat, Type 2 Test, 50th-Percentile Hybrid III Male ATD, Center Seat; Chest Acceleration, x Direction

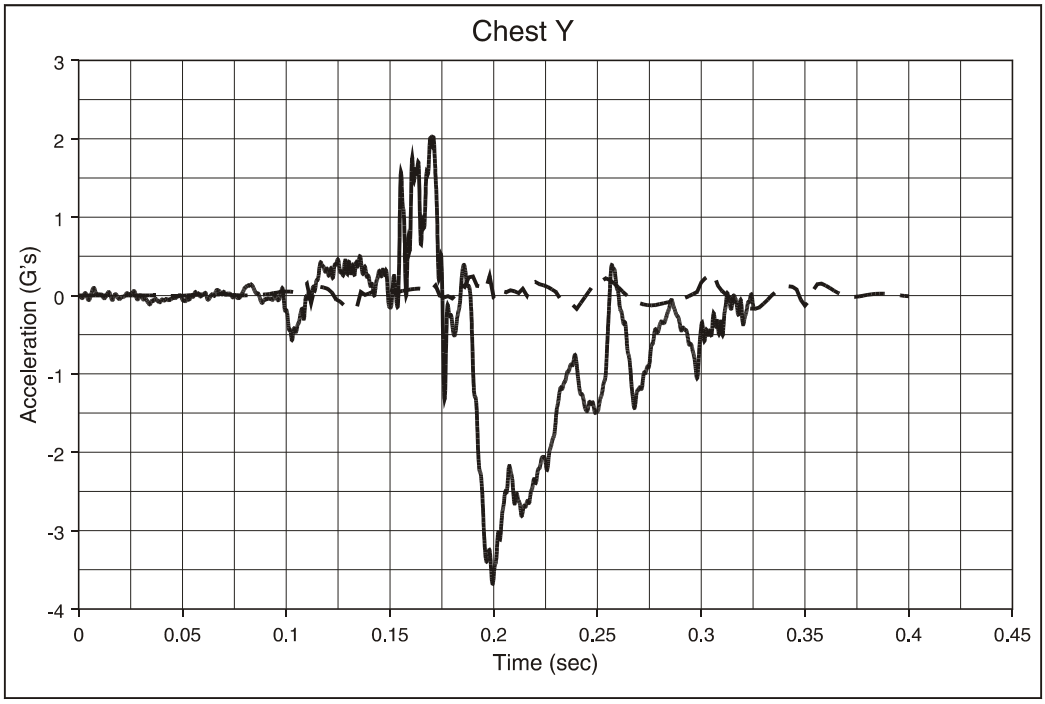

Figure F113. M-Style Seat, Type 2 Test, 50th-Percentile Hybrid III Male ATD, Center Seat; Chest Acceleration, y Direction

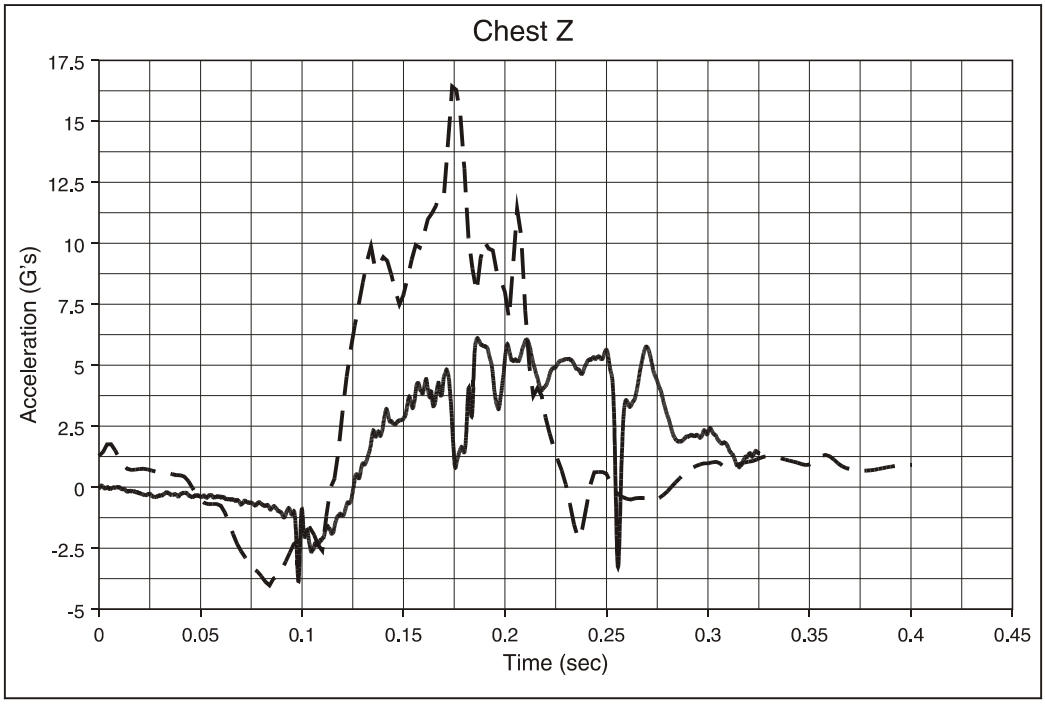

Figure F114. M-Style Seat, Type 2 Test, 50th-Percentile Hybrid III Male ATD, Center Seat; Chest Acceleration, z Direction

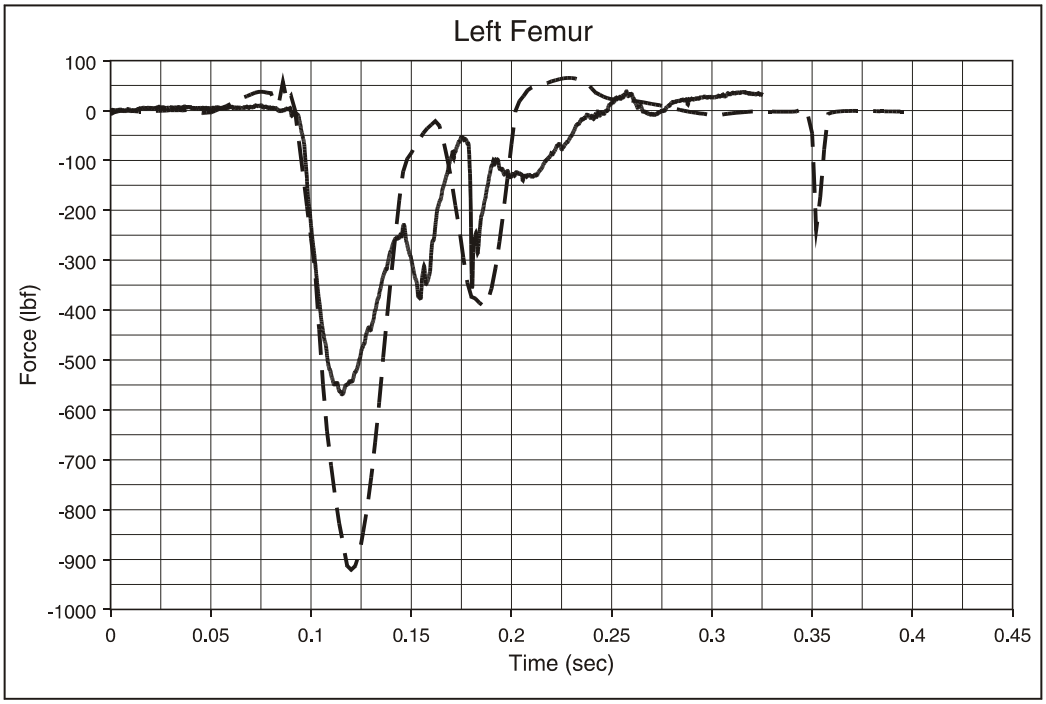

Figure F115. M-Style Seat, Type 2 Test, 50th-Percentile Hybrid III Male ATD, Center Seat; Left Femur Load

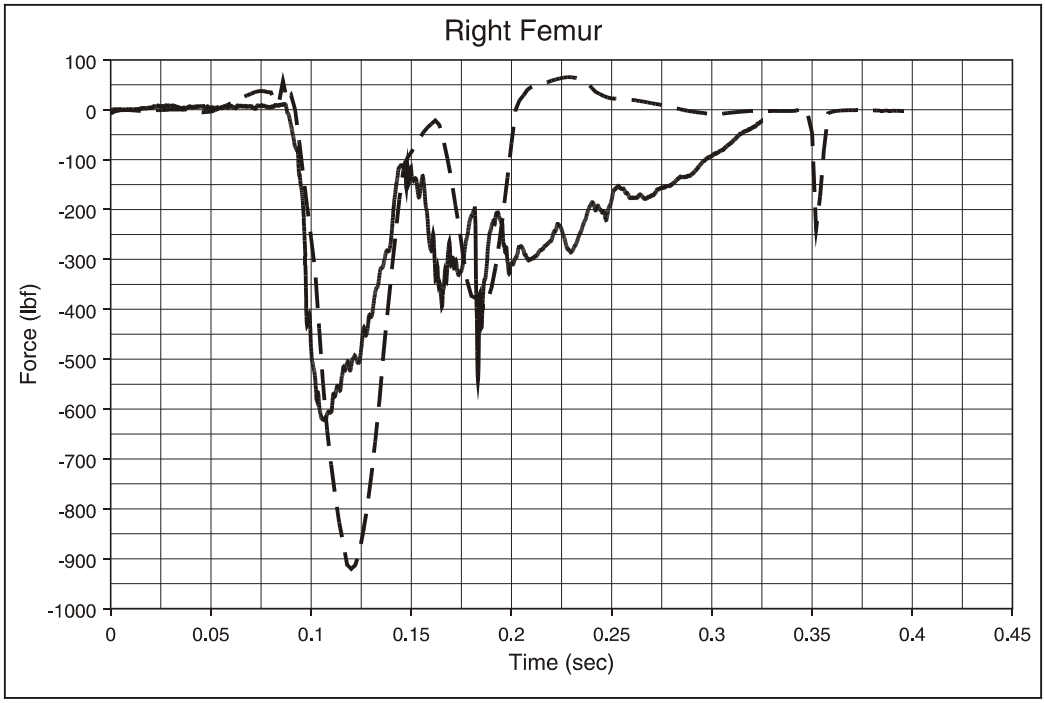

Figure F116. M-Style Seat, Type 2 Test, 50th-Percentile Hybrid III Male ATD, Center Seat; Right Femur Load

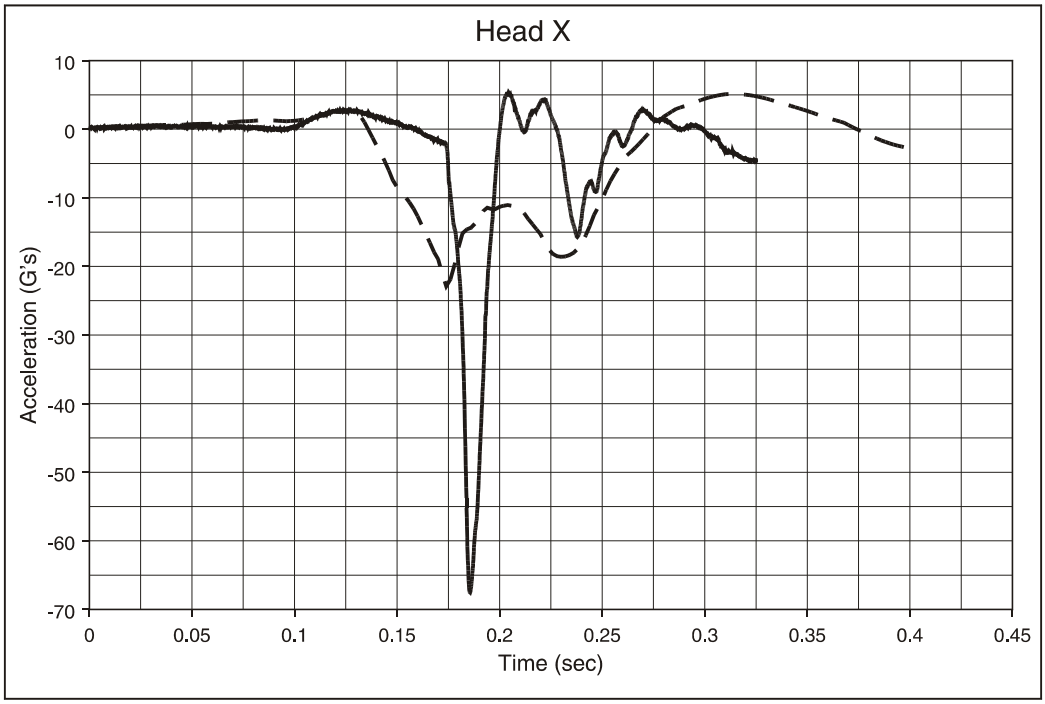

Figure F117. M-Style Seat, Type 2 Test, 50th-Percentile Hybrid III Male ATD, Center Seat; Head Acceleration, x Direction

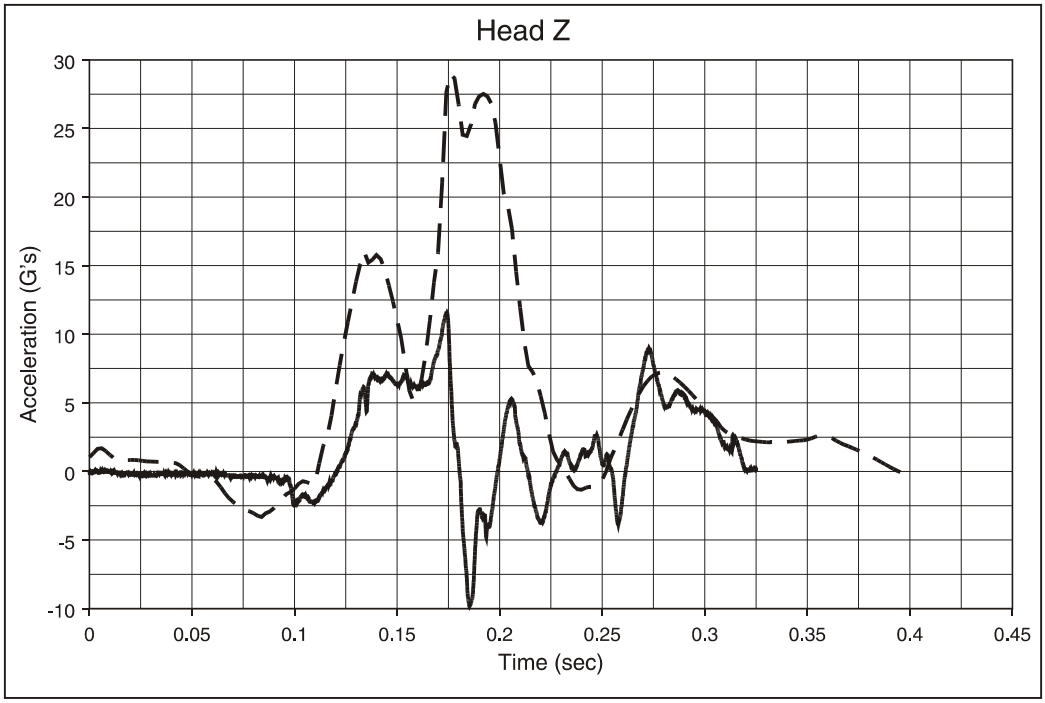

Figure F118. M-Style Seat, Type 2 Test, 50th-Percentile Hybrid III Male ATD, Center Seat; Head Acceleration, z Direction

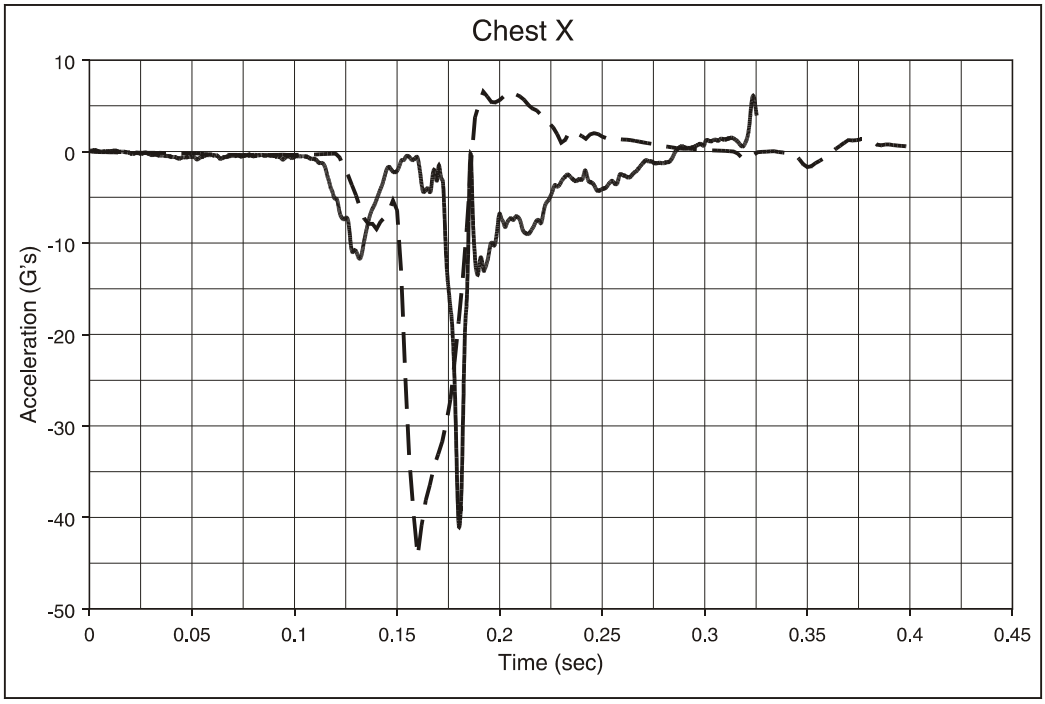

Figure F119. M-Style Seat, Type 2 Test, 5th-Percentile Hybrid III Female ATD, Window Seat; Chest Acceleration, x Direction

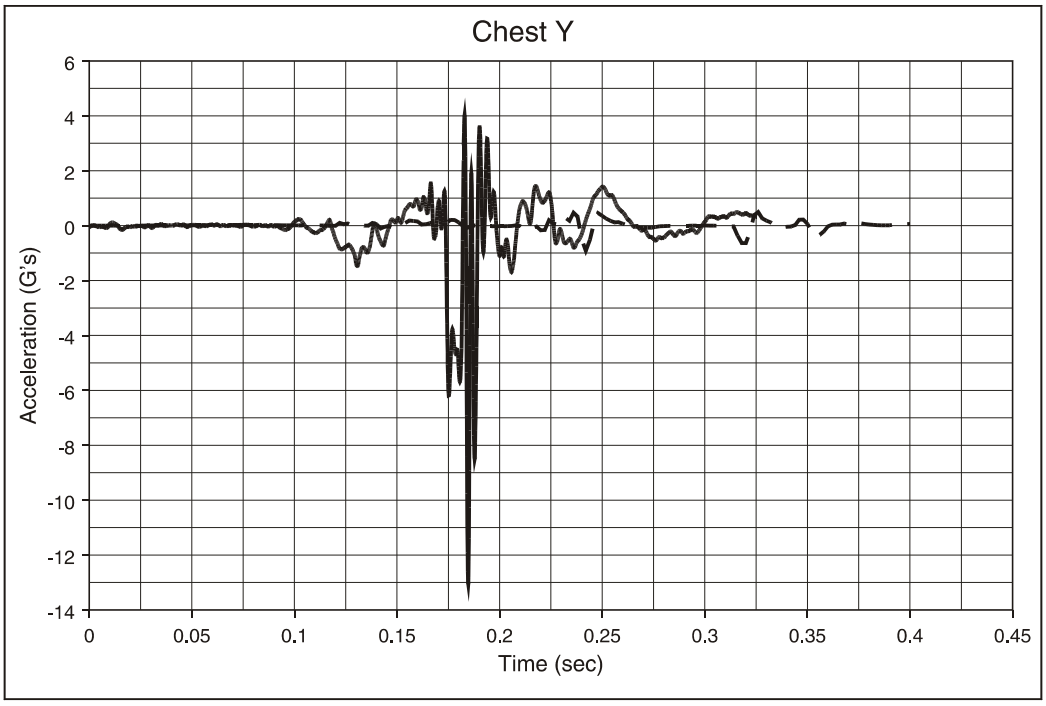

Figure F120. M-Style Seat, Type 2 Test, 5th-Percentile Hybrid III Female ATD, Window Seat; Chest Acceleration, y Direction

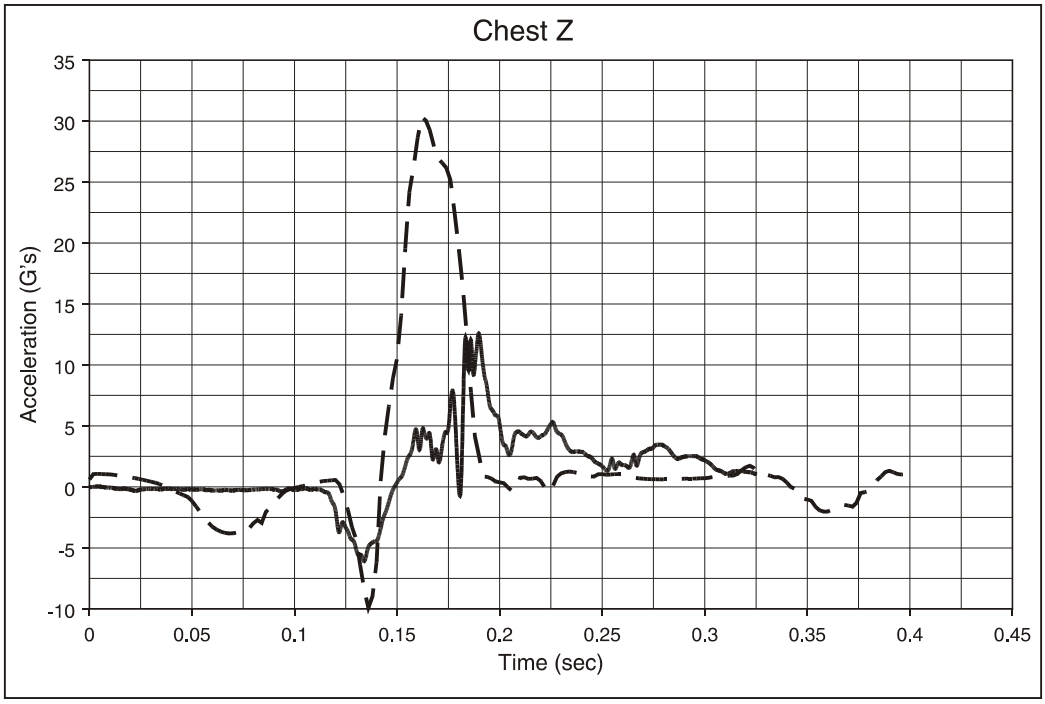

Figure F121. M-Style Seat, Type 2 Test, 5th-Percentile Hybrid III Female ATD, Window Seat; Chest Acceleration, z Direction

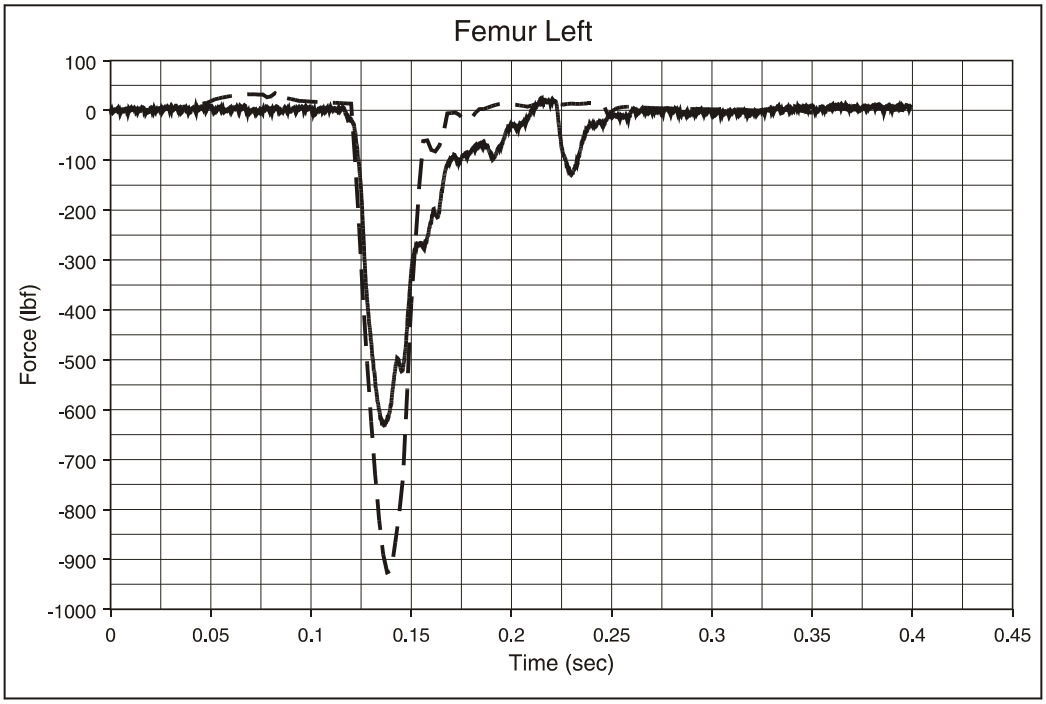

Figure F122. M-Style Seat, Type 2 Test, 5th-Percentile Hybrid III Female ATD, Window Seat; Left Femur Load

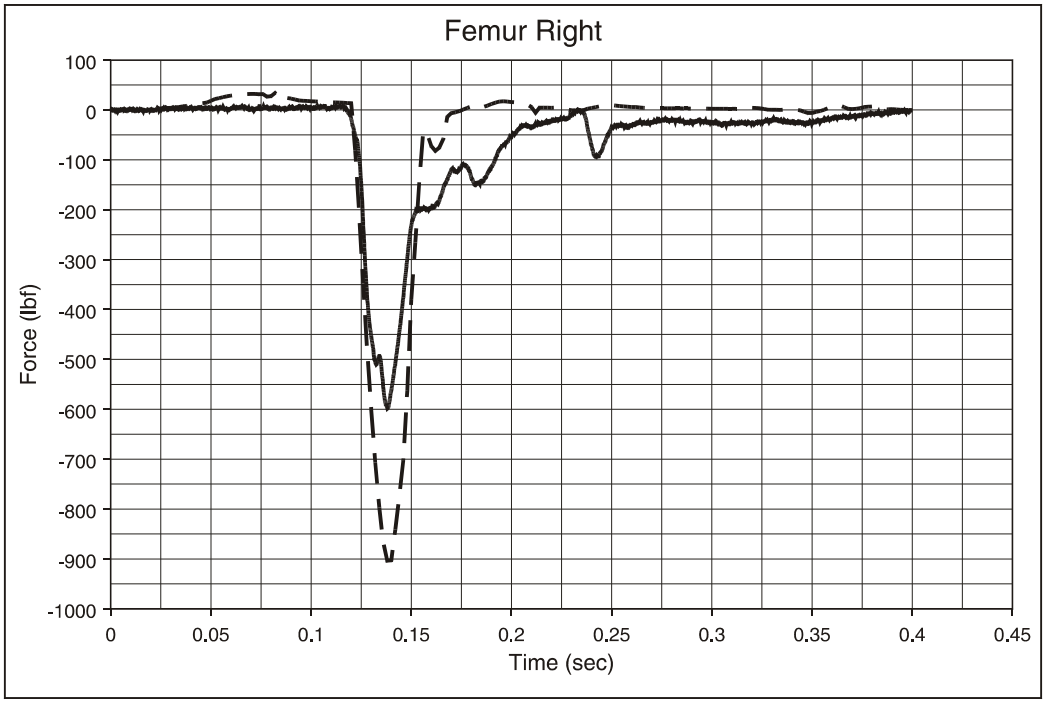

Figure F123. M-Style Seat, Type 2 Test, 5th-Percentile Hybrid III Female ATD, Window Seat; Right Femur Load

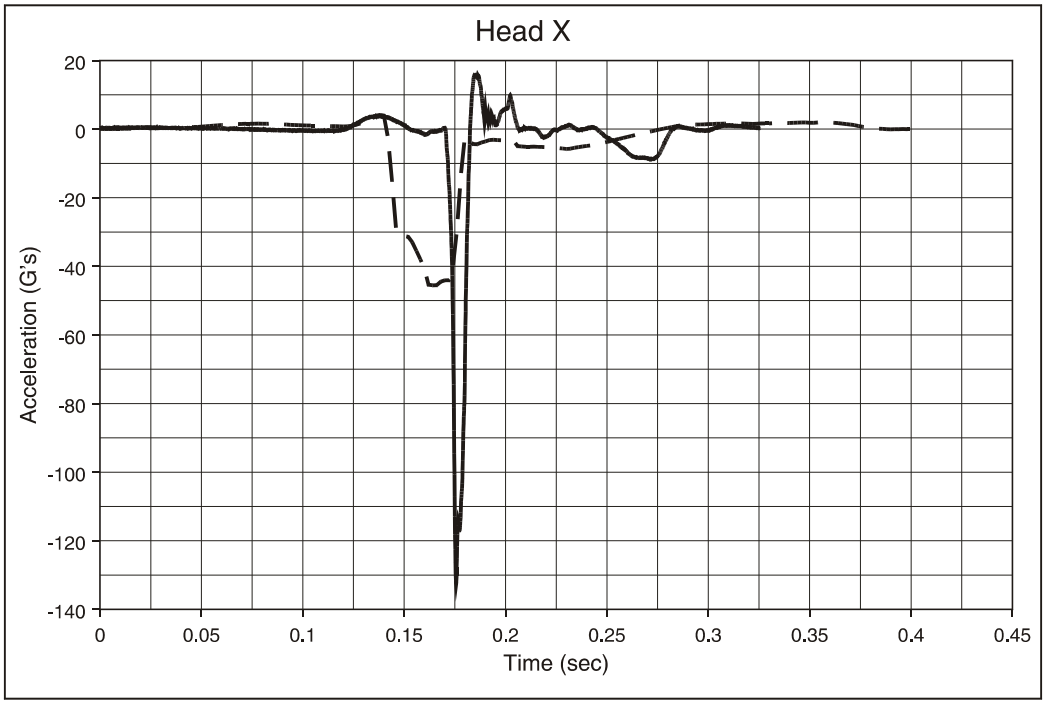

Figure F124. M-Style Seat, Type 2 Test, 5th-Percentile Hybrid III Female ATD, Window Seat; Head Acceleration, x Direction

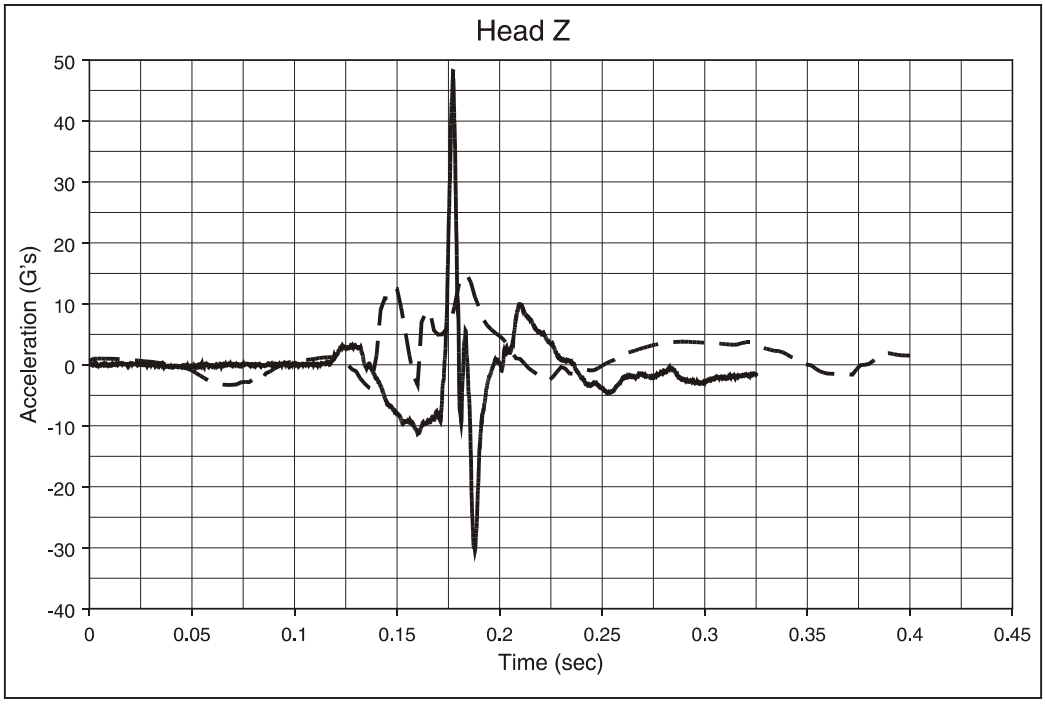

Figure F125. M-Style Seat, Type 2 Test, 5th-Percentile Hybrid III Female ATD, Window Seat; Head Acceleration, z Direction

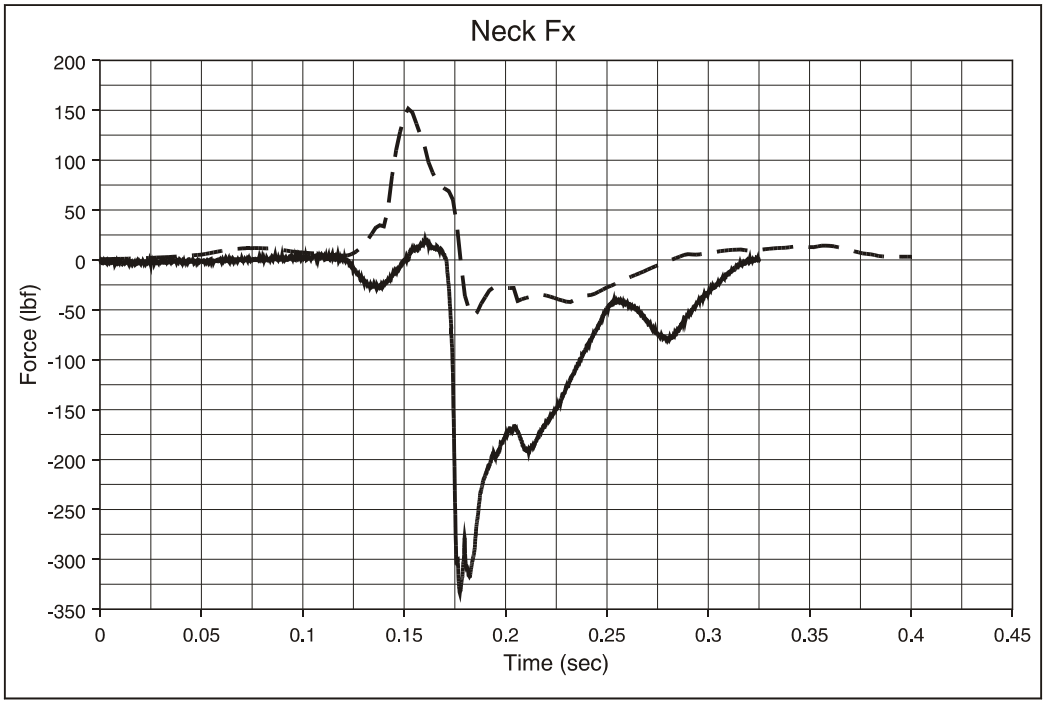

Figure F126. M-Style Seat, Type 2 Test, 5th-Percentile Hybrid III Female ATD, Window Seat; Neck Shear Load

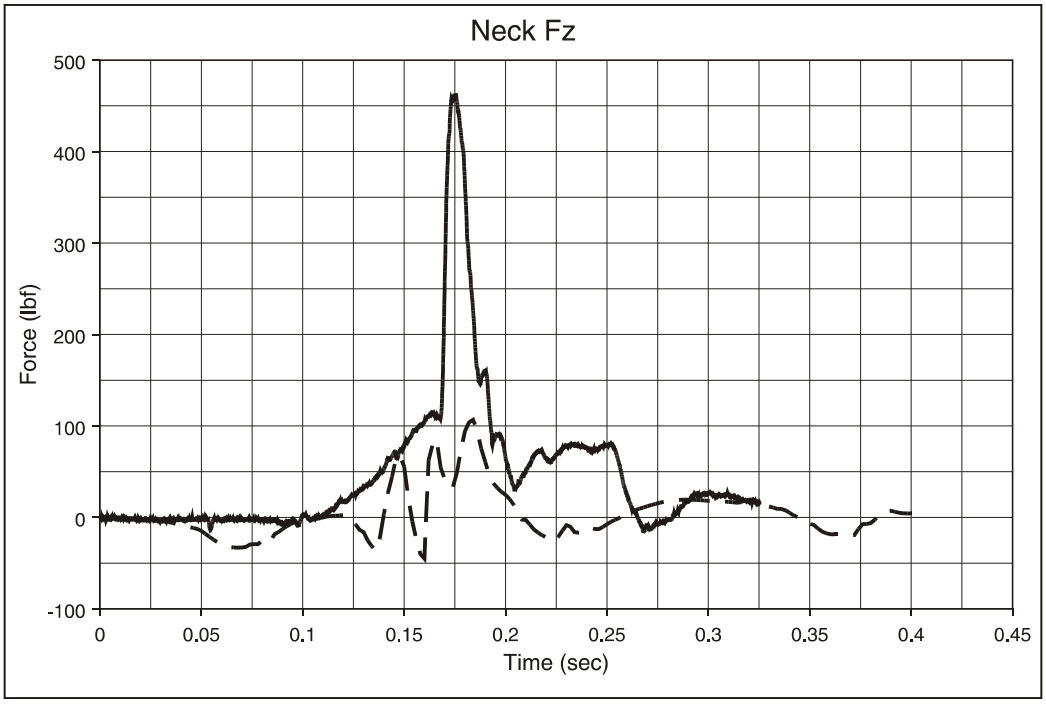

Figure F127. M-Style Seat, Type 2 Test, 5th-Percentile Hybrid III Female ATD, Window Seat; Neck Compression/Tension Load

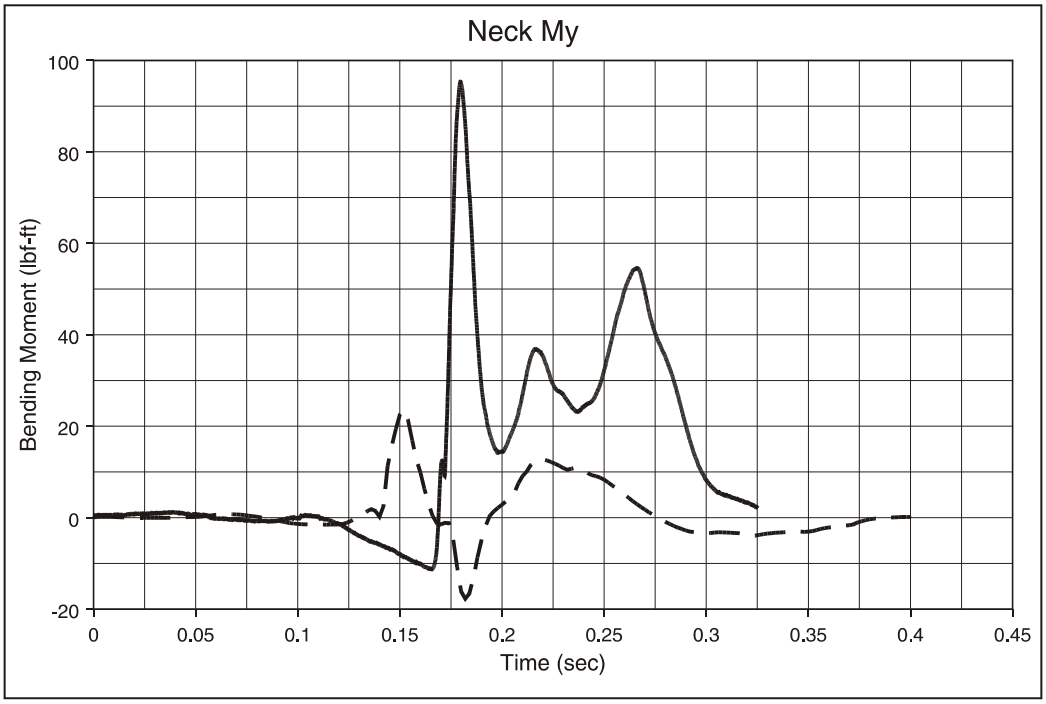

Figure F128. M-Style Seat, Type 2 Test, 5th-Percentile Hybrid III Female ATD, Window Seat; Neck Flexion/Extension Moment

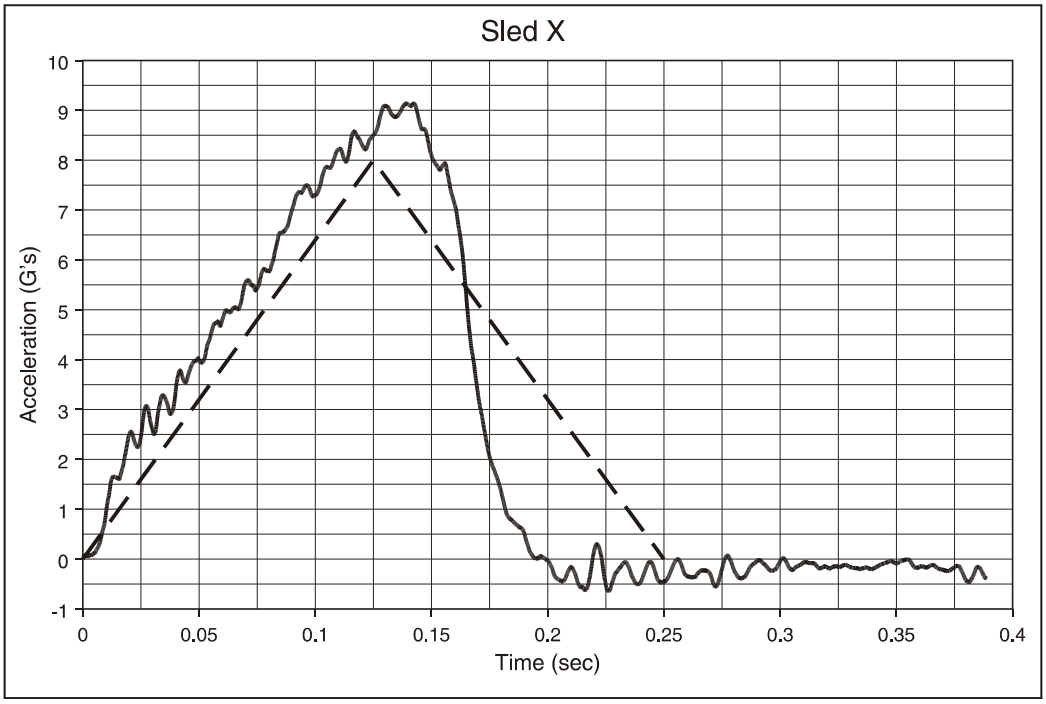

Figure F129. Walkover Seat, Type 1 Test, all 50th-Percentile ATDs: Sled Pulse

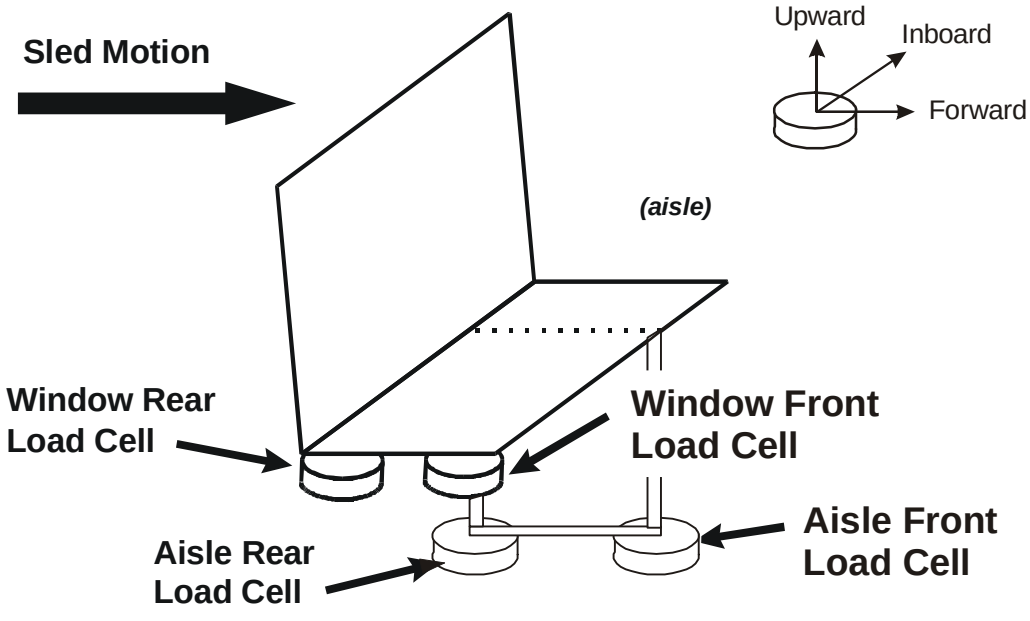

Figure F130. Walkover Seat, Type 1 Test, Seat Attachment Loads: Walkover Seat Load Cell Orientation

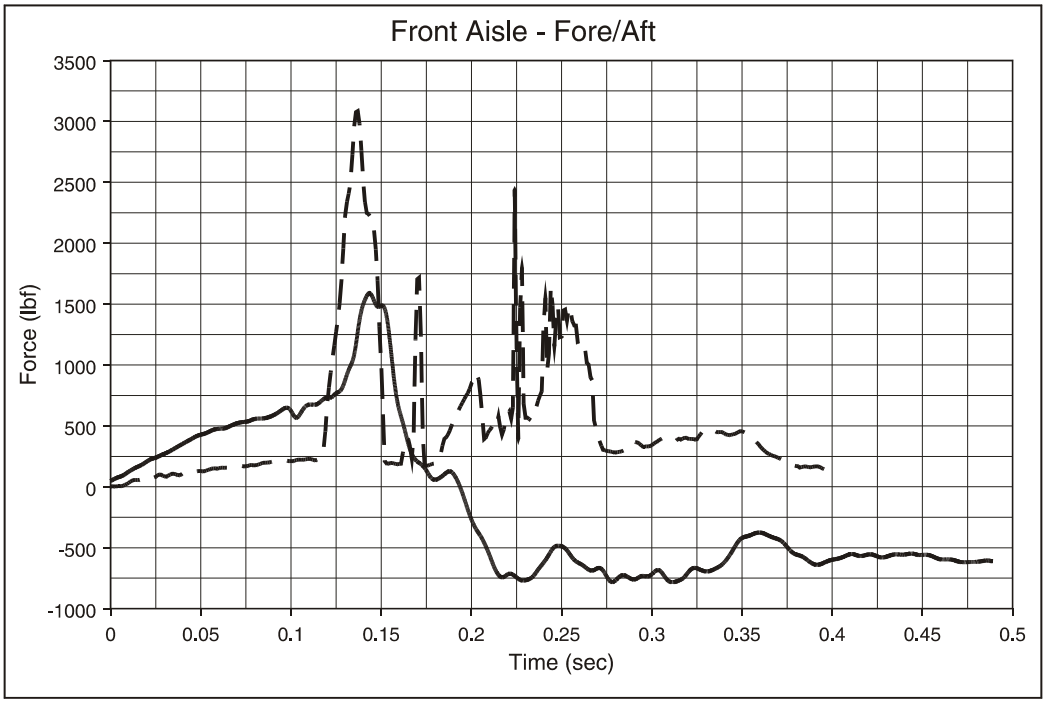

Figure F131. Walkover Seat, Type 1 Test, Seat Attachment Loads: Aisle Front Load Cell, x Direction

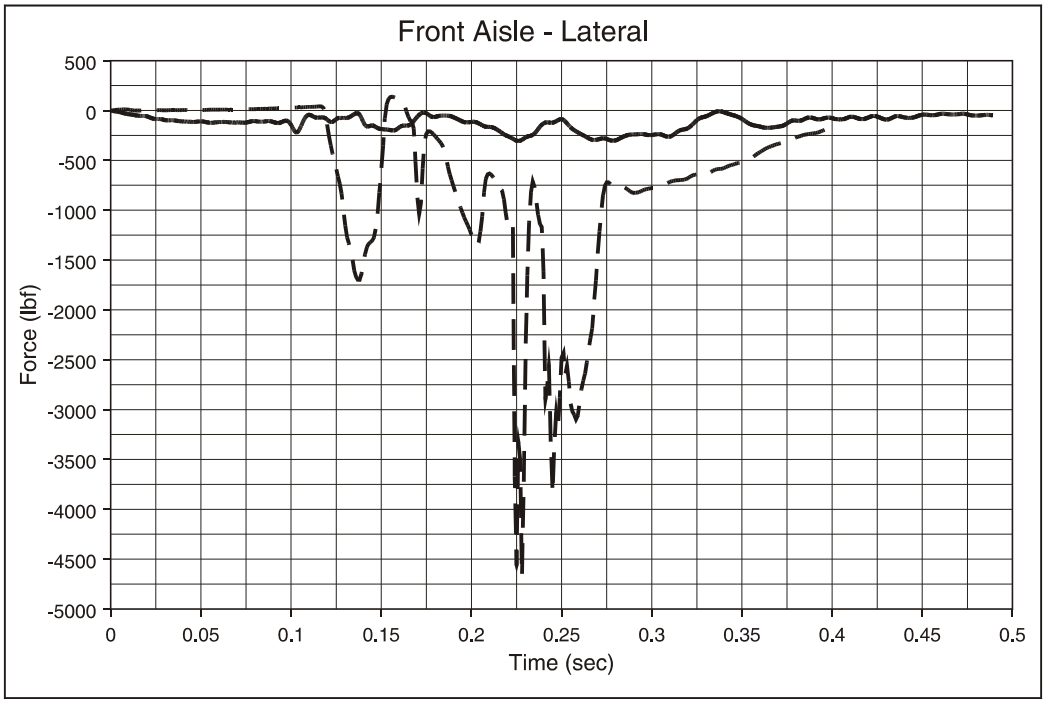

Figure F132. Walkover Seat, Type 1 Test, Seat Attachment Loads: Aisle Front Load Cell, y Direction

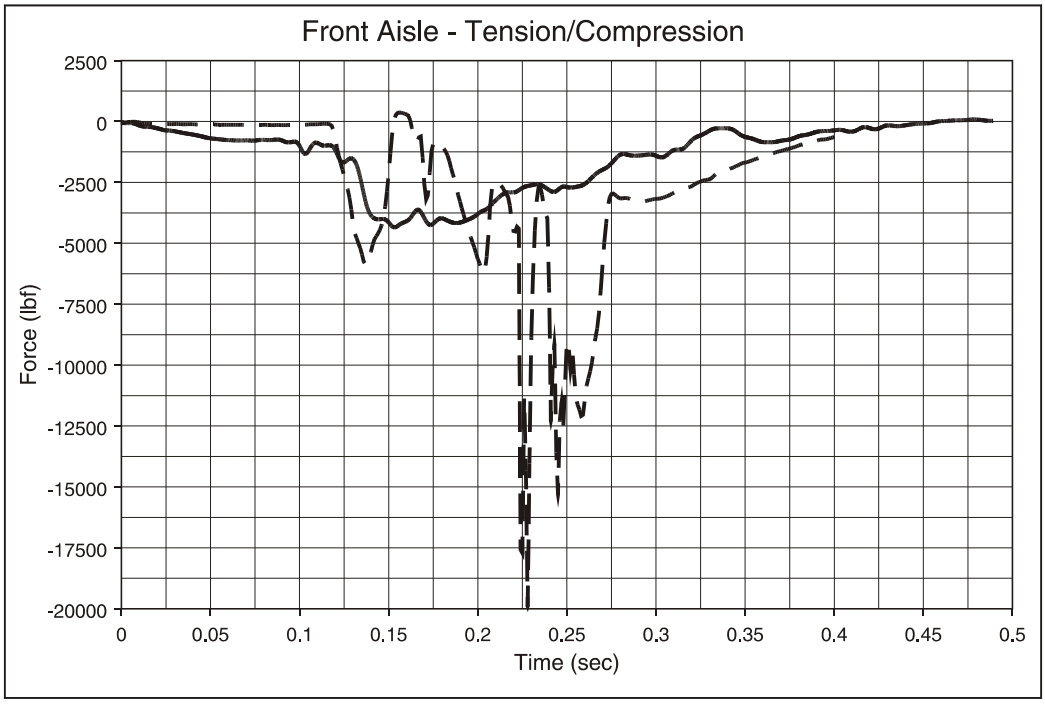

Figure F133. Walkover Seat, Type 1 Test, Seat Attachment Loads: Aisle Front Load Cell, z Direction

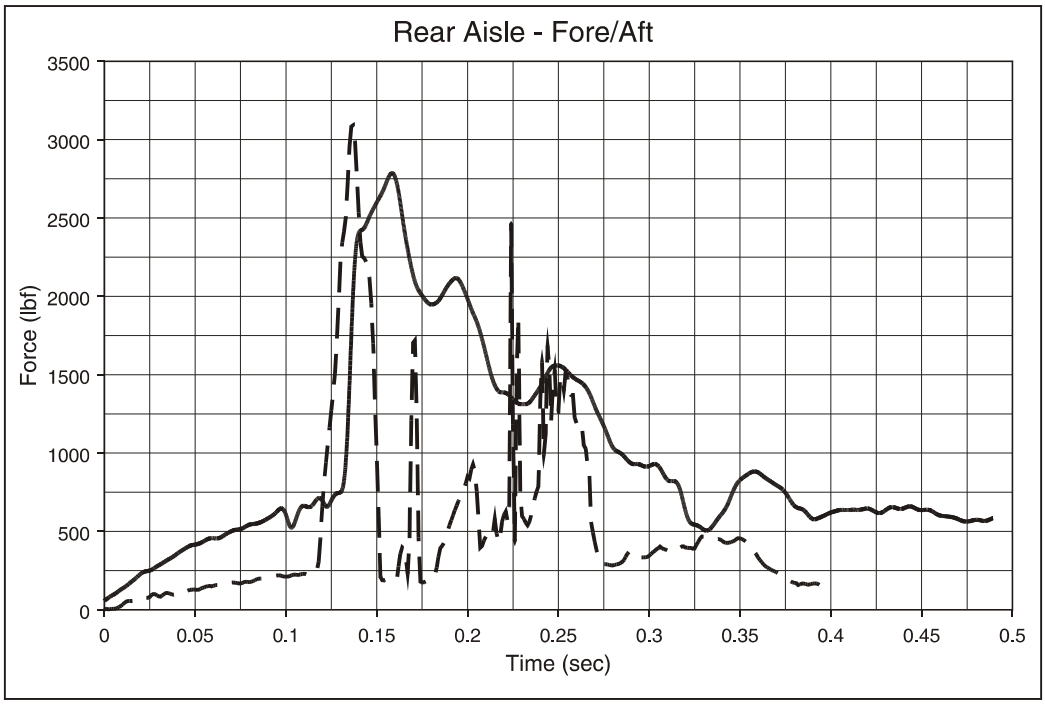

Figure F134. Walkover Seat, Type 1 Test, Seat Attachment Loads: Aisle Rear Load Cell, x Direction

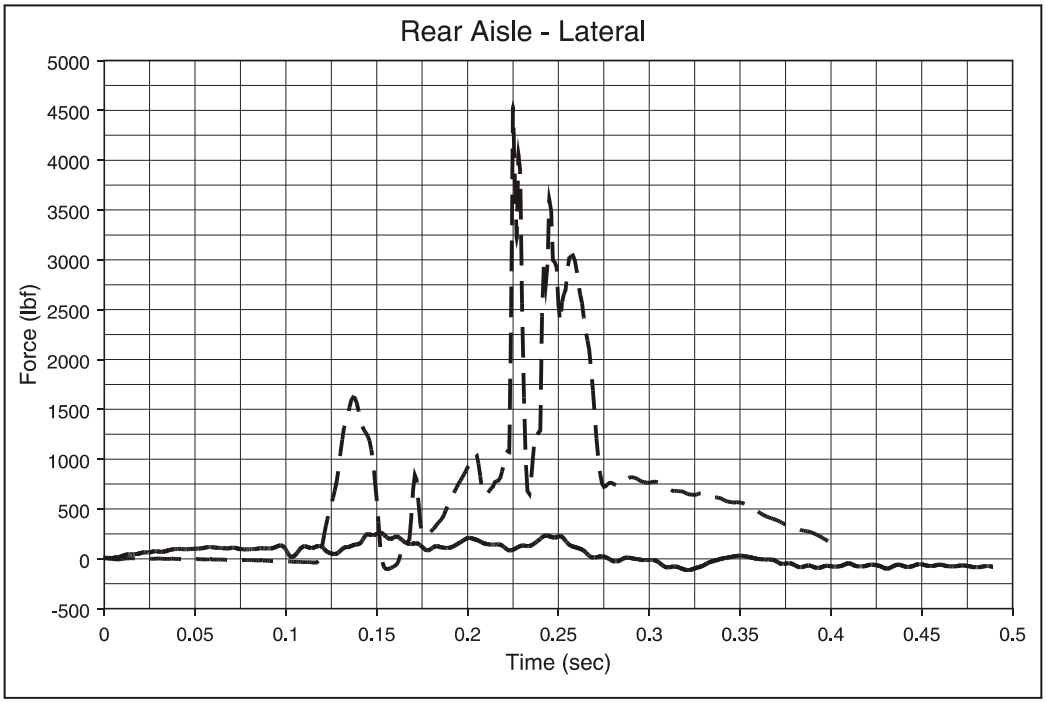

Figure F135. Walkover Seat, Type 1 Test, Seat Attachment Loads: Aisle Rear Load Cell, y Direction

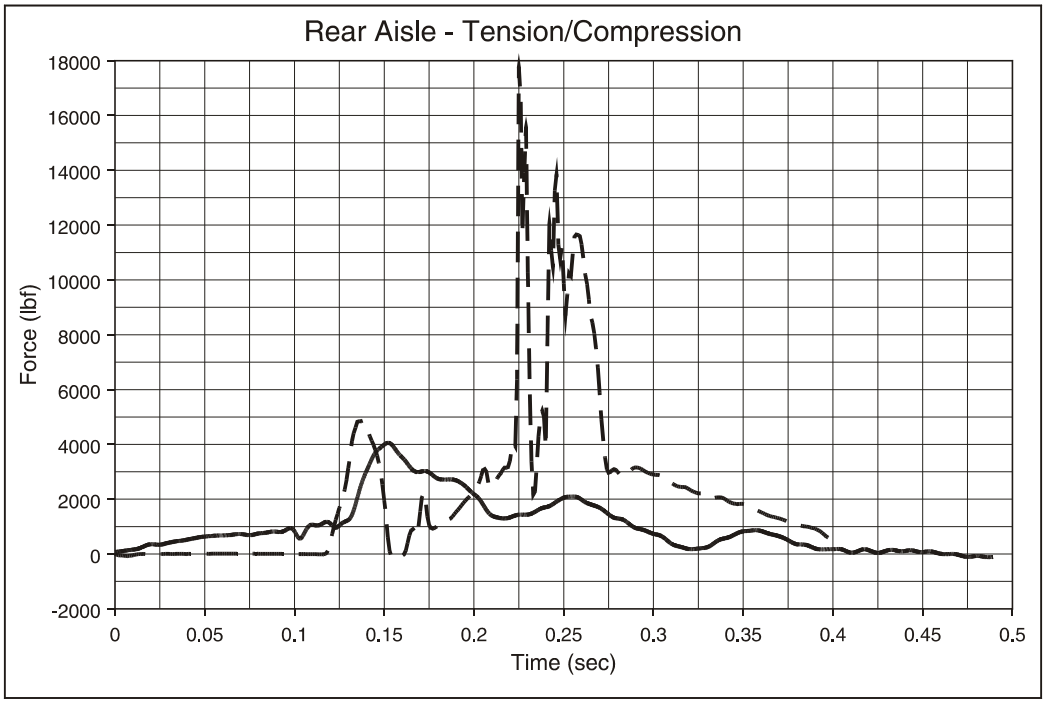

Figure F136. Walkover Seat, Type 1 Test, Seat Attachment Loads: Aisle Rear Load Cell, z Direction

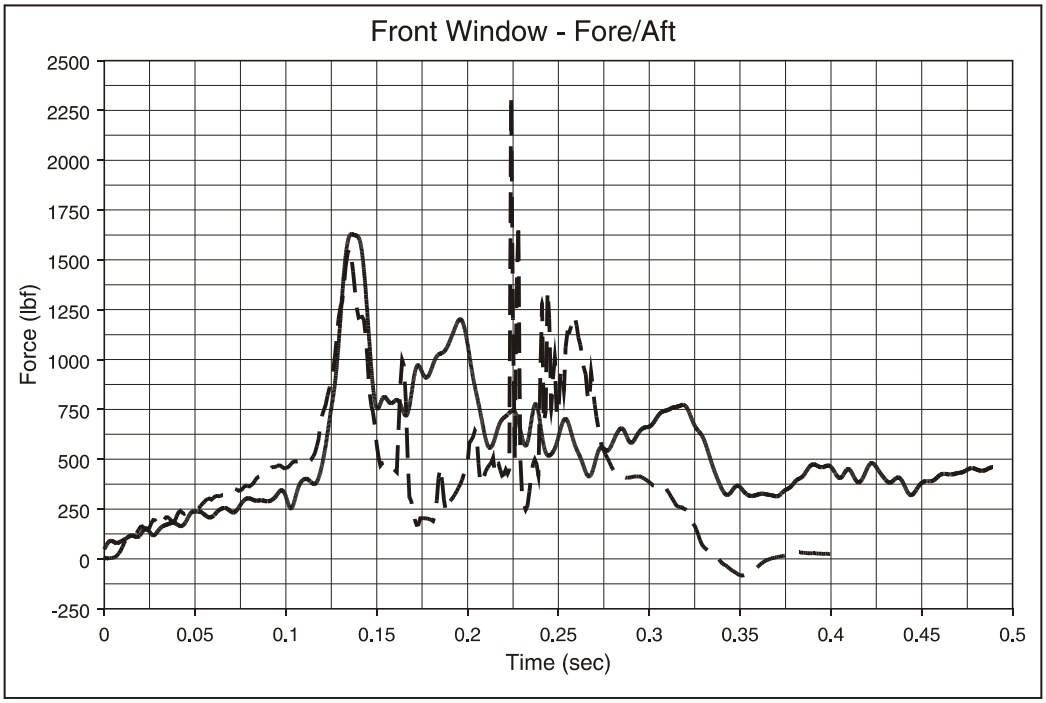

Figure F137. Walkover Seat, Type 1 Test, Seat Attachment Loads Window Front Load Cell, x Direction

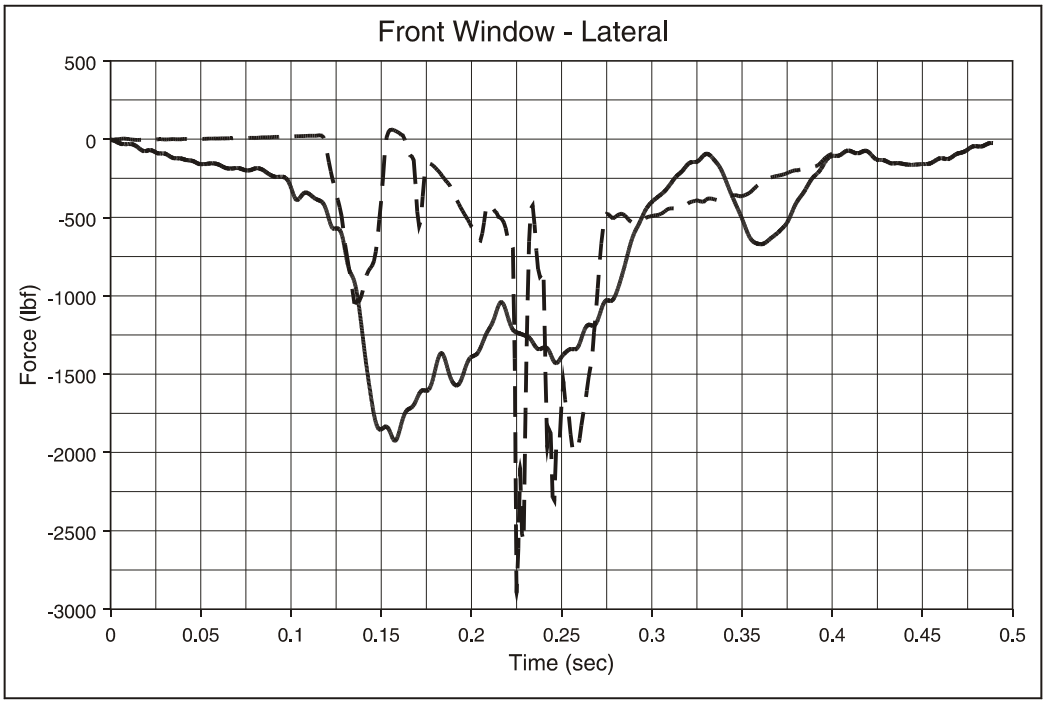

Figure F138. Walkover Seat, Type 1 Test, Seat Attachment Loads: Window Front Load Cell, y Direction

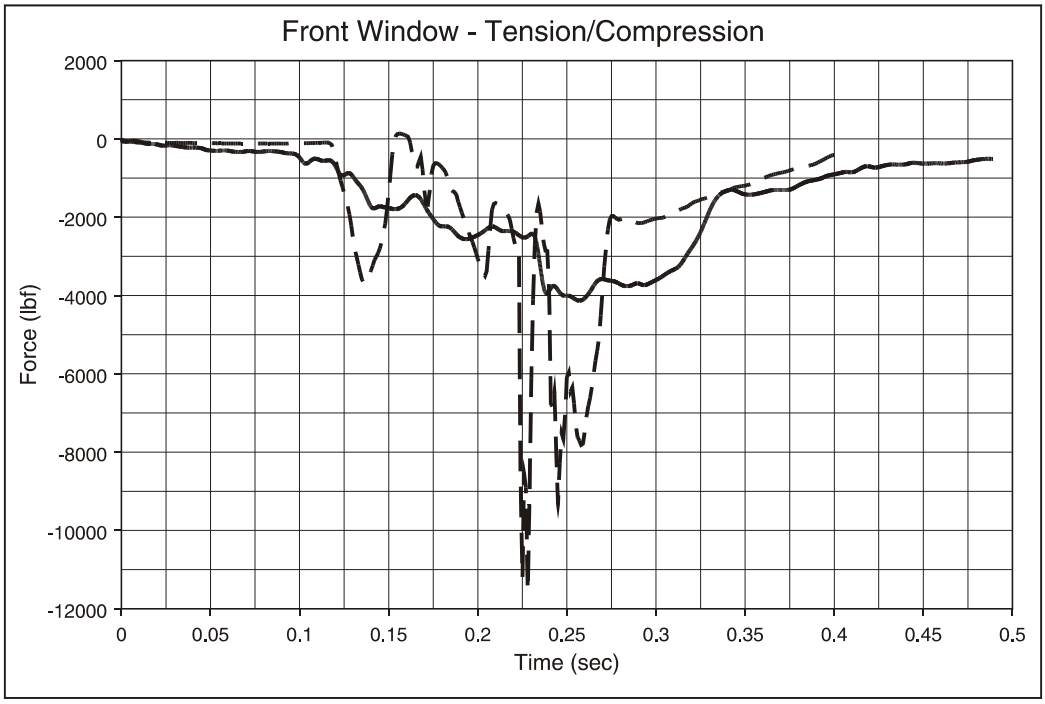

Figure F139. Walkover Seat, Type 1 Test, Seat Attachment Loads: Window Front Load Cell, z Direction

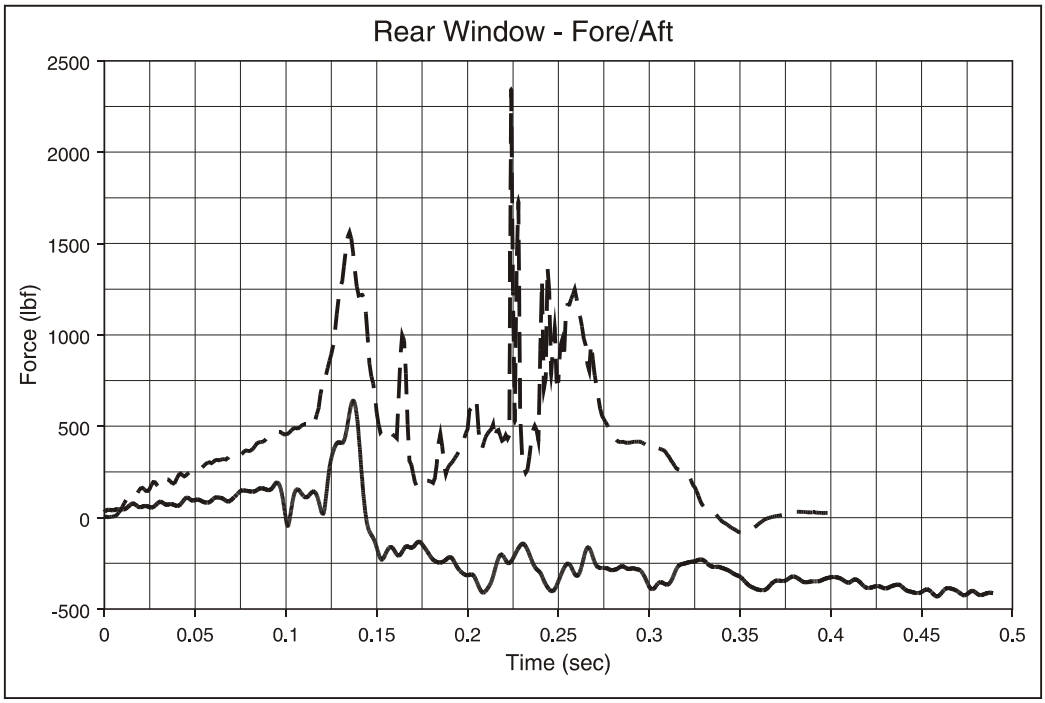

Figure F140. Walkover Seat, Type 1 Test, Seat Attachment Loads: Window Rear Load Cell, x Direction

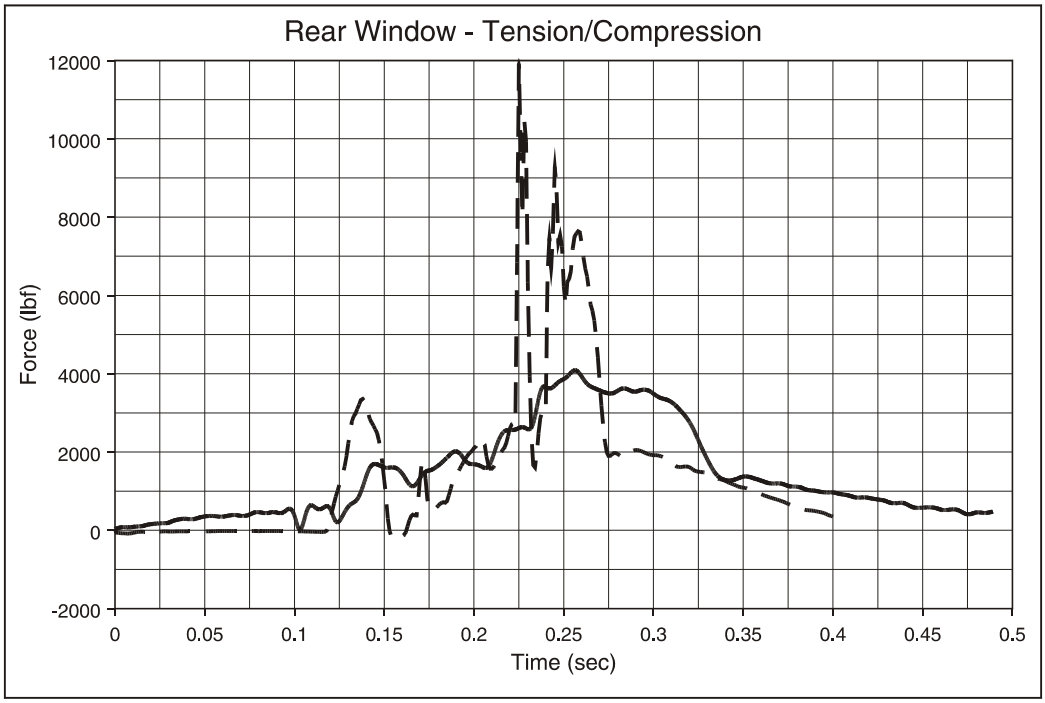

Figure F141. Walkover Seat, Type 1 Test, Seat Attachment Loads Window Rear Load Cell, z Direction

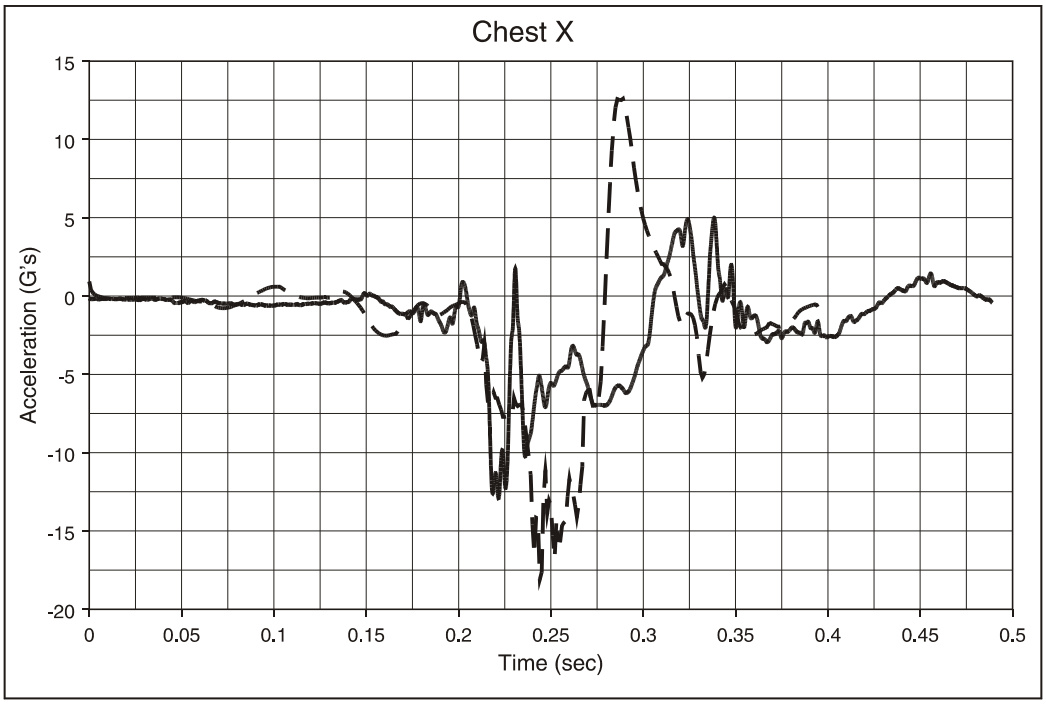

Figure F142. Walkover Seat, Type 1 Test, 50th-Percentile Hybrid II Male ATD, Aisle Seat; Chest Acceleration, x Direction

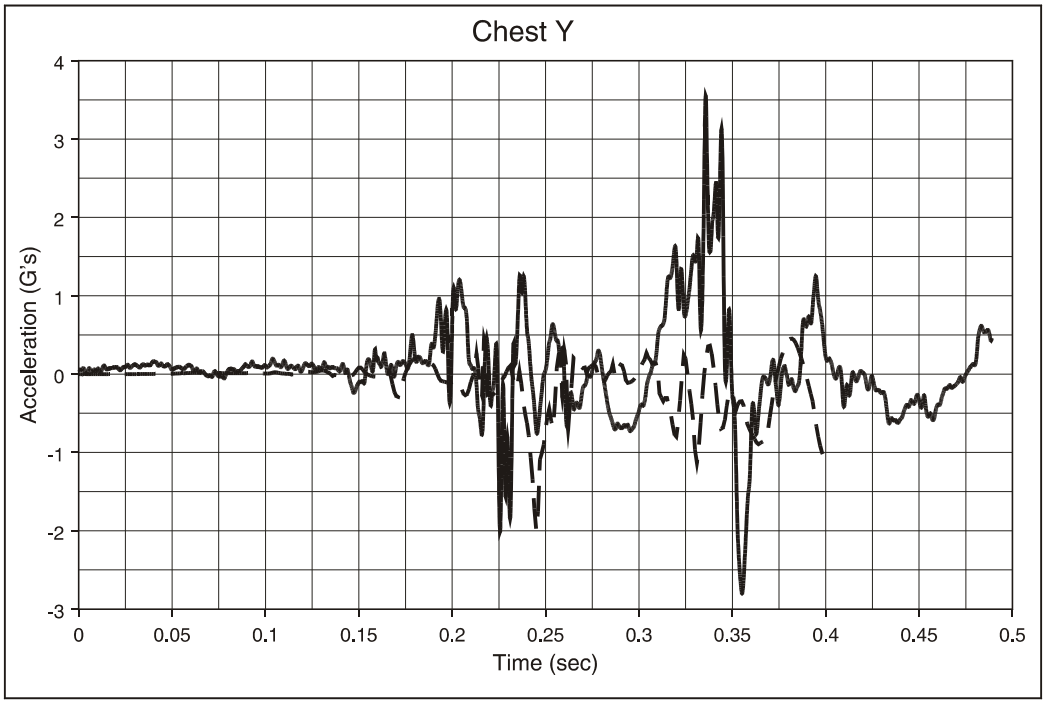

Figure F143. Walkover Seat, Type 1 Test, 50th-Percentile Hybrid II Male ATD, Aisle Seat; Chest Acceleration, y Direction

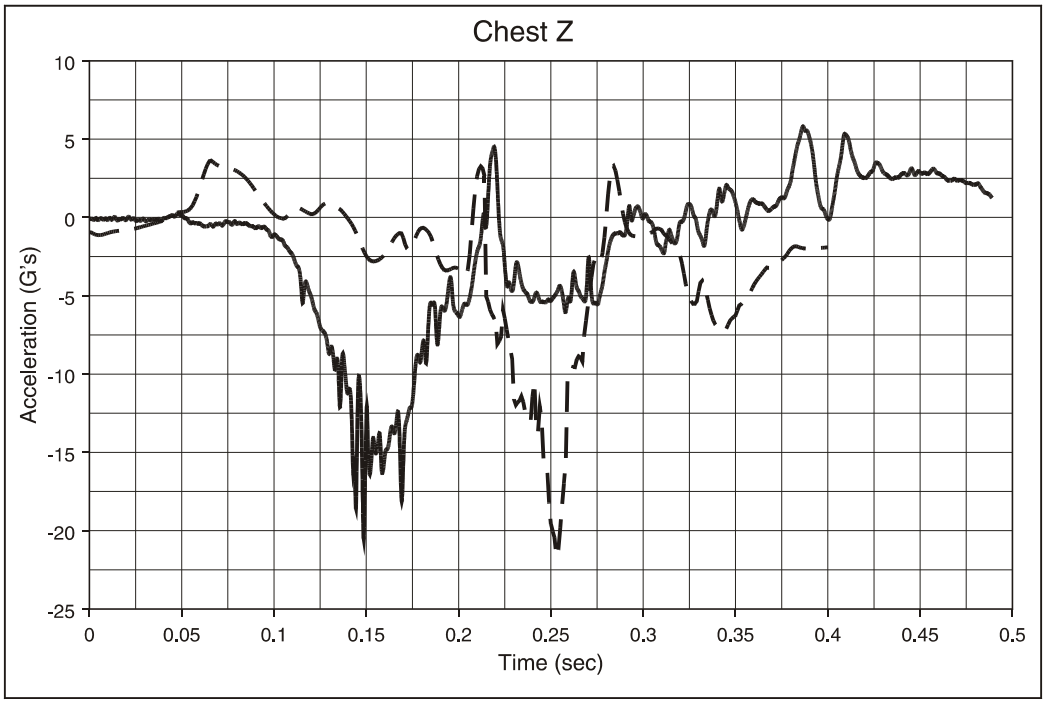

Figure F144. Walkover Seat, Type 1 Test, 50th-Percentile Hybrid II Male ATD, Aisle Seat; Chest Acceleration, z Direction

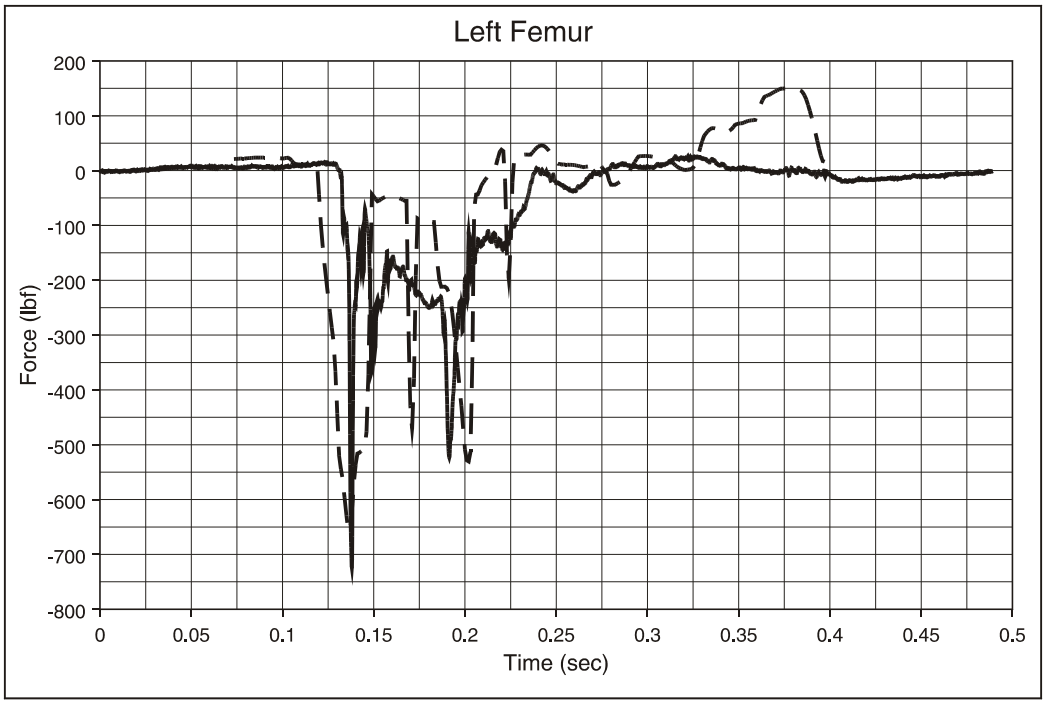

Figure F145. Walkover Seat, Type 1 Test, 50th-Percentile Hybrid II Male ATD, Aisle Seat; Left Femur Load

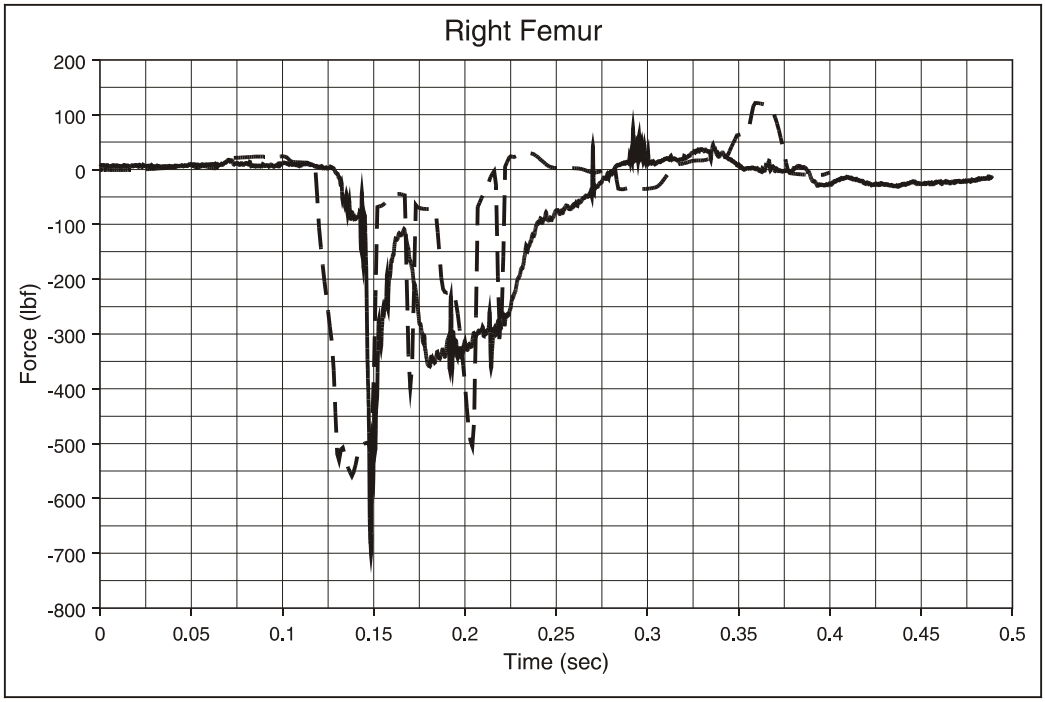

Figure F146. Walkover Seat, Type 1 Test, 50th-Percentile Hybrid II Male ATD, Aisle Seat; Right Femur Load

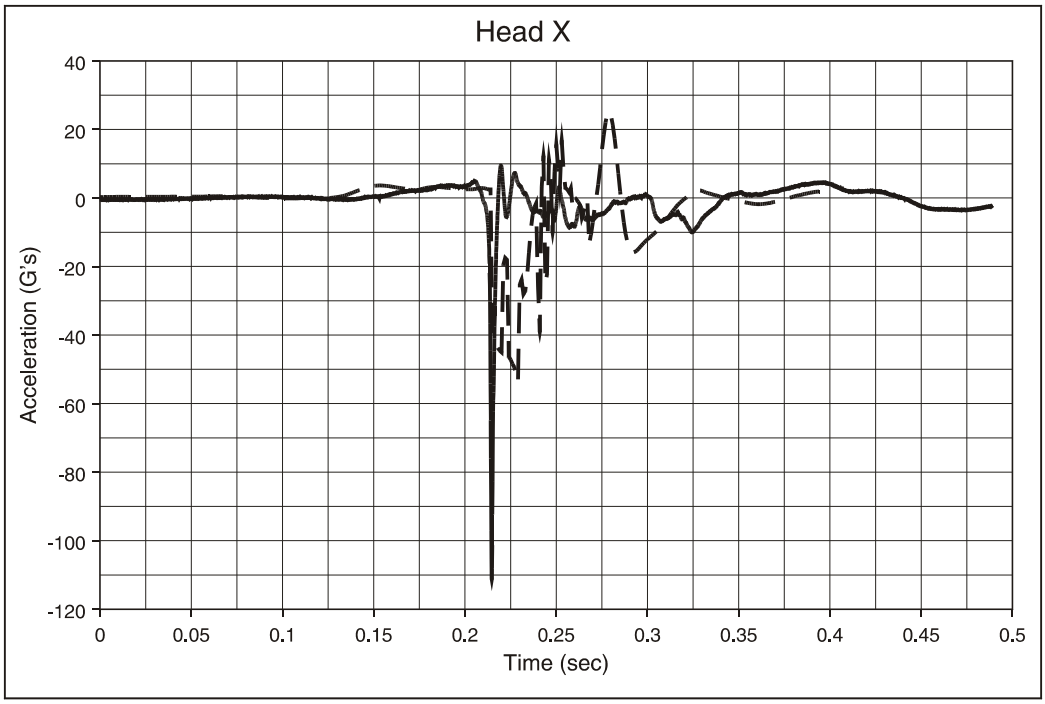

Figure F147. Walkover Seat, Type 1 Test, 50th-Percentile Hybrid II Male ATD, Aisle Seat; Head Acceleration, x Direction

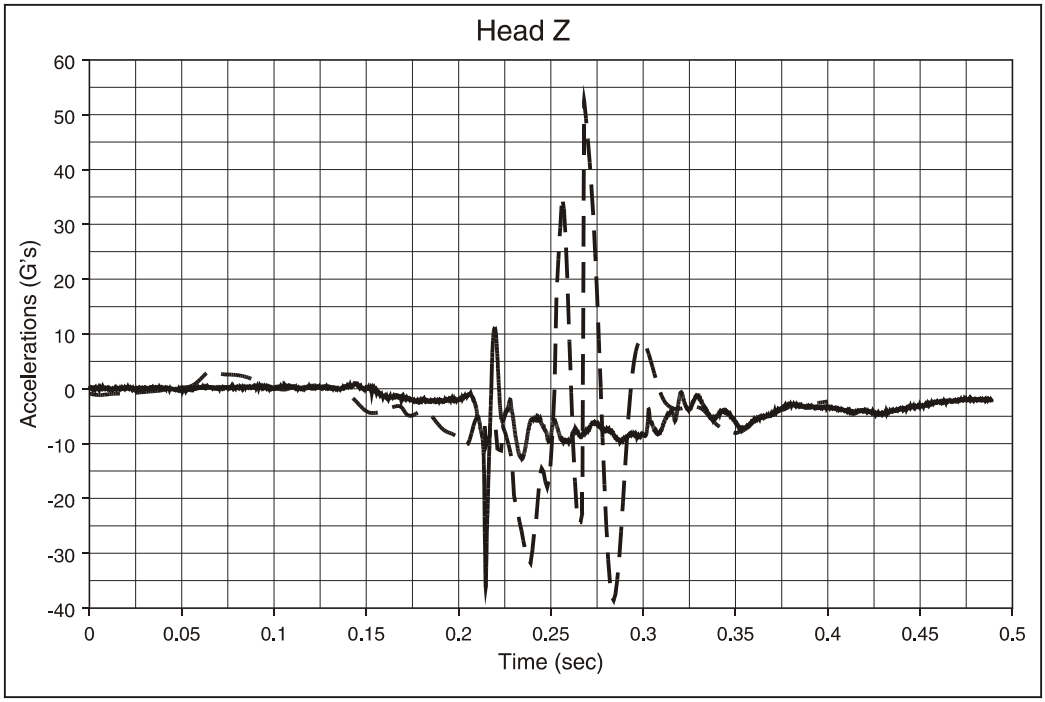

Figure F148. Walkover Seat, Type 1 Test, 50th-Percentile Hybrid II Male ATD, Aisle Seat; Head Acceleration, z Direction

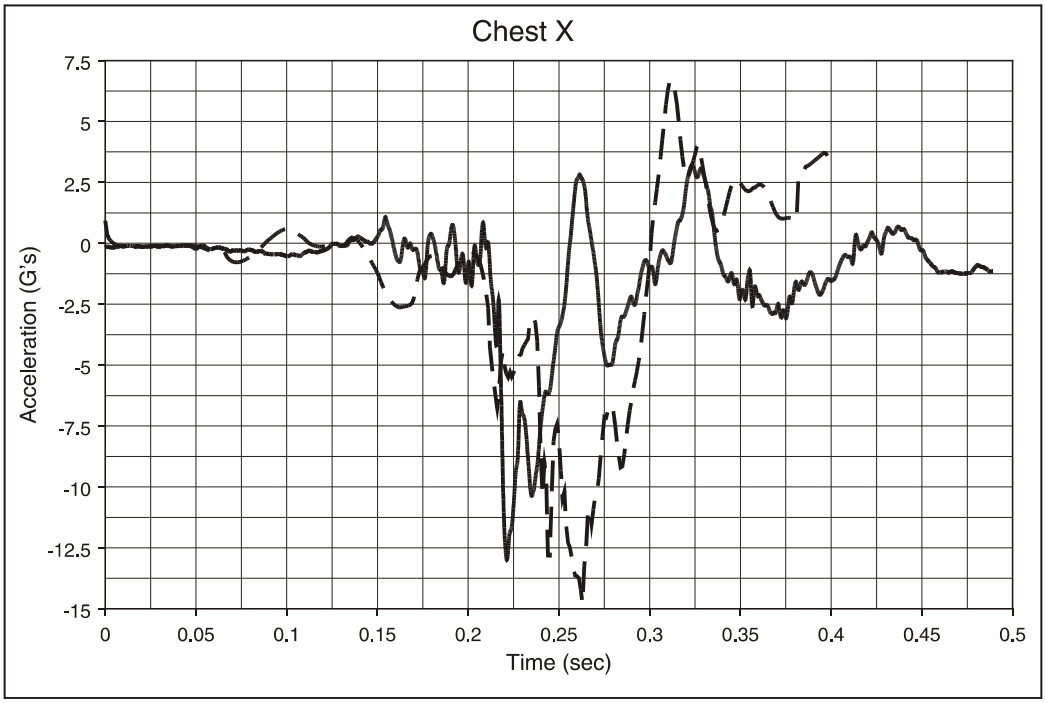

Figure F149. Walkover Seat, Type 1 Test, 50th-Percentile Hybrid II Male ATD, Center Seat; Chest Acceleration, x Direction

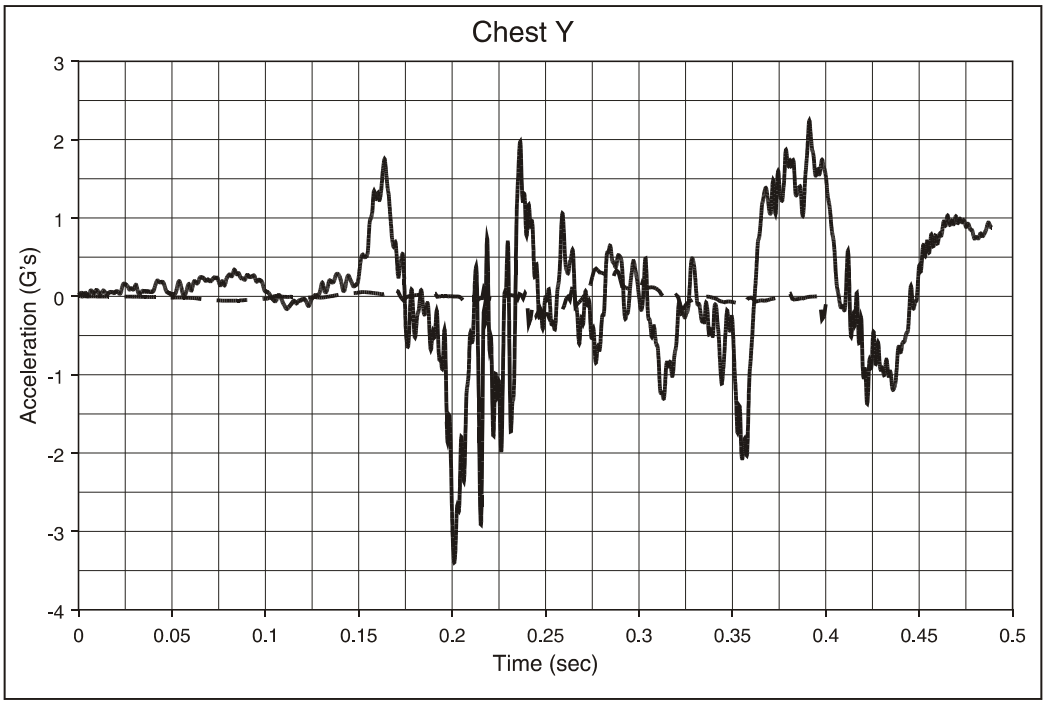

Figure F150. Walkover Seat, Type 1 Test, 50th-Percentile Hybrid II Male ATD, Center Seat; Chest Acceleration, y Direction

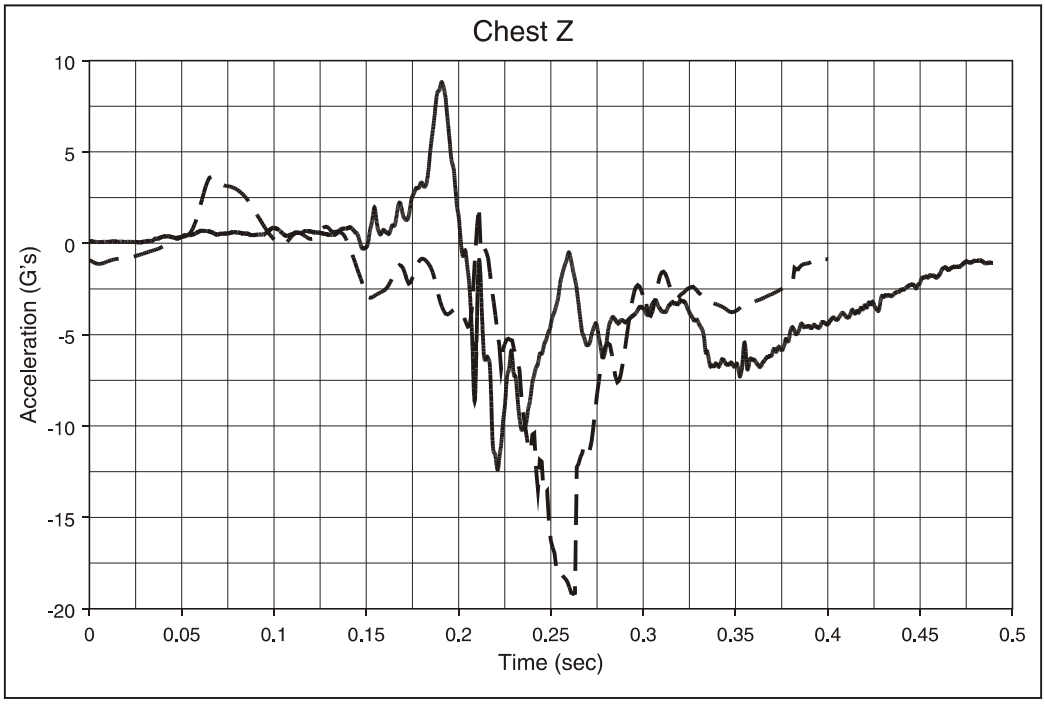

Figure F151. Walkover Seat, Type 1 Test, 50th-Percentile Hybrid II Male ATD, Center Seat; Chest Acceleration, z Direction

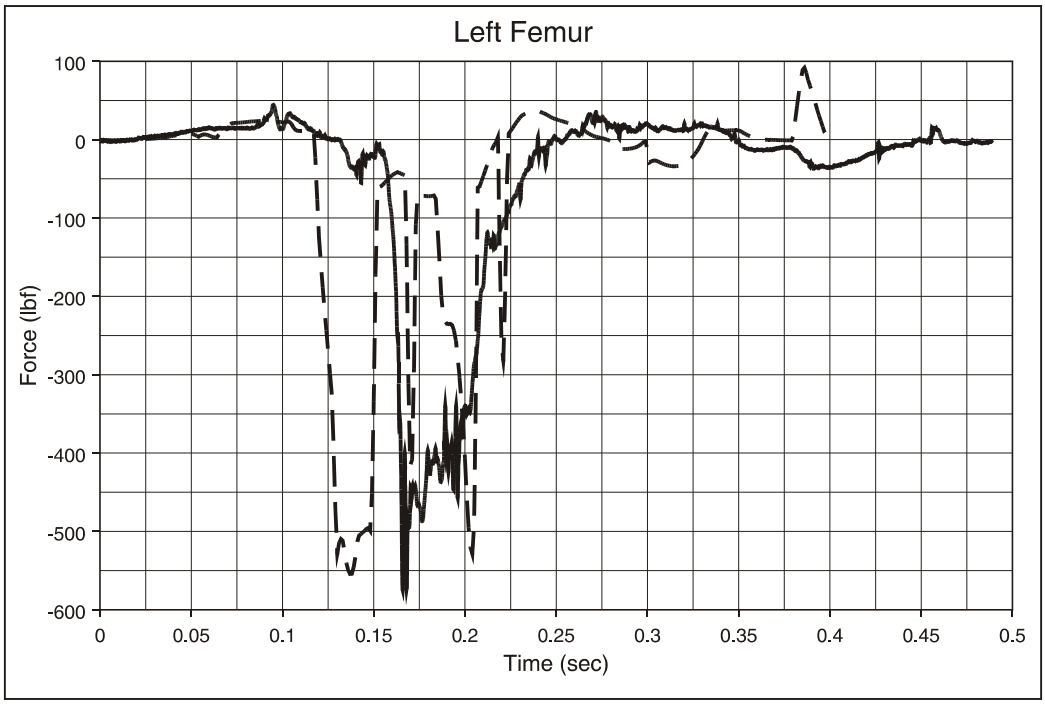

Figure F152. Walkover Seat, Type 1 Test, 50th-Percentile Hybrid II Male ATD, Center Seat; Left Femur Load

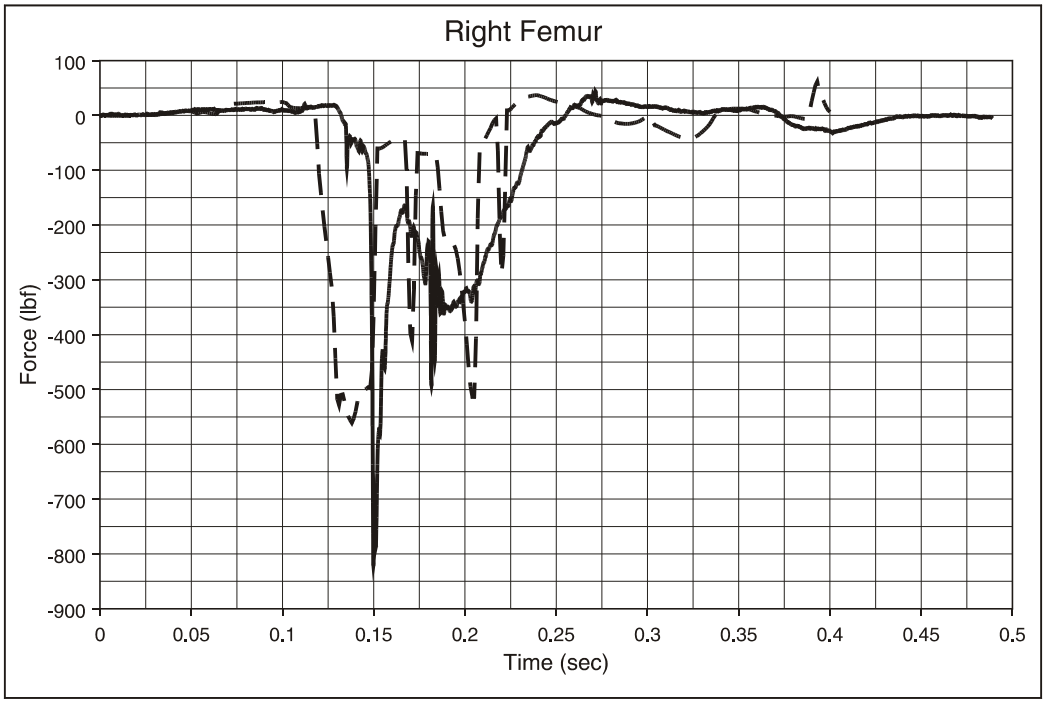

Figure F153. Walkover Seat, Type 1 Test, 50th-Percentile Hybrid II Male ATD, Center Seat; Right Femur Load

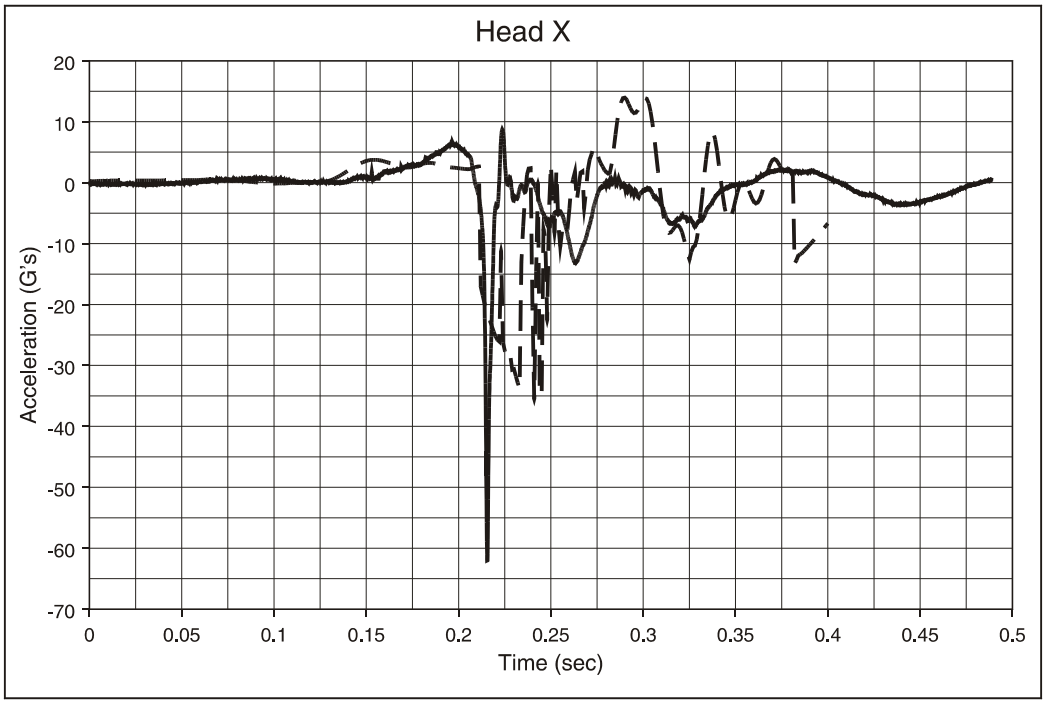

Figure F154. Walkover Seat, Type 1 Test, 50th-Percentile Hybrid II Male ATD, Center Seat; Head Acceleration, x Direction

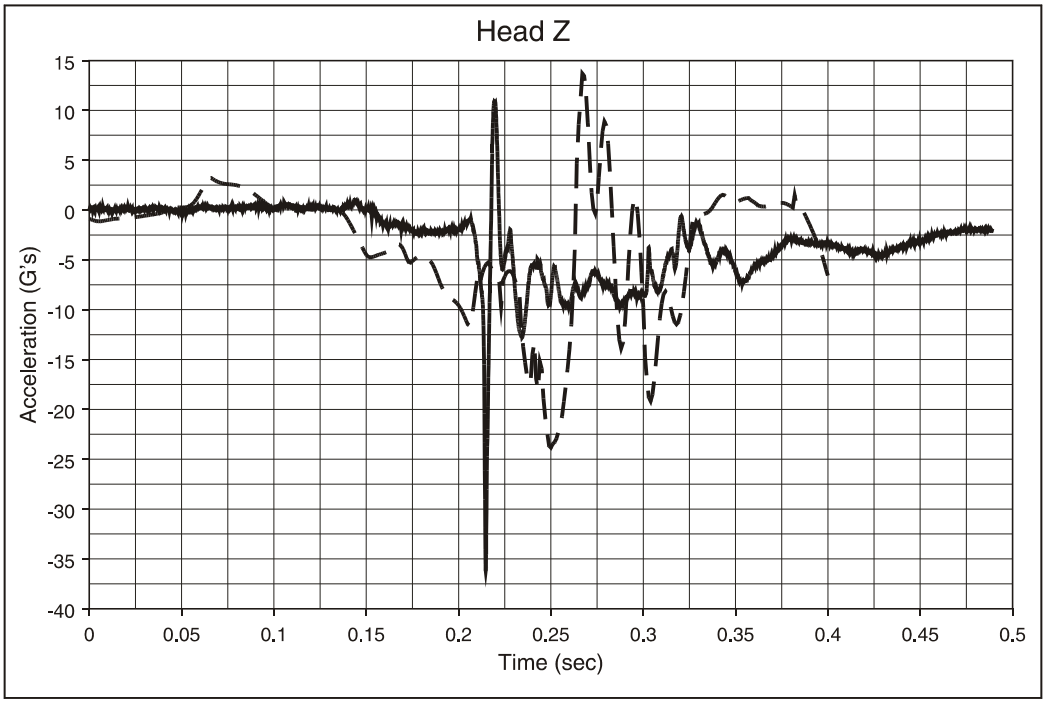

Figure F155. Walkover Seat, Type 1 Test, 50th-Percentile Hybrid II Male ATD, Center Seat; Head Acceleration, z Direction

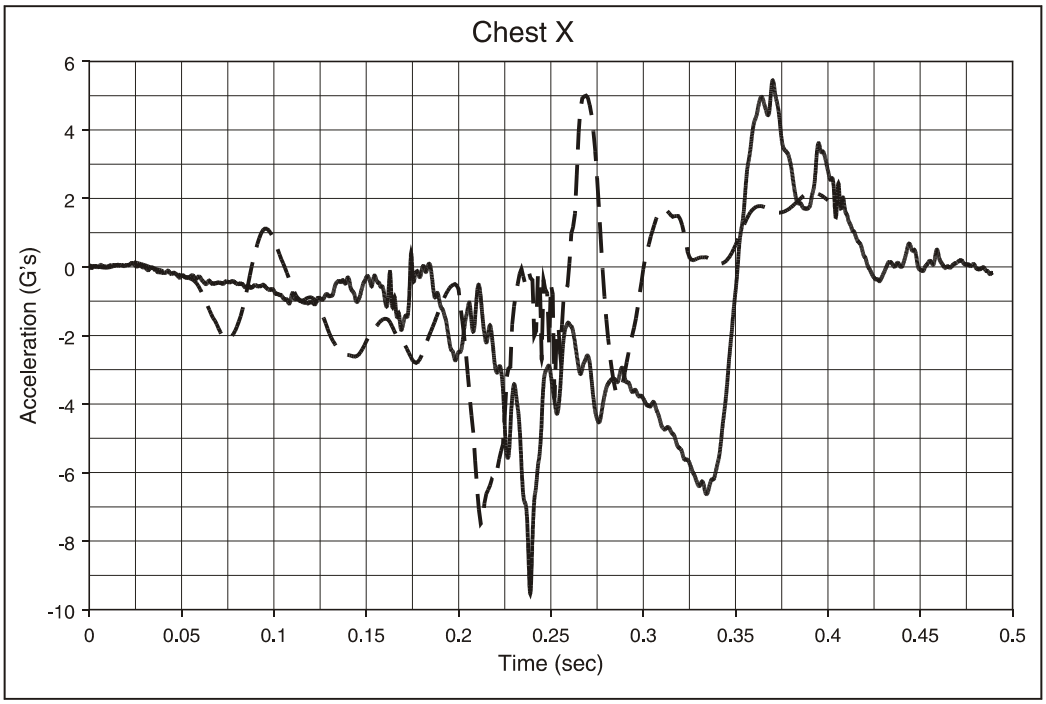

Figure F156. Walkover Seat, Type 1 Test, 50th-Percentile Hybrid III Male ATD, Window Seat; Chest Acceleration, x Direction

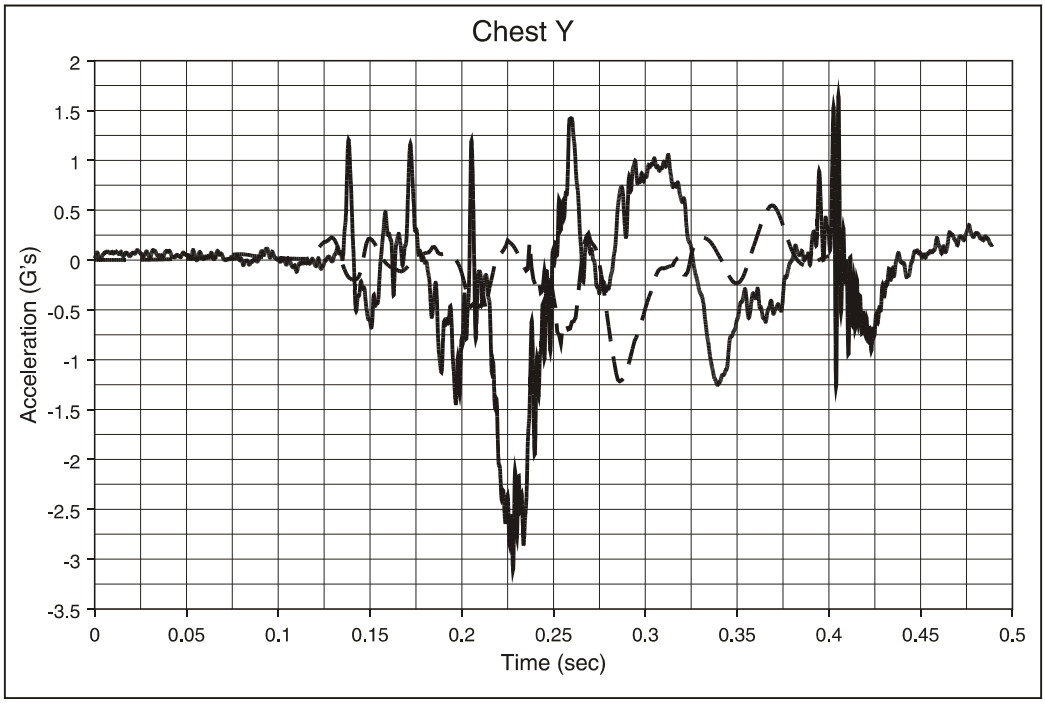

Figure F157. Walkover Seat, Type 1 Test, 50th-Percentile Hybrid III Male ATD, Window Seat; Chest Acceleration, y Direction

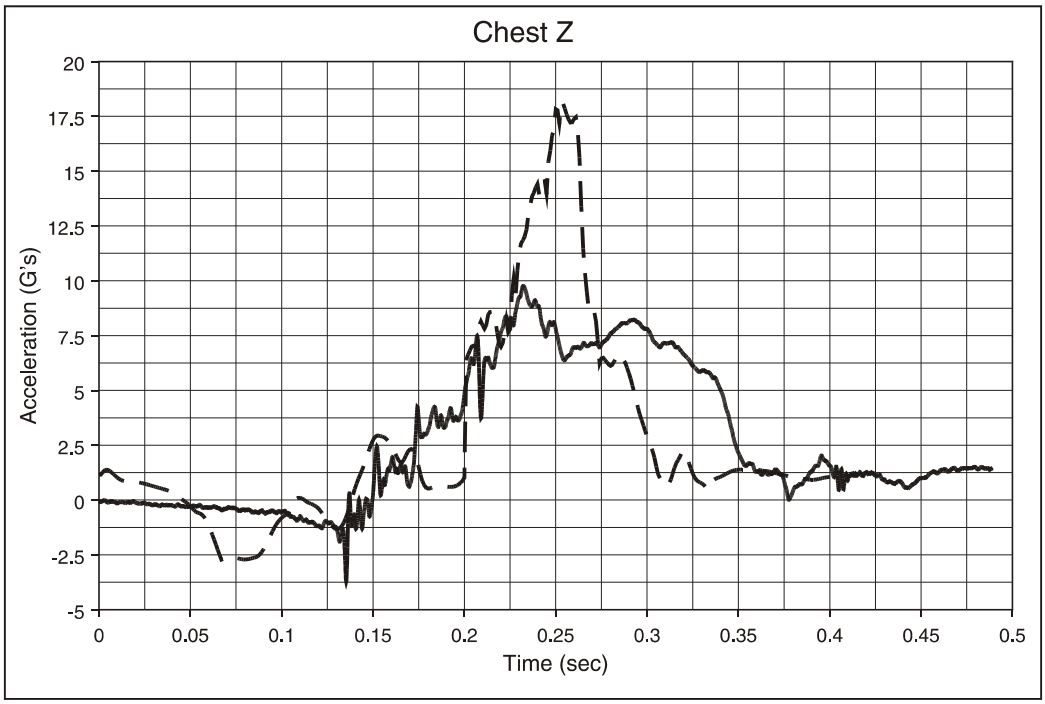

Figure F158. Walkover Seat, Type 1 Test, 50th-Percentile Hybrid III Male ATD, Window Seat; Chest Acceleration, z Direction

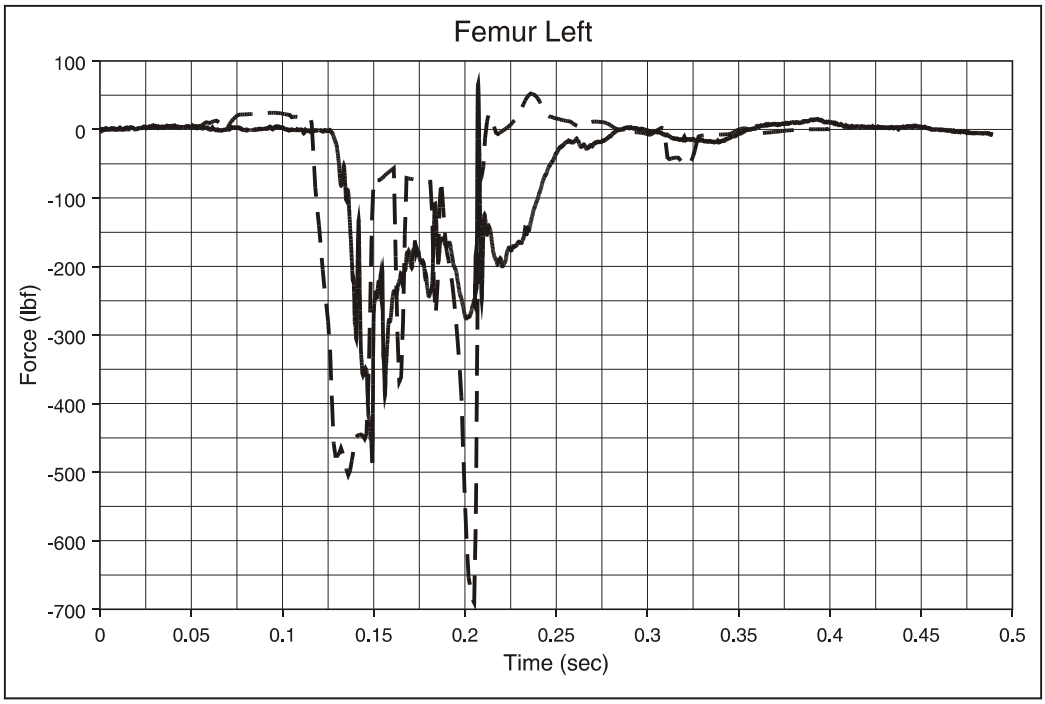

Figure F159. Walkover Seat, Type 1 Test, 50th-Percentile Hybrid III Male ATD, Window Seat; Left Femur Load

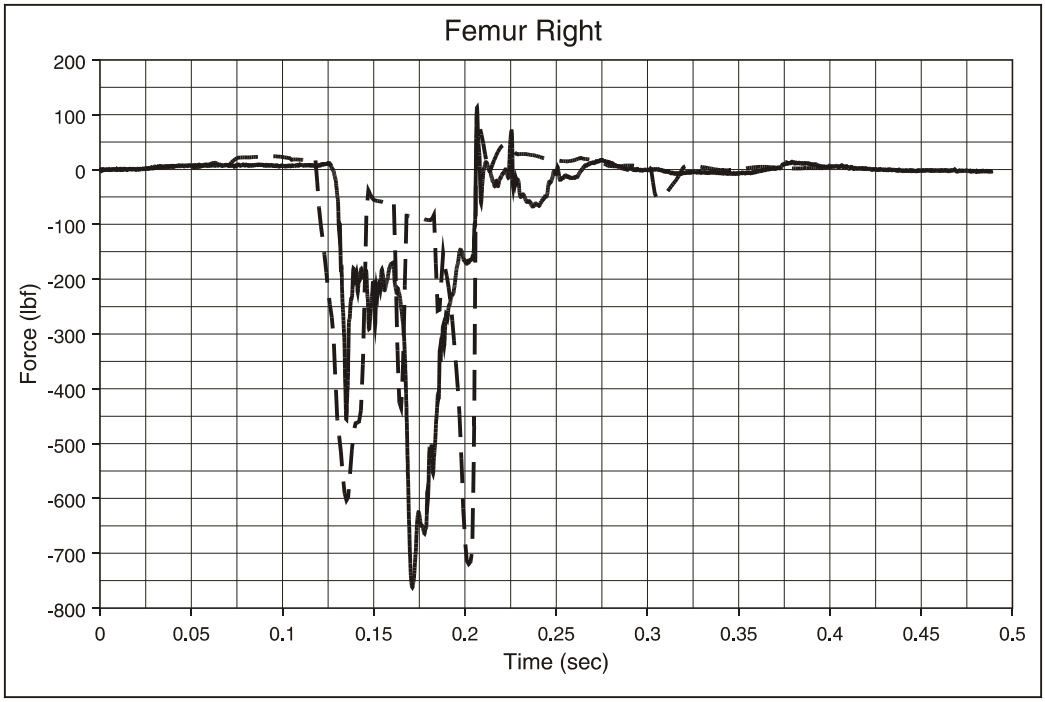

Figure F160. Walkover Seat, Type 1 Test, 50th-Percentile Hybrid III Male ATD, Window Seat; Right Femur Load

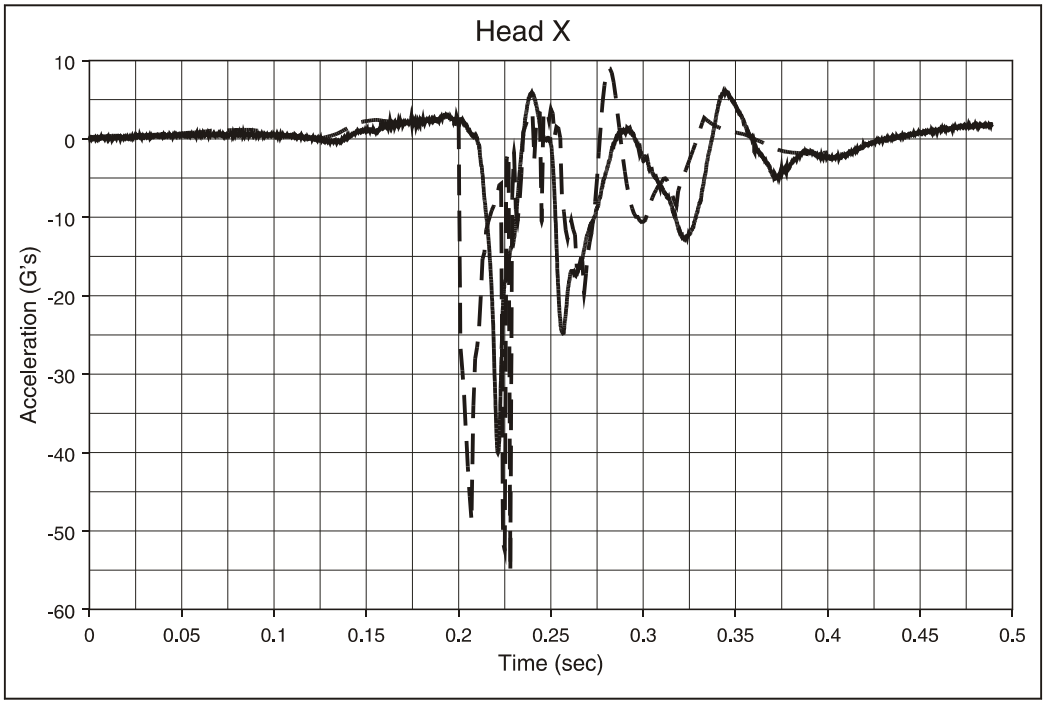

Figure F161. Walkover Seat, Type 1 Test, 50th-Percentile Hybrid III Male ATD, Window Seat; Head Acceleration, x Direction

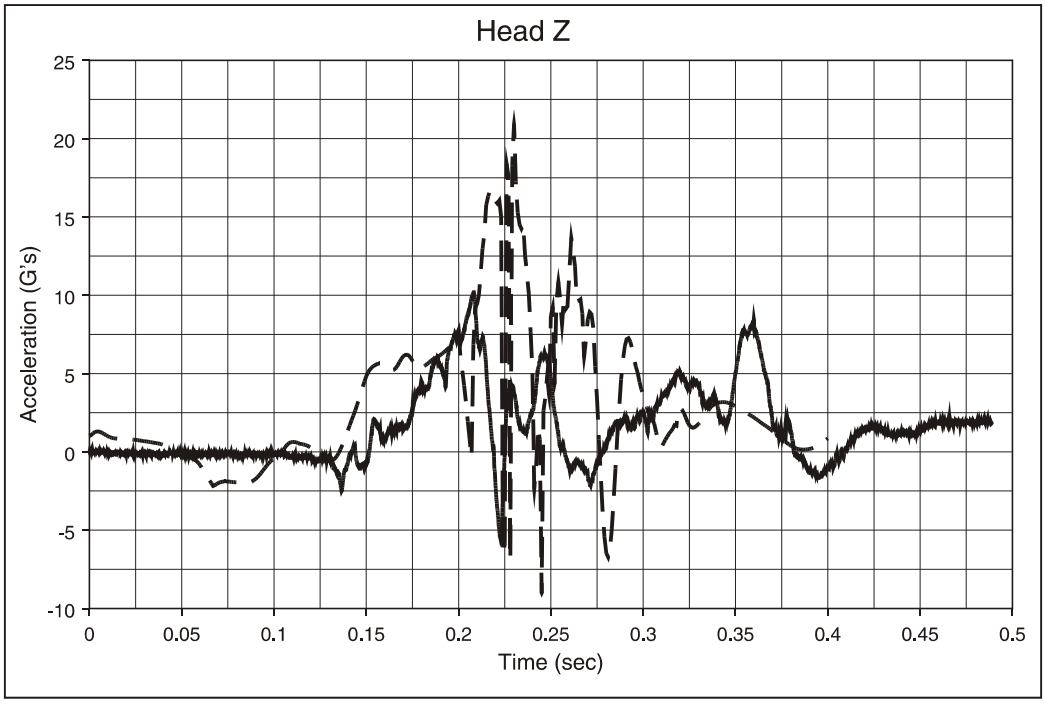

Figure F162. Walkover Seat, Type 1 Test, 50th-Percentile Hybrid III Male ATD, Window Seat; Head Acceleration, z Direction

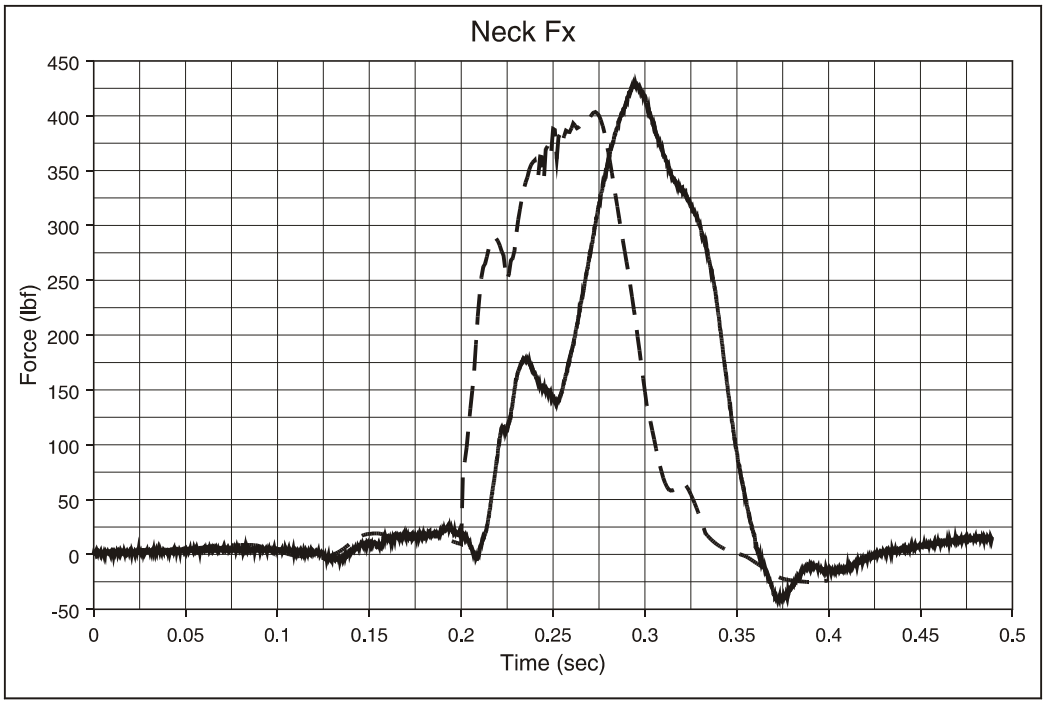

Figure F163. Walkover Seat, Type 1 Test, 50th-Percentile Hybrid III Male ATD, Window Seat; Neck Shear Load

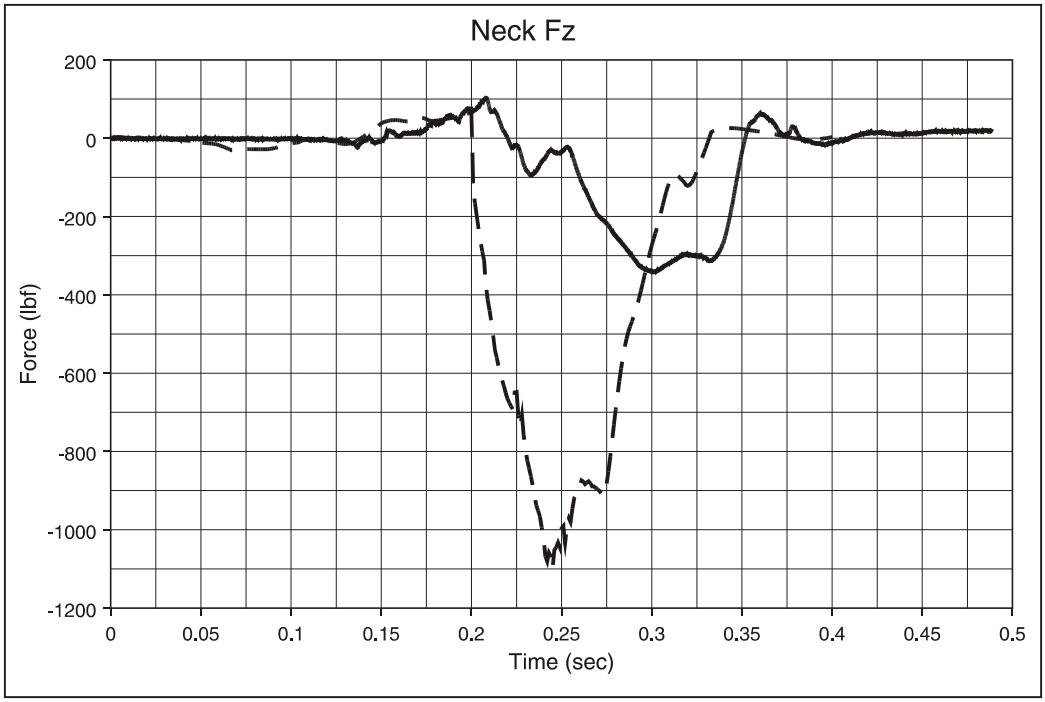

Figure F164. Walkover Seat, Type 1 Test, 50th-Percentile Hybrid III Male ATD, Window Seat; Neck Compression/Tension Load

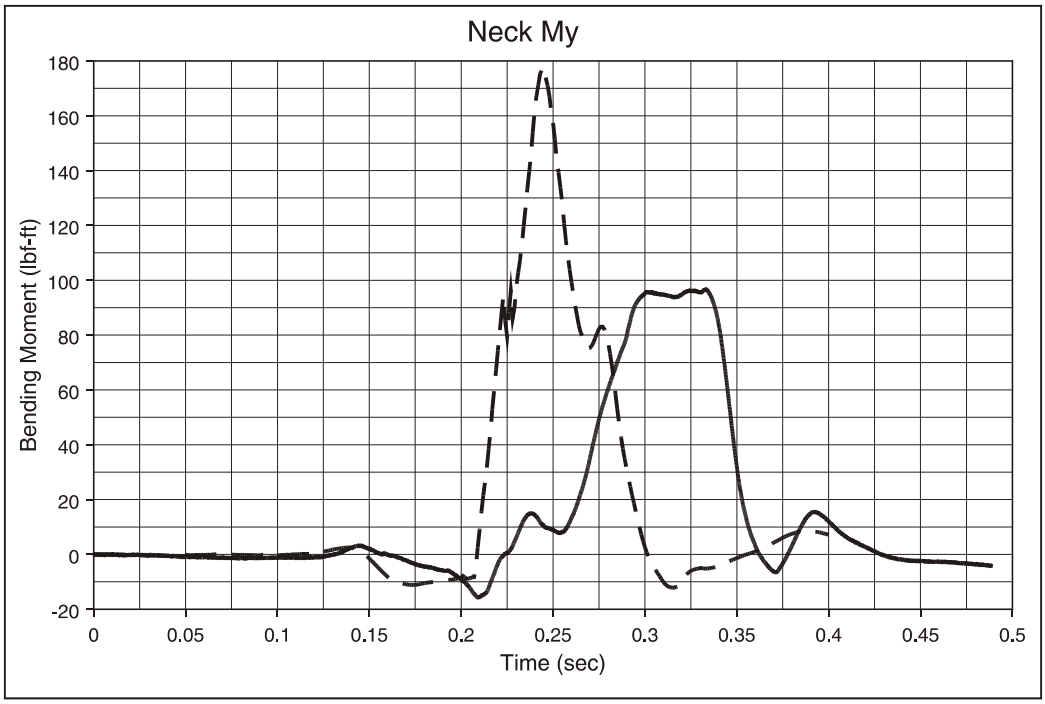

Figure F165. Walkover Seat, Type 1 Test, 50th-Percentile Hybrid III Male ATD, Window Seat; Neck Flexion/Extension Moment

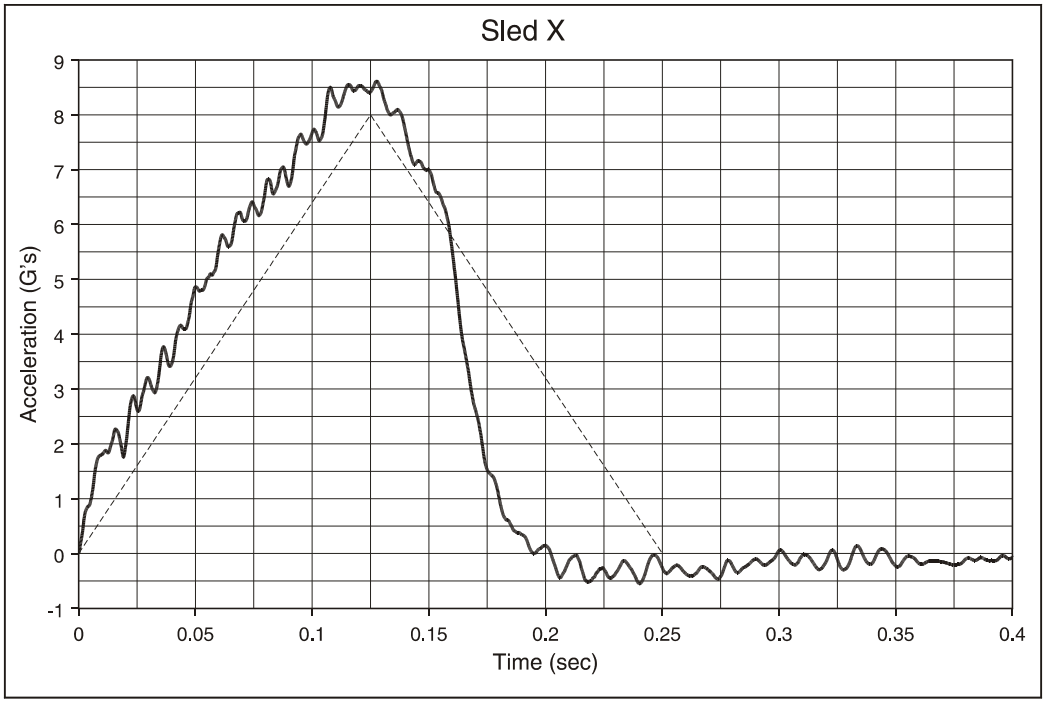

Figure F166. Walkover Seat, Type 2 Test, 95th-, 50th-, and 5th-Percentile ATDs: Sled Pulse

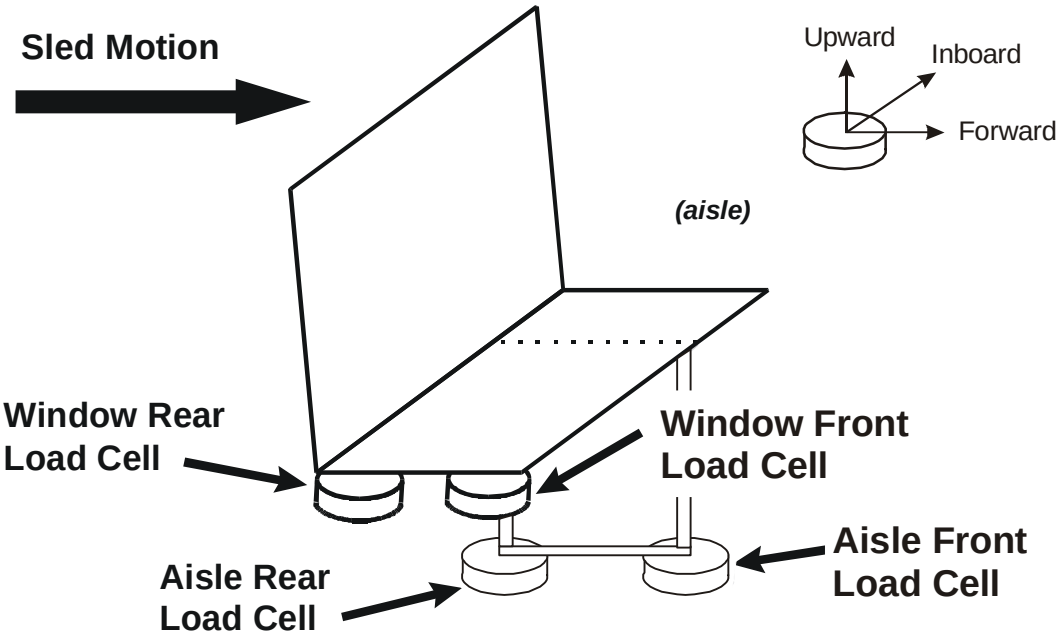

Figure F167. Walkover Seat, Type 2 Test, Seat Attachment Loads: Walkover Seat Load Cell Orientation

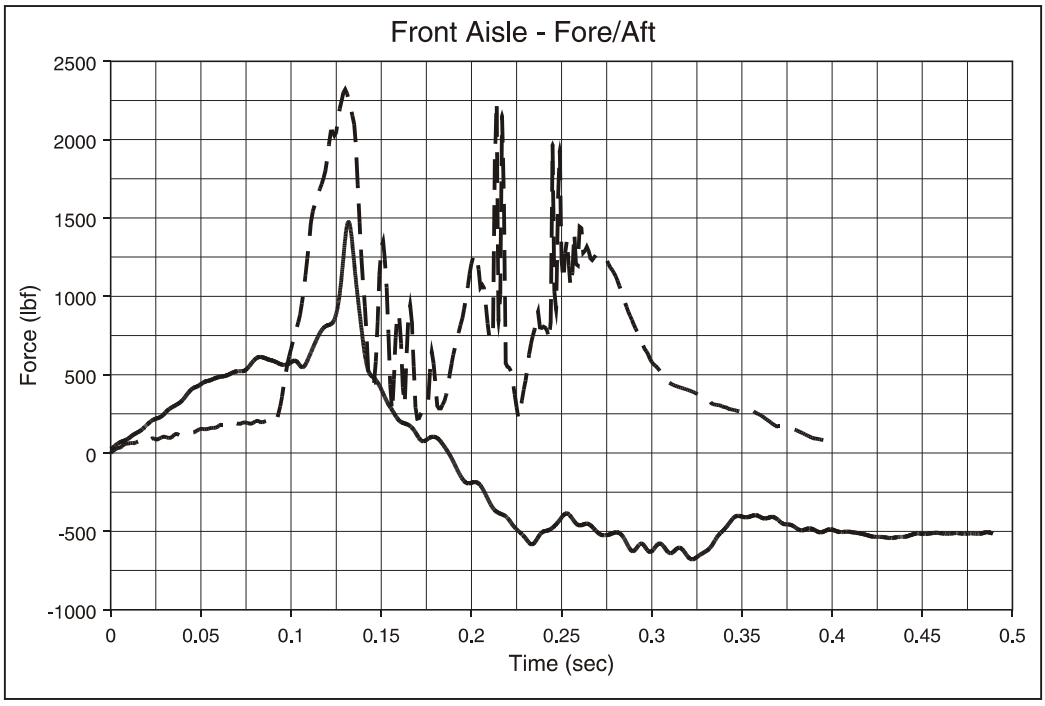

Figure F168. Walkover Seat, Type 2 Test, Seat Attachment Loads: Aisle Front Load Cell, x Direction

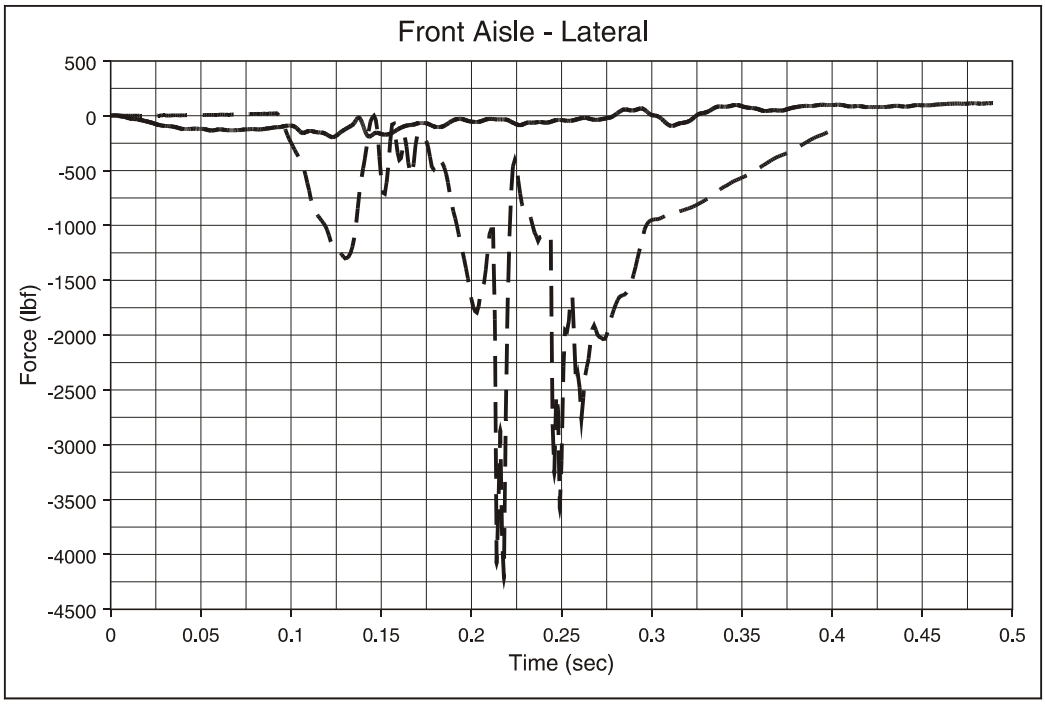

Figure F169. Walkover Seat, Type 2 Test, Seat Attachment Loads: Aisle Front Load Cell, y Direction

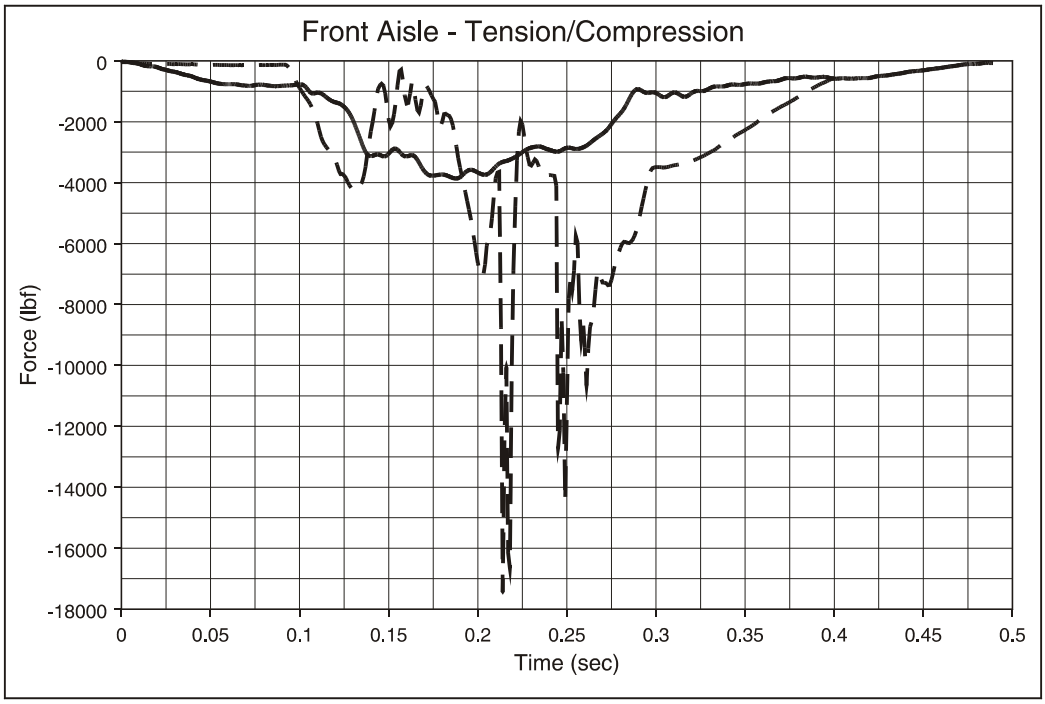

Figure F170. Walkover Seat, Type 2 Test, Seat Attachment Loads: Aisle Front Load Cell, z Direction

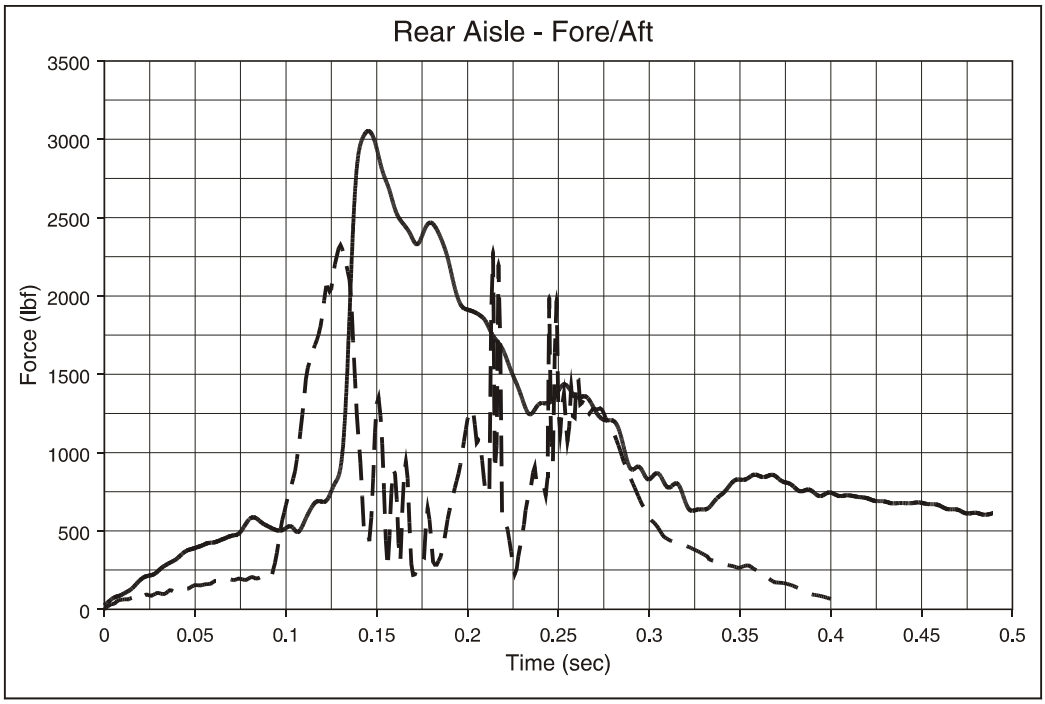

Figure F171. Walkover Seat, Type 2 Test, Seat Attachment Loads: Aisle Rear Load Cell, x Direction

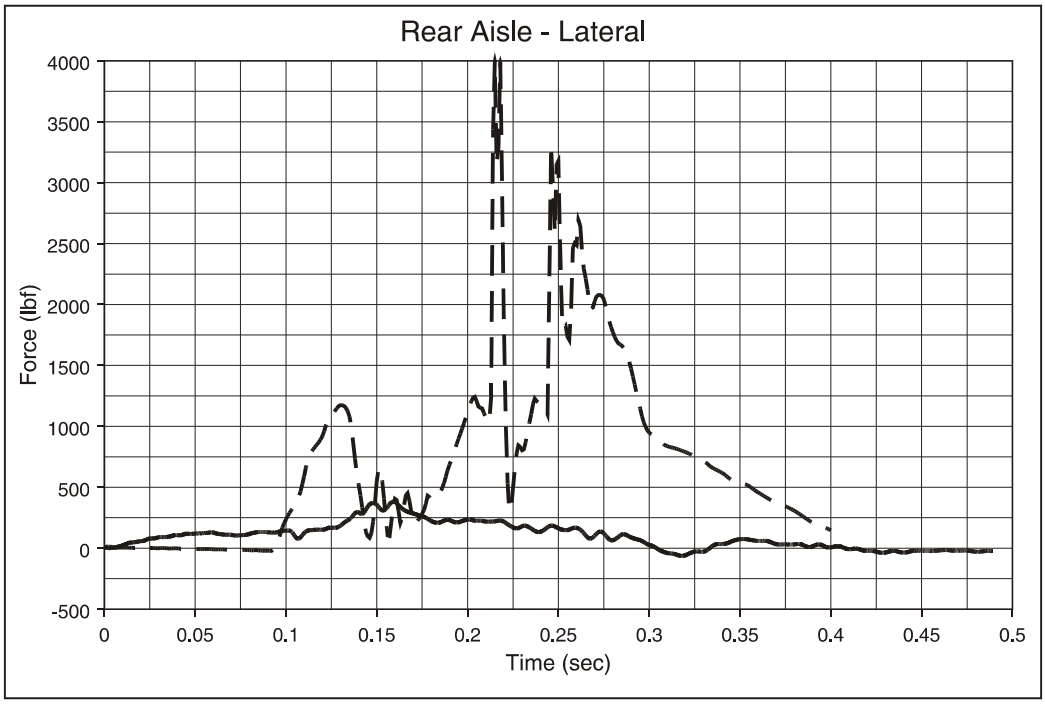

Figure F172. Walkover Seat, Type 2 Test, Seat Attachment Loads: Aisle Rear Load Cell, y Direction

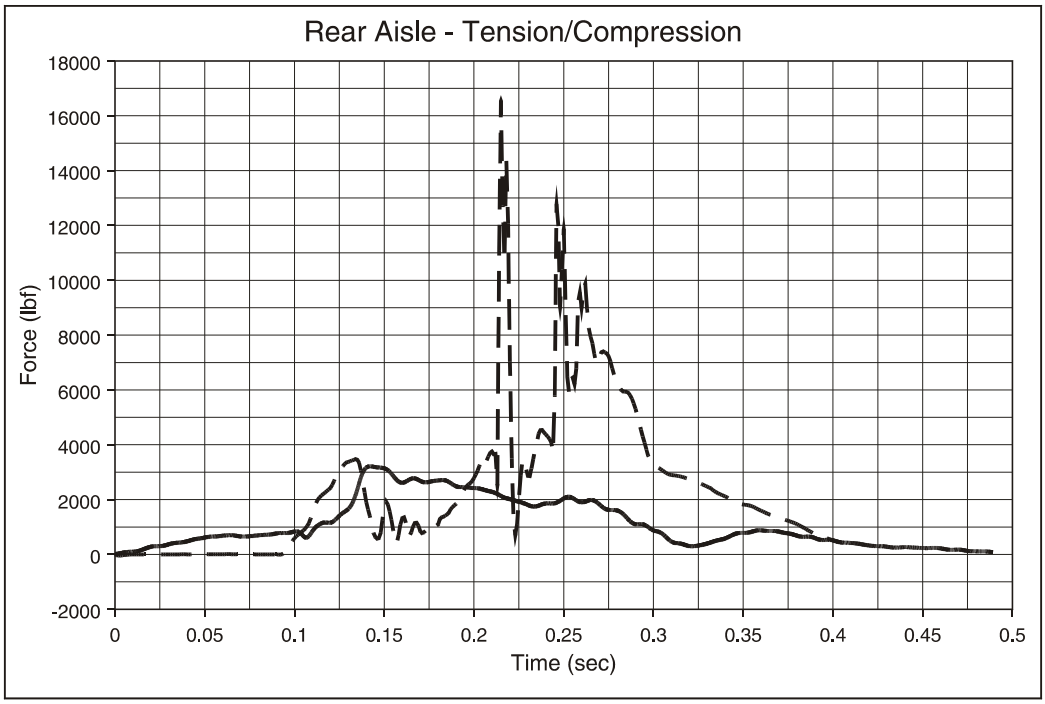

Figure F173. Walkover Seat, Type 2 Test, Seat Attachment Loads: Aisle Rear Load Cell, z Direction

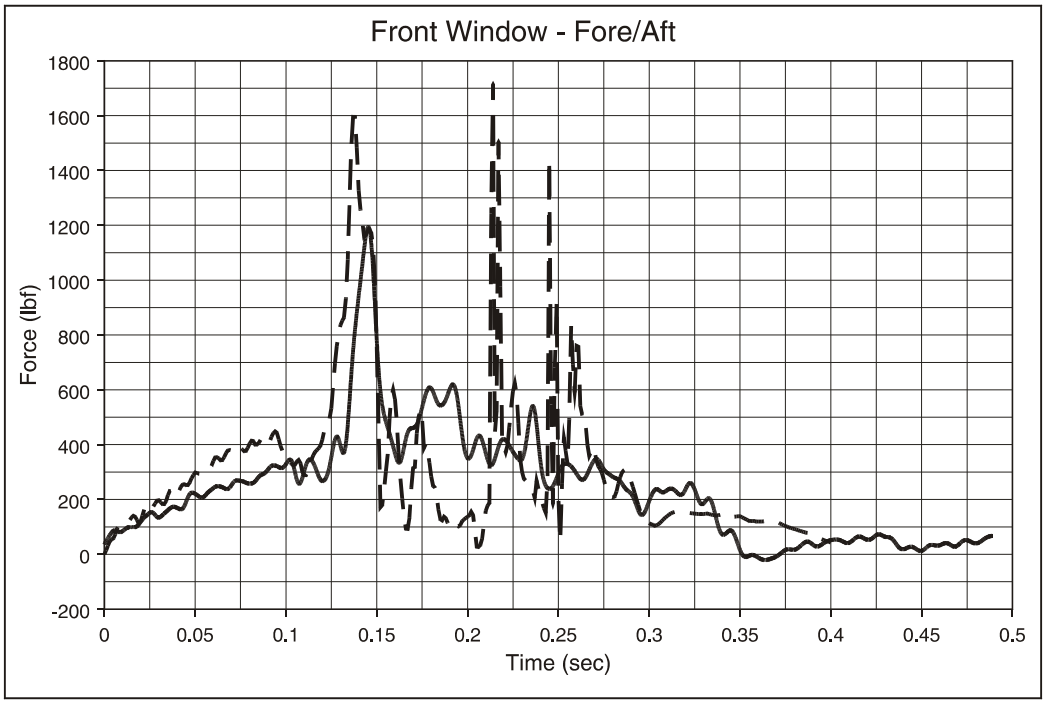

Figure F174. Walkover Seat, Type 2 Test, Seat Attachment Loads: Window Front Load Cell, x Direction

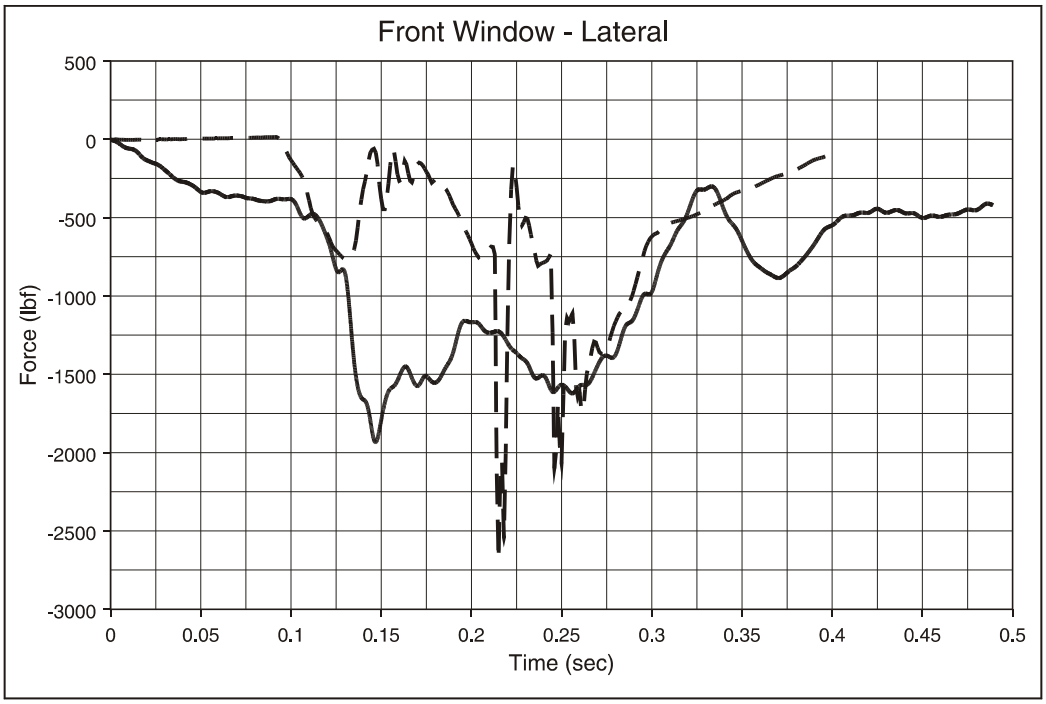

Figure F175. Walkover Seat, Type 2 Test, Seat Attachment Loads: Window Front Load Cell, y Direction

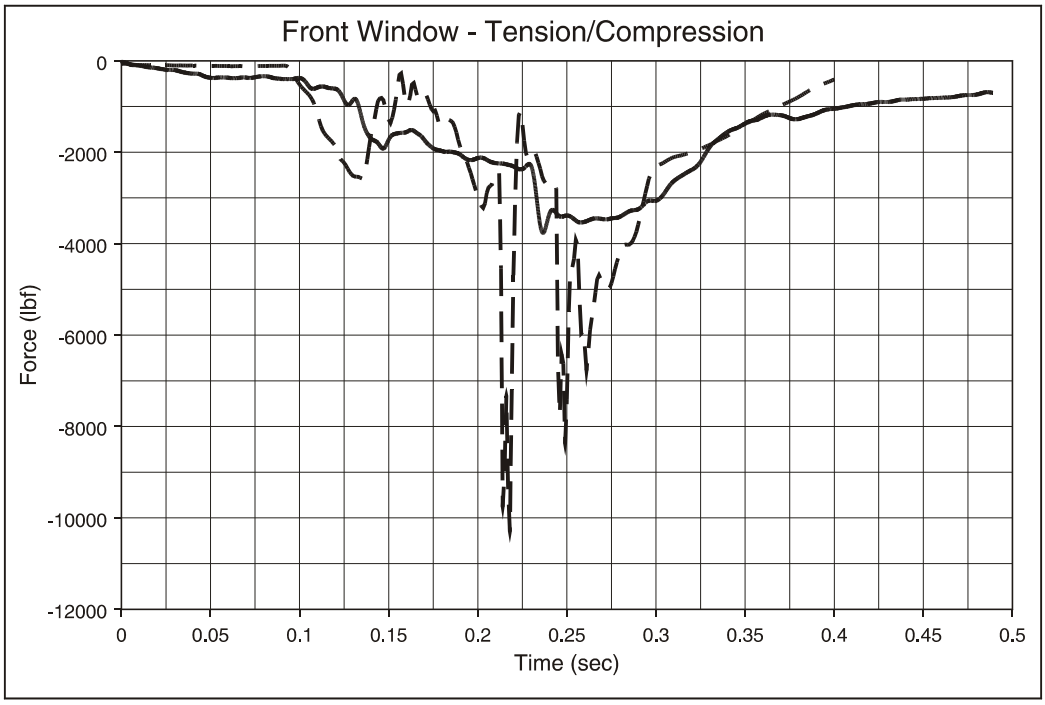

Figure F176. Walkover Seat, Type 2 Test, Seat Attachment Loads: Window Front Load Cell, z Direction

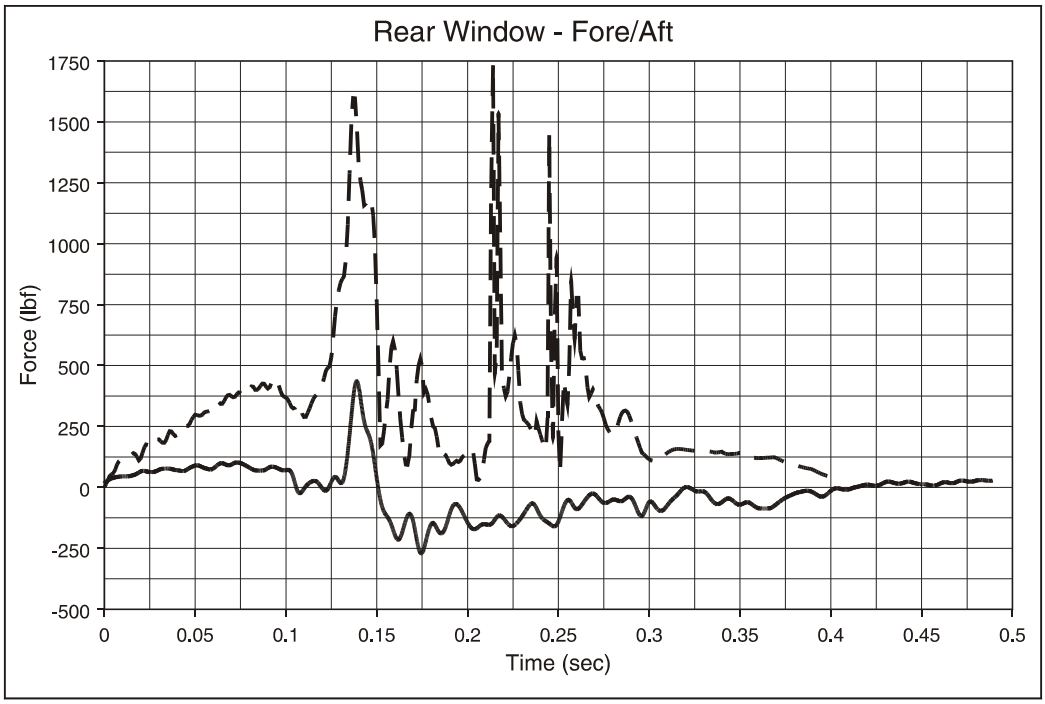

Figure F177. Walkover Seat, Type 2 Test, Seat Attachment Loads: Window Rear Load Cell, x Direction

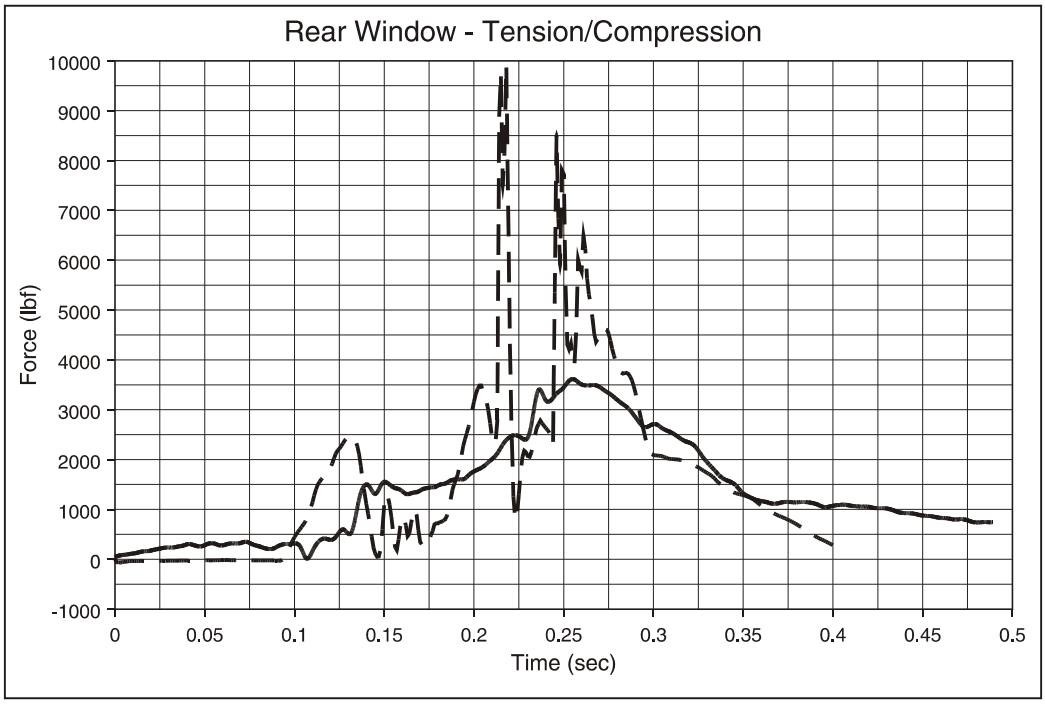

Figure F178. Walkover Seat, Type 2 Test, Seat Attachment Loads: Window Rear Load Cell, z Direction

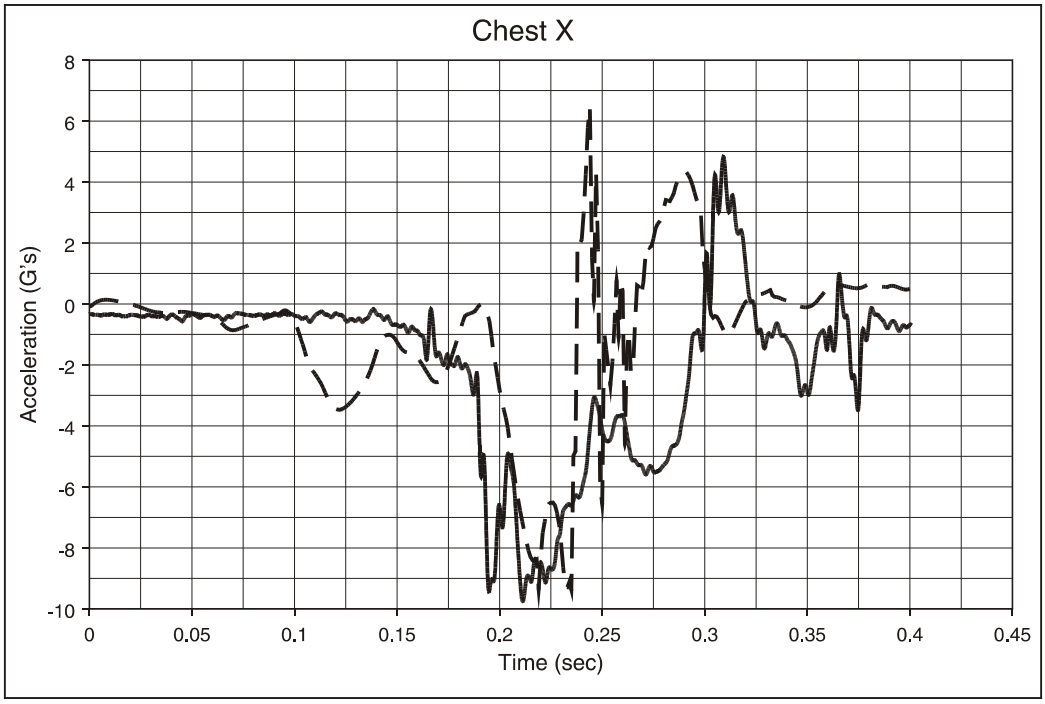

Figure F179. Walkover Seat, Type 2 Test, 95th-Percentile Hybrid III Male ATD, Aisle Seat; Chest Acceleration, x Direction

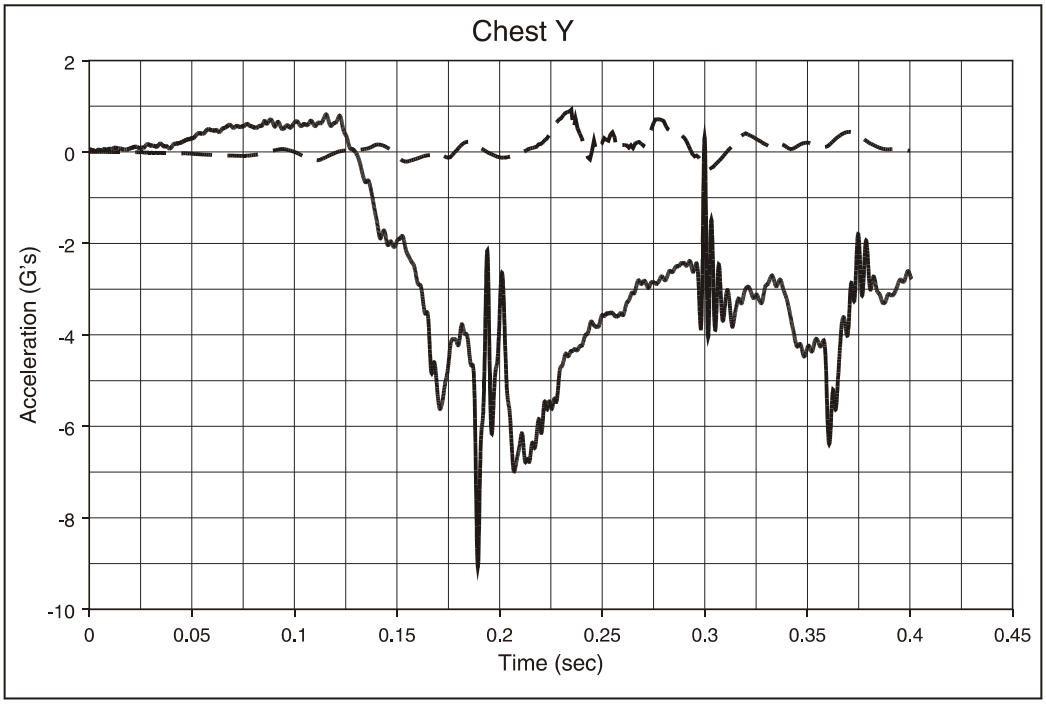

Figure F180. Walkover Seat, Type 2 Test, 95th-Percentile Hybrid III Male ATD, Aisle Seat; Chest Acceleration, y Direction

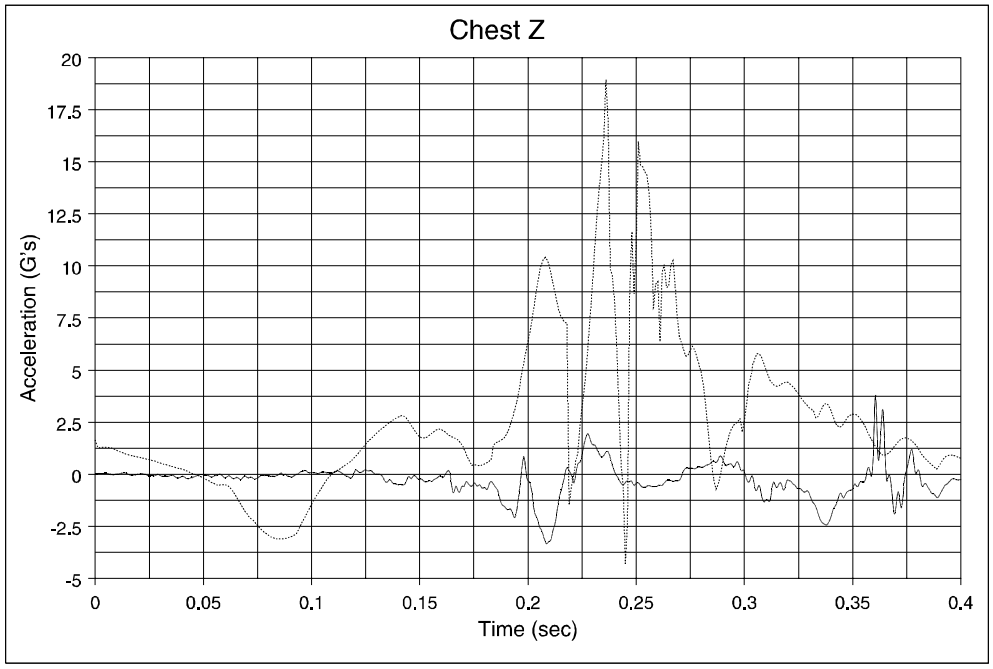

Figure F181. Walkover Seat, Type 2 Test, 95th-Percentile Hybrid III Male ATD, Aisle Seat; Chest Acceleration, z Direction

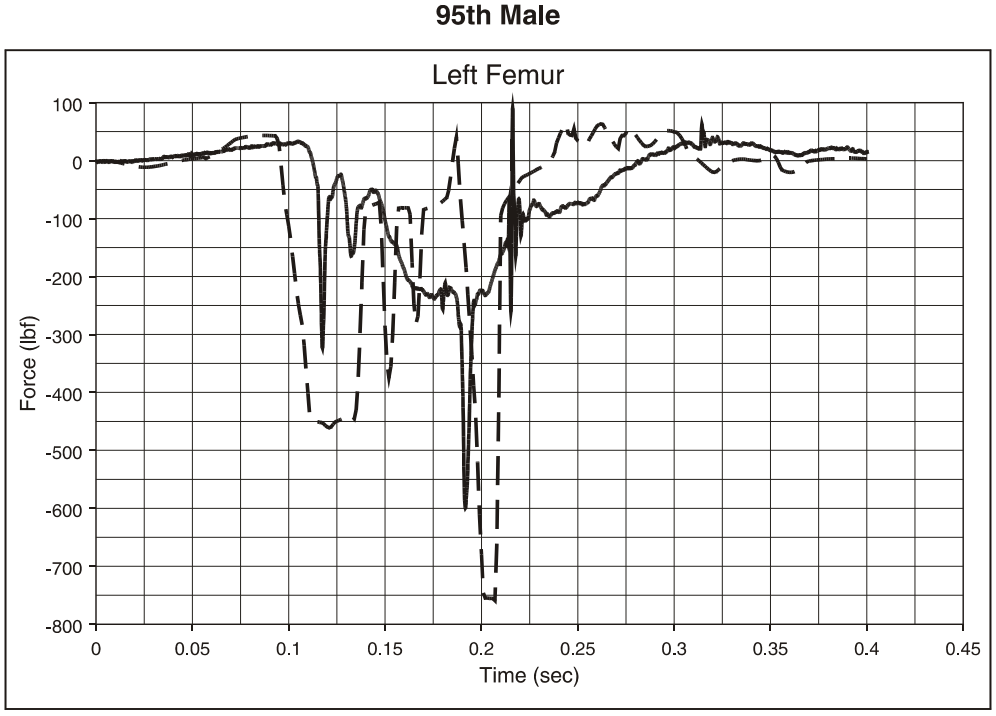

Figure F182. Walkover Seat, Type 2 Test, 95th-Percentile Hybrid III Male ATD, Aisle Seat; Left Femur Load

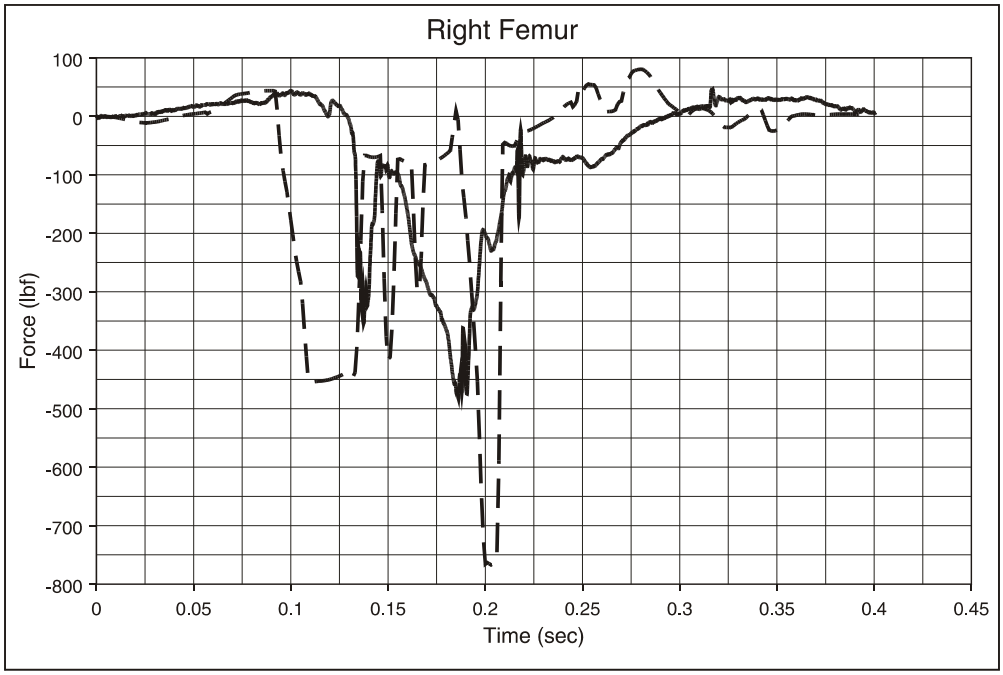

Figure F183. Walkover Seat, Type 2 Test, 95th-Percentile Hybrid III Male ATD, Aisle Seat; Right Femur Load

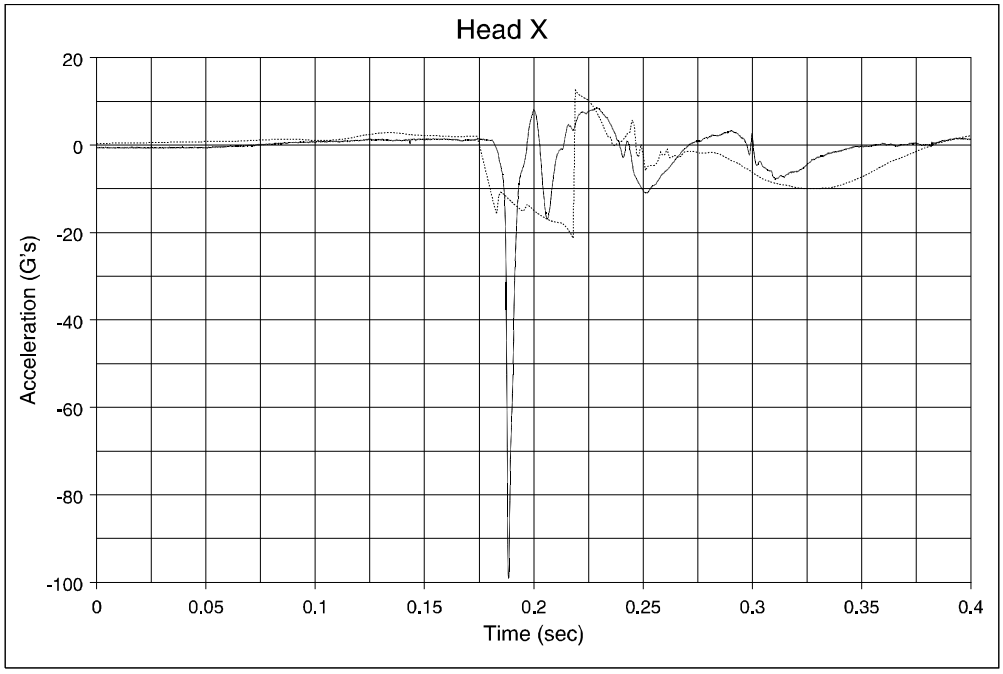

Figure F184. Walkover Seat, Type 2 Test, 95th-Percentile Hybrid III Male ATD, Aisle Seat; Head Acceleration, x Direction

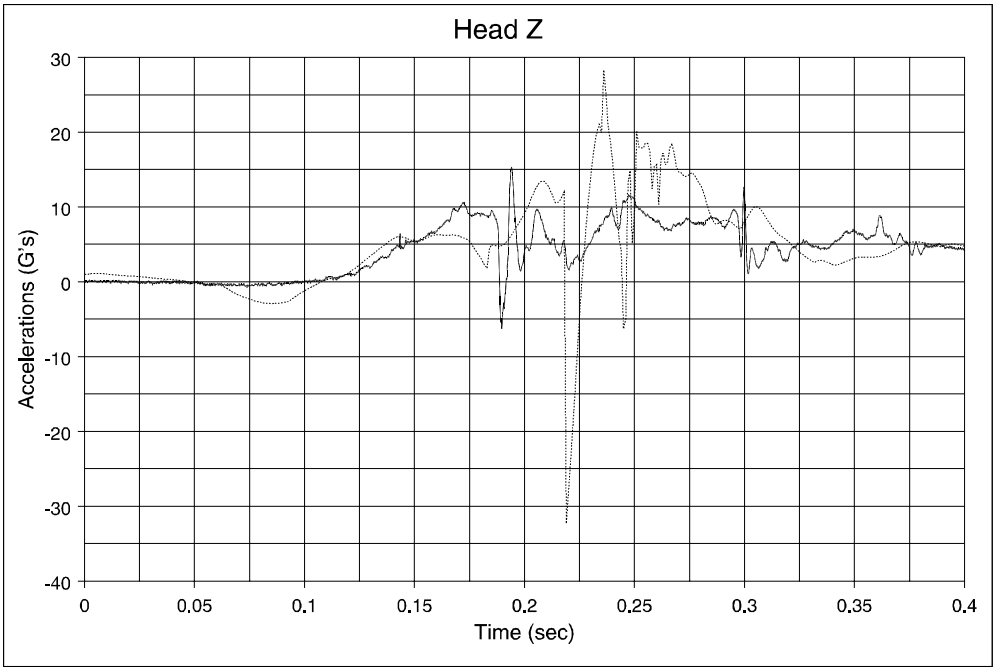

Figure F185. Walkover Seat, Type 2 Test, 95th-Percentile Hybrid III Male ATD, Aisle Seat; Head Acceleration, z Direction

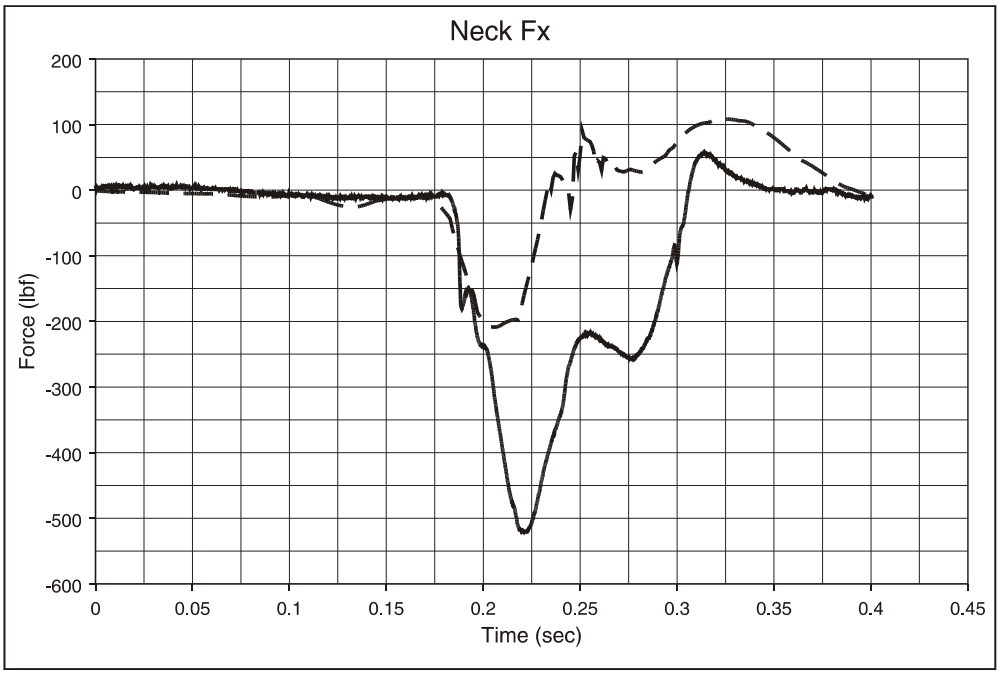

Figure F186. Walkover Seat, Type 2 Test, 95th-Percentile Hybrid III Male ATD, Aisle Seat; Neck Shear Load

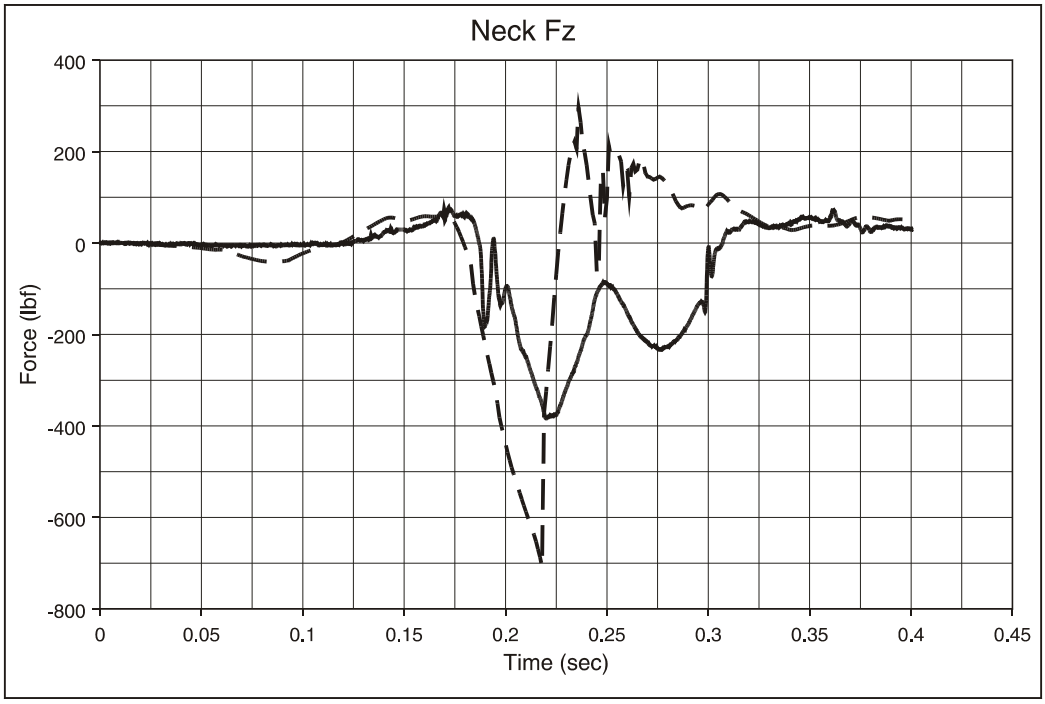

Figure F187. Walkover Seat, Type 2 Test, 95th-Percentile Hybrid III Male ATD, Aisle Seat; Neck Compression/Tension Load

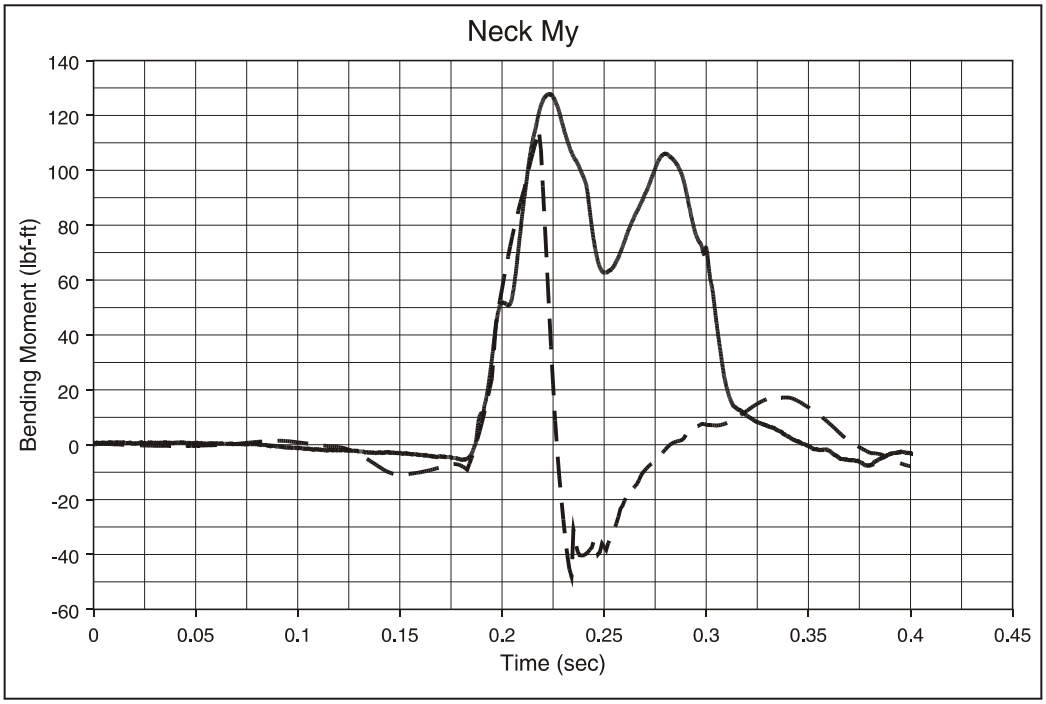

Figure F188. Walkover Seat, Type 2 Test, 95th-Percentile Hybrid III Male ATD, Aisle Seat; Neck Flexion/Extension Moment

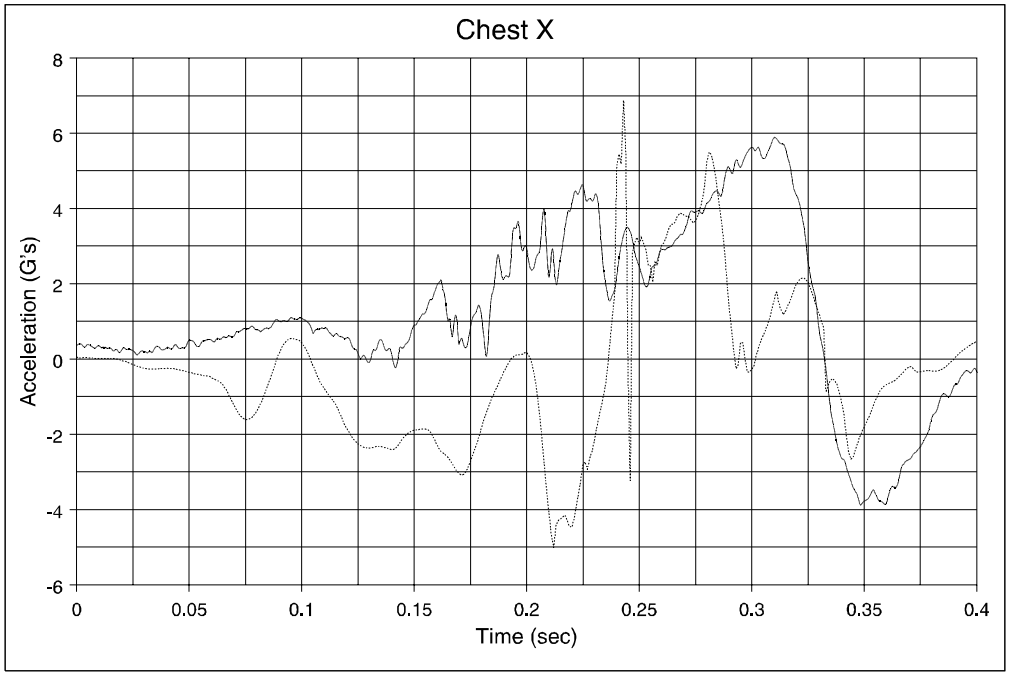

Figure F189. Walkover Seat, Type 2 Test, 50th-Percentile Hybrid III Male ATD, Center Seat; Chest Acceleration, x Direction

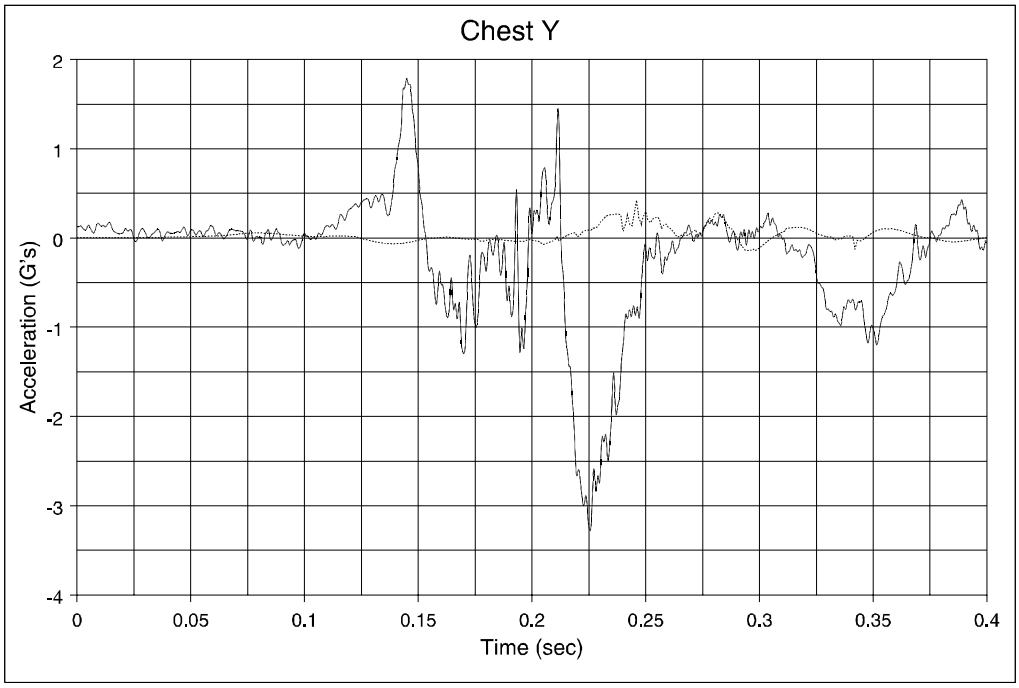

Figure F190. Walkover Seat, Type 2 Test, 50th-Percentile Hybrid III Male ATD, Center Seat; Chest Acceleration, y Direction

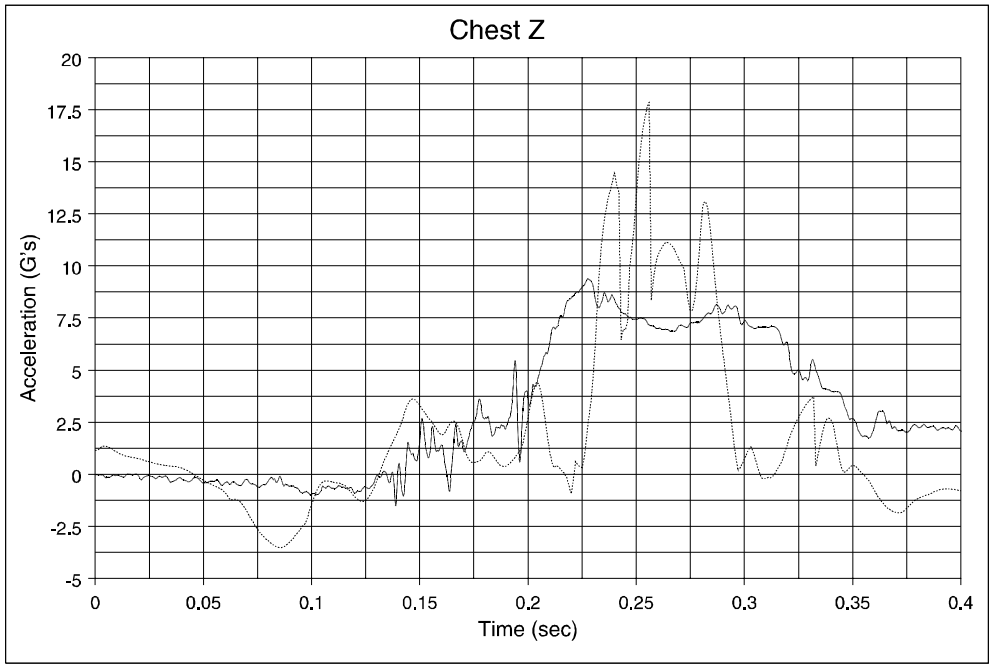

Figure F191. Walkover Seat, Type 2 Test, 50th-Percentile Hybrid III Male ATD, Center Seat; Chest Acceleration, z Direction

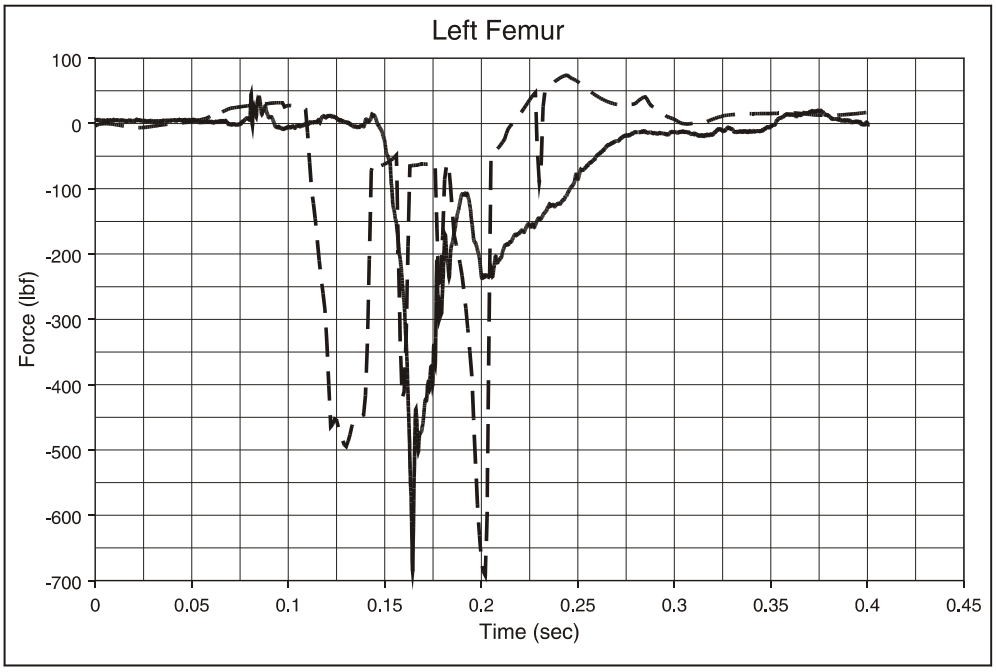

Figure F192. Walkover Seat, Type 2 Test, 50th-Percentile Hybrid III Male ATD, Center Seat; Left Femur Load

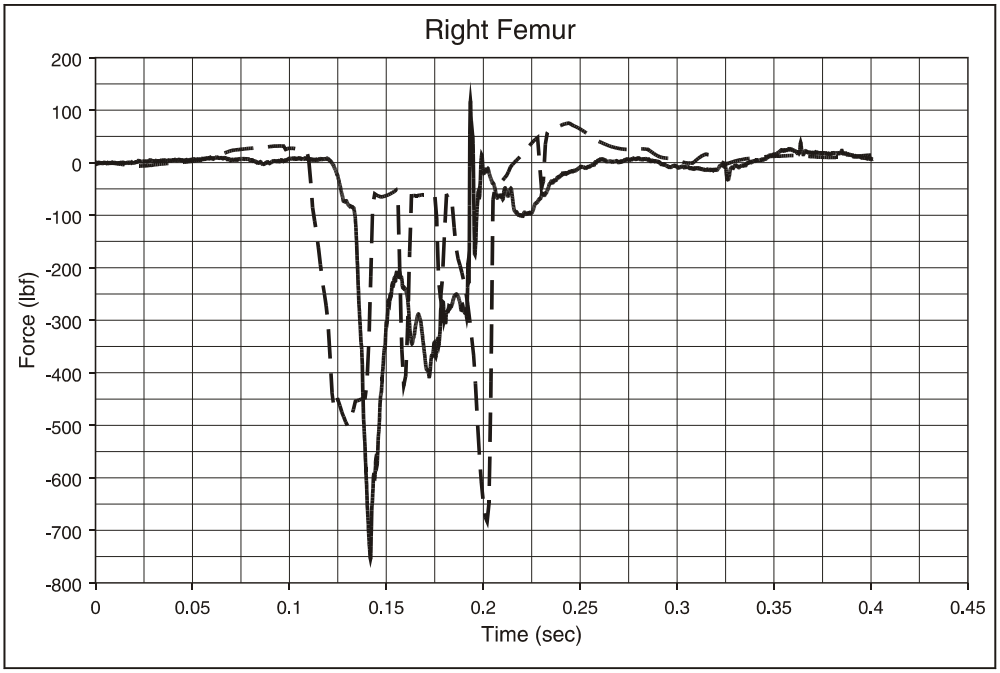

Figure F193. Walkover Seat, Type 2 Test, 50th-Percentile Hybrid III Male ATD, Center Seat; Right Femur Load

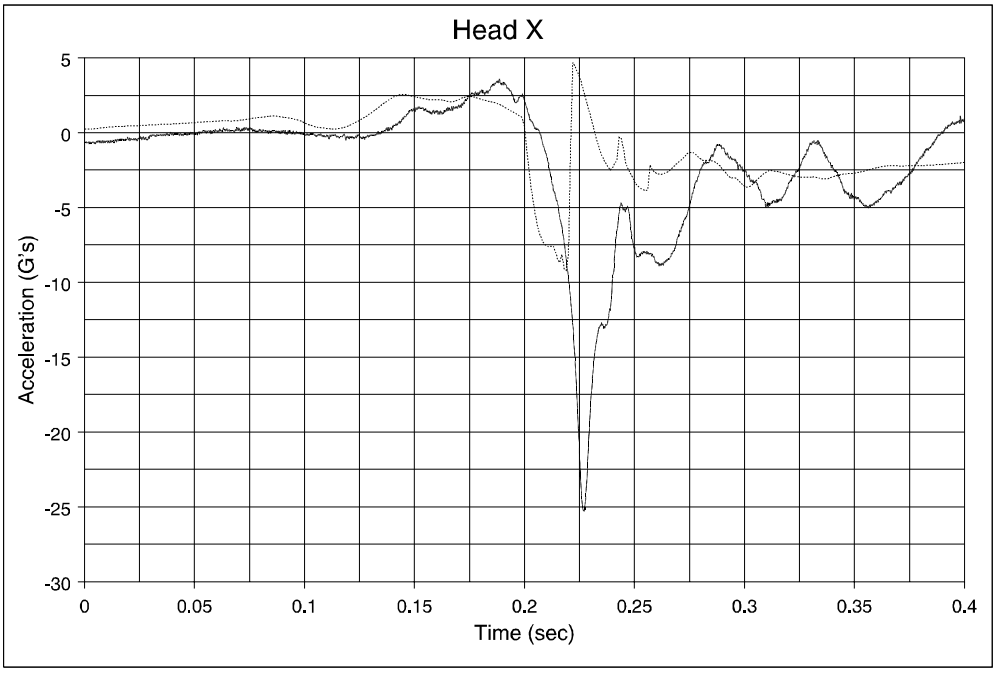

Figure F194. Walkover Seat, Type 2 Test, 50th-Percentile Hybrid III Male ATD, Center Seat; Head Acceleration, x Direction

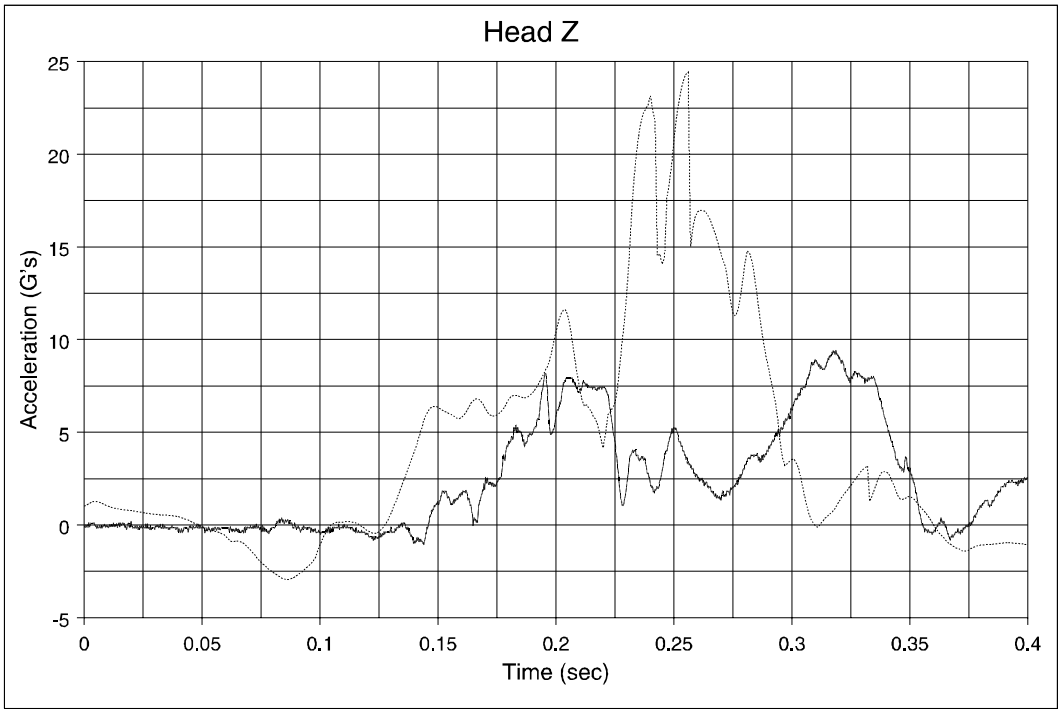

Figure F195. Walkover Seat, Type 2 Test, 50th-Percentile Hybrid III Male ATD, Center Seat; Head Acceleration, z Direction

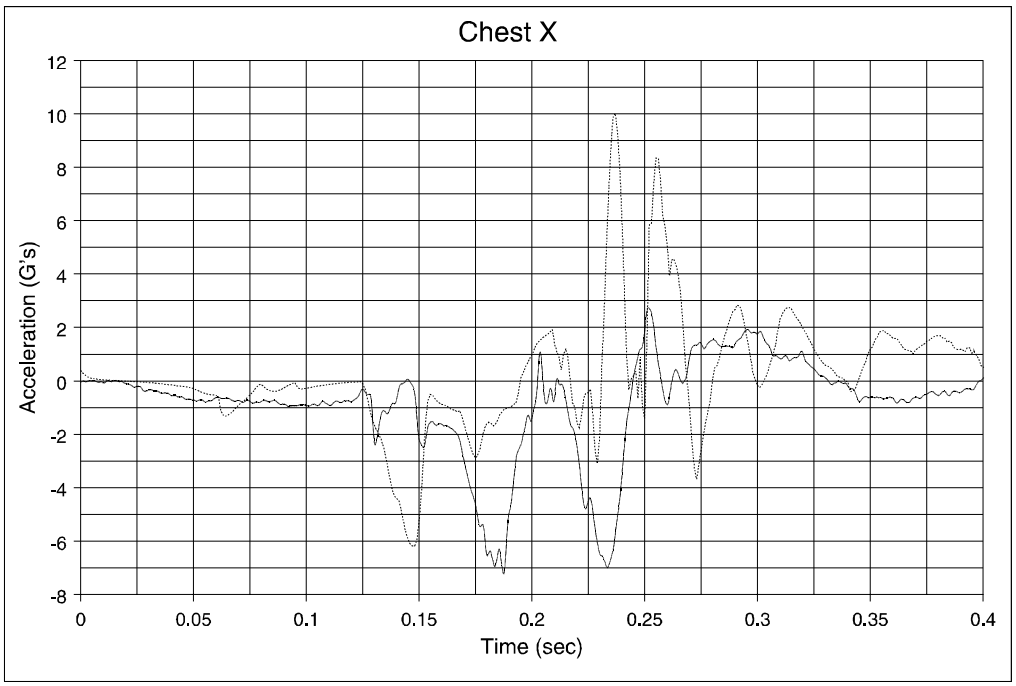

Figure F196. Walkover Seat, Type 2 Test, 5th-Percentile Hybrid III Female ATD, Window Seat; Chest Acceleration, x Direction

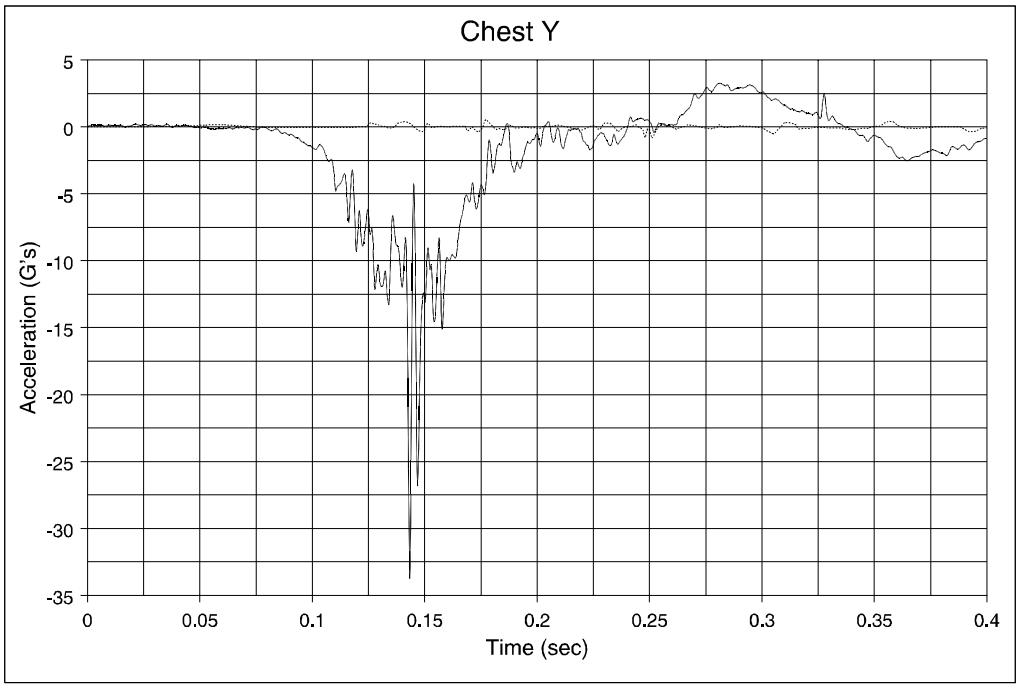

Figure F197. Walkover Seat, Type 2 Test, 5th-Percentile Hybrid III Female ATD, Window Seat; Chest Acceleration, y Direction

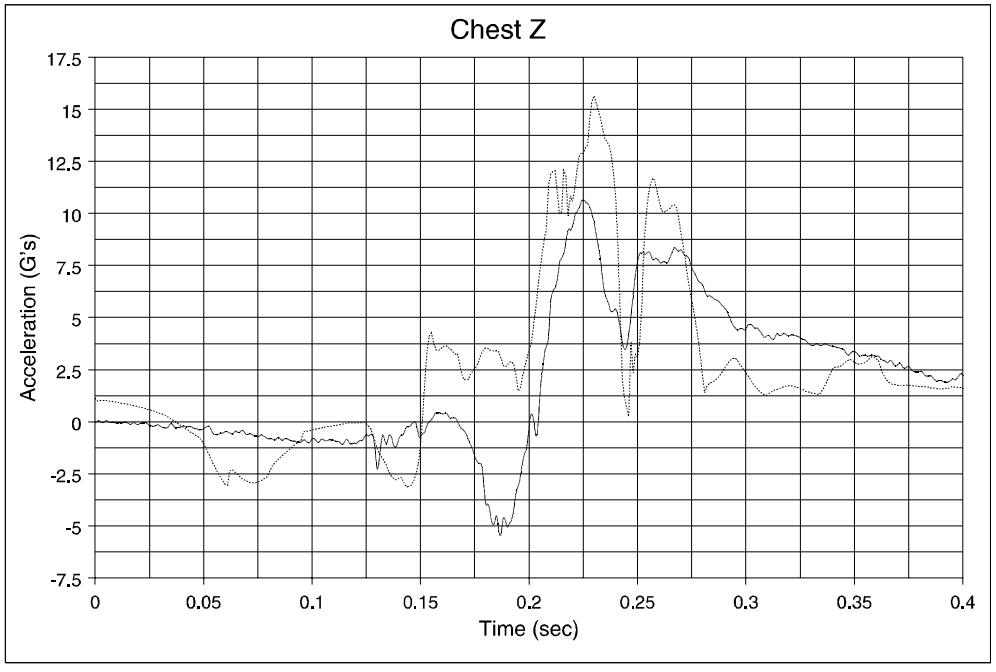

Figure F198. Walkover Seat, Type 2 Test, 5th-Percentile Hybrid III Female ATD, Window Seat; Chest Acceleration, z Direction

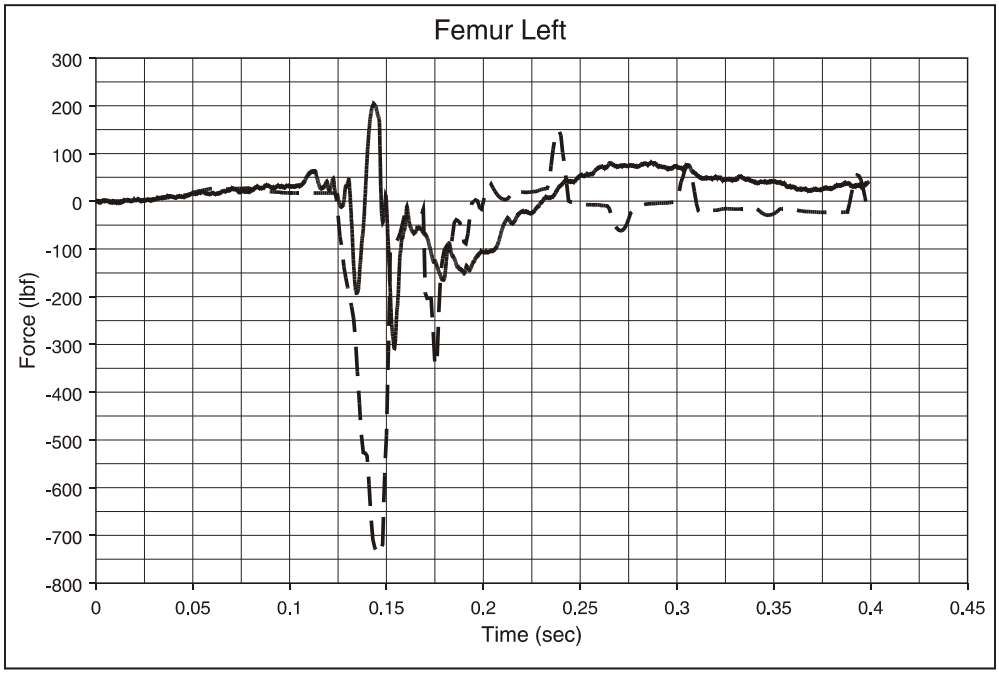

Figure F199. Walkover Seat, Type 2 Test, 5th-Percentile Hybrid III Female ATD, Window Seat; Left Femur Load

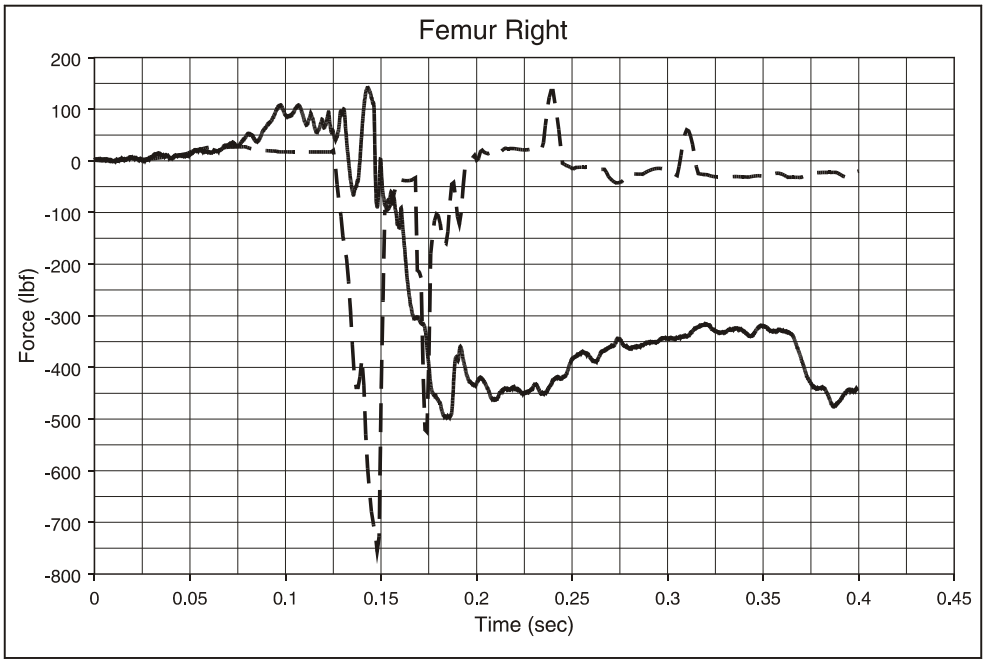

Figure F200. Walkover Seat, Type 2 Test, 5th-Percentile Hybrid III Female ATD, Window Seat; Right Femur Load

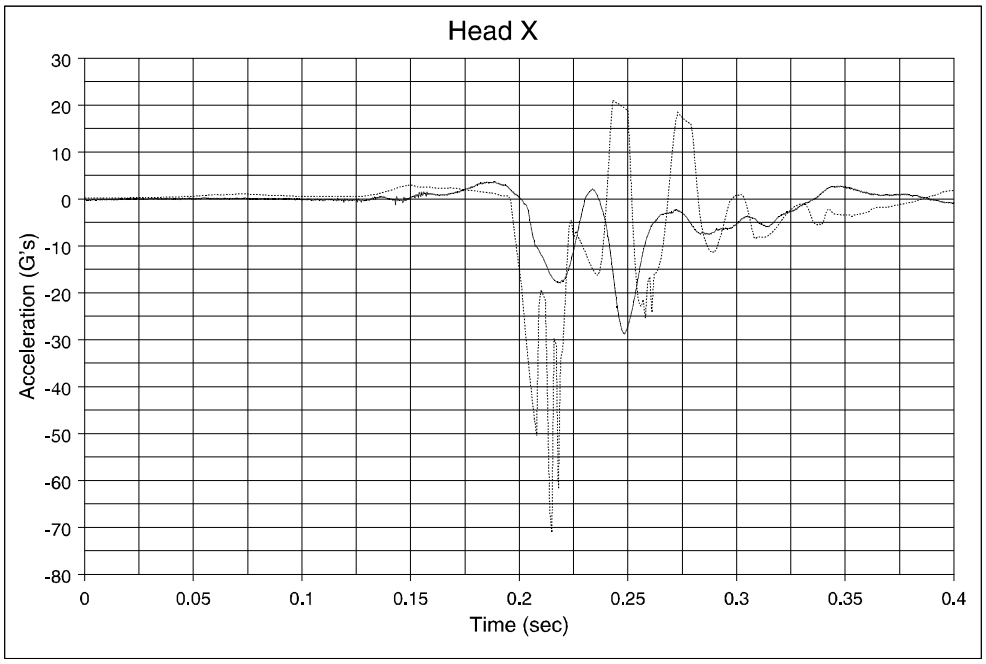

Figure F201. Walkover Seat, Type 2 Test, 5th-Percentile Hybrid III Female ATD, Window Seat; Head Acceleration, x Direction

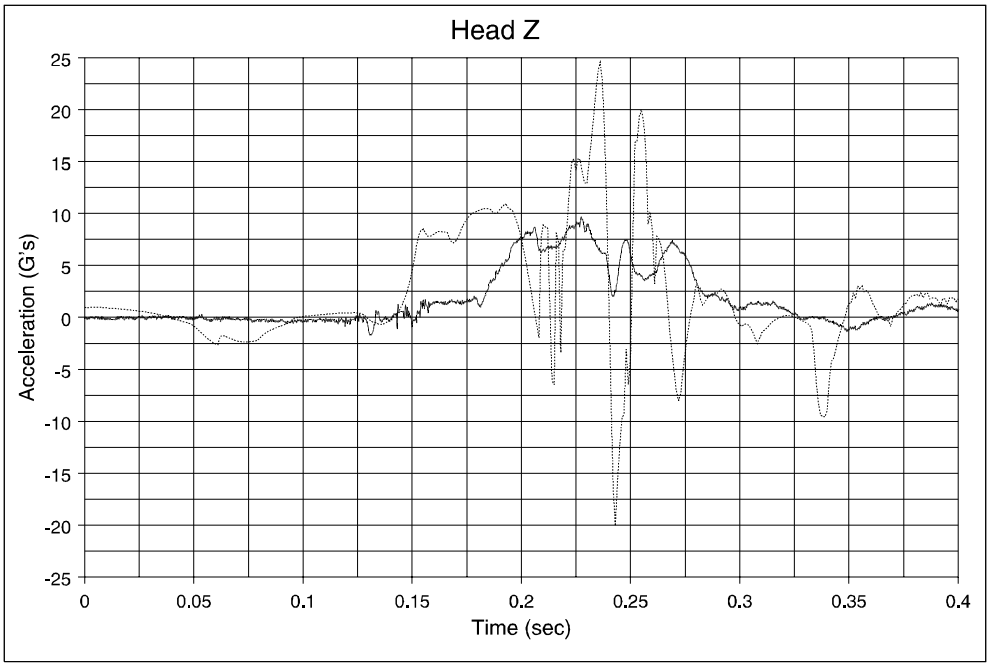

Figure F202. Walkover Seat, Type 2 Test, 5th-Percentile Hybrid III Female ATD, Window Seat; Head Acceleration, z Direction

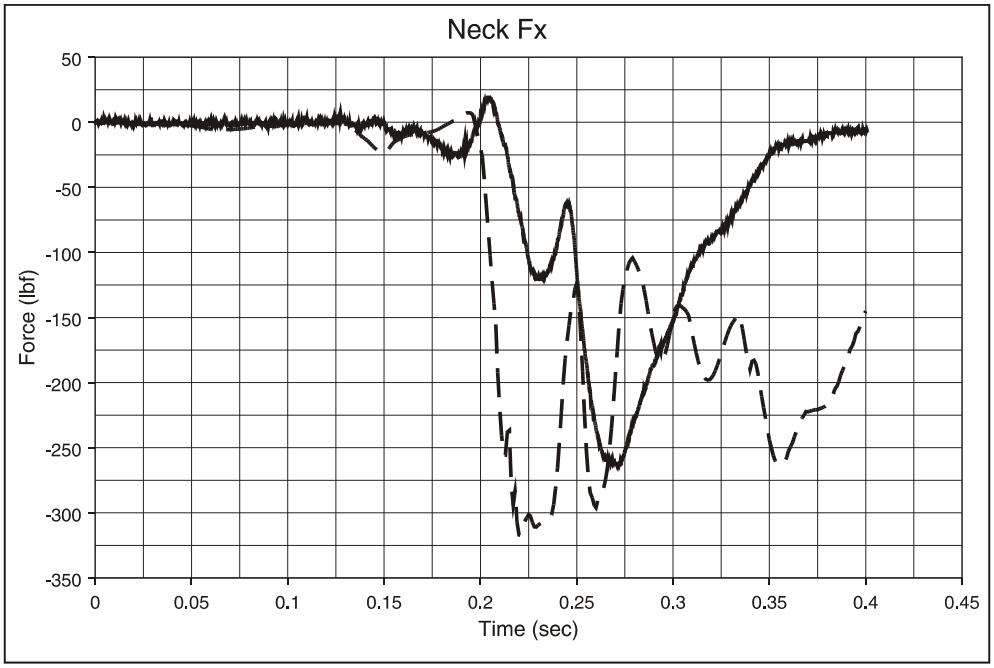

Figure F203. Walkover Seat, Type 2 Test, 5th-Percentile Hybrid III Female ATD, Window Seat; Neck Shear Load

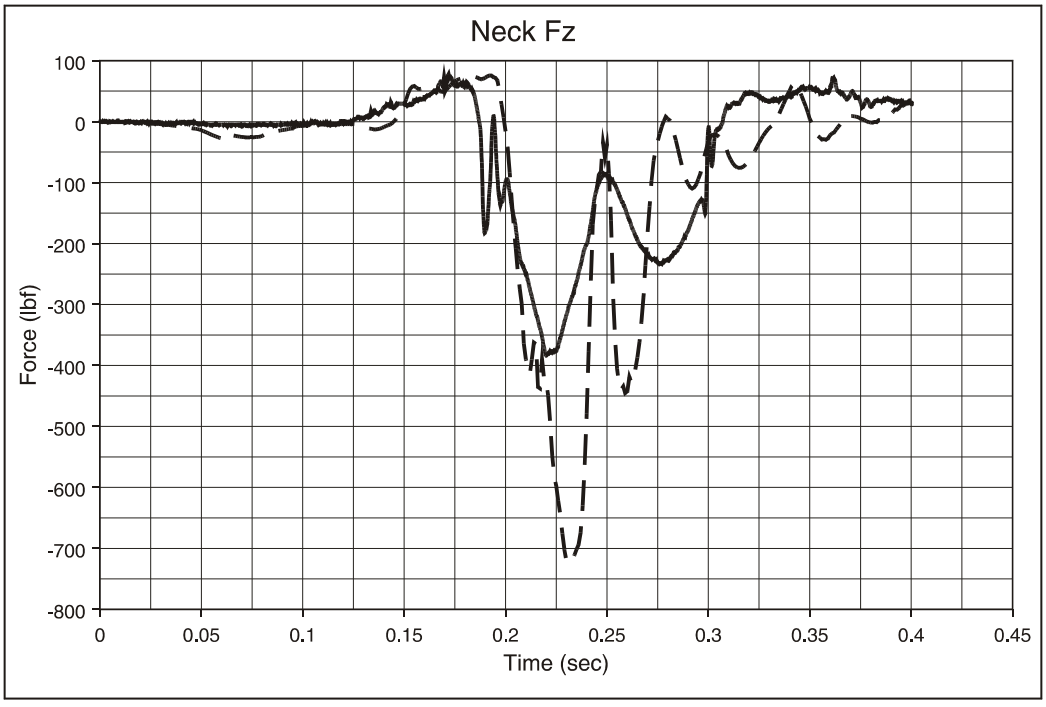

Figure F204. Walkover Seat, Type 2 Test, 5th-Percentile Hybrid III Female ATD, Window Seat; Neck Compression/Tension Load

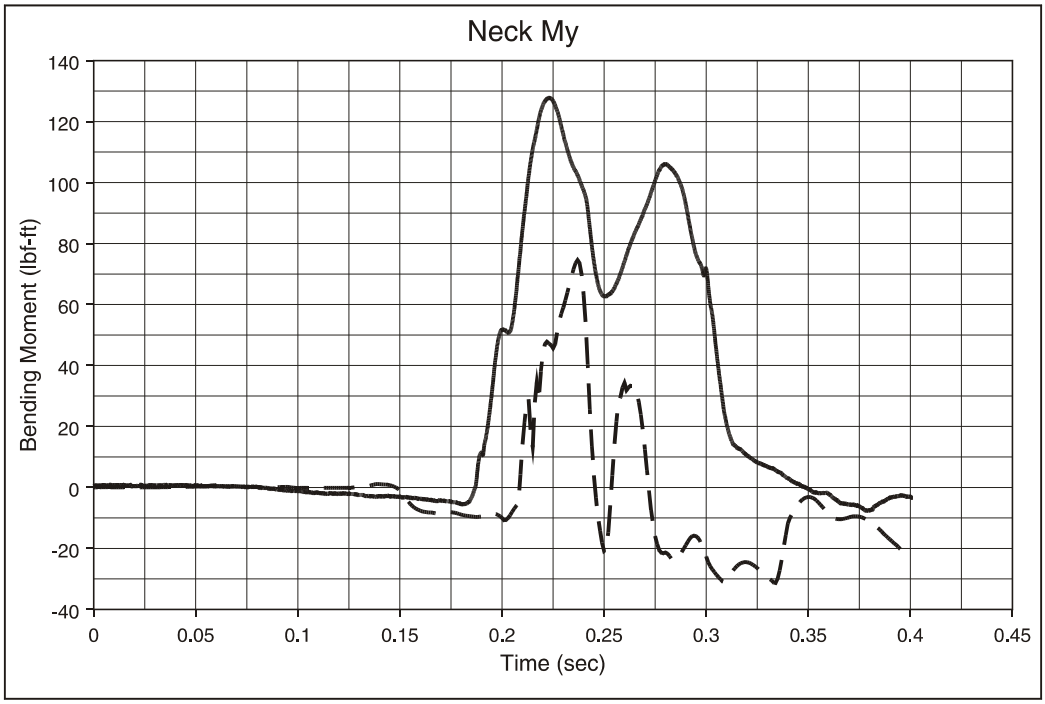

Figure F205. Walkover Seat, Type 2 Test, 5th-Percentile Hybrid III Female ATD, Window Seat; Neck Flexion/Extension Moment

APPENDIX G. PASSENGER RAIL SEAT SAFETY BACKGROUND INFORMATION

EXISTING STANDARDS

A worldwide literature search was conducted for existing regulations and current practice in the commuter rail industry and for other mass transit seating industries (including automotive, aviation, and military) in the United States.

The search revealed that apparently there are no actual regulations in any country in the world governing seat design, strength, and crashworthiness for passenger rail cars. Efforts have been underway for the last five years, however, in Europe to produce European standards under the auspices of an international organization called the Union Internationale des Chemins de Fer (UIC). This has been a difficult task for them to complete.

In the UK, there are a series of standards governing Railway Interior Crashworthiness. Among them are:

- GM/RC2502; Code of Practice for Structural Aspects of Railway Vehicle Interiors.
- BR/BCT609; Code of Practice for Railway Vehicle Interior Crashworthiness.

In the U.S., there are many regulations relating to passenger seating, human tolerance to impacts, passenger restraint systems, etc., in other transportation industries. For highway transportation, these include:

- FMVSS 222; School Bus Passenger Seating and Crash Protection.
- FMVSS 208; Occupant Crash Protection.
- FMVSS 201; Occupant Protection in Interior Impact.
- FMVSS 572.25; Subpart E - Hybrid III Test Dummy.

For air transport, the standards and regulations include:

- Federal Aviation Regulations (FAR) Part 25, Airworthiness Standards for Transport Category Airplanes.
- FAR Part 23, Airworthiness Standards for Commuter Category Airplanes.
- FAR Part 27, Airworthiness Standards for Normal Category of Rotorcraft.
- FAR Part 29, Airworthiness Standards for Transport Category of Rotorcraft.
- SAE AS8049; Performance Standards for Seats in Civil Rotorcraft and Transport Airplanes.
- SAE ARP 750; Passenger Seat Design Commercial Transport Aircraft.

- SAE ARP 767A; Impact Protective Design of Occupant Environment Transport Aircraft.

For rail transportation, the standards and regulations include:

- APTA SS-C&S-016-99 "Standard for Seating in Commuter Rail Cars."
- Federal Register, Vol. 64, No. 91, 5/12/99, Rules and Regulations (49CFR part 238.233).
- AAR RP-026 "Dimensions of Coach Seats" (dating from 1945).
- AAR RP-027 "Passenger Car Floor Plans."

CURRENT PRACTICE

Current practice in commuter rail car seating generally involves static testing of seats, with almost no consideration for limits on the criteria associated with passenger injury. A typical specification for commuter rail seats reads as follows:

1. Seat frame construction, cushions and attachments shall withstand the maximum stresses from…the following Load applications:

a. 300 lb per passenger uniformly distributed perpendicular to the plane of the seat back in both directions three (3) in. below the top of the back.

b. 450 lb per passenger uniformly distributed vertically downward on the seat bottom.

c. 250 lb vertical downward on armrests.

d. On seats equipped with grab handles, 300 lb on the handle applied in both longitudinal directions.

2. The allowable deformation may be an average of 1/2 in. at the top of the seat back.

3. Seat frames shall remain anchored to the floor and shall suffer no damage other than permanent deformation, for a 6-G longitudinal Load applied to passengers of weight equal to 210 lb each.

There is no mention in this specification regarding the safety of the passenger, although on occasion, some commuter rail seating specifications refer to the school bus standard (FMVSS 222) as a design guideline.

Often, the 6-G requirement given in Item No. 3 above is interpreted as a static load; i.e., the seat is statically loaded through the center of gravity of seated passengers to a static force equal to 210 lb x 2 (for a two-passenger seat) x 6 (from the 6-G requirement). A static test is fundamentally different from a dynamic test in that the static test determines only the yield strength of the seating frame, while the characteristic of interest is really the energy absorption capability of the seat.

On occasion, a swinging sandbag test is conducted in a manner such that the kinetic energy delivered into the seat is equal to the kinetic energy determined by calculating the distance through which occupants travel (using the seating pitch dimension) and then calculating the terminal velocity with which the occupants impact the seat back. While this method comes closer to the intent of measuring the energy-absorbing capability of the seat, it is only a crude approximation of the complexity of an actual accident situation and makes no attempt to measure any injury-causing accelerations or impact loads on the occupants.

A notable change in "standard" seating specifications is the recent Amtrak High-Speed Train Project. Although the Amtrak High-Speed seating specification makes an attempt to greatly improve the safety aspect of passenger seating, work remains to develop guidelines that are specific, improve passenger safety, and are as unambiguous as possible.

Another development in commuter rail cars is cantilever-mounted seating; i.e., transverse seats that are attached to the sidewall of the car. The primary reason for this type of design is to ease the task of regularly cleaning the car interior. Structural requirements for cantilever seating, however, can be at odds with requirements for passenger safety. Seat frames and attachments that are strong enough to support cantilever loads are difficult to make compliant enough to absorb the energy of passengers impacting the seat backs.

CURRENT RESEARCH AND DEVELOPMENT

The most relevant current research and development relating to rail passenger seat design has been conducted by the FRA in conjunction with the Volpe Center. The papers and reports associated with this research are:

- Tyrell, D.C, and K.J. Severson, USDOT/FRA *Crashworthiness Testing of Amtrak's Traditional Coach Seat,* October 1996.

- Tyrell, D.C., K.J. Severson, and B.P. Marquis, *Train Crashworthiness Design for Occupant Survivability,* American Society of Mechanical Engineers, AMD-Vol. 210, BED-Vol. 30, 1995.

- Tyrell, D.C., K.J. Severson, and B.P. Marquis, *Analysis of Occupant Protection Strategies in Train Collisions,* American Society of Mechanical Engineers, AMD-Vol. 210, BED-Vol. 30, 1995.

Other current work on seating and crashworthiness includes:

- "Report to Advanced Railroad Research Centre," Sheffield, UK, and associated paper for the Transportation Research Record 1531, Vanderbilt University, Nashville, TN, "Passenger Train Crashworthiness - Secondary Collisions," Chaterjee, S., and J. Carney III.

It is clear that a wealth of data and technology exist in the United States and throughout the world from which an appropriate, effective, and efficient set of specifications for use in the design of new commuter rail seating can be developed. The proposed baseline testing of current passenger rail seats augments this effort to better understand the current level of rail seat crashworthiness; the challenge will be to synthesize the results of these data into meaningful specifications.